

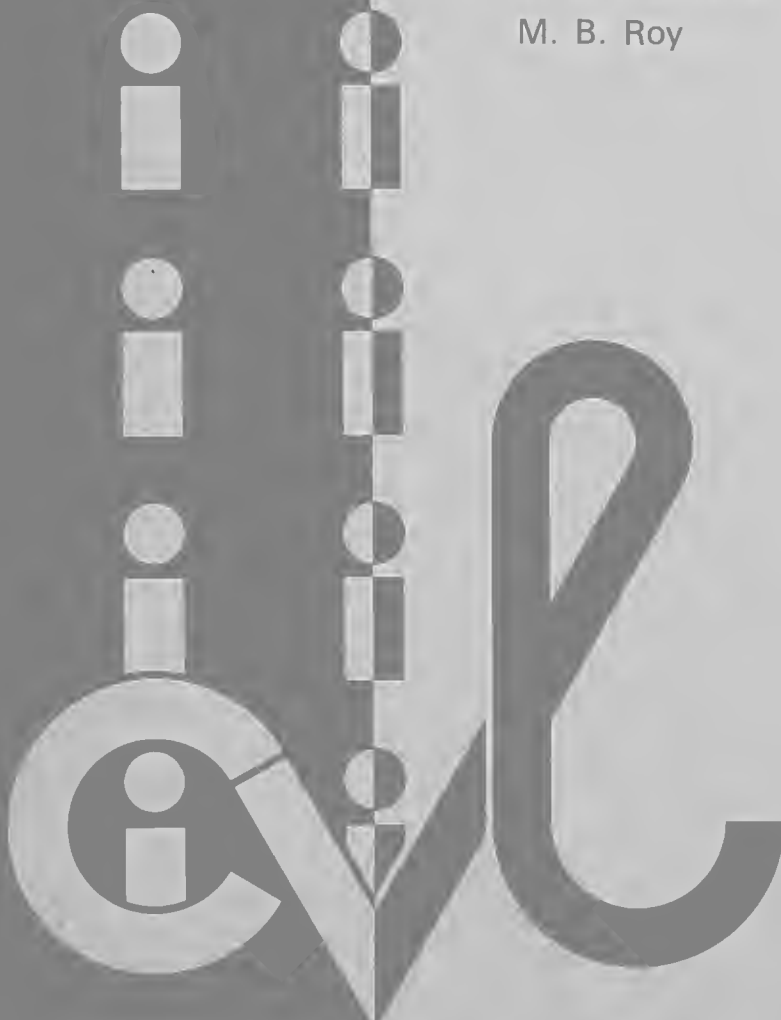


JOINT HIGHWAY RESEARCH PROJECT

JHRP-76-15

PREDICTING PERFORMANCE
OF PIPE CULVERTS BURIED
IN SOIL

G. A. Leonards
M. B. Roy



Digitized by the Internet Archive
in 2011 with funding from
LYRASIS members and Sloan Foundation; Indiana Department of Transportation

Interim Report

PREDICTING PERFORMANCE OF PIPE CULVERTS BURIED IN SOIL

TO: J. F. McLaughlin, Director
Joint Highway Research Project

May 5, 1976

FROM: H. L. Michael, Associate Director
Joint Highway Research Project

Project: C-36-62F

File: 9-8-6

The attached Interim Report of the HPR Part II Study titled "Performance of Pipe Culverts Buried in Soil" is submitted. The title of the report "Predicting Performance of Pipe Culverts Buried in Soil" has been performed by Mr. M. B. Roy, Graduate Instructor on our staff under the direction of Professor G. A. Leonards. This Interim Report covers Phase I of the Study and records total activity for this Phase.

A proposal for Phase II is being prepared and will be submitted shortly and has been detailed in the material submitted for the FY 77 HPR Work Program on this Study. A controlled laboratory study will be proposed for verification and fine-tuning of the computer program developed under Phase I.

The accomplishment of Phase I was fulfillment of the objectives of the Phase, development of an analytical prediction procedure for rational design of buried culverts. The computer program developed is applicable to any desired range of pipe flexibility, using relevant soil properties that can be determined by laboratory tests and including appropriate soil-structure interaction effects.

The Report is submitted for acceptance as fulfillment of the objectives of Phase I. It will be submitted for review, comment and similar acceptance to FHWA. A User's Manual for the computer program FINLIN developed in this research is also available in a second volume.

Respectfully submitted,

Harold L. Michael /ms
Harold L. Michael
Associate Director

HLM/ss

cc: W. L. Dolch	M. L. Hayes	C. F. Scholer
R. L. Eskew	K. R. Hoover	M. B. Scott
G. D. Gibson	G. A. Leonards	K. C. Sinha
W. H. Goetz	C. W. Lovell	L. E. Wood
M. J. Gutzwiller	R. D. Miles	E. J. Yoder
G. K. Hallock	P. L. Owens	S. R. Yoder
D. E. Hancher	G. T. Satterly	

1. Report No. JHRP-76-15	2. Government Accession No.	3. Recipient's Catalog No.	
4. Title and Subtitle PREDICTING PERFORMANCE OF PIPE CULVERTS BURIED IN SOIL		5. Report Date May 1976	6. Performing Organization Code
		8. Performing Organization Report No. JHRP-76-15	
7. Author(s) G. A. Leonards and M. B. Roy		10. Work Unit No.	
9. Performing Organization Name and Address Joint Highway Research Project Civil Engineering Building Purdue University W. Lafayette, Indiana 47907		11. Contract or Grant No. HPR-1(12) Part II	
		13. Type of Report and Period Covered Interim Report of Phase I	
12. Sponsoring Agency Name and Address Indiana State Highway Commission State Office Building 100 North Senate Avenue Indianapolis, Indiana 46204		14. Sponsoring Agency Code	
15. Supplementary Notes Prepared in cooperation with the U. S. Department of Transportation, Federal Highway Administration. From the study, "Performance of Pipe Culverts Buried in Soil"			
16. Abstract <p>An analytical tool based on the finite element method has been developed to analyze buried culvert problems in a realistic fashion.</p> <p>Segments of a curved bar with three degrees of freedom (normal, tangential and rotational) at each end have been used to simulate a thin pipe where nodal moments are important. Triangular, isoparametric elements with one curved boundary (to fit the shape of pipe), and three midside nodes have been used to represent the soil. A special type of 'interaction' element with zero thickness has been used between pipe and soil to simulate interface behavior, including slip and/or the inability to resist tensile stresses.</p> <p>Nonlinear, anisotropic soil properties have been accounted for. Actual test data are used as input for soil properties.</p> <p>A computer program was written to include all the aspects mentioned above, and example problems were solved to demonstrate its versatility and to investigate the influence of such factors as non-linear soil properties, relative stiffness of pipe and soil, inclusion of weak materials near the spring line, and construction procedures. The present program is applicable only for analysis of two-dimensional problems transverse to the pipe in which the state of stress either in the soil mass or in the pipe does not approach failure.</p>			
17. Key Words Pipe Culverts; Design of Pipe Culverts; Finite Element Analysis; Pipe Culverts in Soil		18. Distribution Statement No restrictions. This document is available to the public through the National Technical Information Service, Springfield, Virginia 22161.	
19. Security Classif. (of this report) Unclassified	20. Security Classif. (of this page) Unclassified	21. No. of Pages 219	22. Price

Interim Report

PREDICTING PERFORMANCE OF PIPE CULVERTS BURIED IN SOIL

BY

G. A. Leonards
Professor of Soil Mechanics

and

Mihir Baran Roy
Graduate Instructor in Research

Joint Highway Research Project

Project No.: C-36-62F

File No.: 9-8-6

Prepared as Part of an Investigation

Conducted by .

Joint Highway Research Project
Engineering Experiment Station
Purdue University

in cooperation with the

Indiana State Highway Commission

and the

U. S. Department of Transportation
Federal Highway Administration

The contents of this report reflect the views of the authors who are responsible for the facts and the accuracy of the data presented herein. The contents do not necessarily reflect the official views or policies of the Federal Highway Administration. This report does not constitute a standard, specification, or regulation.

Purdue University
West Lafayette, Indiana
May 5, 1976

ACKNOWLEDGEMENTS

The writers are indebted to Drs. V. J. Meyers and T. Y. Yang for valuable assistance with the formulation of the finite element computer program. They also wish to thank members of the staff at the Purdue University Computing Center, especially Mr. Ladd J. Wheeler and Dr. D. V. Pathak, for their suggestions and discussions about the computer program.

Careful typing of the manuscript by Mary Kerkhoff and Carole Montgomery is gratefully acknowledged.

TABLE OF CONTENTS

LIST OF TABLES.	Page vii
LIST OF FIGURES	viii
LIST OF SYMBOLS	xi
HIGHLIGHT SUMMARY	xv
CHAPTER I - INTRODUCTION.	1
CHAPTER II - LITERATURE REVIEW.	5
Current Design Practice	5
Concrete Culverts:	5
Marston Theory	6
Flexible Culverts.	10
Literature Review	13
Need for Further Research	20
CHAPTER III - FINITE ELEMENT METHOD	21
Historical Background	21
Requirements for Finite Element Methods	23
Selection of Finite Elements to Represent the Soil	25
Selection of Displacement Function.	27
Derivation of Element Stiffness Matrix for Linear Strain Triangular Finite Element.	33
Finite Element Representation for Pipe Culverts	37
Curved-Ring Element	48
Soil-Pipe Interaction Element	51
CHAPTER IV - MATERIAL PROPERTIES.	53
Introduction.	53
Pipe Properties	54
Soil-Pipe Interaction	54
Properties for the Interaction Element	56
Soil Properties	57
Need for Incremental Analysis.	64
Method of Considering Stress-Strain Parameters.	66
Spline Functions	69

	Page
CHAPTER IV - (Continued)	
Poisson's Ratio	78
Anisotropy.	86
Anisotropic Pipe Properties (for thick pipe only)	87
Determination of Elasticity Matrix [D] for Soil	92
Use of Spline Function for Material Properties. . .	94
Procedure for Data Reduction	95
CHAPTER V - COMPUTER PROGRAM	106
Introduction.	106
Program Outline	108
Overlay.	109
(Disc) Tape Unit	110
Random Mass Storage	110
Type 1, Curved Bar Element	117
Type 2, Interaction Element.	119
Triangular Element	120
Structural Assembly.	122
Solution of Stiffness Equation	123
No-tension Analysis.	127
CHAPTER VI - FINITE ELEMENT ANALYSIS.	134
Selection of Boundaries and Boundary Conditions . .	134
Selection of Example Problems	136
Properties of Soil	136
Finite Element Idealization.	139
Problems Selected.	139
CHAPTER VII - PRESENTATION AND DISCUSSION OF RESULTS. .	144
Group One	145
Group Two	155
Group Three	158
CHAPTER VIII - SUMMARY.	167
Results	167
Conclusions	168
Recommendations for Future Research	170
LIST OF REFERENCES.	172
APPENDICES	
APPENDIX - ISOPARAMETRIC LINEAR-STRAIN TRIANGULAR ELEMENT WITH ONE CURVED BOUNDARY. . .	182

APPENDICES - (Continued)	Page
APPENDIX - B CURVED BAR ELEMENT.	199
APPENDIX - C INTERACTION ELEMENT	209
APPENDIX - D DERIVATION OF $\frac{\tau_{oct}}{\sigma_{oct}}$ failure	215
APPENDIX - E DERIVATION OF TANGENT MODULUS (E_t) AND POISSON'S RATIO (ν_t)	217
VITA.	220

LIST OF TABLES

Table		Page
3.1	Comparison of Ring Solutions	38
6.1 (a)	Layer Heights for Incremental Analysis, 20 Ft. Fill	141
6.1 (b)	Layer Heights for Incremental Analysis, 40 Ft. Fill	141
6.2	Example Problem Description - I. Single Layer, 20 Feet of Cover	142
6.3	Example Problem Description - II. Multi-Layer, Nonlinear Soil, 20 Feet of Cover	143
7.1	Comparison of Results for Linear Soil Properties, Single Layer, No Interface Slip, 20 Feet of Soil Cover	146
7.2	Comparison of Results for Single and Multilayer, Nonlinear Soil Properties, with and without Interface Slip, 20 Feet of Cover	156
7.3	Comparison of Results for Single and Multilayer, Nonlinear Soil Properties, with and without Interface Slip, 40 Feet of Cover	159

LIST OF FIGURES

Figure		Page
2.1	FREE BODY DIAGRAM FOR DITCH CONDUIT. (After Spangler, 1960).	7
3.1	TYPICAL SECTION OF PIPE CULVERT	26
3.2	TRIANGULAR ISOPARAMETRIC ELEMENT.	28
3.3	DISTRIBUTION OF CIRCUMFERENTIAL NORMAL STRESS AT THE SPRING LINE	40
3.4	DISTRIBUTION OF CIRCUMFERENTIAL NORMAL STRESS AT THE SPRING LINE	41
3.5	DISTRIBUTION OF CIRCUMFERENTIAL NORMAL STRESS AT THE SPRING LINE	42
3.6	DISTRIBUTION OF CIRCUMFERENTIAL NORMAL STRESS AT THE SPRING LINE	43
3.7	DISTRIBUTION OF CIRCUMFERENTIAL NORMAL STRESS AT THE SPRING LINE	44
3.8	DISTRIBUTION OF CIRCUMFERENTIAL NORMAL STRESS AT THE SPRING LINE	45
3.9	ERROR IN $\sigma_{\theta_{\max}}$ DETERMINED USING ISOPARAMETRIC TRIANGULAR ELEMENTS VS. RATIO OF PIPE WALL THICKNESS TO INTERNAL RADIUS.	46
4.1	PROPERTIES OF INTERACTION ELEMENT	58
4.2	ERRORS IN INCREMENTAL ANALYSIS.	68
4.3	INTERVAL OF A CUBIC SPLINE FUNCTION	70
4.4	SUBINTERVAL OF SPLINE FUNCTION.	73
4.5(a)	TYPICAL STRESS - STRAIN CURVES.	77
4.5(b)	TANGENT MODULUS - OCTAHEDRAL NORMAL STRESS CURVES	77

Figure	Page
4.6(a) LOG-LOG PLOT OF $\epsilon_3\%$ VS. $\epsilon_1\%$ (Data From Duncan and Chang, 1970).	80
4.6(b) LOG-LOG PLOT OF P VS. σ_3/p_a (Data From Duncan and Chang, 1970).	82
4.6(c) COMPARISON OF TANGENT MODULUS FOR PLANE STRAIN CONDITION (1) DETERMINED FROM PLANE STRAIN TEST, E_p (2) CALCULATED FROM TRIAXIAL TEST USING FORMULATION (4.4), (4.34) AND (4.25), E_{TX}	84
4.6(d) COMPARISON OF TANGENT POISSON'S RATIO FOR PLANE STRAIN CONDITION (1) DETERMINED FROM PLANE STRAIN TEST, ν_p (2) CALCULATED FROM TRIAXIAL TEST USING FORMULATION (4.4), (4.34) AND (4.35), ν_{TX}	85
4.7 CO ORDINATE SYSTEM FOR TRANSFORMATION OF ANISOTROPIC MATERIAL PROPERTIES	89
4.8 PLANE STRAIN TEST ON LOOSE MONTEREY NO. O SAND.	96
4.9 TANGENT MODULUS VS. OCTAHEADRAL NORMAL STRESS AND FAILURE RATIO FOR LOOSE SAND	98
4.10 TANGENT POISSON'S RATIO VS. OCTAHEADRAL NORMAL STRESS AND FAILURE RATIO FOR LOOSE SAND.	99
4.11 OCTAHEADRAL SHEAR STRESS VS. OCTAHEADRAL NORMAL STRESS AT FAILURE, LOOSE SAND.	100
4.12 PLANE STRAIN TEST ON DENSE MONTEREY NO. O SAND. (After Lade, 1972).	101
4.13 TANGENT MODULUS VS. OCTAHEADRAL NORMAL STRESS AND FAILURE RATIO FOR DENSE SAND	103
4.14 TANGENT POISSON'S RATIO VS. OCTAHEADRAL NORMAL STRESS AND FAILURE RATIO FOR DENSE SAND.	104
4.15 OCTAHEADRAL SHEAR VS. OCTAHEADRAL NORMAL STRESS AT FAILURE, DENSE SAND	105
5.1 General Flow Chart of Program FINLIN.	112
5.2 Flow Chart for OVERLAY (0,0).	113

Figure		Page
5.3	Flow Chart for OVERLAY (1,0) (Continued)	114
5.4	Flow Chart for OVERLAY (2,0)	116
5.5	Flow Chart for OVERLAY (3,0)	118
5.6	Flow Chart for OVERLAY (4,0)	125
5.7	Flow Chart for OVERLAY (5,0)	125
5.8	Flow Chart for OVERLAY (6,0)	126
5.9	SCHEME FOR 'NO-TENSION' ANALYSIS	130
6.1	GEOMETRY OF SAMPLE CULVERT PROBLEM	137
6.2	FINITE ELEMENT MESH FOR EXAMPLE PROBLEM	138
7.1(a)	EFFECT OF RELATIVE STIFFNESS OF PIPE AND SOIL ON CHANGE IN VERTICAL DIAMETER OF PIPE	148
7.1(b)	EFFECT OF RELATIVE STIFFNESS OF PIPE AND SOIL ON MAXIMUM MOMENT AND MAXIMUM THRUST IN THE PIPE	149
7.1(c)	EFFECT ON RELATIVE STIFFNESS OF PIPE AND SOIL ON MAXIMUM EXTREME FIBER STRESS IN THE PIPE	150
7.1(d)	FRACTION OF EXTREME FIBRE STRESS IN PIPE INDUCED BY MOMENT VS. NORMALIZED PIPE STIFFNESS	150(a)
7.1(e)	INFLUENCE OF PIPE STIFFNESS ON MARSTON- SPANGLER SOIL MODULUS	150(b)
7.2	DISTRIBUTION OF MOMENT AND DEFORMED SHAPE OF PIPE, PROBLEM L-14	152
7.3	DISTRIBUTION OF NORMAL AND SHEAR FORCES IN PIPE, PROBLEM L-14	153
7.4	NORMAL AND SHEAR STRESS AT SOIL-PIPE INTERFACE PROBLEM L-14	154
7.5	DEFLECTED SHAPE AND DISTRIBUTION OF MOMENT IN PIPE, NONLINEAR ANALYSIS, PROBLEM NL-1	160
7.6	DISTRIBUTION OF NORMAL AND SHEAR FORCE IN PIPE, NONLINEAR ANALYSIS, PROBLEM NL-1	161
7.7	DISTRIBUTION OF NORMAL AND SHEAR STRESS IN INTERACTION LAYER, NONLINEAR ANALYSIS, PROBLEM NL-1	162
7.8	DEFLECTED SHAPE AND DISTRIBUTION OF MOMENT IN PIPE, MULTI LAYER ANALYSIS, PROBLEM ML-1, ML-3	163

Figure		Page
7.9	DISTRIBUTION OF NORMAL AND SHEAR FORCE IN PIPE, MULTI LAYER ANALYSIS, PROBLEM ML-1, ML-3.	164
7.10	DISTRIBUTION OF NORMAL AND SHEAR STRESS IN INTERACTION LAYER, MULTI LAYER ANALYSIS, PROBLEM ML-1, ML-3.	165
Appendix		
Figure		
A.1	ISOPARAMETRIC LINEAR STRAIN TRIANGULAR ELEMENT	183
B.1	CURVED BAR ELEMENT.	200
B.2	TRANSFORMATION OF CO ORDINATE SYSTEM FOR CURVED BAR ELEMENT.	206
C.1	REPRESENTATION OF INTERACTION ELEMENT	210

LIST OF SYMBOLS

A, A^*	Cross-sectional area
a	Inner radius of ring, constant
B	Constant
b	Constant, vector
B_c	External diameter of pipe
C	Soil cohesion, constant
D_d	Constant
D	Nominal diameter of pipe
D_L	Deflection lag factor
d	Nominal diameter of pipe
E	Young's modulus
E'	Modulus of passive earth resistance
F	Shape function
F_b	Buckling stress of pipe material
f_u	Minimum tensile strength of pipe material
G	Shear modulus
g	Plastic potential
H	Height of fill
h	Distance
I	Moment of inertia
i, j	Index number

K	Bulk modulus, Coefficient of active earth pressure, bedding constant
k	Stiffness matrix
M	Nodal moment
m	Exponent value
N	Factor of safety
n	Exponent value
P	Vertical load, nodal point; constant
p_a	Atmospheric pressure
Q	Nodal point
q	Exponent value
R	Radius of pipe, nodal point
r	Radial distance
s	Arc length
t	Unit thickness
U	Strain energy
u	Displacement
V	Force, elastic potential
v	Displacement
W_c	Vertical load on pipe
X,x	Co-ordinate axis
Y,y	Co-ordinate axis
α	Angle
β	Angle
γ	Unit weight of soil, shear strain

Δ	Increment, sub-interval of spline function
δ	Partial derivative
ϵ	Strain
η	Area ratio
θ	Rotation
λ	Constant
μ	Coefficient of friction
ν	Poisson's ratio
π	Ratio of circumference to diameter of circle
σ	Principal stress
σ_{θ}	Circumferential normal stress
σ_{oct}	Octahedral normal stress
τ	Shear stress
τ_{oct}	Octahedral shear stress
ϕ	Potential function
ϕ	Angle of friction of soil
ψ	Matrix of derivative of shape function
ξ	Natural co-ordinate

HIGHLIGHT SUMMARY

An analytical tool, based on the finite element method, has been developed to analyze buried culvert problems in a realistic fashion.

Segments of a curved bar with three degrees of freedom (normal, tangential and rotational) at each end have been used to simulate a thin pipe where nodal moments are important. Triangular, isoparametric elements with one curved boundary (to fit the shape of pipe), and three midside nodes have been used to represent the soil. A special type of 'interaction' element with zero thickness has been used between pipe and soil to simulate interface behavior, including slip.

Nonlinear, anisotropic soil properties have been accounted for. Actual test data are used as input for soil properties; the data are interpolated using a cubic spline function, incremental Young's modulus and Poisson's ratio are calculated in terms of octahedral normal and shear stresses and the result is stored in the computer. 'Interaction' elements offer high resistance to movements in the normal and tangential directions until the stress ratio (shear to normal stress) exceeds a limiting value. Once the ratio is exceeded, stiffness in the shear direction is reduced to zero. Actual construction sequences can be simulated and 'no-tension' analysis is incorporated if the soil and/or the soil-pipe interface cannot resist tension.

A computer program was written to include all the aspects mentioned above, and some example problems were solved to demonstrate its versatility and to investigate the influence of such factors as non-linear soil properties, relative stiffness of pipe and soil, inclusion of weak materials near the spring line, and construction procedures. It was found that for circular corrugated metal pipe buried in granular soil:

(a) maximum circumferential thrust in the pipe depends mainly on pipe diameter and height of fill, although interface friction has some influence.

(b) the effect of nonlinear soil properties on culvert performance must be accounted for but, for high fills placed and loaded symmetrically, neither construction sequence nor partial slip at the soil-pipe interface had significant effects.

(c) Marston-Spangler soil modulus E' can not be used as a soil parameter in rational predictions of culvert performance.

The study did not consider time-dependent soil properties, prestress of soil during compaction, or cracking or yielding of the pipe, although the latter can readily be accounted for. The present program is applicable only for analysis of two-dimensional problems transverse to the pipe in which the state of stress in the soil mass does not approach failure.

CHAPTER I

INTRODUCTION

Culverts and conduits under highway and railway embankments are commonly used structures. Depending upon the purpose, they may be large or small, deep or shallow, rigid or flexible. Culverts can be classified in two broad categories, based on their relative stiffness: (1) rigid and (2) flexible. Rigid culverts are those for which the diametral change under load prior to rupture is assumed to be too small to influence the resulting distribution of soil pressure. Before cracking, concrete pipe culverts are usually considered to be rigid. Flexible culverts are designed on the basis that sufficient deflection of the culvert will occur to mobilize additional lateral resistance from the surrounding soil mass. Accordingly, for rigid culverts, the "Marston Theory" (Marston and Anderson, 1913; Marston, 1930) is commonly used for design while flexible culverts are designed using the well-known "Iowa Formula", (Spangler, 1962; FHWA, 1970). For rigid culverts bedded within an earth fill, the Marston approach assumes that the total load applied to the horizontal projection of a conduit is equal to the weight of the fill above the conduit, modified by a factor

which purports to account for the relative displacement of the prism of soil above the conduit with respect to the surrounding soil. For design purposes, Spangler (1962) recommends that this factor be equal to or greater than unity, depending upon the foundation condition. The rigid culvert is designed to resist this uniform vertical load in addition to those transmitted by external dead and live loads. But in determining the lateral pressure, which assists in supporting the culvert, no account is taken of the stresses in the soil surrounding the pipe. For flexible culverts, the design is based on limiting the change in vertical diameter of the pipe, as well as providing adequate resistance against critical buckling of the pipe wall, or failure of the longitudinal (riveted, welded or bolted) seams (White and Layer, 1960; Spangler, 1962; FHWA, 1970). The lateral resistance offered by the soil is characterized by a so-called modulus of soil reaction (E'), which is defined (Spangler, 1962) as the ratio of the lateral stress to the displacement at the spring line of the pipe, times the pipe radius. Values of E' are recommended based on field experience and model tests.

The semi-empirical nature of present design methods, especially in evaluating the soil-structure interaction, renders them difficult to extrapolate to situations other than those which have been considered in the past. This feature is of particular importance in view of the recent trend toward high fills (Davis and Bacher, 1968), and large

diameter culverts under shallow fills. Extrapolation becomes even more difficult when new materials such as plastics and composites are introduced.

The main purpose of this study is to develop an analytical design tool which can be used to simulate actual conditions realistically, and to predict the performance of culverts embedded in soil under different construction and loading situations. All efforts have been directed towards representative simulation of pipe, soil, and soil-pipe interaction. For this purpose the technique of finite element analysis was chosen. Flexible pipes were simulated by segments of a curved bar. Isoparametric triangular elements with stress dependent, nonlinear soil properties were used to represent the soil medium. A special type of interaction element was introduced between soil and pipe which permits slip to occur between soil and pipe at shear stresses less than the strength of the soil. Incremental analysis to simulate construction in steps has been accommodated.

A finite element computer program has been written which incorporates all the factors mentioned above. This program has been used in a few example problems to show its capability for the purpose of predicting culvert performance in practical situations. Examples were selected to show the effects of various soil parameters and different types of loadings.

The finite element technique developed in this study was used to investigate non-linear vs. linear soil properties, the effects of construction in layers, inclusion of stiffer or softer material at different locations on the pipe, slip between pipe and soil and various combinations of superimposed loadings. It is believed that the significant aspects of culvert behavior have been realistically represented and that it should be possible to predict performance under a wide variety of field conditions. Comparison of such predictions with measured performance (from controlled laboratory tests and field installations) are needed to establish the practical utility of the newly developed method to predict actual field performance.

CHAPTER II

LITERATURE REVIEW

2.1 Current Design Practice

In this section current design approaches of different types of culverts are reviewed with emphasis on the assumptions made and their validity.

Concrete Culverts: (Rigid culverts) - California Culvert Practice (1944) mentions the importance of differential settlement between the pipe and surrounding soil and its effect on the loads carried by the culvert. For a rigid culvert on unyielding foundation, the earth alongside the culvert moves downwards relative to the material in the prism over the culvert. This causes load to be transferred to the prism over the culvert which will result in an excess load over the culvert. When the culvert settles or deflects an amount equal to the settlement of the surrounding material, the load on culvert will be the same as the weight of the prism of material directly above it. This mechanistic picture of behavior is very realistic but the amount of relative settlement and their effects must be evaluated by qualitative judgment. Once this is done certain specific design approaches are available. For example, Spangler, (1960)

presents a formulation for determining vertical loads for unyielding culverts, which he named 'projecting' culverts. Townsend (1963) presented design charts for estimating loads on pipes for various projecting conditions. His specifications estimating loads of ASTM standard (ASTM, C76-59T) pipes are based mainly on Marston's formula, and his charts merely transform Marston's formula into graphical form.

Marston Theory - Marston's theory is often used to determine vertical loads on flexible or rigid culverts. The mechanism and assumptions of this theory is illustrated in Figure (2.1), in which

P = External vertical load

V = Vertical force on a horizontal plane

dV = Increment of vertical force

B_c = External diameter of pipe

B_d = Horizontal width of ditch

H = Height of fill on top of pipe

h = Variable distance from top of soil

dh = Increment of h

K = Coefficient of active earth pressure

$\mu' = \tan \phi' =$ Coefficient of friction between fill material and side of ditch

γ = Unit weight of fill.

For equilibrium of vertical forces in the element of thickness dh , the following equation can be written per unit length of pipe (assuming $P=0$):

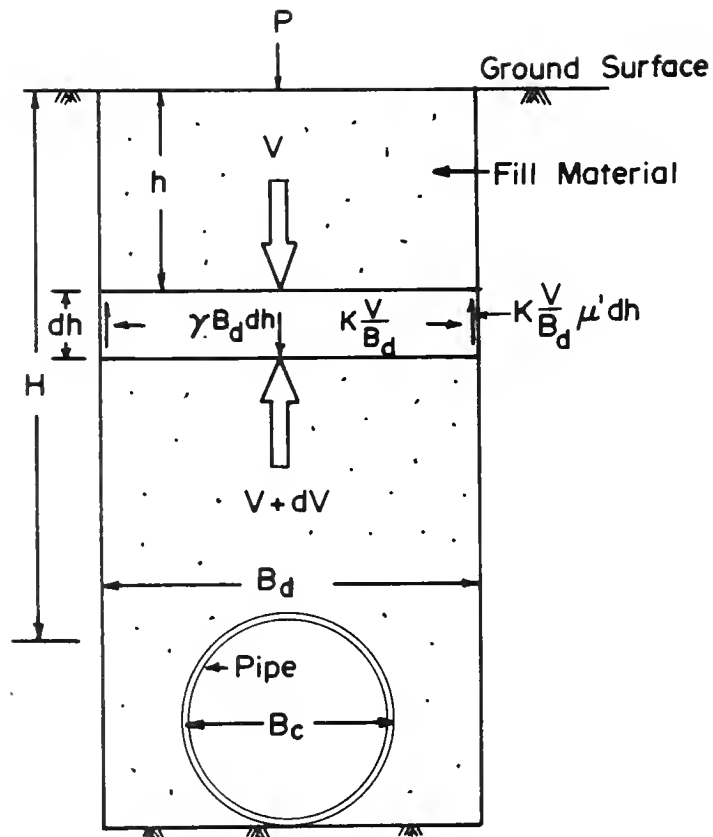


FIGURE 2.1 FREE BODY DIAGRAM FOR DITCH CONDUIT. (After Spangler, 1960)

$$V + dV + 2K\mu' \frac{V}{B_d} dh = V + \gamma B_d dh \quad (2.1)$$

Solving for V,

$$V = \gamma B_d^2 \frac{1 - e^{-2K\mu' \left(\frac{h}{B_d}\right)}}{2K\mu'} = C_d \gamma B_d^2 \quad (2.2)$$

On substitution of $h = H$, total vertical load on the pipe can be evaluated. According to Marston theory equation (2.2) represents the total vertical load on pipe for rigid culverts with relatively compressible side fills. For flexible culvert, with thoroughly compacted side fills which have essentially the same degree of stiffness as the pipe, V is modified as:

$$V = C_d \gamma B_c B_d \quad (2.3)$$

Spangler (1963) points out that in actual cases V will lie between the values given by equations (2.2) and (2.3). This formulation is logical, but leaves some questions unanswered.

(1) For how wide a ditch are the formulas applicable? Spangler (1963) presented charts for C_d values for $\frac{H}{B_d}$ values ranging up to 15, which shows values of C_d increases for $\frac{H}{B_d}$ up to about 8. He mentioned the width of the ditch as "relatively narrow" and he did not present any criteria for establishing limiting values of B_d .

(2) Is it proper to consider active earth pressure condition with the wall of trench without knowing the deflection?

(3) What will be the changes in the load on pipe for different specifications for degree of compaction of fill surrounding the pipe?

(4) Will there be any difference in load if there is slip between pipe and soil?

(5) Will the load P be distributed to the pipe according to the Boussinesq solution, as proposed by Marston?

These and other factors were accounted for by Spangler (1963) by defining specific restraint conditions (positive projection, negative projection, imperfect ditch, settlement ratio) and preparing design charts based on model tests and field experiences.

After the load on the pipe has been computed, selection of pipe is based on either of two criteria, (i) 0.01 inch crack strength, or (ii) ultimate pipe strength divided by an appropriate value of Factor of Safety. Recommended values of Factor of Safety are 1.5 for the first criteria and 1.33 for the second. Pipe strengths are determined by conventional three-edge-bearing tests.

Concrete pipe culverts do not collapse when cracking is initiated, and as further cracking develops the rigidity of the pipe changes sufficiently to redistribute the soil pressures on the pipe. Important research to predict performance of cracked concrete pipe is underway at Northwestern University, (Krizek et. al. (1971)).

Flexible Culverts - Wolf and Townsend (1970) proposed that the following criteria should guide the design of flexible culverts.

- (1) deflection or flattening of pipe
- (2) buckling of pipe wall
- (3) longitudinal seam strength
- (4) handling and installation strength.

Deflection criterion - Change in nominal pipe diameter for flexible culverts can be determined using the "Iowa Formula" (Spangler, 1960):

$$\Delta x = \frac{D_L K W_C R^3}{EI + 0.061 R^3 E'} \quad (2.4)$$

where

Δx = horizontal deflection of pipe in inches,
assumed equal to vertical deflection

D_L = deflection lag factor, (1.25 for $E' = 1400$ psi
or more 1.5 for $E' = 700$ psi)

R = radius of pipe in inches

K = bedding constant, depending on the bedding angle
 α (0.11 for $\alpha = 0$ to 0.083 for $\alpha = 90^\circ$)

W_C = vertical load on pipe as predicted by Marston
theory

E & I = Young's modulus and moment of inertia of the
pipe

E' = modulus of "soil reaction", in pounds
per square inch

This formula has been derived based on the theory of curved beams and arches on elastic foundation and assumes a parabolic distribution of horizontal stresses at side of pipe. The Iowa Formula is based on an assumed distribution of load around pipe, and parameters D_L , K and E' are empirically derived. Parmelee and Corotis (1972) took a closer look into the assumptions and validity of Iowa Formula. They studied data from 18 tests and conducted statistical analysis of the three important parameters D_L , K and E' . They concluded that there is no rational basis for assigning any value for E' which is greater than the modulus value (E) of the medium. They also pointed out that extreme caution should be exercised in choosing values for the parameters in the Iowa Formula, including values of W_c .

The deflection criterion arbitrarily specifies failure at 5 percent deflection of nominal pipe diameter. Experiments suggest that a 20 percent change in vertical diameter is necessary to develop plastic hinges in corrugated metal pipes, provided local buckling does not occur. In such cases, the deflection criterion has a nominal Factor of Safety of 4.

Buckling criterion - This criterion provides for the design of pipe based on the wall thickness required for a limiting buckling stress which takes into account the restraining effect of soil-structure interaction around pipe. This restraining effect is solely due to confinement of the

pipe in soil. If the pipe cross-section is considered as ring, then the ring compression becomes critical for buckling when, [Wolf and Townsend (1970).]

$$F_b \geq f_u - \frac{f_u^2}{48E} \left(\frac{k d}{r} \right)^2 \quad (2.5)$$

for diameter less than $\frac{r}{k} \sqrt{\frac{24E}{f_u}}$

where

F_b = buckling stress, psi

f_u = minimum tensile strength, psi

k = soil stiffness coefficient (0.22 for $E' = 1400$ psi or above and 0.44 when $E' = 700$ psi.)

d = nominal diameter of pipe, inch

r = radius of gyration of pipe wall, inch.

E = Young's modulus of pipe material, psi

Design for buckling is accomplished by limiting the ring compression thrust to the buckling stress multiplied by the conduit wall area, divided by Factor of Safety.

Longitudinal seam strength and handling stresses are not considered in this study, although their relevancy to the total problem is recognized. It might be mentioned, however, that yielding (as opposed to rupture) of a seam is often beneficial as it is equivalent to an increase in pipe flexibility without necessarily reducing the buckling resistance.

It is seen that the Iowa Formula assumes both soil and pipe as linear, elastic and homogeneous materials during

the entire loading range, hence values of W_c , D_L , K and E' are difficult to establish for wide ranges in design conditions. Several manuals provide numerical values of these parameters based mostly on past experience. Culvert design methods suggested by pipe manufacturers (e.g., Republic Steel, ARMCO) follow simplified procedures as follows:

- (1) Dead load - the total weight of the prism of soil directly above the pipe.
- (2) Live load - specified by empirically derived charts.
- (3) Ring thrust - vertical pressure multiplied by the pipe radius.

From the value of ring thrust the required sectional properties of pipe are chosen. None of these manuals attempt to evaluate soil-structure interaction, nonlinear soil properties, or installation sequence, but most mention the importance of compacting the backfill materials close to pipe wall.

2.2 Literature Review

Krizek and Parmelee (1968) prepared an extensive bibliography on analysis, design and installation of highway culverts, which covers publications from year 1900 to 1968. A review of selected recent studies follows.

Davis (1966) reported results of a field study of a large reinforced concrete arch culvert buried under an embankment 200 feet high in natural soil. This report concluded that

- (1) stresses at any depth are proportional to the fill height
- (2) soil stresses remain essentially constant after the fill is completed
- (3) side walls of arch moved inwards while the crown moved upwards during back filling
- (4) a layer of organic material around the pipe reduced vertical pressure to about half of that expected
- (5) distribution of soil pressure around culvert was vastly different from the values predicted from a model prepared by Brown (1967).

Brown, Green and Pawsey (1968) conducted tests on culverts under high fill with soft inclusions (straw) at different locations around pipe, which showed significant difference in stress distribution around pipe. Theoretical results using incremental finite element analysis did not predict the nature of the experimental results.

Watkins and Moser (1971) presented simple design criteria for flexible pipes based on test data from a number of field and laboratory studies. They assumed a section of a pipe as a ring and related the ring compression strength, f_c with the applied stress by the simple formula.

$$\frac{PD}{2A} = \frac{f_c}{N} \quad (2.6)$$

where

P = vertical soil pressure determined by adding
pressure on pipe due to weight of prism of soil
and that produced by any imposed live load.

D = nominal diameter of pipe

A = cross-sectional area of pipe

N = Factor of Safety

Equation (2.6) states that for limiting equilibrium, applied stress is equal to the strength of pipe divided by adequate Factor of Safety. Based on this, and the results of laboratory tests, the authors presented a design chart, which includes the effect of degree of compaction of the surrounding soil. This procedure does not take into account soil-structure interaction due to arching and terminal shear between pipe and soil. Spangler (1971) points out that the model proposed by Watkins and Moser (1971) ignores the moments developed in the pipe which, when neglected, is not representative of pipe behavior. Spangler (1971) concluded that the similarity between the field test results and equation (2.6) is coincidental. However, Neilson (1972) pointed out that the test results by Watkins and Moser (1971) have good agreement with the results given by elastic theory using constrained soil modulus values, and proposed that agreement of laboratory and field results by Watkins and Moser (1971) may be due to same degree of confinement in both cases.

Allgood and Takahashi (1972) have shown the similarity between Iowa Formula and the solution for an elastic ring in an elastic medium, and presented a semi-empirical procedure for culvert design whose principal advantages are:

- (1) Arching of soil can be considered
- (2) Effects of backpacking can be considered
- (3) Moment in pipe can be taken into account
- (4) Several modes of failure are taken into account.

This procedure assumes both soil and pipe as linearly elastic material and ignores potential slip at the soil-structure interface.

Allgood and Takahashi (1972) also presented results of three dimensional finite element analysis of culvert problems. Changes in elastic modulus were considered by specifying values at different depths. Poisson's ratio was kept unchanged at a given value. Possibility of slip between pipe and soil, non-linear soil properties, sequence of construction, and variations in state of compaction around pipe were neglected. As a result, the authors acknowledged that large differences can be expected between their predictions and field performance.

Kirkland and Walker (1972) performed model studies of culverts on 6 inch diameter steel pipes with different wall thickness so as to consider both rigid and flexible culverts. Soil properties were modeled in two ways: (1) use of bulk and shear modulus updated for state of volumetric and shear

strains, (2) by fitting second degree curves for bulk and shear modulus. Behavior for soil-structure interaction was simulated by two curves, one for initial near-straight line portion and the second for the portion where the curve begins to flatten. Comparison of predicted and experimental results always show significant deviation. This may be attributed to the following sources of error (1) assumption of isotropic behavior of soil, (2) linear displacement function for finite elements, (3) homogeneous soil properties. The authors indicated the need for more research on the effects of slip at the soil-pipe interface.

Howard and Metzger (1973), Howard (1973) conducted a large number of laboratory and field tests on a variety of pipes which includes soil, fiberglass, reinforced resin and reinforced plastic mortar for pipe materials. Results show significant effects of various types of bedding and compaction around pipe. For well compacted backfills, pipes of all variety of materials show similar response. But for poorly compacted backfills, the results vary over a wide range. The spread of results can be attributed to the variation of friction between soil and different pipe materials, which has significant effects for relatively low soil density. It also shows that behavior of pipes with reinforced laminates significantly differs from that of steel pipes. These aspects need further study. Davis, Bacher and Obermüller (1974) conducted field tests of an under-designed reinforced

concrete pipe culvert of large diameter (84") in a high embankment (136 ft). Main purpose of this study was to investigate the structural behavior of several methods of backfilling and bedding. It was found that with proper attention to bedding and backfilling procedures, in particular, providing adequate lateral support by placing the pipe in a trench and surrounding it by a well-compacted high quality structural backfill, culverts of much lesser thickness than normal can be used satisfactorily. In a related paper, Davis and Bacher (1974) concluded that for embankments of appreciable height, earth pressure loads are of far more consequence than any external live loads. The authors expressed their concern over the design and backfill procedures specified by California Division of Highways Specifications. They indicated a need for future research in the following areas:

- (1) Soil-pipe interface around pipe
- (2) Different types and thickness of bedding
- (3) Use of a layer of polystyrene surrounding the pipe to reduce friction
- (4) Revision of current tables and design charts.

Dar and Bates (1974) presented a method for analysis of culvert problems based on theory of elasticity for ideal linear elastic, isotropic and homogeneous soil and pipe properties. Their derivation treats the pipe as a circular elastic material and the medium as an elastic plate with a circular hole. Stresses in the pipe are determined from a

harmonic displacement function and the stresses in the medium is determined from traction stresses around the opening. Matching the stresses and displacements at the boundary between pipe and soil, and permitting no slip at the boundary, a solution to the problem is obtained. Experimental results for concrete pipes were compared with those predicted by the formula. Results show that the method provides an upper bound for radial stresses in thin pipes, and a lower bound for thick pipes. This distinct difference in behavior may be due to the interface conditions and simplifying assumptions used in the analysis. The approach is of value in estimating upper and lower bounds in the pipe stresses but more comparisons with field measurements are needed.

A long-range research project concerning soil-structure interaction of concrete culverts is underway at Northwestern University, Evanston, Illinois. This research program consists of two parts, (i) a series of full scale field installation of concrete culverts including instrumentation, (ii) development of finite element program to predict behavior. Nonlinear properties for both soil and pipe have been considered. Cracking of concrete pipes will be modelled in this research program. Parmelee (1973) mentioned that decisions about the soil-structure interface will be made after developing considerable data about their interaction through a series of laboratory and field tests.

2.3 Need for Further Research

Both flexible and rigid culverts are commonly in use. Their size varies from several inches to tens of feet (Fisher, 1969). Shapes vary over a wide range which includes circular, elliptical, bullet-shape, arch, and combinations of different shapes. Depth of cover vary from several feet to several hundred feet. Methods of construction include trenching, bedding, backfilling and compaction. Different backfill materials, ranging from loose straw to foamed plastics are used around the pipe to change stress distribution patterns. The soil medium varies from coarse granular material to plastic clay. Materials used for the pipe include reinforced concrete, prestressed concrete, plate steel, corrugated steel, aluminum, clay tile, reinforced plastic, etc. Superimposed loads may vary over a wide range. Thus, the number of variables encountered in a real culvert problems is enormous, and can only increase in the future. This imposes severe restrictions on approaches that rely on empirically derived parameters and simplified design procedures.

It is proposed in this study to develop an analytical tool which will permit a realistic study of culvert problems with a minimum number of restrictive, simplifying assumptions. This tool is intended to be capable of handling generalized soil properties, soil-culvert interaction including slip at the interface, and any combination of construction conditions and superposed loadings.

CHAPTER III

FINITE ELEMENT METHOD

3.1 Historical Background.

The finite element method of analysis is a well-known tool in many branches of engineering science and technology. Many complex problems can be solved satisfactorily by the use of this method.

The concept of Ritz (Ritz, 1909) and Raleigh's (Strutt, 1870) method of variational analysis has been in existence for long time. In the Rayleigh-Ritz method, the expression for total potential energy of a system is formulated and the displacement pattern is assumed to vary with a finite number of undetermined parameters. A set of simultaneous equations are formulated minimizing the total potential energy with respect to the displacement parameters. So far both the finite element and Rayleigh-Ritz methods are identical. In the Ritz procedure, the displacement pattern is specified in the whole region, whereas in the finite element method the displacements (or loads) are specified at nodal points of discrete elements.

The organized matrix approach to structural analysis based upon the finite element idealization was prescribed clearly by Turner, et. al. (1956) in their pioneering paper.

In this paper important concepts of compatibility at the boundary between two elements in terms of nodal displacements, nodal equilibrium, and determination of stiffness influence coefficients were presented in step by step development. The main criteria of variational methods in linear static structural mechanics is the principle of minimum potential energy (Washizu, 1968), which provides a basis for the direct formulation of element stiffness equations. The paper by Turner, et. al. did not make reference to variational considerations, rather, it took a "direct" approach, in which direct consideration was given to conditions of equilibrium and compatibility. Consequently, the paper stimulated numerous efforts to develop formulations for stiffness influence coefficients for a variety of different types of elements (Turner, 1959; Clough, 1960; Melosh, 1961; Melosh, 1963; Clough and Tocher, 1965).

In the last decade, research in finite element methods were directed mainly to new techniques of analysis for complex structures with nonlinear material properties, heat-flow and seepage (with moving boundaries), large displacements, etc. (Mallett and Marcal, 1968; Przemieniecki, 1968; Zienkiewicz, 1971; Desai and Abel, 1972). The method has been extended to deal with three-dimensional geometries using sub and superparametric elements, curvilinear elements, and account has been taken of inertia effects.

3.2 Requirements for Finite Element Methods

As discussed in Chapter II, the behavioral aspects of culverts can be analyzed with confidence provided each component of the structure such as soil, pipe, and soil-structure interface can be modeled realistically using a minimum number of restrictive assumptions. To achieve this, the first step is to idealize all components of the problem by an appropriate geometric shape. A good choice of element shape should consider the following factors.

- (1) The elements can be assembled to form the complete structure with correct shapes at the boundaries.
- (2) The element should have a sufficient number of degrees of freedom to simulate the actual structural response.
- (3) The element should not be ill-conditioned, i.e., convergence is too slow or is prevented.

Once the element shape is chosen, the next step is to choose the displacement function (also known as shape function). Careful consideration of the following factors are essential for the choice of shape function.

- (1) The displacement function should ensure minimum potential energy.
- (2) Continuity is maintained at the boundary between adjacent elements.
- (3) Straining of an element due to rigid body motion is precluded.
- (4) Criteria for convergence to the true solution should be met, which are as follows:

(a) The displacement function must be continuous within the element and compatible between adjacent elements.

(b) The function includes rigid body displacement of the element.

(c) The function reduces an element to a state of uniform strain when the element approaches a very small size.

Once the shape and displacement function of an element is chosen, the next important decision is the choice of material properties. The most attractive feature of the finite element method is the versatile way of considering the material properties. Theoretically each element can be assigned different properties, which can be changed in each step of analysis. This possibility enables one to analyze complex cases, like different material properties at different portions of a structure, nonlinear, and anisotropic materials, and limiting values for certain element properties, which permits accounting for slip or limiting the magnitude of tensile resistance between two elements.

The last and final step in the sequence of analysis deals with techniques for numerical analysis. Basic requirements for success and efficiency of a finite element analysis depends heavily on the solution scheme. Solution of a real problem involves a vast number of mathematical and numerical operations, which can only be dealt with by the use of high speed digital computers. Hence, a good knowledge of computer language, mechanism and peripheral systems of computers,

numerical techniques, data storage and data structures are essential. A few general requirements for efficient solution are stated below.

- (1) Total number of numerical operations should be minimized.
- (2) Repetitions of calculations should be avoided or minimized.
- (3) Use of core-memory storage spaces should be as low as possible.
- (4) Input data should be easy to prepare and store. The output should be easy to interpret.
- (5) Scheme for solution of stiffness-influence matrix should be efficient.
- (6) Ill-conditions and "blow-ups" should be avoided.
- (7) Solution should be performed at the minimum possible cost.

3.3 Selection of Finite Elements to Represent the Soil.

Figure 3.1 shows a section through a culvert buried in soil. The components, which are believed to affect the system's behavior are labeled. These are (1) the pipe, (2) soil-structure boundary materials, (3) bedding, (4) surrounding zones of select materials having prescribed states of compaction, (5) the earth fill, and (6) externally applied loads. To analyze a real problem all of the above mentioned components require appropriate consideration.

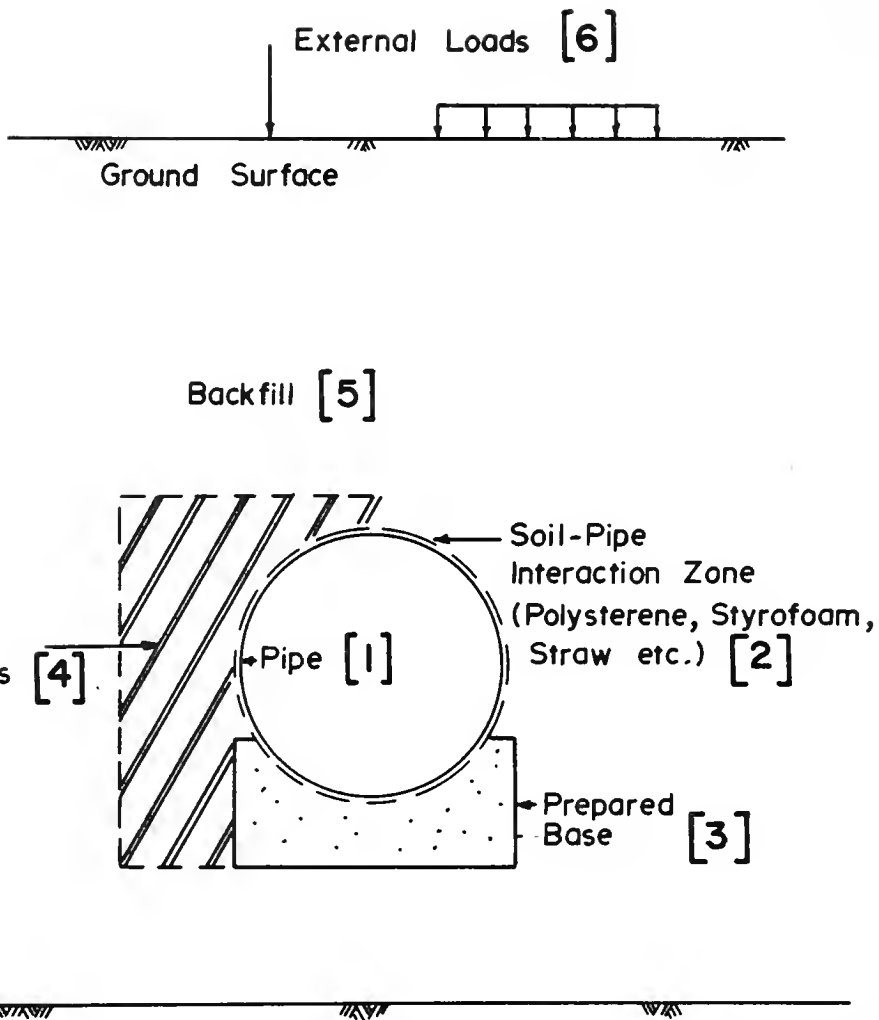


FIGURE 3.1 TYPICAL SECTION OF PIPE CULVERT.

In addition, culvert problems are three-dimensional in nature; in many cases, differential displacements in the longitudinal direction have adverse effects on performance. However, in this study, emphasis is placed on better representation of soil materials and on the soil-pipe interaction. Accordingly, a two-dimensional finite element analysis was chosen to represent the structure.

Triangular shaped elements were chosen to represent the soil. As culverts usually have a curvilinear shape (often circular) triangular elements with one curved boundary were selected (Figure 3.2). The element has a total of six nodes, three corner nodes and three intermediate nodes at the midpoints of each side. The reason for taking three intermediate nodes is given in next section. To avoid tendencies towards instability of solution, any one side of the triangle should not be too large compared to other sides, i.e., the element should not be a 'flat' triangle.

3.4 Selection of Displacement Function.

In the finite element method it is not necessary that the geometry and displacements of an element be expressed by the same ordered model. Accordingly there can be three distinct combinations between the order of displacement function and order of geometry. (1) Subparametric, where geometry is determined by a lower order model than displacement, (2) Superparametric, in which the reverse is true, and (3) Isoparametric, where the geometry and displacements

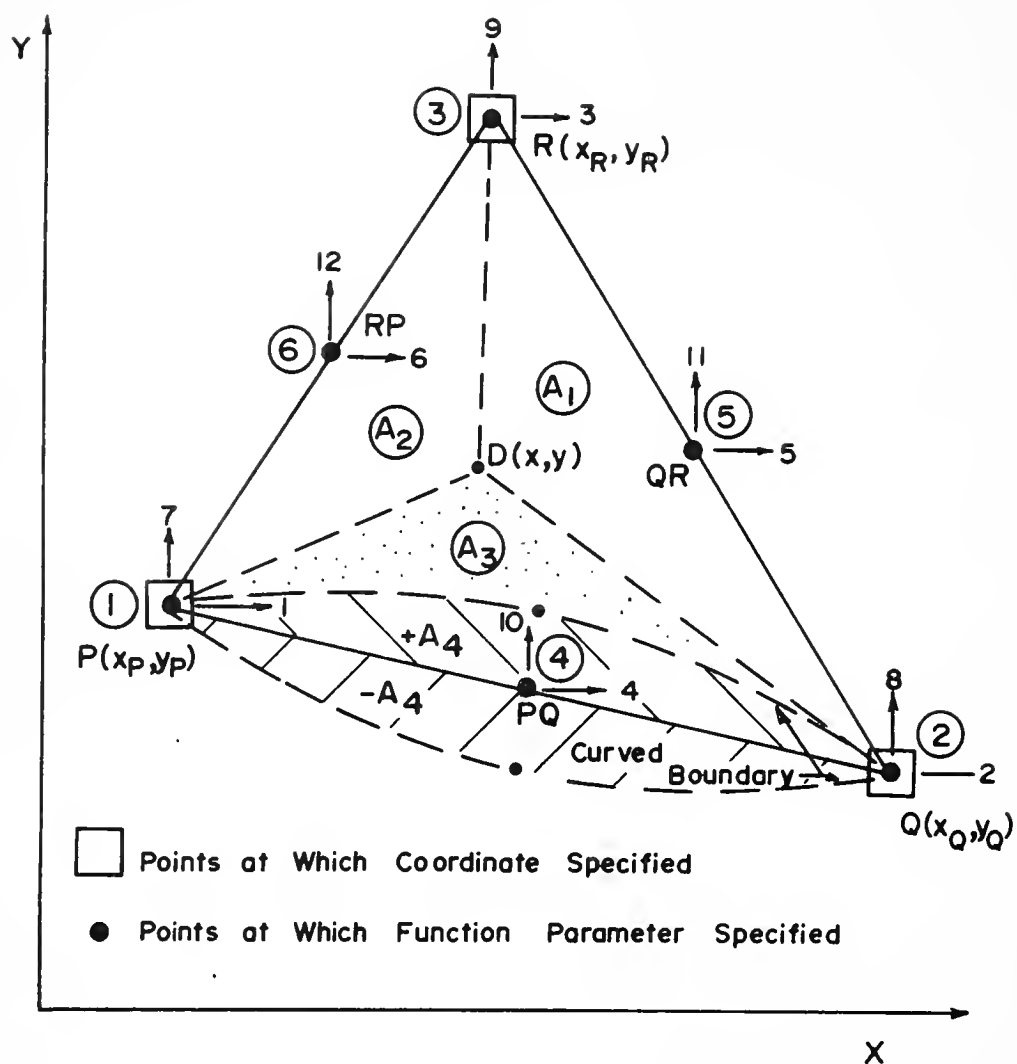


FIGURE 3.2 TRIANGULAR ISOPARAMETRIC ELEMENT.

are defined by the same order model. Zienkiewicz, et. al. (1969), summarized the Isoparametric finite element concept, a powerful generalized tool for formulating complete and conforming elements with models of any polynomial order. Also, Felippa (1966), presented a rigorous treatment of the systematic development of refined two-dimensional elements for plane stress, plane strain, and plate bending. The advantages of isoparametric elements will be discussed later.

Before selecting the order of the displacement function, one should investigate the type of results required from the analysis. In the culvert problem, stresses in the immediate vicinity of the pipe are very important factors controlling performance. Also, soil properties depend strongly on the state of stress so that regions of high stress gradients must be carefully delineated. Hence, accurate determination of stresses anywhere within an element (including its boundaries) is required in this study. Accordingly, a quadratic displacement function was selected, which ensures a linear variation of strain (and hence stress) across the element.

Before treating the derivation of element stiffness coefficients, three additional factors had to be discussed.

- (1) The natural coordinate system
- (2) Primary and secondary nodes and
- (3) Interpolation displacement function.

The natural coordinate system, or "area coordinates", is a local system defined for a particular element which permits the specification of a point within the element by a set of dimensionless numbers whose magnitude never exceeds unity. This system is general and easy to use, and integration of element stiffness coefficients is greatly simplified. In Figure 3.2, $D(x,y)$ is any floating point within the element (or at its boundary). In the natural coordinate system $D(\xi_1, \xi_2, \xi_3)$, ξ_1, ξ_2, ξ_3 are natural coordinates, which are defined as

$$\xi_1 = \frac{A_1}{A^*} ; \xi_2 = \frac{A_2}{A^*} , \xi_3 = \frac{A_3}{A^*} \quad (3.1)$$

in which A^* is total area of the curvilinear triangle PQR, and A_1 is the area of sub-triangle DQR, and so on. The relation between the Cartesian coordinate system and the natural coordinate system can be determined as follows: (for convenience nodal points are designated by numbers given below)

$$P = 1, Q = 2, R = 3, PQ = 4, QR = 5, RP = 6.$$

$$x = \xi_1 x_1 + \xi_2 x_2 + \xi_3 x_3$$

$$y = \xi_1 y_1 + \xi_2 y_2 + \xi_3 y_3 \quad (3.2)$$

$$1 - 2\eta = \xi_1 + \xi_2 + \xi_3$$

in which

$$2\eta = \frac{A_4}{A^*}$$

and

$$A^* = A_1 + A_2 + A_3 + A_4$$

Solving (3.2), ξ_1, ξ_2, ξ_3 can be determined in terms of (x_i, y_i) , $i = 1, 2, 3$ and $D(x, y)$, which can be expressed in a general form

$$\xi_i = (a_i + b_i x + c_i y) / 2A^*, \quad i = 1, 2, 3, \dots \quad (3.2-a)$$

where a_i, b_i and c_i are constants. In terms of area coordinates

$$\text{Node } 1 = (1 - 2\eta, 0, 0)$$

$$\text{Node } 2 = (0, 1 - 2\eta, 0)$$

$$\text{Node } 3 = (0, 0, 1 - 2\eta)$$

$$\text{Node } 4 = \left(\frac{1}{2} - \eta, \frac{1}{2} - \eta, 0\right)$$

$$\text{Node } 5 = \left(0, \frac{1}{2}, \frac{1}{2} - 2\eta\right)$$

$$\text{Node } 6 = \left(\frac{1}{2}, 0, \frac{1}{2} - 2\eta\right)$$

Primary (external) nodes are corner nodes like P, Q, R. Secondary (internal) nodes are intermediate midpoint nodes like PQ, QR and RP.

By definition an interpolation function is a function which has unit value at one nodal point and zero values at all other nodes. The interpolation functions are polynomials. The order of polynomial is selected to satisfy the requirement of the displacement function. Let F_1 define the interpolation displacement function for the primary node 1. According to the requirement at node 1, $F_1 = 1$ and $F_1 = 0$ at all other nodes.

Let $F_1 = \xi_1 (A\xi_1 + B)$ be a quadratic function; where A and B are constants to be evaluated.

At node 1, $\xi_1 = 1 - 2\eta$, $F_1 = 1$

$$F_1 \text{ at } 1 = \xi_1 (A(1 - 2\eta) + B) = 1 \quad (3.3)$$

At node 4 $\xi_1 = \frac{1 - 2\eta}{2}$, $F_1 = 0$

$$F_1 \text{ at } 4 = \xi_1 (A (\frac{1 - 2\eta}{2}) + B) = 0 \quad (3.4)$$

Solving for A and B from (3.3) and (3.4)

$$A = \frac{2}{1 - 2\eta}$$

$$B = -1$$

So,

$$F_1 = \xi_1 (\frac{2}{1 - 2\eta} \xi_1 - 1) \quad (3.5)$$

For a secondary node say, node 4, $F_4 = 1$ at node 4 and $F_4 = 0$ at all other nodes. By inspection, it is seen $\xi_1 = 0$ at nodes 2, 3, 5 and $\xi_2 = 0$ at nodes 1, 3, 6.

Hence, $\xi_1 \cdot \xi_2 = 0$ at nodes 1, 2, 3, 5, 6

Let $F_4 = B\xi_1\xi_2$, where B is a constant to be determined.

At node 4, $\xi_1 = \frac{1}{2} - \eta$, $\xi_2 = \frac{1}{2} - \eta$, $F_4 = 1$.

$$\therefore F_4 = B(\frac{1}{2} - \eta)(\frac{1}{2} - \eta) = 1$$

$$\text{Solving, } B = \frac{4}{(1 - 2\eta)^2}$$

So,

$$F_4 = \frac{4}{(1 - 2\eta)^2} \xi_1 \xi_2 \quad (3.6)$$

Following similar procedure for all other nodes, the interpolation functions can be developed and are summarized below:

$$\begin{aligned}
F_1 &= \xi_1 \left(\frac{2}{1-2\eta} \xi_1 - 1 \right) \\
F_2 &= \xi_2 \left(\frac{2}{1-4\eta} \xi_2 - \frac{1}{1-4\eta} \right) \\
F_3 &= \xi_3 (2\xi_3 - 1 + 4\eta) \\
F_4 &= \frac{4}{(1-2\eta)^2} \xi_1 \xi_2 \\
F_5 &= \frac{4}{(1-4\eta)} \xi_2 \xi_3 \\
F_6 &= \frac{4}{(1-4\eta)} \xi_3 \xi_1
\end{aligned} \tag{3.7}$$

In matrix notation,

$$F = \{F_1 \quad F_2 \quad F_3 \quad F_4 \quad F_5 \quad F_6\} \tag{3.8}$$

F defines the displacement functions which is quadratic in nature, normalized with respect to the area ratio and dependent only on the global coordinate system.

3.5 Derivation of Element Stiffness Matrix for Linear Strain Triangular Finite Element

Given the displacement functions and nodal displacements in both x and y directions at all nodes, the general expression for displacement of point D in Figure 3.2 can be written as follows:

$$\begin{aligned}
u &= \sum_{i=1}^6 u_i F_i \\
v &= \sum_{i=1}^6 v_i F_i
\end{aligned} \tag{3.9}$$

where u and v are displacements in x and y directions respectively and F_i are defined in (3.7).

In matrix form (3.9) can be written:

$$f = \begin{Bmatrix} u \\ v \end{Bmatrix} = \begin{bmatrix} F & 0 \\ 0 & F \end{bmatrix} \cdot \begin{Bmatrix} u \\ v \end{Bmatrix} \quad (3.10)$$

in which F as defined in (3.8) and

$$u^T = \{u_1 \quad u_2 \quad u_3 \quad u_4 \quad u_5 \quad u_6\}$$

$$v^T = \{v_1 \quad v_2 \quad v_3 \quad v_4 \quad v_5 \quad v_6\}$$

are the nodal displacement vectors.

To determine element strains the partial derivative of equation (3.10) is taken with respect to x and y . If the vector \tilde{e} defines strain components, then it can be written as:

$$\tilde{e} = \begin{Bmatrix} e_x \\ e_y \\ e_{xy} \end{Bmatrix} = \begin{Bmatrix} \frac{\delta u}{\delta x} \\ \frac{\delta v}{\delta y} \\ \frac{\delta u}{\delta y} + \frac{\delta v}{\delta x} \end{Bmatrix} = \begin{Bmatrix} \tilde{f}_x u \\ \tilde{f}_y v \\ \tilde{f}_y u + \tilde{f}_x v \end{Bmatrix} \quad (3.11)$$

in which

$$\tilde{f}_x = \frac{\delta F}{\delta x} = \frac{\delta F}{\delta \xi_1} \frac{\delta \xi_1}{\delta x} + \frac{\delta F}{\delta \xi_2} \frac{\delta \xi_2}{\delta x} + \frac{\delta F}{\delta \xi_3} \frac{\delta \xi_3}{\delta x}$$

$$\tilde{f}_y = \frac{\delta F}{\delta y} = \frac{\delta F}{\delta \xi_1} \frac{\delta \xi_1}{\delta y} + \frac{\delta F}{\delta \xi_2} \frac{\delta \xi_2}{\delta y} + \frac{\delta F}{\delta \xi_3} \frac{\delta \xi_3}{\delta y}$$

Taking derivatives of equations (3.2) and (3.7) and multiplying appropriate coefficients, \tilde{f}_x and \tilde{f}_y can be

determined and the expression for strains can be written as:

$$\underline{\underline{e}} = \frac{1}{2A^*} \begin{bmatrix} B_1 & 0 \\ 0 & B_2 \\ B_2 & B_1 \end{bmatrix} \cdot \begin{bmatrix} \psi & 0 \\ \sim & \\ 0 & \psi \end{bmatrix} \cdot \begin{Bmatrix} u \\ v \end{Bmatrix} \quad (3.12)$$

in which

$$B_1 = \left(\frac{\delta \xi_1}{\delta x} \quad \frac{\delta \xi_2}{\delta x} \quad \frac{\delta \xi_3}{\delta x} \right)$$

$$B_2 = \left(\frac{\delta \xi_1}{\delta y} \quad \frac{\delta \xi_2}{\delta y} \quad \frac{\delta \xi_3}{\delta y} \right)$$

and

$$\underline{\underline{\psi}} = \begin{Bmatrix} \frac{\delta F}{\delta \xi_1} \\ \frac{\delta F}{\delta \xi_2} \\ \frac{\delta F}{\delta \xi_3} \end{Bmatrix}$$

Equation (3.12) can be written in matrix form as:

$$\underline{\underline{e}} = [\underline{\underline{b}}] \cdot \begin{Bmatrix} u \\ v \end{Bmatrix} \quad (3.13)$$

$$\text{where } [\underline{\underline{b}}] = \frac{1}{2A^*} \cdot \begin{bmatrix} B_1 & 0 \\ 0 & B_2 \\ B_2 & B_1 \end{bmatrix} \cdot \begin{bmatrix} \psi & 0 \\ 0 & \psi \end{bmatrix}$$

According to the definition of stiffness matrix, the element stiffness matrix k can be written

$$k = \int \int \int_{\text{vol}} [b]^T \cdot [D] \cdot [b] \cdot d(\text{vol}). \quad (3.14)$$

in which [D] is the elasticity matrix, generated from material properties and type of analysis such as plane strain or plane stress. Detailed discussion about material properties and development of [D] matrix will be presented in a later section.

Equation (3.14) can be expanded as follows:

$$k = \frac{1}{4A^*2} \int \int \int_{\text{vol}} \begin{bmatrix} \psi^T & 0 \\ 0 & \psi^T \end{bmatrix} \cdot \begin{bmatrix} B_1^T & 0 & B_2^T \\ 0 & B_2^T & B_1^T \end{bmatrix} \cdot$$

(1)

(2)

$$\begin{bmatrix} D_{11} & D_{12} & D_{13} \\ D_{21} & D_{22} & D_{23} \\ D_{31} & D_{32} & D_{33} \end{bmatrix} \cdot \begin{bmatrix} B_1 & 0 \\ 0 & B_2 \\ B_2 & B_1 \end{bmatrix} \cdot \begin{bmatrix} \psi & 0 \\ 0 & \psi \end{bmatrix} \cdot d(\text{vol})$$

(3)

(4)

(5)

(3.14a)

Multiplying (2), (3) and (4) yields

$$k = \frac{1}{4A^*2} \int \int \int_{\text{vol}} \begin{bmatrix} \psi^T & 0 \\ 0 & \psi^T \end{bmatrix} \cdot \begin{bmatrix} C_{11} & C_{12} \\ C_{21} & C_{22} \end{bmatrix} \cdot \begin{bmatrix} \psi & 0 \\ 0 & \psi \end{bmatrix} \cdot d(\text{vol})$$

Carrying out the remaining multiplications and for constant thickness of element 't'

$$k = \frac{t}{4A^*2} \int \int_{\text{area}} \begin{bmatrix} \tilde{\psi}^T \cdot C_{11} \cdot \tilde{\psi} & \tilde{\psi}^T \cdot C_{12} \cdot \tilde{\psi} \\ \tilde{\psi}^T \cdot C_{21} \cdot \tilde{\psi} & \tilde{\psi}^T \cdot C_{22} \cdot \tilde{\psi} \end{bmatrix} d(\text{area}) \quad (3.15)$$

The final step in the evaluation of the stiffness matrix is to perform the integration of all coefficients in the matrix over the whole area of the element. Each element of the stiffness matrix is defined in terms of area coordinates. To facilitate integration of these coefficients over the area of element, the following expression is helpful.

$$\int \int_{\text{Area}} \xi_1^a \xi_2^b \xi_3^c dx dy = \frac{a! b! c!}{(a + b + c + 2)!} 2 (\text{area}) \quad (3.16)$$

Details of derivation of element stiffness matrix for isoparametric elements, are given in Appendix A.

3.6 Finite Element Representation for Pipe Culverts

Thorough review of existing literature revealed that in most cases finite elements used to represent pipes are either triangular or rectangular in shape, and these shapes were initially adopted for this study. In the course of internal checks of the general program the validity of this procedure was brought into question in cases where the pipe thickness becomes small. The triangular element (with two degrees of freedom at each node) is incapable of considering rotation at any node, which means that flexure cannot be adequately represented if the triangle has a linear strain

distribution. To examine this problem further, two types of problems were solved. In the first type a ring of uniform thickness having internal radius a , and outer radius b , is acted upon by two line loads 180 degrees apart. In the second problem relatively thick rings are acted upon by an externally applied uniform, all-around pressure. Table 3.1 shows the error in the resulting change in diameter, $\Delta x\%$, and of the change in outer radius, $\Delta b\%$, determined using isoparametric triangular finite elements compared with the results of a formal solution from the theory of elasticity.

Table 3.1 Comparison of Ring Solutions

Line Loads					Uniform Pressure				
a	b	b-a	$\frac{b-a}{a}$	% Error Δx	a	b	b-a	$\frac{b-a}{a}$	% Error Δb
5"	6"	1"	0.2	2.2	4"	6"	2"	0.5	2.5
10"	11"	1"	0.1	40.0	10"	14"	4"	0.4	5.0
10.5"	11.5"	1"	0.095	60.0	5"	6"	1"	0.2	11.0

From Table 3.1 it is seen that as the ratio of thickness over internal radius decreases, the error increases, with the effect being far more pronounced for the line load than for the uniform pressure, which clearly indicated the need for further investigation. For this purpose a ring subjected to two line loads (P) applied diametrically opposite to each other, with internal radius $a = 10$ inches and outer radii

$b = 11, 12, 14, 16, 18,$ and 20 inches was chosen. Solutions were obtained in three different ways:

(1) by elastic theory

(2) using isoparametric triangular finite elements having linear strain distribution

(3) using segments of curved beams as finite elements. The distribution of circumferential normal stress (σ_θ) across the pipe thickness at a section 90 degrees from the point of loading (spring line) is considered for comparison. In Figures 3.3 to 3.8 the normalized circumferential stress $\sigma_\theta / \frac{2P}{\pi b}$ is plotted against $\frac{r-a}{b-a}$ ratio (where r is the radial distance from center of ring). The solid line represents the solution given by the theory of elasticity. Plotted points are from finite element solutions using isoparametric triangular elements, and curved bar elements. For the latter elements the stress distribution due to nodal moments is calculated including a correction for element curvature (Roark, 1943). From these figures it is clearly seen that the triangular and curved bar finite element solutions agree closely with each other, and with the formal solution, for $\frac{b-a}{a}$ equal to one, but for $(b-a/a) = 0.1$ the use of triangular elements introduces large errors. This is illustrated more specifically in Figure 3.9, where the error in $\sigma_{\theta_{\max}}$ is plotted against the ratio of wall thickness to internal radius. It is seen that the error may be unacceptable when the ratio of wall thickness to internal radius is less than about 0.4 . It is concluded that:

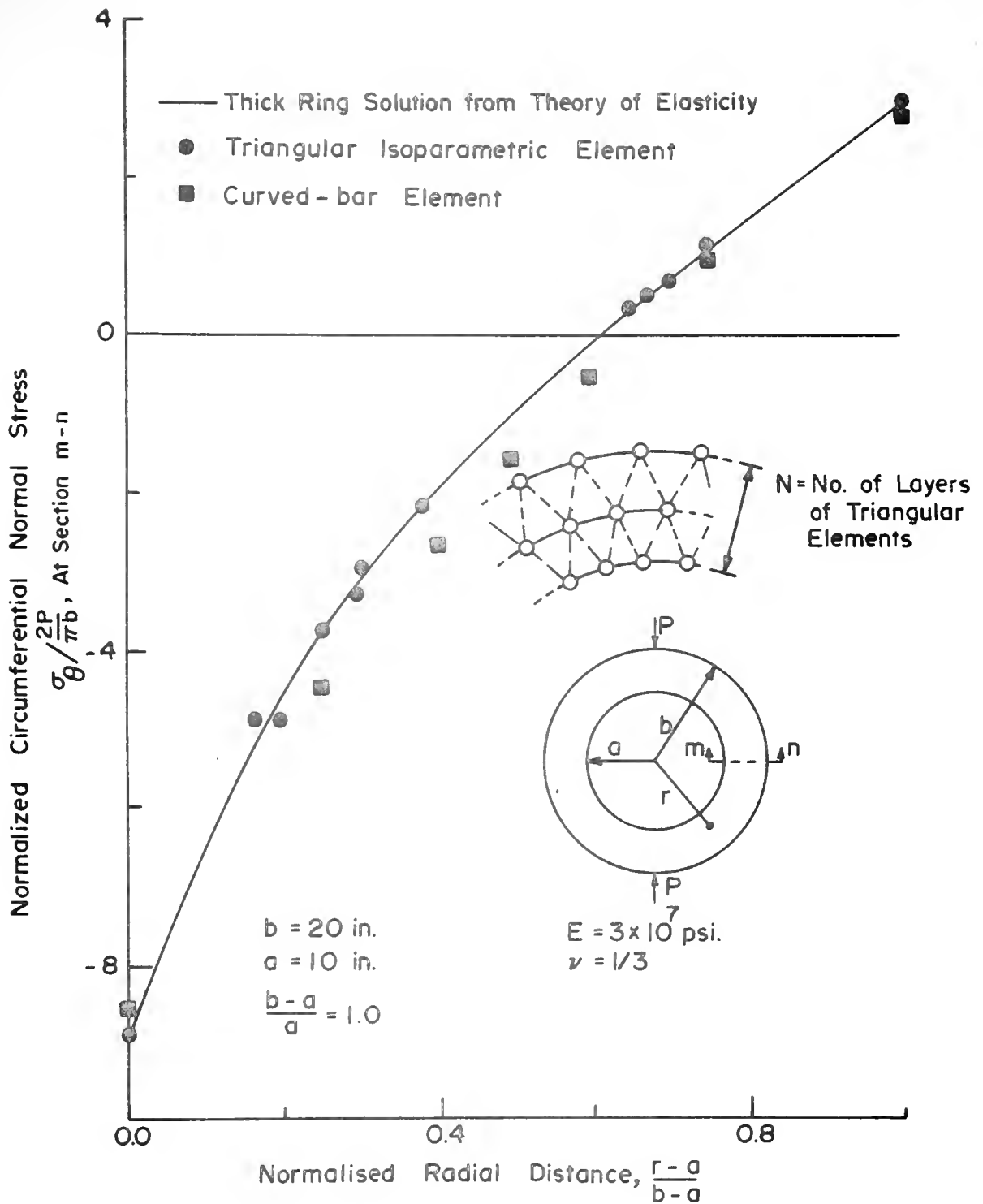


FIGURE 3.3 DISTRIBUTION OF CIRCUMFERENTIAL NORMAL STRESS AT THE SPRING LINE. ($N=4$)

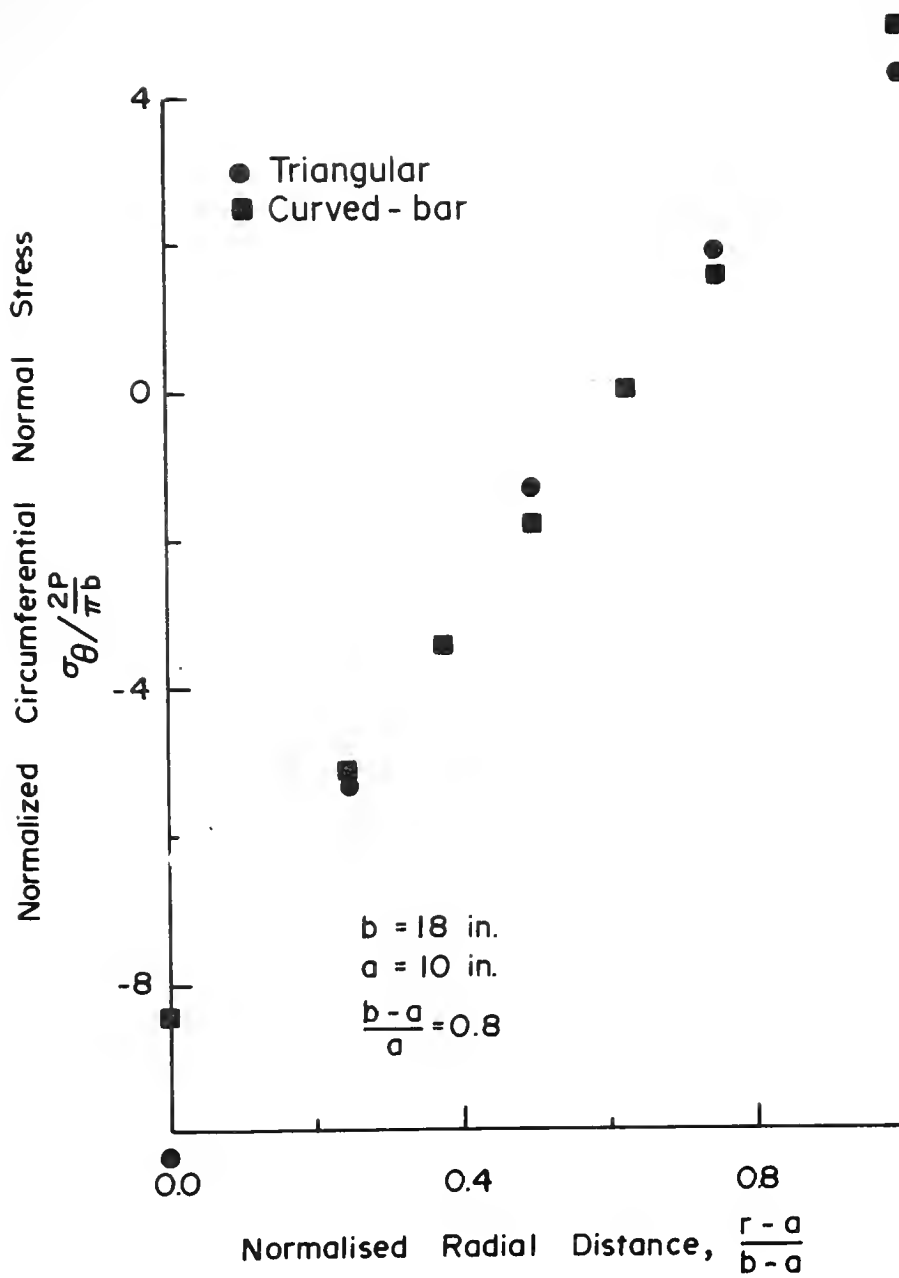


FIGURE 3.4 DISTRIBUTION OF CIRCUMFERENTIAL
NORMAL STRESS AT THE SPRING LINE. (N=4)

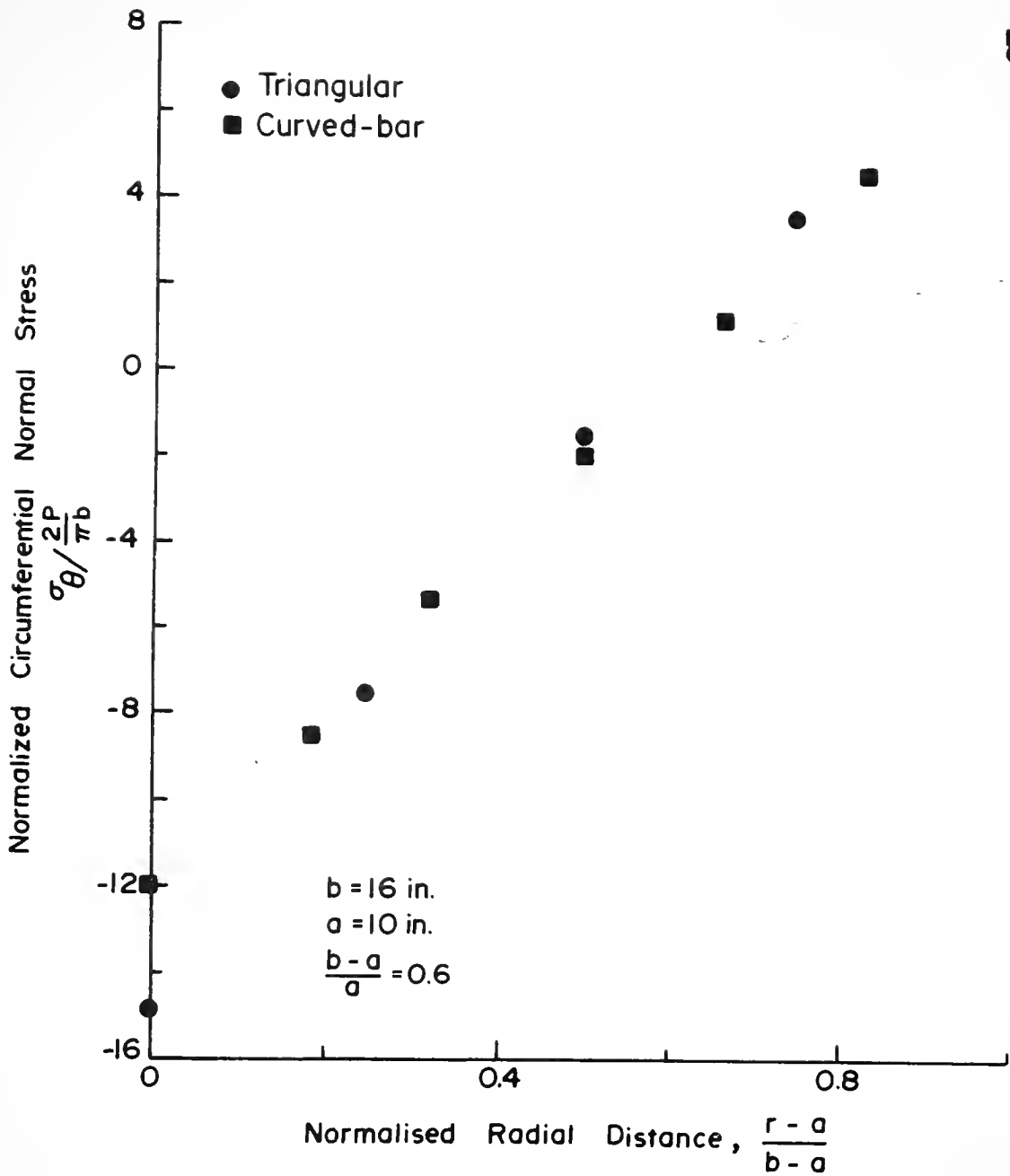


FIGURE 3.5 DISTRIBUTION OF CIRCUMFERENTIAL NORMAL STRESS AT THE SPRING LINE. (N=2)

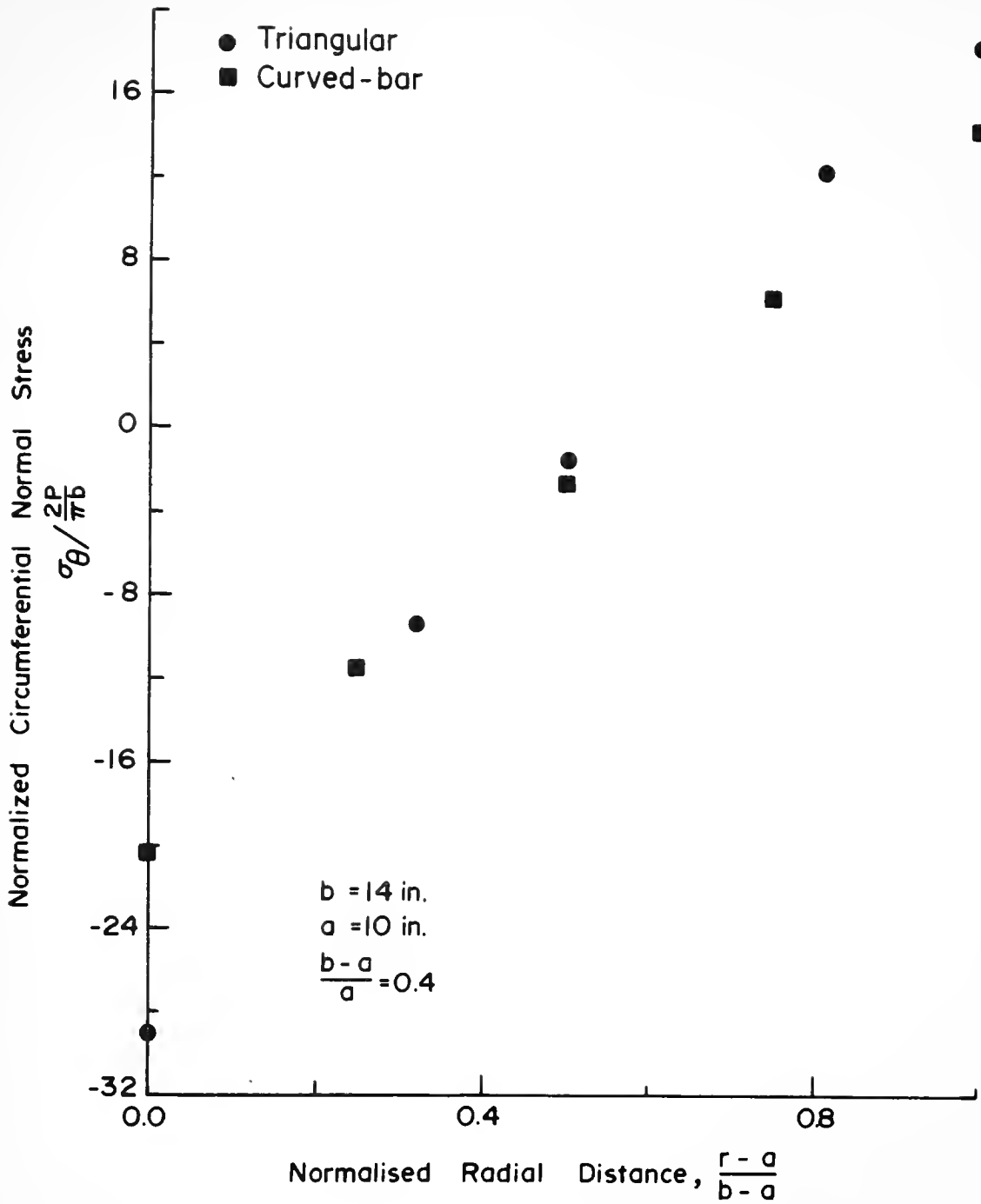


FIGURE 3.6 DISTRIBUTION OF CIRCUMFERENTIAL NORMAL STRESS AT THE SPRING LINE.(N=2)

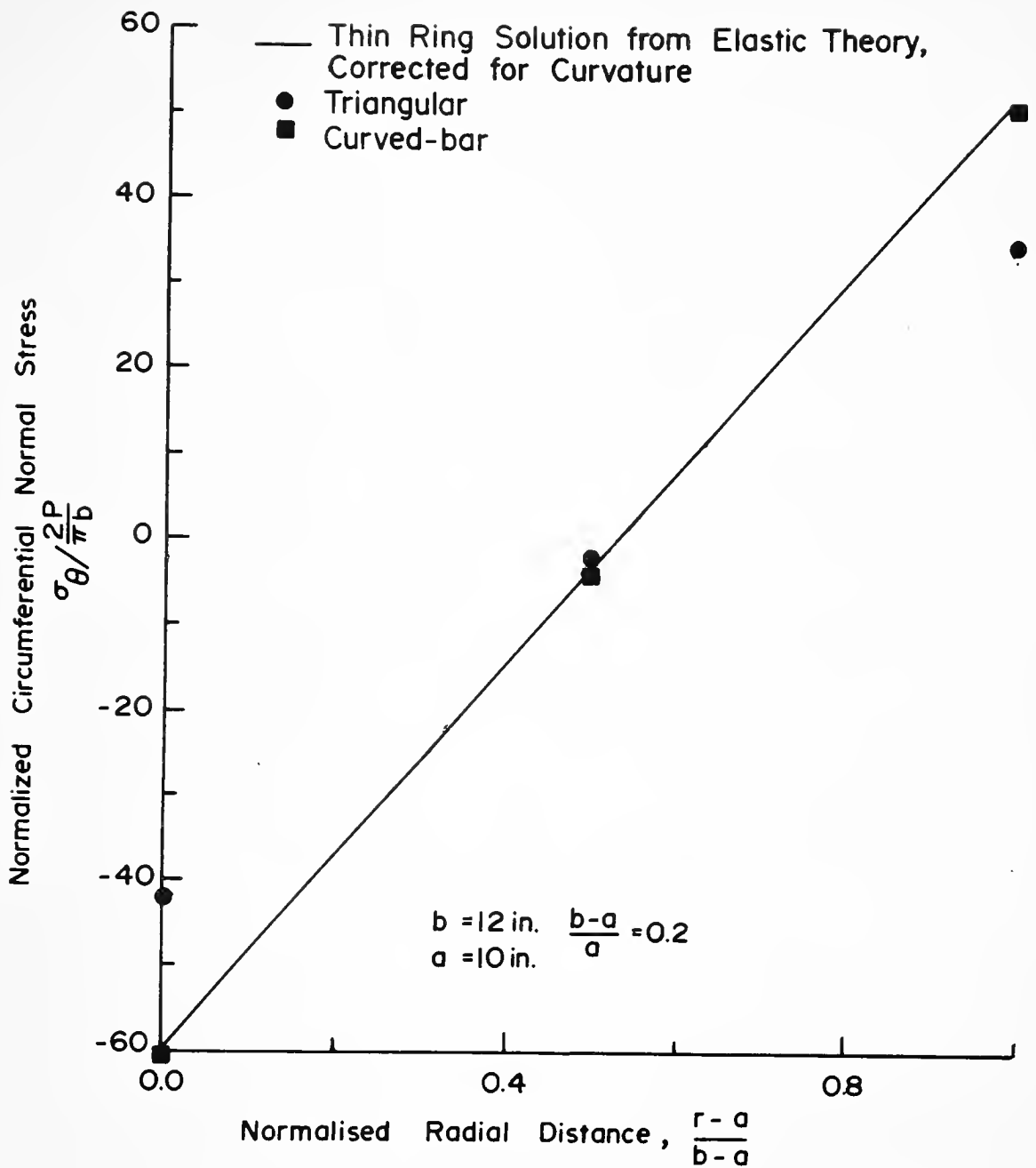


FIGURE 3.7 DISTRIBUTION OF CIRCUMFERENTIAL NORMAL STRESS AT THE SPRING LINE. (N=1)

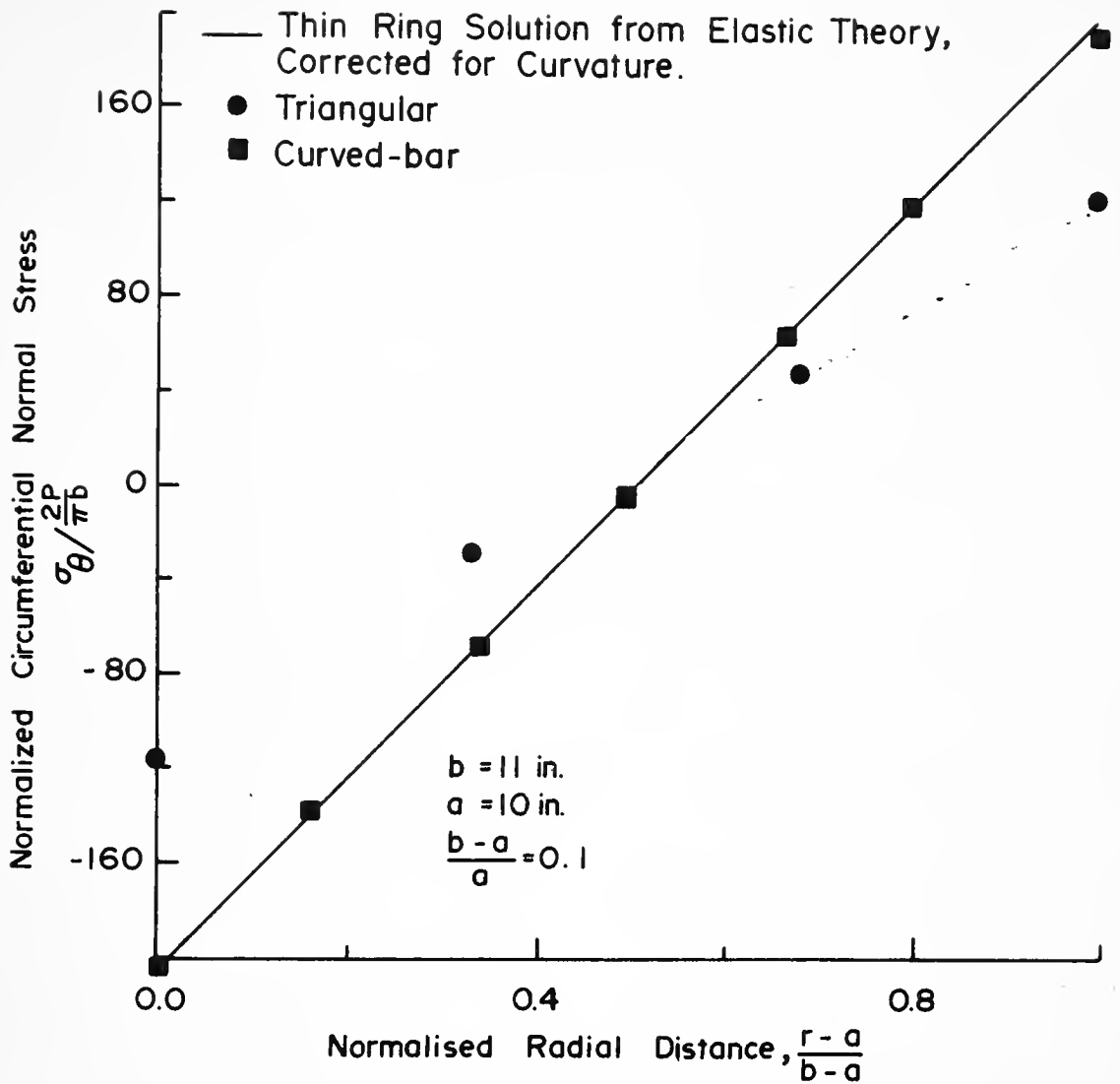


FIGURE 3.8 DISTRIBUTION OF CIRCUMFERENTIAL NORMAL STRESS AT THE SPRING LINE. (N=1)

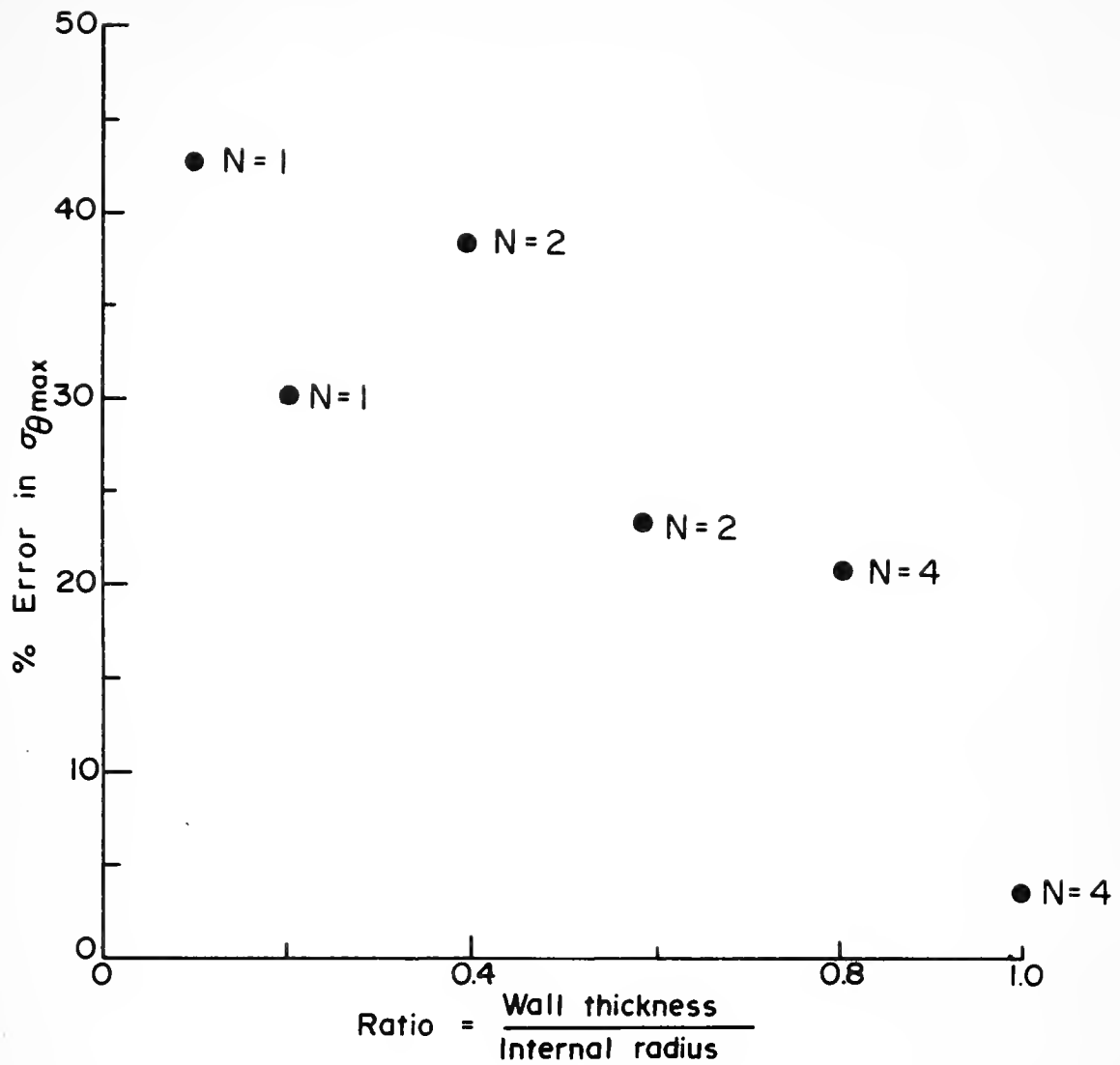


FIGURE 3.9 ERROR IN $\sigma_{\theta_{max}}$ DETERMINED USING ISOPARAMETRIC TRIANGULAR ELEMENTS VS. RATIO OF PIPE WALL THICKNESS TO INTERNAL RADIUS.

(1) isoparametric triangular finite elements can be used to represent "thick" rings, ($\frac{b-a}{a}$ greater than 0.4) where compression plays the major role and bending is of much lesser importance, provided the ring thickness is subdivided sufficiently.

(2) for $\frac{b-a}{a}$ less than 0.2 bending becomes significant and finite elements without a degree of freedom in rotation can result in significant errors in the calculated stresses, unless an extremely fine mesh is used.

(3) for $\frac{b-a}{a}$ ratio less than 0.1, bending of the ring is dominant, and rotation at nodes must be considered in the finite element idealization.

In the case of corrugated metal culverts, $\frac{b-a}{a}$ values are nearly always less than 0.1. In this range, any finite element using equivalent thickness and without rotational stiffness at the nodes is bound to have built-in errors and triangular isoparametric finite elements are not suitable for use. This led to the search for a pipe element which

- (1) provides rotational stiffness at the nodes
- (2) has circumferential and shear stiffness
- (3) can represent actual pipe thicknesses that are small compared to the radius
- (4) would not require adjacent soil elements to have rotational stiffness.

These requirements have been satisfied in a curved-bar element which is described in the following section.

3.7 Curved-Ring Element

Martin (1966) presented a development for the stiffness matrix of curved beam elements. In this procedure a section of a circular ring is acted upon by a normal force, a tangential force, and by a moment at each node. Each node has three degrees of freedom namely, normal and tangential displacements, and rotation. Total moment (M) at any point due to applied forces and moments is calculated. Total strain energy U is given as

$$U = \frac{1}{2EI} \int M^2 \cdot ds \quad (3.17)$$

where ds is increment of length of arc of bar, E is the Young's modulus of pipe material and I is the moment of inertia of the pipe section.

Displacements and rotations in each degree of freedom is determined using Castigliano's theorem which yields:

$$u = \frac{\delta U}{\delta P} = \text{shear displacement} \quad (3.18)$$

$$v = \frac{\delta U}{\delta Q} = \text{normal displacement} \quad (3.19)$$

$$\theta = \frac{\delta U}{\delta M} = \text{rotation} \quad (3.20)$$

where u and P are shear displacement and force, similarly v and Q are in the normal direction, and θ is the rotation and M is the moment. Substituting in the equations for u , v and θ the values of M , differentiating with respect to P , Q and M and integrating over the arc length, one obtains for node 1

$$\begin{Bmatrix} u_1 \\ v_1 \\ \theta_1 \end{Bmatrix} = [A_{11}] \cdot \begin{Bmatrix} P_1 \\ Q_1 \\ M_{1/R} \end{Bmatrix} \quad (3.21)$$

where R is the mean radius of arc, and A_{11} is a (3×3) matrix consisting of functions of known quantities like R , EI , and β , the angle subtended by the arc at the center. Inverting the above matrix-equation

$$\begin{Bmatrix} P_1 \\ Q_1 \\ M_1 \end{Bmatrix} = [K_{11}] \cdot \begin{Bmatrix} u_1 \\ v_1 \\ \theta_1 \end{Bmatrix} \quad (3.22)$$

where $[K_{11}] = \text{inverse of } [A_{11}]$

For the other end of the arc, (node 2), another matrix equation can be written in a similar fashion.

$$\begin{Bmatrix} P_2 \\ Q_2 \\ M_2 \end{Bmatrix} = [K_{22}] \cdot \begin{Bmatrix} u_2 \\ v_2 \\ \theta_2 \end{Bmatrix} \quad (3.23)$$

Considering total equilibrium of the arc under the system of forces and moments,

$$\begin{Bmatrix} P_2 \\ Q_2 \\ M_2 \end{Bmatrix} = [K_{21}] \cdot \begin{Bmatrix} u_1 \\ v_1 \\ \theta_1 \end{Bmatrix} \quad (3.24)$$

Combining all these matrix equations

$$\begin{Bmatrix} u_1 \\ v_1 \\ \theta_1 \\ u_2 \\ v_2 \\ \theta_2 \end{Bmatrix}_{6 \times 1} = \begin{bmatrix} k_{11} & k_{12} \\ k_{21} & k_{22} \end{bmatrix}_{6 \times 6} \begin{Bmatrix} P_1 \\ Q_1 \\ M_1 \\ P_2 \\ Q_2 \\ M_2 \end{Bmatrix}_{6 \times 1} \quad (3.25)$$

where k_{12} = transpose of matrix k_{21} . The result is a (6 x 6) stiffness matrix for a curved beam element. Details of this derivation can be found in Martin, (1966) and are given in Appendix B. The final step in the formulation of the stiffness matrix for a curved beam element is the transformation to the global coordinate system, which can be accomplished by matrix multiplication of the stiffness matrix with the transformation matrix whose coefficients consist of appropriate direction cosine (For details see Appendix B).

3.8 Soil-Pipe Interaction Element

Many researchers have expressed the need for considering interaction between pipe and enclosing soil medium. This interaction can involve slip between the pipe and the soil at shear stresses less than the shear strength of the soil, especially if the pipe is wrapped in a polyesterene film. A suitable interaction element should have the following features:

- (1) In contact with granular soils, no net tensile resistance in the normal direction
- (2) Negligible displacement in the normal direction
- (3) Small shear displacements as long as the ratio of shear stress to normal stress is less than a given limiting value (limiting wall friction)
- (4) When the ratio of shear stress to normal stress exceeds the limiting value, the shear stress is sustained but there is negligible resistance to shear displacement.

Accordingly, an element of zero thickness was chosen, which is capable of offering resistance to shear deformation until a limiting ratio of shear to normal stress is exceeded.

Goodman, Taylor and Brekke (1968) presented a model for the mechanics of jointed rock. Discontinuities or joints in the rock mass are considered as different material with distinct properties which are different from those of adjoining rock blocks. To represent joints in terms of finite elements, the authors derived the stiffness matrix for

these joints based on the minimum potential energy concept. The procedure presented by Goodman et. al. (1968) had been used in this study to develop the stiffness matrix for interaction elements. The element has four nodes, each node having two degrees of freedom in the normal and tangential direction of the interaction element. A pair of nodes of the interaction element (Figure C.1) separated by a finite distance are connected to two consecutive nodes of a pipe segment. The other pair of nodes are connected to the adjacent soil elements. Initially the normal distance between these two pairs of nodes is zero. Properties for the interaction element are described in Chapter IV, and detailed derivation of the stiffness matrix for this element with eight degrees of freedom is presented in Appendix C.

CHAPTER IV

MATERIAL PROPERTIES

4.1 Introduction

One of the primary advantages of the finite element method is the capacity of handling realistic material properties which may differ from place to place in the structure. Referring to Figure 3.1, there are three basic types of material behavior in the culvert problem; (1) pipe, (2) soil-pipe interaction and (3) soil medium. Depending upon the number of different compacted zones several soil types with distinct properties may exist. At the interface between the pipe and soil the behavior is different from the properties of either of the two media. This will be modeled by an interaction element of zero thickness with its own inherent properties.

It is well-known that an isotropic elastic material requires two independent parameters to define its properties. Most commonly used elastic parameters are Young's modulus (E) and Poisson's ratio (ν). For linearly elastic material both E and ν remain constant over the entire range of loading and unloading. Soil is not an ideal material in this respect; on the contrary its stress-strain relation is non-linear and stress path dependent. Natural clay soils,

up to a certain limit, show linearly elastic behavior, but sands are nonlinear and inelastic even at low stress levels. For this reason, analyses that assume the soil to be a linearly-elastic material are not appropriate.

4.2 Pipe Properties

Commonly used culvert materials, such as steel, aluminum or concrete show linear elastic behavior both in compression and in tension up to the yield point. Within this stress range it is reasonable to assume that the properties of the pipe materials remain constant. It is recognized that before collapse concrete pipes will crack and steel culverts will yield. However, in this study it was decided to concentrate on the behavior of the soil medium and the soil-pipe interaction effects. Accordingly, it was initially assumed that values of E and ν for the pipe would remain constant and to consider only problems in which the yield point stress of the pipe materials is not exceeded.

4.3 Soil-Pipe Interaction

Introduction

A number of investigators conducted model and field tests on flexible and rigid pipes buried in soil; Krizek, et. al. (1974); Kirkland and Walker, (1972); Neilson, (1972); Brown, (1966); Davis, (1966, 1969); Abel, (1973) and Allgood, (1972). Most of this research shows that measured results deviate from the analytical predictions even under

controlled test conditions. Among the factors considered to explain the discrepancy is the interaction between soil and pipe, Krizek (1972), Linger (1972), Corotis et. al. (1974), Abel et. al. (1973) and others. The term soil-structure interaction refers to the general phenomenon involved in the behavior of a buried structure as a result of different properties at the interface of the structure and the surrounding soil medium in response to the imposed loading system. This concept has existed in the literature for a long time, however, until recently, the phenomenon received little attention. Linger (1972) presented a historical development of soil-structure interaction. The concept may be stated as the process of pressure distribution between soil and structure, which depends on the degree to which relative displacements along the interface has mobilized the contact shear strength.

In the conduit problem, the existence of soil-structure interaction was first recognized by Spangler and Marston (1941) and they introduced the concept of the "imperfect ditch method." As a result, different methods of pipe installation have been developed. For example, in the "Soil-Arch" method a layer of material is compacted around the pipe after a relatively stiffer material has been placed at both abutments. The soil arch helps transfer load from overburden to a base away from the pipe. Fisher (1969) described the installation of "super-span"

culverts whose successful performance he attributes to slip along the soil-pipe interface and to transfer of load by arching to well-compacted zones beside the base of the arch.

Properties for the Interaction Element

Interaction between soil and structure may be looked at as a phenomenon which occurs as a result of existence of one material next to another. Because of the fact that the two materials have different properties the behavior at the interface is different from that of either material by itself. The mechanism of shear transfer between a structure and clay soil is little understood whereas for sandy soil some information is available (Brumund and Leonards, (1973)). Interface friction depends on several factors, among which are the normal pressure, roughness of contact surfaces, relative displacements, and environmental conditions. For a granular soil, the following characteristics are recognized as representative of behavior:

- (1) In two-dimensional representation, the interaction element should approach zero thickness.
- (2) Tension normal to the pipe cannot be tolerated.
- (3) Compression displacements normal to the pipe are negligible.
- (4) The shearing resistance is purely frictional in nature, and is proportional to the normal stress.
- (5) The resistance to shear deformation is high until the ratio of shear stress to normal stress exceeds a

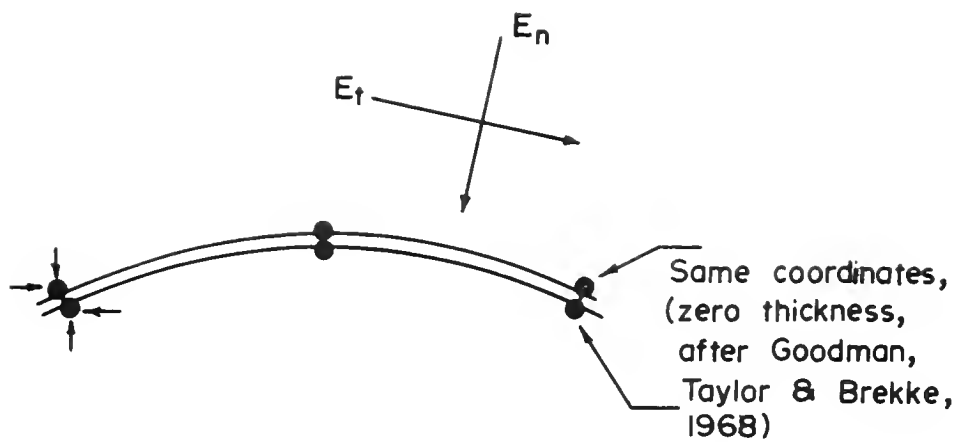
limiting value. Beyond this limit, the shear stress is maintained but full slip is permitted.

Based on the above mentioned features, the model for the properties of the interaction element is shown in Figure 4.1. High values for stiffness in the normal and shear direction (E_n and E_s in equation C.9) are initially assigned. If after application of an increment of load, the net normal stress is tensile, E_n and E_s are reduced to zero. If the net normal stress is compressive but the stress ratio exceeds the limiting value, then E_s is reduced to zero while E_n is left unchanged, which simulates slip in interaction element.

4.4 Soil Properties

In general, stress-strain properties for soil are non-linear in nature; even at small strains, the stress-strain curves are slightly nonlinear and there are plastic components of strain. However, the amount of plastic strain is not large in the initial stages. Frydman and Zeitlen (1969) concluded from triaxial tests performed on dense dune sand and glass microspheres that only insignificant amounts of plastic strain occur before a yield point is reached. A major factor which influences the stress-strain behavior for sand is the confining pressure (Lee and Seed, 1967, Duncan and Chang, (1970).

Three stress-strain models for soils are commonly in use: linear elastic, elastoplastic and non-linear. A



$$E_n \rightarrow \infty$$

$E_s = E_n$ until $\tau/\sigma = \tan \delta$ (interaction friction)
 then, $E_s \rightarrow 0$

FIGURE 4.1 PROPERTIES OF INTERACTION ELEMENT.

drawback of the linear elastic model is that it does not consider shear dilatancy. The state of stress at a point can be expressed in terms of octahedral normal stress

$$\sigma_{\text{oct}} = \frac{1}{3} (\sigma_1 + \sigma_2 + \sigma_3) \quad (4.1)$$

and the octahedral shear stress:

$$\tau_{\text{oct}} = \frac{1}{3} \sqrt{(\sigma_1 - \sigma_2)^2 + (\sigma_2 - \sigma_3)^2 + (\sigma_3 - \sigma_1)^2} \quad (4.2)$$

Frydman and Zeitlen (1969) showed that in triaxial tests with σ_{oct} constant, no volume change took place before a particular ratio of $\tau_{\text{oct}}/\sigma_{\text{oct}}$ was exceeded regardless of the value of σ_{oct} . The point at which volume change started was called the yield point, after which the stress-strain curve showed increasing change in curvature; this aspect is important for determination of deformations.

Several models for simulating nonlinear stress-strain behavior of soils are available in literature. Chen (1948) concluded from triaxial tests on cohesionless soils that axial strain can be expressed in terms of an exponential function of deviator stress for a stress range of 15% to 50% of maximum deviator stress. A hyperbolic function was proposed by Kondner (1963) to represent stress-strain relations for cohesive soils. He used

$$(\sigma_1 - \sigma_3) = \frac{\varepsilon}{a + b\varepsilon} \quad (4.3)$$

in which 'a' and 'b' are constants to be evaluated from experimental results. Taking derivatives of equation (4.3) one can find the value of tangent modulus. He also proposed methods to determine the constants 'a' and 'b'.

Brinch Hansen (1963) proposed a parabolic relationship as $\sigma = \frac{\sqrt{\epsilon}}{r - s \cdot \epsilon}$. Where r and s are constants of the parabola. The initial tangent modulus value is indefinite at $\epsilon = 0$.

Duncan and Chang (1970) used the hyperbolic model for stress-strain relations proposed by Kondner (1963) modified to account for the stress-dependency of the model. They also developed relations for tangent modulus which is suitable for use in incremental analysis, such as the finite element analysis. The main advantage of using the tangent modulus instead of initial modulus is that in-situ stresses can be taken into account and incremental analysis can be performed, taking state of stress and strain dependency effects into account. Their expression for tangent modulus was given as

$$E_t = \left[1 - \frac{R_f (1 - \sin \phi) (\sigma_1 - \sigma_3)}{2c \cdot \cos \phi + 2\sigma_3 \cdot \sin \phi} \right]^2 \cdot K \cdot p_a \cdot \left(\frac{\sigma_3}{p_a} \right)^n \quad (4.4)$$

in which R_f = failure ratio, c and ϕ are cohesion and friction angle values of the soil, p_a is the atmospheric pressure, K and n are constants to be determined. This model is useful for soils which show hyperbolic stress-strain

relations. For soils in which the stress-strain relation deviates from hyperbolic shape, use of the model introduces significant errors. Duncan and Chang (1970) used the proposed relationship for tangent modulus in calculation of footing behavior, which show significant improvements on previous analytical predictions. Domaschuk and Wade (1969) proposed the use of bulk modulus, K and shear modulus G , as opposed to Young's modulus, E and Poisson's ratio, ν because K and G can be evaluated independently.

Lade (1972) did an extensive study of stress-strain relations for soil. He presented a three-dimensional, elastoplastic stress-strain relationship for cohesionless soils. This development is based on the concept that during loading both elastic and plastic strain occur. The elastic part is evaluated using elastic theory and plastic component is determined using plastic stress-strain relations.

$$\Delta \epsilon_x = \Delta \epsilon_x^e + \Delta \epsilon_x^p \quad (4.5)$$

in which $\Delta \epsilon_x$ is the total increment of strain, $\Delta \epsilon_x^e$ is the elastic and $\Delta \epsilon_x^p$ is the plastic component of strain. This model is based on three requirements:

(1) There must exist a yield surface such that if the stress condition is within this surface, the soil will behave elastically. If the point is outside the surface, it will deform plastically. When the point is on the surface, it represents yield a condition.

(2) A flow rule should relate plastic stresses to plastic strain.

(3) A work-hardening law is required from which the magnitudes of strain increments caused by a given stress increment can be determined. The yield criterion adopted is of the form:

$$I_1^3 - k_1 I_3 = 0 \quad (4.6)$$

$$f = I_1^3 / I_3$$

in which I_1 and I_3 are the first and third principal stress invariants and k_1 is a constant whose values depend on the type of sand, and f is stress level. When an increment of stress is applied, the material will yield plastically if $df > 0$, and will yield elastically if $df = 0$ or $df < 0$. Lade (1972) assumed the following function for plastic potential.

$$g = I_1^3 - k_2 I_3 \quad (4.7)$$

in which g is the plastic potential and k_2 is a constant for given value of f . The plastic stress-strain relation is given by:

$$d\epsilon_{ij}^p = d\lambda \cdot \frac{dg}{d\sigma_{ij}} \quad (4.8)$$

in which $d\epsilon_{ij}^p$ is the plastic strain increment in i, j directions due to an increase in stresses $d\sigma_{ij}$ in the same directions; $d\lambda$ is constant, which relates to the work hardening rule. Total plastic work done due to applied stress

system can be written as a function of f .

$$w_p = F(f) \quad (4.9)$$

$$w_p = \text{plastic work, } f = I_1^3/I_3.$$

Lade (1972) has shown that for cubical stress conditions

$$\Delta\lambda = \frac{dw_p}{3g} \quad (4.10)$$

Taking derivatives for all strain components in equation (4.8) substituting for I_2 and $\Delta\lambda$ the plastic strain components can be written as:

$$\begin{Bmatrix} \Delta\epsilon_x^p \\ \Delta\epsilon_y^p \\ \Delta\epsilon_z^p \\ \Delta\epsilon_{yz}^p \\ \Delta\epsilon_{zx}^p \\ \Delta\epsilon_{xy}^p \end{Bmatrix} = \frac{K_2}{3(I_1^3 - K_2 I_1)} dw_p \begin{Bmatrix} \frac{3}{K_2} I_1^2 - \sigma_y \sigma_z + \tau_{yz}^2 \\ \frac{3}{K_2} I_1^2 - \sigma_z \sigma_x + \tau_{zx}^2 \\ \frac{3}{K_2} I_1^2 - \sigma_x \sigma_y + \tau_{xy}^2 \\ 2\sigma_x \tau_{yz} - 2\tau_{xy} \tau_{zx} \\ 2\sigma_y \tau_{zx} - 2\tau_{xy} \tau_{yz} \\ 2\sigma_z \tau_{xy} - 2\tau_{yz} \tau_{zx} \end{Bmatrix} \quad (4.11)$$

Lade (1972) presented methods for evaluating the constants of equation 4.11 from standard tests. He used these relations in a variety of cases including cubical triaxial tests and has shown that predicted results compare well with the experimental results. To investigate the influence of intermediate principal stress, σ_2 , Bishop (1966) proposed a parameter b , which is defined as

$$b = \frac{\sigma_2 - \sigma_3}{\sigma_1 - \sigma_3} \quad (4.12)$$

Lade (1972) presented results for range in values of b varying from 0 to 1.

Need for Incremental Analysis

Geotechnical engineering construction often involves either filling or making excavations in soil which is done in layers. Classical methods of analysis do not take into account this real situation. For example, in classical analysis in the case of construction of an embankment, a decision has to be taken regarding full shear, full slip or partial slip between layers. In such cases use of finite element method has an important advantage over many other existing methods.

Goodman and Brown (1963) were among the first to recognize the importance of considering the effects of construction or excavation in layers. If construction is accomplished in layers and the soil possesses nonlinear behavior, simulation of this process in analytical models is important. Even if the material is linearly elastic and deformations are small, construction in layers would have an effect because of incompatibility at the interface between layers. One of the great advantages of the finite element method is its ability to simulate the layer-by-layer construction sequence. To minimize the cost of such analyses, the general practice is to use actual lift heights in the

zones of major influence on the structure and relatively larger lift heights elsewhere.

The influence of the construction sequence is of importance in many other types of problems; for example, retaining walls, locks, dams and buried conduits. In particular, for problems of flexible culverts in soil, many investigators have pointed out that slip between pipe and soil may occur and this might have an important effect on the behavior of the system. To account for this slippage, the characteristics of which depend on normal thrust on the interface, incremental finite element analyses is very convenient.

The construction of a culvert may be considered as a three phase process. The first phase, a trench may be excavated (changing the free-field stress system) and the bedding is prepared. In the second phase, the pipe is placed and initial back packing takes place up to the crown. During this phase the pipe is not fully constrained by surrounding soil and considerable displacements may occur. The third phase includes filling and backpacking operations up to the top of the embankment or trench. These three processes take place step-by-step and may not be carried out symmetrically with respect to the pipe. Accordingly, construction effects may be simulated by incremental analysis but the real situation can not be fully recreated.

In this study a combination of incremental and iterative procedures has been used depending upon the requirements of the problem. In general the incremental approach is used in the analysis until some ill-condition like tension in the soil or slip in the interaction element occurs. In such cases an iterative approach must be used. Details of this approach are presented in a later chapter.

4.5 Method of Considering Stress-Strain Parameters

For incremental finite element analyses, the following factors are important in selection of soil parameters:

- (1) Stress-strain relations are non-linear and dependent on the state of stress and the stress path.
- (2) A tangent modulus and tangent Poisson's ratio is more representative of non-linear behavior
- (3) A single stress-strain formulation, which is reasonably accurate over a wide range of conditions, probably does not exist.

Solutions of nonlinear problems using the finite element method can be done in three ways - (1) stepwise or incremental procedure, (2) iterative technique and (3) combination of incremental and iterative methods. In the incremental method the total load is divided into predetermined numbers of increments. Results such as stresses, displacements of each step are added to the results at the end of previous step. This process is continued till the total load is applied. The underlying assumption in this method

is that the material behaves linearly during each increment. The accuracy of this approach depends largely on the number of increments. The source of error is illustrated in Figure 4.2.

In Figure 4.2, A and B are two points representing an increment on the stress-strain curve. AC is the tangent modulus at point A, which is different from the tangent modulus at point B. Use of a tangent modulus value either at A or at B for the increment will introduce an unavoidable error. Somewhat better result may be expected by using an average value of the tangent modulus between points A and B, (EF). But there are two difficulties: (1) before analyzing for the increment, point B is undefined and (2) segment of the curve between A and B may be strongly curved. Using an iterative technique the error can be reduced. One drawback of this approach is that the solution becomes expensive. To eliminate these sources of errors, cubic spline functions were used to simulate the actual stress-strain curve. The basic principles of spline functions are consistent with the discretization principle of finite elements.

Desai (1971) presented a method for using spline functions for nonlinear finite element analysis. From a given set of stress-strain curves for different confining pressures, another set of splines can be generated for tangent modulus versus confining pressure for any given strain or stress ratio as desired. Desai (1971) solved a footing

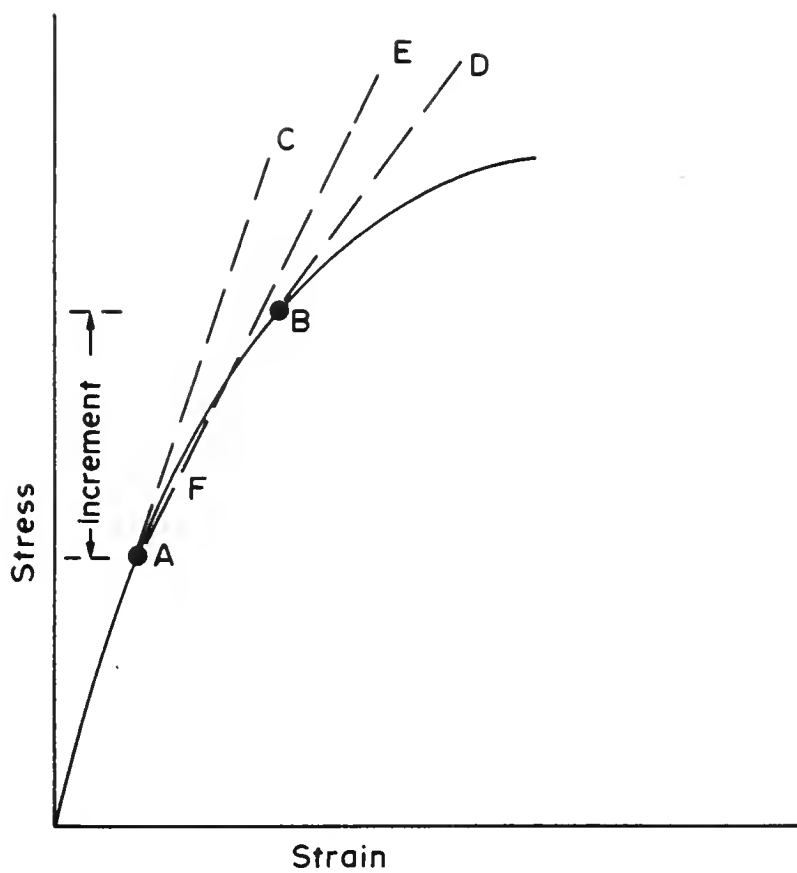


FIGURE 4.2 ERRORS IN INCREMENTAL ANALYSIS.

problem with nonlinear stress-strain properties using spline functions, keeping Poisson's ratio constant, which shows better agreement than assuming hyperbolic stress-strain relations. Desai (1972) presented another method of approximating stress-strain relationships using bicubic spline functions. In this process continuity in all three spaces (e.g., stress, strains and confining pressure) is ensured. However, due to computational difficulties of bicubical spline functions, cubical spline functions were used in this study. The approach taken is slightly different from that proposed by Desai (1971). The advantage of using spline functions in incremental analysis is that the parameter in question can vary continuously within a stress (or strain) interval.

Spline Functions

In this study a general method for handling incremental loadings and non-linear material properties has been adopted making use of spline functions. Ahlberg et. al. (1967) presented a comprehensive mathematical background of a variety of spline functions and their application. In Figure 4.3, (a,b) represents an interval Δ of a typical stress-strain curve. The interval has been subdivided into a number of subintervals so that

$$\Delta : a = x_0 < x_1 < \dots x_N = b$$

and corresponding ordinates are:

$$Y : y_0, y_1, y_2, \dots y_N \quad (4.13)$$

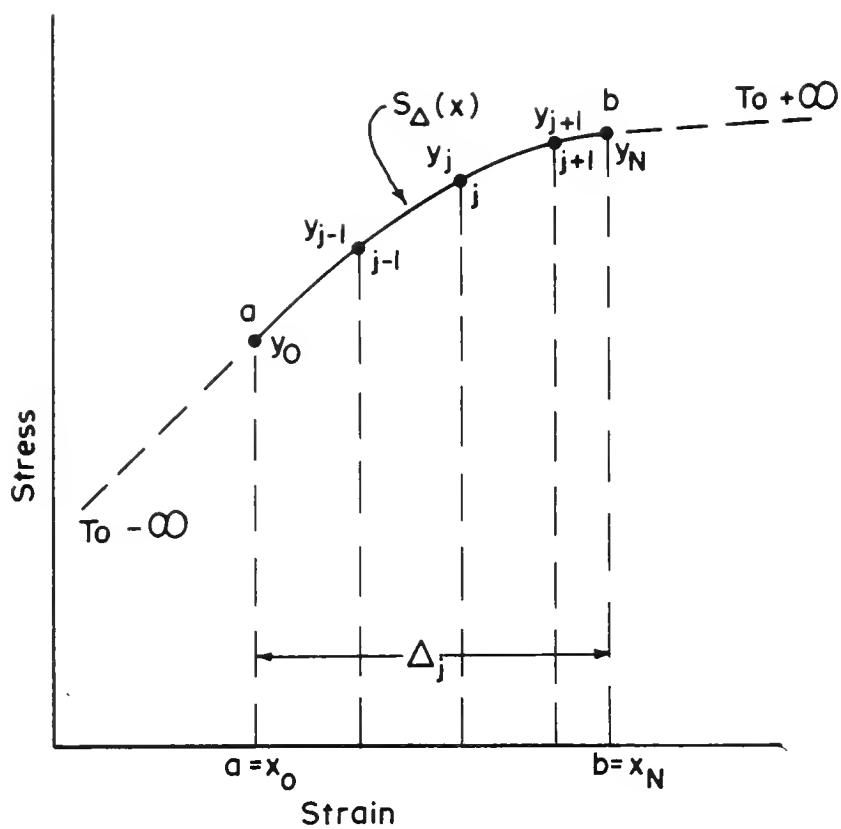


FIGURE 4.3 INTERVAL OF A CUBIC SPLINE FUNCTION.

in which Y is the vector of ordinate at each x_i value.

Spline function may be defined as

$$S_{\Delta}(x) = Y \quad (4.14)$$

S_{Δ} is continuous together with its first and second derivatives in the interval (a, b) and coincides with a cubic in each subinterval, i.e.,

$$\begin{aligned} x_{j-1} \leq x \leq x_j \text{ for } j = 1, 2, \dots, N \text{ and} \\ S_{\Delta}(x_j) = Y_j \text{ for } j = 0, 1, 2, \dots, N \end{aligned} \quad (4.15)$$

The second derivative of S_{Δ} may be considered as "moment" of spline (M_j).

$$S''_{\Delta}(x) = M_{j-1} \frac{x_j - x}{h_j} + M_j \frac{x - x_{j-1}}{h_j} \quad (4.16)$$

where $h_j = x_j - x_{j-1}$ is the size of subinterval and x is a variable point. Integrating equation (4.16) twice,

$$S_{\Delta}(x) = - \frac{M_{j-1}}{h_j} \frac{(x - x_j)^3}{6} + \frac{M_j}{h_j} \cdot \frac{(x - x_{j-1})^3}{6} + C_1 x + C_2 \quad (4.17)$$

in which C_1 and C_2 are constants to be determined from the end conditions at point $j-1$ and j which are:

$$\text{at } x = x_{j-1}, \quad S_{\Delta}(x_{j-1}) = Y_{j-1}$$

$$\text{and } x = x_j, \quad S_{\Delta}(x_j) = Y_j$$

After determining C_1 and C_2 and substitution in equation (4.17) yields:

$$\begin{aligned}
S_{\Delta}(x) &= \frac{M_{j-1}}{6h_j} (x_j - x)^3 + \frac{M_j}{6h_j} (x - x_{j-1})^3 \\
&+ \left(Y_{j-1} - \frac{M_{j-1} h_j^2}{6} \right) \cdot \left(\frac{x_j - x}{h_j} \right) \\
&+ \left(Y_j - \frac{M_j h_j^2}{6} \right) \cdot \left(\frac{x - x_{j-1}}{h_j} \right) \quad (4.18)
\end{aligned}$$

To ensure continuity, the first derivative of equation (4.18) is taken and the following continuity condition is applied (Figure 4.4).

$$\lim_{dx \rightarrow 0} S'_{\Delta}(x_j - dx) = \lim_{dx \rightarrow 0} S'_{\Delta}(x_j + dx) \quad (4.19)$$

After simplification,

$$\begin{aligned}
\frac{h_j}{6} M_{j-1} + \frac{h_j + h_{j+1}}{3} M_j + \frac{h_{j+1}}{6} M_{j+1} \\
= \frac{Y_{j+1} - Y_j}{h_{j+1}} - \frac{Y_j - Y_{j-1}}{h_j} = d_j \quad (4.20)
\end{aligned}$$

Similar equations are written for each interval and can be written in a matrix form as below

$$\begin{bmatrix}
2(h_1 + h_2) & h_2 & 0 & \dots \\
h_2 & 2(h_2 + h_3) & h_3 & \dots \\
0 & h_3 & 2(h_3 + h_4) & \dots \\
\vdots & \vdots & \vdots & \ddots \\
& & 2(h_n + h_{n+1}) &
\end{bmatrix} \cdot \begin{bmatrix} M_1 \\ M_2 \\ M_2 \\ \vdots \\ M_n \end{bmatrix} = \begin{bmatrix} d_1 \\ d_2 \\ d_3 \\ \vdots \\ d_n \end{bmatrix} \quad (4.21)$$

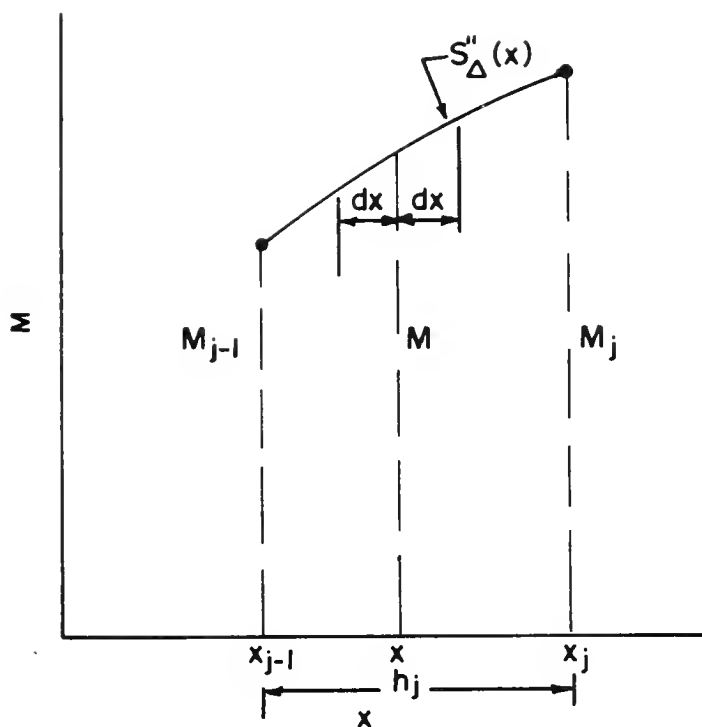


FIGURE 4.4 SUBINTERVAL OF SPLINE FUNCTION.

In equation (4.21) the vector M_j is unknown, but can be solved for using matrix algebra. For any value of x in $x_{j-1} < x < x_j$, the ordinate can be determined using equation (4.18). But the primary interest is to find the slope at any point which in fact is the tangent modulus. Slope of a cubic spline is determined by taking the first derivative of equation (4.18), which can be written as:

$$S'_\Delta(x) = -\frac{M_{j-1}}{2h_j}(x_j-x)^2 + \frac{M_j}{2h_j}(x-x_{j-1})^2 + \frac{Y_j - Y_{j-1}}{h_j} - \frac{M_j - M_{j-1}}{6}h_j \quad (4.22)$$

In this study, taking first derivative as in equation (4.22) is avoided by starting with slopes rather than ordinate values.

Say $S'_\Delta(x_j) = m_j$ = slope at point j . In the interval (x_{j-1}, x_j) the expression for $S_m(x)$ can be written as:

$$S_m(x) = m_{j-1} \frac{(x_j-x)^2 (x-x_{j-1})}{h_j^2} - m_j \frac{(x-x_{j-1})^2 (x_j-x)}{h_j^2} + Y_{j-1} \frac{(x_j-x)^2 [2(x-x_{j-1}) + h_j]}{h_j^3} + Y_j \frac{(x-x_{j-1})^2 [2(x_j-x) + h_j]}{h_j^3} \quad (4.23)$$

and slope $s'_m(x)$ is given by

$$\begin{aligned}
S'_m(x) = & m_{j-1} \frac{(x_j - x)(2x_{j-1} + x_j - 3x)}{h_j^2} \\
& - m_j \frac{(x - x_{j-1})(2x_j + x_{j-1} - 3x)}{h_j^2} \\
& + 6 \cdot \frac{y_j - y_{j-1}}{h_j^3} \cdot (x_j - x) \cdot (x - x_{j-1}) \quad (4.23a)
\end{aligned}$$

Taking second derivative of equation (4.23), enforcing continuity condition as x approaches x_j from both sides, it can be written in matrix form.

$$\begin{bmatrix}
2 & \mu_0 & 0 \\
\lambda_1 & 2 & \mu_1 \\
0 & \lambda_2 & 2 & \mu_2 \\
\cdot & \cdot & \cdot & \cdot & \cdot & \cdot \\
\cdot & \cdot & \cdot & \cdot & \cdot & \cdot \\
& & & \lambda_{n-1} & 2 & \mu_{n-1} \\
& & & & \lambda_n & 2
\end{bmatrix} \cdot \begin{bmatrix} m_0 \\ m_1 \\ m_2 \\ \cdot \\ \cdot \\ \cdot \\ m_n \end{bmatrix} = \begin{bmatrix} c_0 \\ c_1 \\ c_2 \\ \cdot \\ \cdot \\ \cdot \\ c_n \end{bmatrix} \quad (4.24)$$

in which

$$\lambda_j = \frac{h_{j+1}}{h_j + h_{j+1}} \quad \text{and} \quad \mu_j = 1 - \lambda_j$$

and

$$c_j = 3\lambda_j \frac{y_j - y_{j-1}}{h_j} + 3\mu_j \cdot \frac{y_{j+1} - y_j}{h_{j+1}}$$

Whence vector m can be solved for. Using appropriate values of m , the slope at any point can be determined by equation (4.23a).

In Figure 4.5(a) typical stress-strain curves for different confining pressures (σ_3) are shown. Tangent moduli for nonlinear material behavior can be determined using spline functions as follows.

- (1) From the given data points, λ_j , μ_j and C_j are determined and the tridiagonal matrix along with right hand side of equation (4.24) is formed. The system of equations are solved for values of m .
- (2) In the next step, slopes at the curve (which is tangent modulus) at predetermined failure stress ratios (τ_{oct}/τ_{oct_f}) are evaluated using equation 4.23. Steps (1) and (2) are repeated for all curves.
- (3) Another set of splines are used to fit tangent modulus and confining pressure (σ_{oct}) for various values of failure stress ratios. Because only values of ordinates are required, equation (4.21) is used in this stage. Values of tangent modulus for a given stress ratio and for an interval of confining pressure can be determined by using equation (4.18). Figure 4.5(b) shows curves for tangent modulus versus confining pressure for different octahedral shear stress ratios obtained from the stress-strain curves shown in Figure 4.5a. Using this process, finite element analysis can be performed for nonlinear stress-strain relations, which in turn are influenced by the stress level.

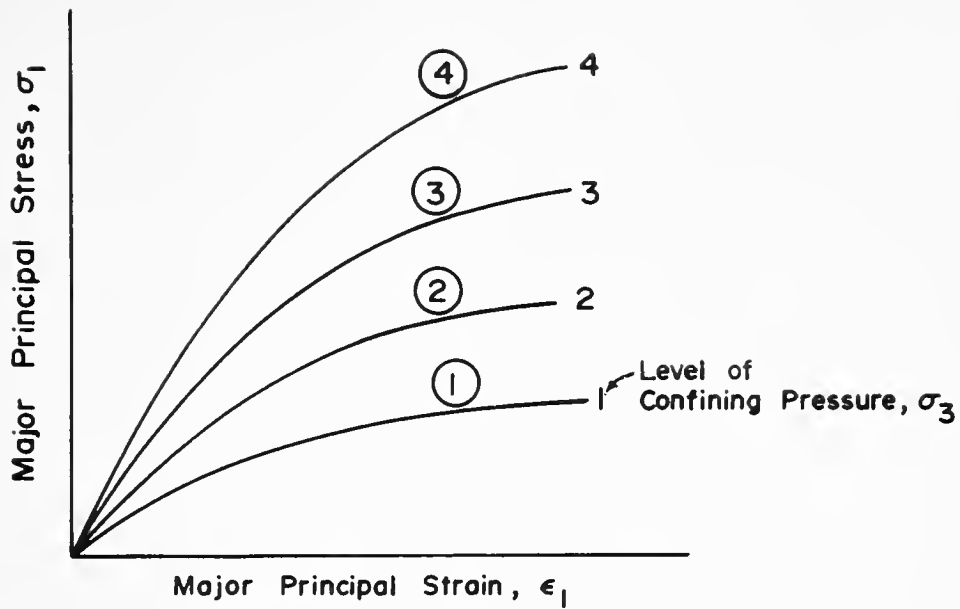


FIGURE 4.5 (a) TYPICAL STRESS-STRAIN CURVES.

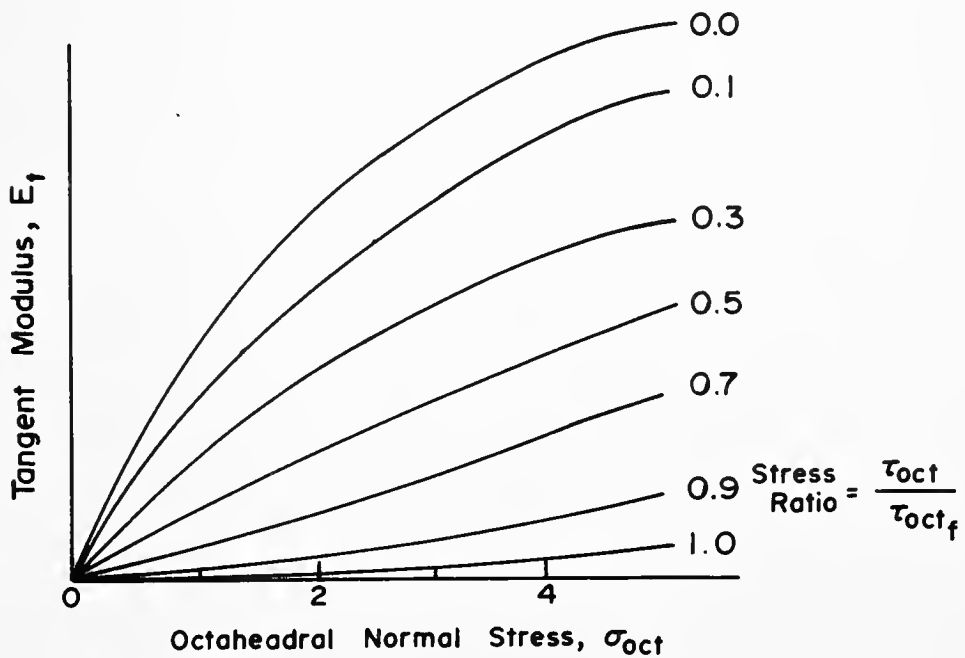


FIGURE 4.5 (b) TANGENT MODULUS - OCTAHEDRAL NORMAL STRESS CURVES.

4.6 Poisson's Ratio

Although Poisson's ratio ν and modulus of elasticity E are both important for calculations of stresses and deformations in soil, the effect of variations in Poisson's ratio has received very little attention and this parameter has frequently been assumed to be constant. For a uniaxial stress increment, Poisson's ratio is defined as the ratio of lateral to axial strain.

$$\nu = - \frac{\epsilon_3}{\epsilon_1} \quad (4.25)$$

in which ν = Poisson's ratio, ϵ_3 and ϵ_1 are the lateral and axial strains respectively. Chen (1948) found that the value of Poisson's ratio for cohesionless soils varies with strain. He defined the tangent Poisson's ratio as

$$\nu_t = - \frac{\Delta\epsilon_3}{\Delta\epsilon_1} \quad (4.26)$$

where ν_t denotes tangent or incremental Poisson's ratio, $\Delta\epsilon_3$ and $\Delta\epsilon_1$ are incremental values of ϵ_3 and ϵ_1 . Tangent Poisson's ratio as given by equation (4.26) has been used by several authors. Duncan and Chang (1970) used the same equation in a different form for incremental analysis, in which incremental Poisson's ratio has been defined as

$$\nu_t = \frac{\Delta\epsilon_1 - \Delta\epsilon_v}{2\Delta\epsilon_1} \quad (4.27)$$

in which $\Delta\epsilon_v$ is the increment in volumetric strain. They

found values of Poisson's ratio ranging from 0.11 to 0.65. Values of tangent Poisson's ratio may range from as low as 0.1 to as high as 1.6.

Poisson's ratio can be expressed in terms of shear modulus G and bulk modulus K , which can be written as:

$$\nu = \frac{3K - 2G}{6K + 2G} \quad (4.28)$$

In some cases (vibration analysis) it is more convenient to obtain K and G , whence ν can be calculated from equation (4.28)

Lade (1972) presented a formulation of tangent Poisson's ratio assuming the hyperbolic stress-strain function proposed by Duncan and Chang (1970).

$$\nu_t = \frac{G - F \log\left(\frac{\sigma_3}{p_a}\right)}{\left[1 - \frac{d \cdot (\sigma_1 - \sigma_3)}{K \cdot p_a \left(\frac{\sigma_3}{p_a}\right)^n \cdot \left[1 - \frac{R_f \cdot (\sigma_1 - \sigma_3) (1 - \sin\phi)}{2 C \cdot \cos\phi + 2 \sigma_3 \cdot \sin\phi} \right]} \right]^2} \quad (4.29)$$

in which G is the value of tangent Poisson's ratio ν_i at $\sigma_3 = 1$ atmosphere, F is the decrease in value of ν_i per log-cycle increase in σ_3 and d is a constant of hyperbolic variation, other parameters have been defined in equation (4.4). Lade (1972) showed that a plot of $-\epsilon_3$ and ϵ_1 for a given confining pressure on a log-log diagram approximates a straight line (Figure 4.6a). This straight line can be

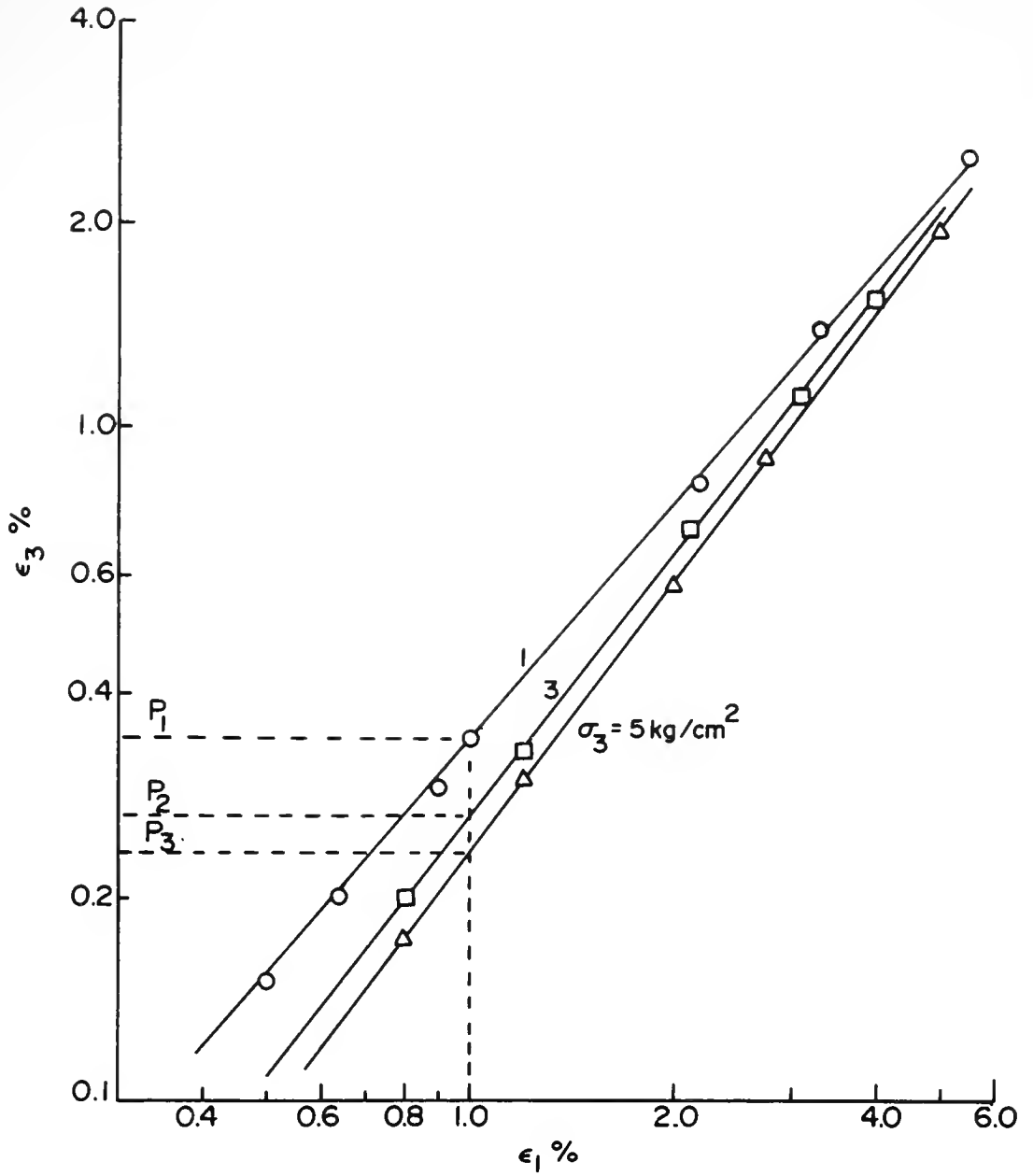


FIGURE 4.6(a) LOG-LOG PLOT OF ϵ_3 % VS. ϵ_1 %.
(Data From Duncan and Chang, 1970)

expressed as an exponential function

$$- \epsilon_3 = P \cdot \epsilon_1^m \quad (4.30)$$

where P is the value of $-\epsilon_3$ at $\epsilon_1 = 1\%$ and m is the slope of the straight line. For some soils similar plots for various confining pressures show more or less the same slope of the line; in other words value of m is independent of confining pressure. The position of the line is shifted with confining pressure; that is, values of P will be different. If values of P are plotted against $(\frac{\sigma_3}{p_a})$ in a log-log diagram, it results in a straight line (Figure 4.6b). This line can be expressed as:

$$P = L \left(\frac{\sigma_3}{p_a} \right)^q \quad (4.31)$$

in which L is the intercept at $\frac{\sigma_3}{p_a} = 1$ and q is the slope of the line. Substituting for P from equation (4.31) into equation (4.30) results

$$- \epsilon_3 = L \left(\frac{\sigma_3}{p_a} \right)^q \epsilon_1^m \quad (4.32)$$

Tangent Poisson's ratio can be determined from the above equation (4.32) by taking the first derivative with respect to ϵ_1 .

$$\nu_{\tan} = - \frac{d\epsilon_3}{d\epsilon_1} = L \cdot m \cdot \left(\frac{\sigma_3}{p_a} \right)^q \cdot \epsilon_1^{m-1} \quad (4.33)$$

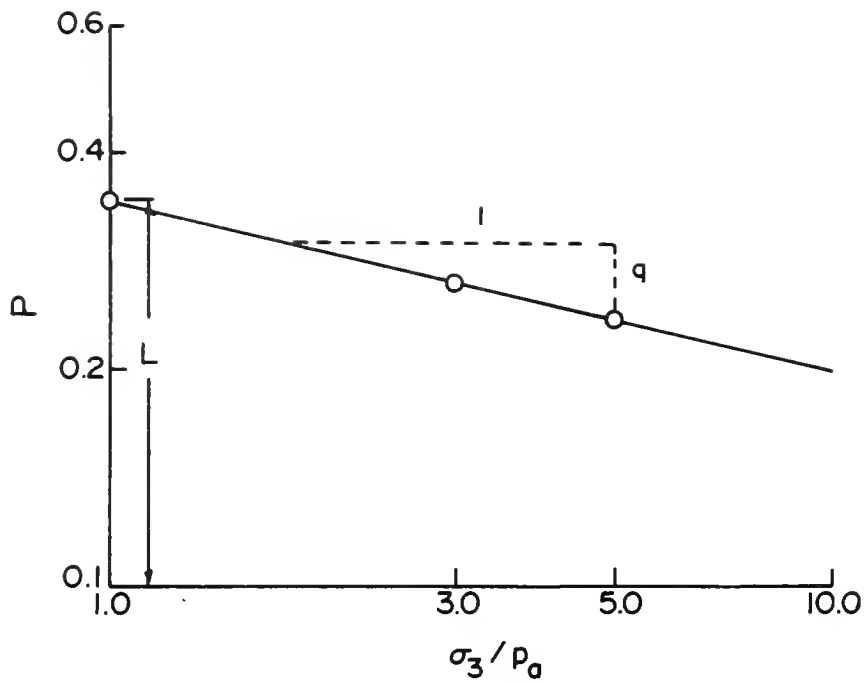


FIGURE 4.6 (b) LOG-LOG PLOT OF P VS. σ_3/p_0 .
(Data From Duncan and Chang, 1970)

value of ϵ_1 in this equation is the total major principal strain in percent. Using parameters L , m , q and values of ϵ_1 the tangent Poisson's ratio for primary loading can be determined for any state of stress in triaxial compression. Lade (1972) has shown good agreement of the experimental and predicted values of tangent Poisson's ratio up to about 2% axial strain.

From the results of triaxial tests the coefficients in equations (4.4) and 4.33) can be evaluated and values of E_t and ν_t can be obtained for plane stress conditions. In principle, the corresponding values for plane strain conditions should be given by

$$E_{pl} = \frac{E_t}{(1 - \nu_t^2)} \quad (4.34)$$

$$\nu_{pl} = \frac{\nu_t}{1 - \nu_t} \quad (4.35)$$

but the carefully conducted triaxial and plane strain tests by Lade (1972) showed that this is not the case (Figures 4.6c and 4.6d). For this reason, it was decided to fit spline functions to the actual test data and obtain E_t and ν_t directly from the data for any given stress state, which is defined in terms of octahedral stresses. Details of the procedure are given in Section 4.9. It is recognized that an incrementally elastic representation of soil properties is inaccurate if the soil is approaching failure, or is in a post-peak stress-strain range, because for these conditions plastic strains dominate behavior. However, suitable elastic-plastic formulations are still in too formative a stage (Lade and Duncan, 1976) for practical use.

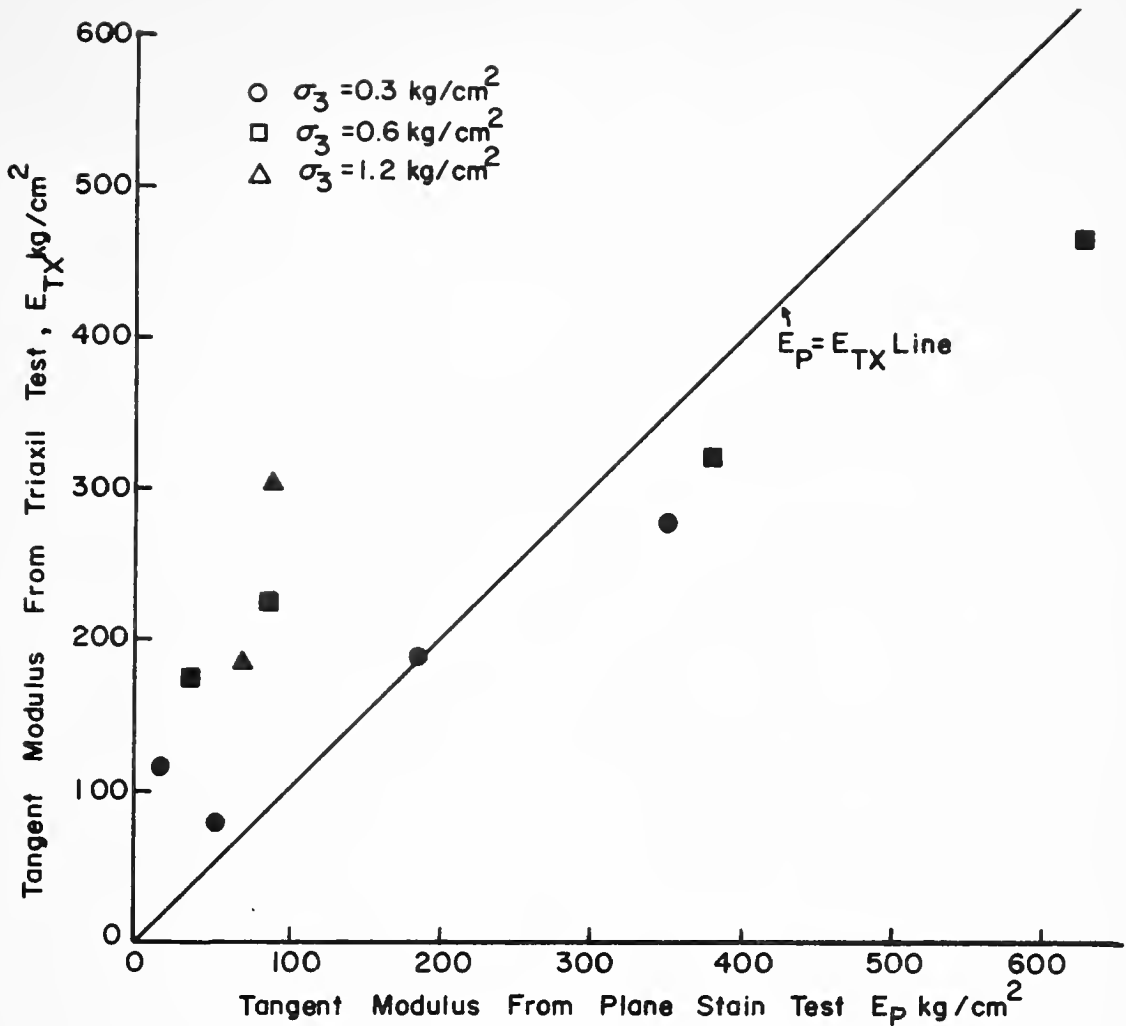


FIGURE 4.6 (c) COMPARISON OF TANGENT MODULUS FOR PLANE STRAIN CONDITION
 (1) DETERMINED FROM PLANE STRAIN TEST, E_P
 (2) CALCULATED FROM TRIAXIAL TEST USING FORMULATION (4.4), (4.34) AND (4.35), E_{TX}

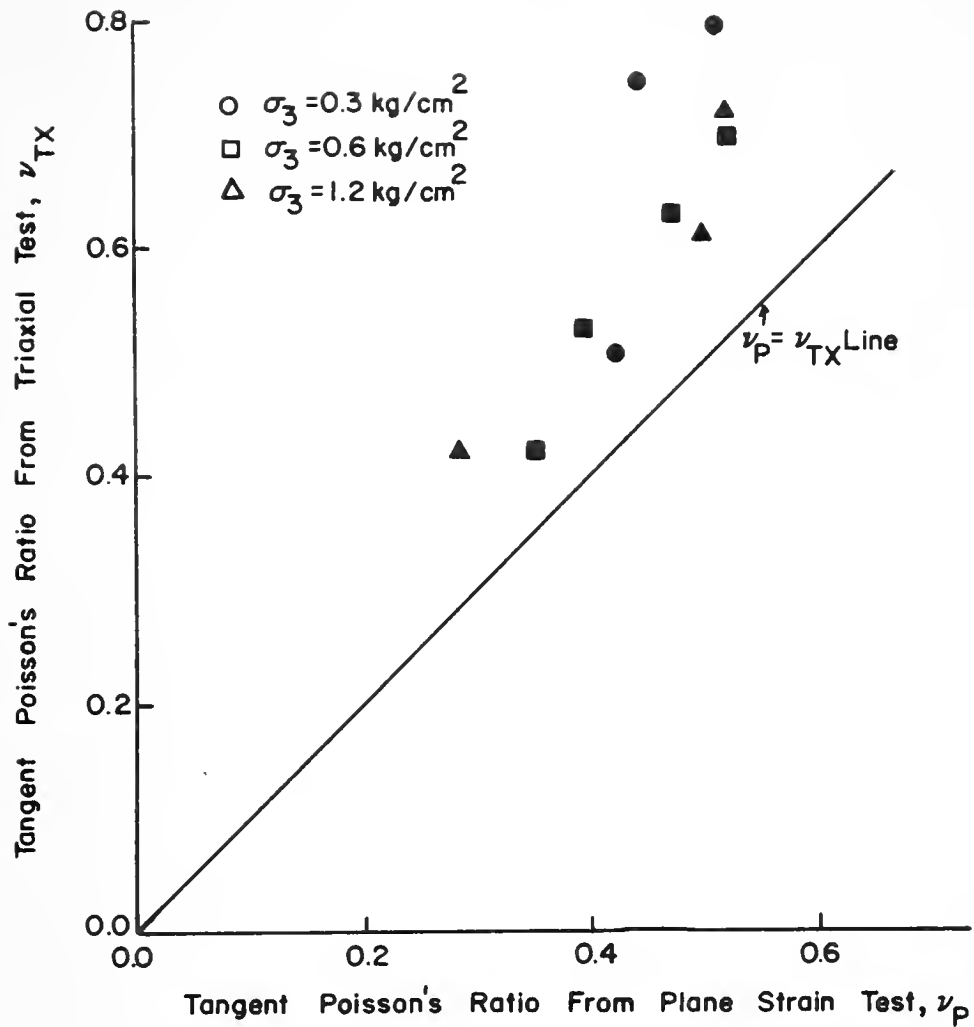


FIGURE 4.6 (d) COMPARISON OF TANGENT POISSON'S RATIO FOR PLANE STRAIN CONDITION

- (1) DETERMINED FROM PLANE STRAIN TEST, ν_P
- (2) CALCULATED FROM TRIAXIAL TEST USING FORMULATION (4.4), (4.34) AND (4.35), ν_{TX}

4.7 Anisotropy

Strength anisotropy in vertical and horizontal directions of naturally deposited soil is well accepted in the literature. The reason for strength anisotropy is that during deposition of a soil layer by a natural process, soil particles attain some preferred orientation. It is also known that soil particles do not have any regular shape. As a result, a soil layer offers more resistance to deformation due to an imposed load in one direction than another direction. Madhav and Roy (1970) have determined the anisotropy ratio of vertical to horizontal shear strength about 1.5. Holubec (1968) has shown that for cohesionless soil Young's modulus in vertical direction, E_v is greater than that in horizontal direction, E_H , i.e., $E_v > E_H$ as shearing increases. For initial equal all around pressure Poisson's ratio in vertical direction, ν_v is greater than that in horizontal direction ν_H . i.e., $\nu_v > \nu_H$; and as shearing increases, a reversal occurs, $\nu_v < \nu_H$. If $E_v > E_H$, no matter what is the relation between ν_v and ν_H , horizontal stress will be less than if $E_v = E_H$.

Poulos (1972) has shown that horizontal deflection of a foundation can not be predicted assuming soil as homogeneous, elastic isotropic material. He cited the following parameters as having important effects on the mechanism of stress and strain distribution in a soil medium: (1) Horizontal soil modulus value, E_H and the ratio of E_v/E_H ,

(2) Horizontal Poisson's ratio, ν_H has greater influence, as vertical deflection is a function of $(1-\nu^2)$ whereas horizontal deflection is a function of $(1+\nu)(1-2\nu)$.

Wright and Duncan (1972) studied sliding of the Waco Dam. Investigation showed that undrained shear strength of the material was highly anisotropic. Ratio of horizontal to vertical strength was about 0.4. Analyses based on the assumption that the soil is isotropic indicates a stable condition of the dam, whereas use of anisotropic strength as determined by experiments, produced results in agreement with the observed failure. This study shows the significance of considering anisotropy in analysis.

The most commonly used pipe materials are concrete, steel and aluminum, which can reasonably be considered as isotropic materials in the stress range preceding failure. Hence no consideration of anisotropy is given to these materials. For pipes constructed of composite plastic laminates, the effects of anisotropic properties are important, and can be handled by following the procedure described in the next section.

Anisotropic Pipe Properties (for thick pipe only)

Pipes constructed of composite plastics may be highly anisotropic; also, the directions of principal anisotropy change continually along the perimeter of pipe. This requires transformation of elastic properties according to its geometric orientation.

Stavsky and Hoff (1969) presented a procedure for transformation of elastic properties for orthotropic composite materials. The method is based on the theory of elasticity and was presented in detail by Lakhnitskii (translated from Russian by P. Fern, 1963). In Figure 4.7 a block of an orthotropic material is shown along with the global coordinate direction (x,y) . At any point the normal direction N , and the tangential direction S , is shown at an angle α with the global coordinate axes. In the following developments subscripts x and y will denote quantities in X and Y directions. Similarly subscripts n and s will be used to refer to quantities in normal, N and tangential, S directions.

According to the theory of elasticity, in the most general case the expression for elastic potential, V , can be considered in terms of component stresses and strains, and can be written as:

$$V = \frac{1}{2}(\sigma_x \epsilon_x + \sigma_y \epsilon_y + \dots + \tau_{xy} \gamma_{xy}) \quad (4.36)$$

in which σ and ϵ refer to normal stress and strain, τ and γ represent shear stress and shear strain. Then the elastic potential is expressed in terms of rotated coordinate system. As the elastic potential is independent of the coordinate system, the two expressions can be equated. Then, equating the coefficients of similar terms, the unknown constants of transformation can be determined. After simplification, the following set of equations can be written, which relate properties in the transformed axes to those in the global axes.

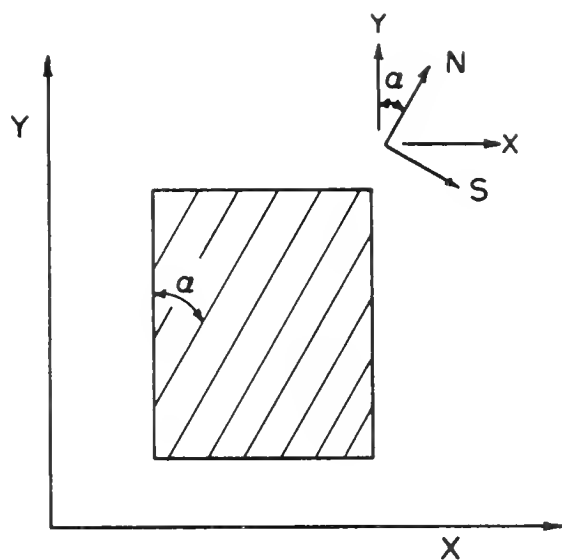


FIGURE 4.7 CO ORDINATE SYSTEM FOR TRANSFOR-
MATION OF ANISOTROPIC MATERIAL
PROPERTIES.



$$\frac{E_n}{E_y} = \cos^4 \alpha + \frac{E_n}{E_s} \cdot \sin^4 \alpha + \frac{1}{4} \left[\frac{E_n}{G_{ns}} - 2\nu_{ns} \right] \cdot \sin^2 2\alpha \quad (4.37a)$$

$$\frac{E_n}{E_x} = \sin^4 \alpha + \frac{E_n}{E_s} \cdot \cos^4 \alpha + \frac{1}{4} \left[\frac{E_n}{G_{ns}} - 2\nu_{ns} \right] \cdot \sin^2 2\alpha \quad (4.37b)$$

$$\nu_{yx} = \frac{E_y}{E_n} \left[\nu_{ns} - \frac{1}{4} \left(1 + 2 \cdot \nu_{ns} + \frac{E_n}{E_s} - \frac{E_n}{G_{ns}} \right) \cdot \sin^2 2\alpha \right] \quad (4.37c)$$

in which G and ν denotes shear modulus and Poisson's ratio.

According to Maxwell's reciprocal theorem the two strains ϵ_n and ϵ_s must be equal if the two stresses σ_n and σ_s are of equal magnitude and sense. Consequently,

$$\frac{\nu_{ns}}{\nu_{sn}} = \frac{E_n}{E_s} \quad (4.37d)$$

Shear strain γ_{yx} due to stress σ_y is

$$\gamma_{yx} = \frac{-m_1 \sigma_y}{E_n} \quad (4.37e)$$

in which m_1 is given by

$$m_1 = \sin 2\alpha \cdot \left[\nu_{ns} + \frac{E_n}{E_s} - \frac{E_n}{2 \cdot G_{ns}} - \cos^2 \alpha \cdot (1 + 2\nu_{ns} + \frac{E_n}{E_s} - \frac{E_n}{G_{ns}}) \right] \quad (4.37f)$$

Shear stress τ_{yx} will produce a component of strain ϵ_x , which is given as

$$\epsilon_x = - \frac{m_2 \tau_{yx}}{E_y} \quad (4.37g)$$

where m_2 is given by

$$m_2 = \sin 2\alpha \cdot \left[\nu_{ns} + \frac{E_n}{E_s} - \frac{E_n}{2G_{ns}} - \sin^2 \alpha \cdot (1 + 2\nu_{ns} + \frac{E_n}{E_s} - \frac{E_n}{G_{ns}}) \right] \quad (4.37h)$$

In the above equations G_{ns} is given as

$$\frac{G_{ns}}{G_{yx}} = \frac{G_{ns}}{E_n} \left[(1 + 2\nu_{ns} + \frac{E_n}{E_s}) - (1 + 2\nu_{ns} + \frac{E_n}{E_s} - \frac{E_n}{G_{ns}}) \cdot \cos^2 2\alpha \right] \quad (4.37i)$$

In equation (4.37a) through (4.37i) E_n , E_s and ν_{ns} will be defined for an orthotropic material. Values of E_x , E_y , G_{yx} will be calculated for a given element depending on its position on the pipe.

The next step is to write the equations for the generalized Hook's law for plane strain conditions in the global coordinate system. In matrix form these equations can be written as

$$\begin{Bmatrix} \epsilon_x \\ \epsilon_y \\ \gamma_{xy} \end{Bmatrix} = \begin{bmatrix} \frac{1}{E_x} & -\frac{\nu_{yx}}{E_y} & -\frac{m_2}{E_n} \\ -\frac{\nu_{xy}}{E_x} & \frac{1}{E_y} & -\frac{m_1}{E_n} \\ -\frac{m_2}{E_n} & -\frac{m_1}{E_n} & \frac{1}{G_{yx}} \end{bmatrix} \cdot \begin{Bmatrix} \sigma_x \\ \sigma_y \\ \tau_{yx} \end{Bmatrix} \quad (4.38)$$

or

$$\{\sigma\} = [D] \{\epsilon\} \quad \dots \quad (4.39)$$

Inversion of the above equation (4.39) will result in the appropriate [D] matrix, which will be used as the elasticity matrix in equation (3.14a) to generate the stiffness matrix of the orthotropic pipe element.

4.8 Determination of Elasticity Matrix [D] for Soil

The stiffness matrix for a finite element consists of two key ingredients, one of them is geometry and displacement function, the other is material property and type of analysis. In equation (3.14) [b] matrix takes care of geometry and shape function; [D] matrix reflects the material properties and type of analysis. In this section development of [D] matrix considering anisotropy and plane strain conditions is presented.

The general stress strain relations for an elastic anisotropic medium can be written by assuming material properties are known in two mutually perpendicular directions

(namely vertical, y and horizontal x and z directions).

(Lekhnitskii, 1963)

$$\epsilon_x = \frac{\sigma_x}{E_x} - \nu_{yx} \cdot \frac{\sigma_y}{E_y} - \nu_{xy} \cdot \frac{\sigma_z}{E_x} \quad (4.40a)$$

$$\epsilon_y = -\nu_{yx} \cdot \frac{\sigma_x}{E_x} + \frac{\sigma_y}{E_y} - \nu_{yx} \cdot \frac{\sigma_z}{E_x} \quad (4.40b)$$

$$\epsilon_z = -\nu_{xy} \cdot \frac{\sigma_x}{E_x} - \nu_{yx} \cdot \frac{\sigma_y}{E_y} + \frac{\sigma_z}{E_x} \quad (4.40c)$$

$$\gamma_{xz} = 2(1 + \nu_{xy}) \cdot \frac{\tau_{xz}}{E_x} \quad (4.40d)$$

$$\gamma_{xy} = 2(1 + \nu_{yx}) \cdot \frac{\tau_{xy}}{E_y} \quad (4.40e)$$

$$\gamma_{yz} = 2(1 + \nu_{yx}) \cdot \frac{\tau_{yz}}{E_y} \quad (4.40f)$$

For plane, strain condition $\epsilon_z = 0$ and also γ_{xz} and γ_{yz} are zero. σ_z can be determined in terms of σ_x and σ_y from equation (4.40c) for $\epsilon_z = 0$. σ_z in equations (4.40a) and (4.40b) can be eliminated. Ratio of moduli can be defined as modular ratios $\frac{E_x}{E_y} = r$ and $m = \frac{G_{xy}}{E_y}$ where

$$G_{xy} = \frac{E_x E_y}{E_x + E_y + 2\nu_{yx} E_x}$$

Using these definitions, the stress-strain relations can be written in matrix form similar to equation (4.38). The [D] matrix can be determined by inverting the stress-strain matrix and can be written as:

$$[D] = \frac{E_y}{(1+v_{xy}) \cdot (1-v_{xy} - 2 \cdot r v_{yx}^2)} \begin{bmatrix} a & b & 0 \\ b & c & 0 \\ 0 & 0 & d \end{bmatrix} \quad (4.41)$$

where

$$a = r \cdot (1 - r v_{yx}^2)$$

$$b = r \cdot v_{yx} (1 + v_{xy})$$

$$c = (1 - v_{xy})^2$$

$$d = m \cdot (1 + v_{xy}) \cdot (1 - v_{xy} - 2r \cdot v_{yx}^2)$$

The expression for [D] as given by equation (4.41) considers both anisotropic soil properties and plane strain condition. In the above equation E_y will be determined using equation (4.18); and corresponding Poisson's ratio v_{xy} ; v_{yx} from (4.37d) and values of r will be defined as input data. This completes the evaluation of [D] matrix, which will be used in equation (3.14) to evaluate stiffness matrix for soil elements.

4.9 Use of Spline Function for Representation of Material Properties

Use of spline function for representing non-linear, stress dependent properties for soil have been presented in sections 4.5 and 4.6. In this section a procedure for reduction of test data is presented, which requires no assumptions--such as parabolic, hyperbolic, or exponential--to obtain a "fit" to the test data.

Lade (1972) conducted plane strain tests on loose sand (Monterey No. 0) for several values of confining pressure and presented results of deviator stress $(\sigma_1 - \sigma_3)$, major principal strain, ϵ_1 and volume strain, ϵ_v . Figure 4.8 shows the stress-strain and volume change curves that were obtained. In this study octahedral stresses are used, so it is necessary to change the test data from principal stress to an octahedral stress system. Every point on a curve has unique value of σ_1 and σ_3 . Value of σ_2 can be determined for plane strain conditions from equation (4.40) as values of ϵ_3 can be determined from ϵ_1 and ϵ_v and $\epsilon_2 = 0$. For, each point, octahedral normal stress σ_{oct} , and octahedral shear stress τ_{oct} are obtained from equations (D.1) and (D.2), and equation (D.8) can be used to evaluate $\tau_{oct/f}$ at failure for a given σ_{oct} . The stress ratio at failure $\tau_{oct}/\tau_{oct/f}$ is determined.

Procedure for Data Reduction

- (1) Select successive values of $(\sigma_1 - \sigma_3)$, ϵ_v and ϵ_1 from the test data at a given σ_3 starting from zero.
- (2) Cubic splines are fitted to the data following the procedure described in section 4.5.
- (3) Values of tangent modulus E_t , and tangent Poisson's ratio, ν_t , are evaluated using equation (E.16) and (E.10). (See Appendix E)

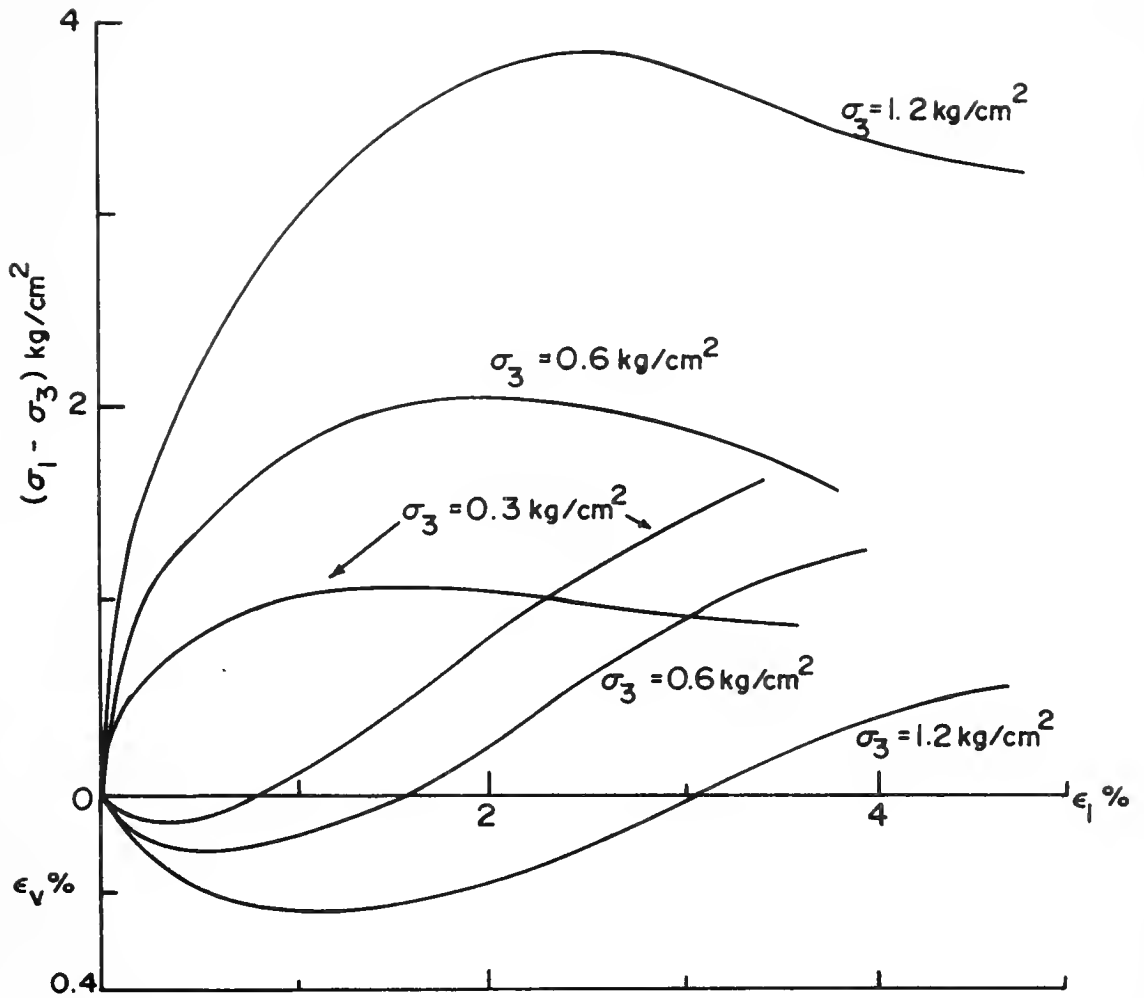


FIGURE 4.8 PLANE STRAIN TEST ON LOOSE MONTEREY NO. 0 SAND.

(4) Small increments of ϵ_1 are chosen and for each ϵ_1 , values of σ_1 , σ_2 , σ_3 , σ_{oct} , τ_{oct} , τ_{oct}/f and the failure stress ratio are evaluated using procedures described above and in section 4.5.

(5) Step 3 is repeated for each increment of ϵ_1 up to failure.

(6) Step 1 through 5 are repeated for test data at different values of σ_3 .

(7) All values of E_t are plotted against their corresponding values of σ_{oct} and values of stress ratio $\tau_{oct}/\tau_{oct/f}$ are noted for all points.

(8) Contours are drawn for selected values of the stress ratio. For convenience, values of stress ratio should range from zero to unity with increments of 0.1. This will generate 11 curves of E_t vs. σ_{oct} for stress ratio ranging from 0.0 to 1.0 (Figure 4.9).

(9) Steps 7 and 8 are repeated for tangent Poisson's ratio ν_t (figure 4.10).

(10) From the peak points in Figure 4.8 values of $\tau_{oct/f}$ and $\sigma_{oct/f}$ are calculated and shown plotted in Figure 4.11.

Lade (1972) also conducted plane strain tests on dense sand. Figure 4.12 shows typical stress-strain and volume change results. Following the procedure outlined above values of E_t and ν_t are plotted against σ_{oct} for different

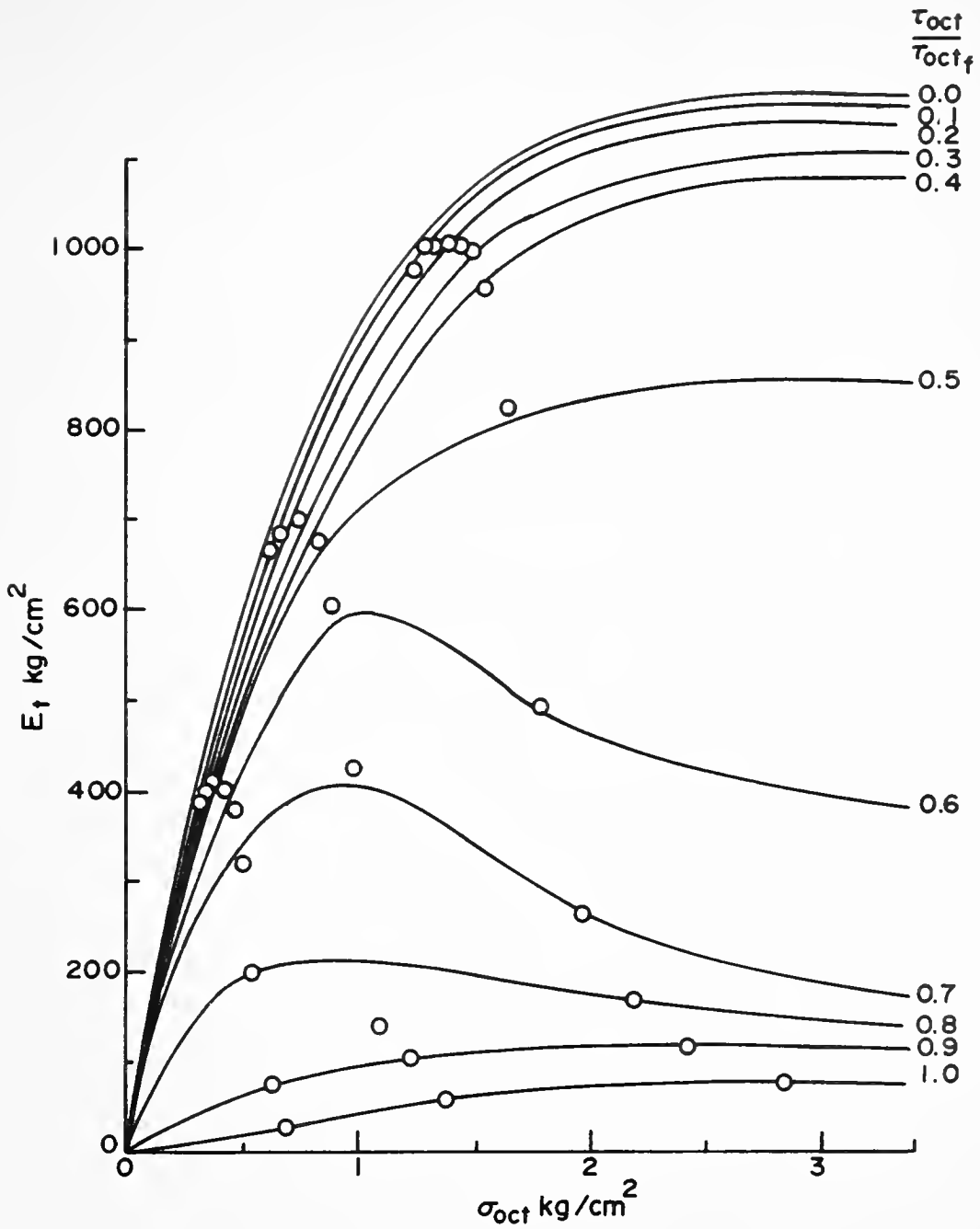


FIGURE 4.9 TANGENT MODULUS VS. OCTAHEADRAL NORMAL STRESS AND FAILURE RATIO FOR LOOSE SAND.

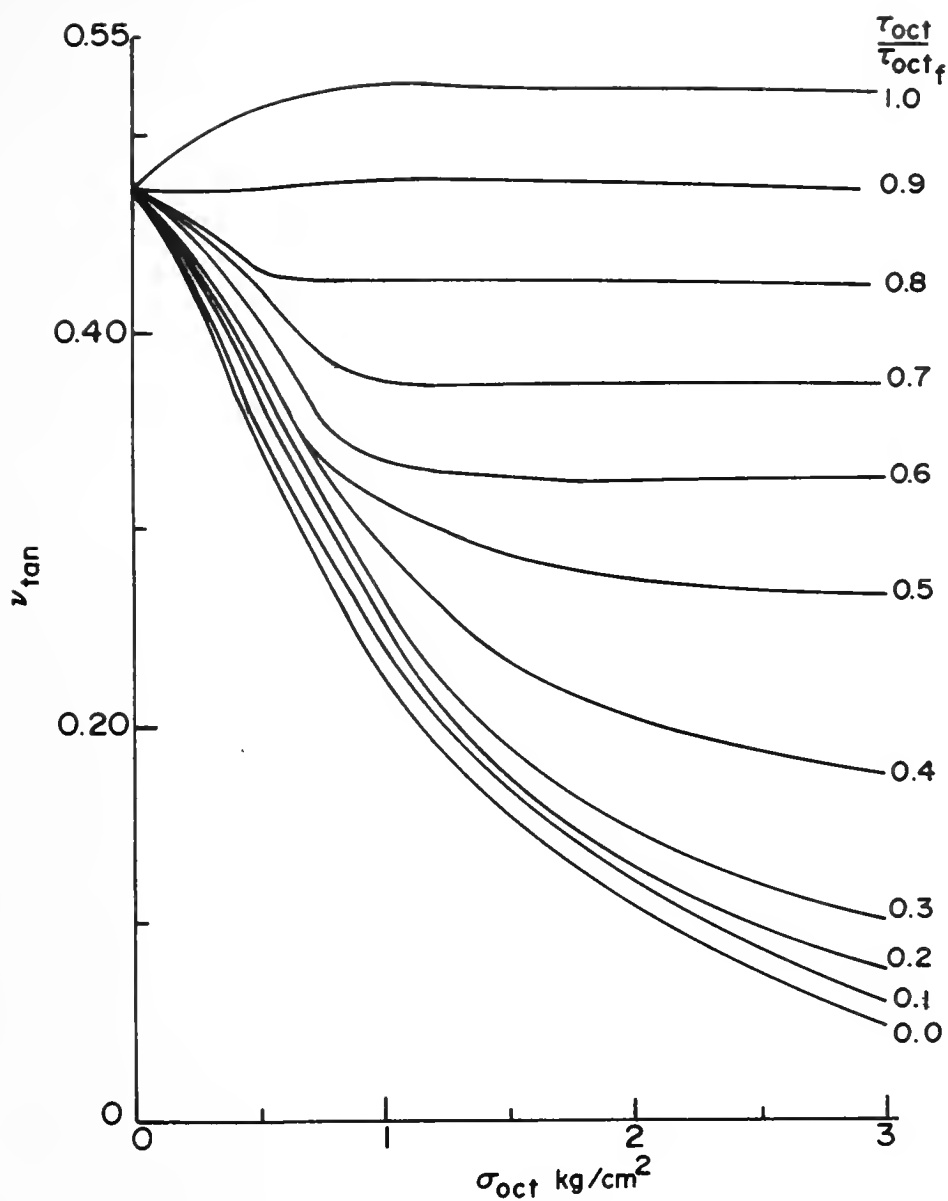


FIGURE 4.10 TANGENT POISSON'S RATIO VS. OCTAHEDRAL NORMAL STRESS AND FAILURE RATIO FOR LOOSE SAND.

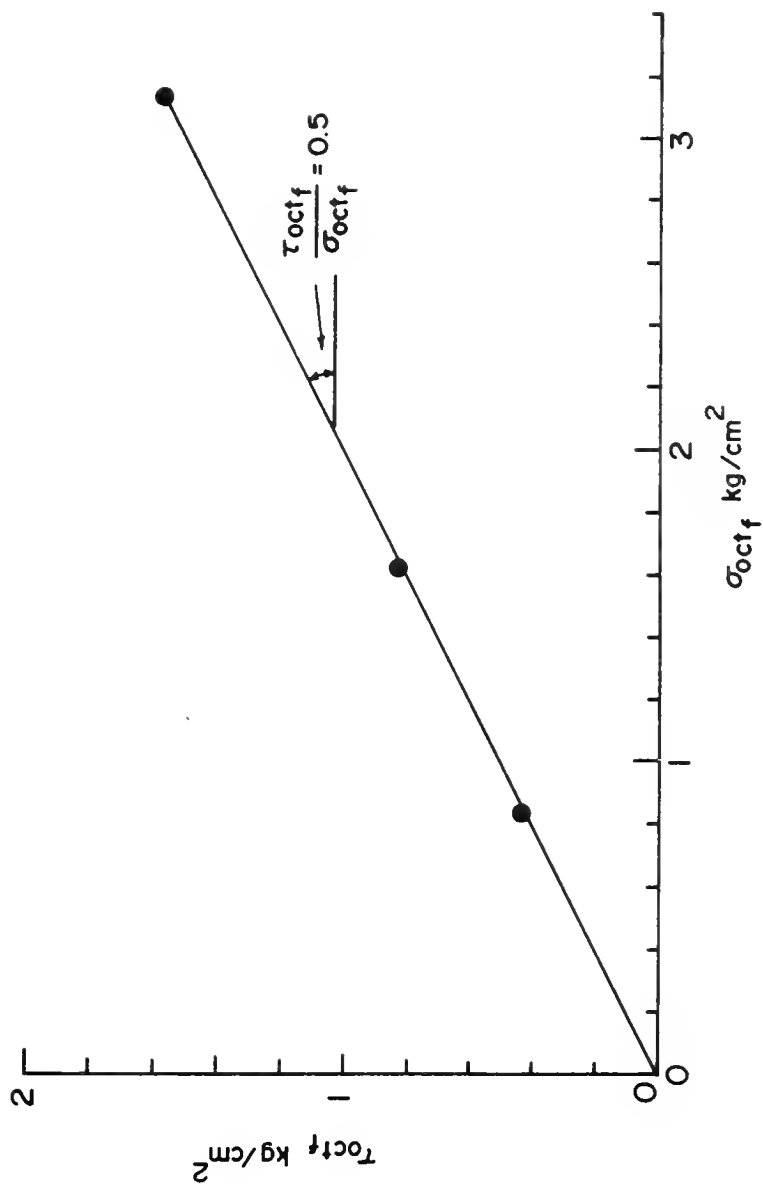


FIGURE 4.11 OCTAHEDRAL SHEAR STRESS VS. OCTAHEDRAL NORMAL STRESS AT FAILURE, LOOSE SAND.

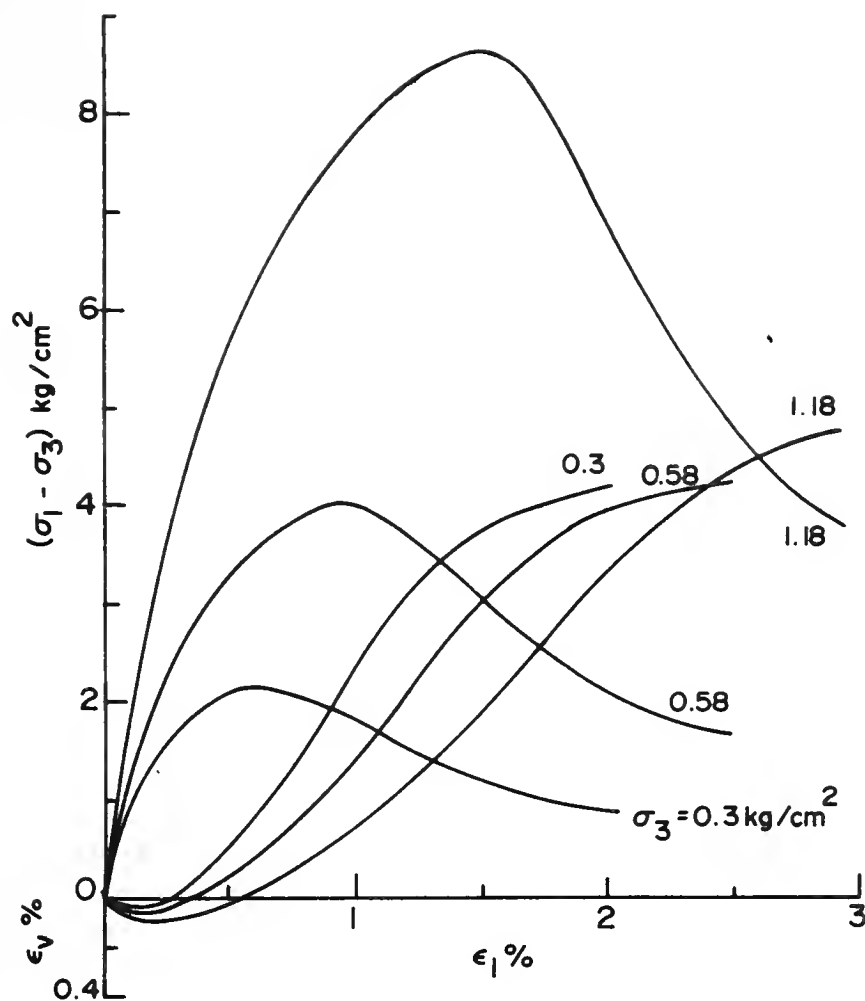


FIGURE 4.12 PLANE STRAIN TEST ON DENSE MONTEREY NO. 0 SAND. (After Lade, 1972)

values of stress ratio at failure and shown in Figure 4.13 and 4.14, respectively. Figure 4.15 shows the plot of $\tau_{oct/f}$ and $\sigma_{oct/f}$ for dense sand.

If, as in the plane strain test, the principal planes remain fixed then the procedure described previously is a precise general method for representing the constitutive relations for granular soils and storing the results in the computer. Only states of stress below failure are considered, and loading must increase continuously. However, if the principal planes rotate during loading, the directions of the principal stress and principal strain increments may not coincide. The potential effects on the stress-strain relation is not accounted for in this study.

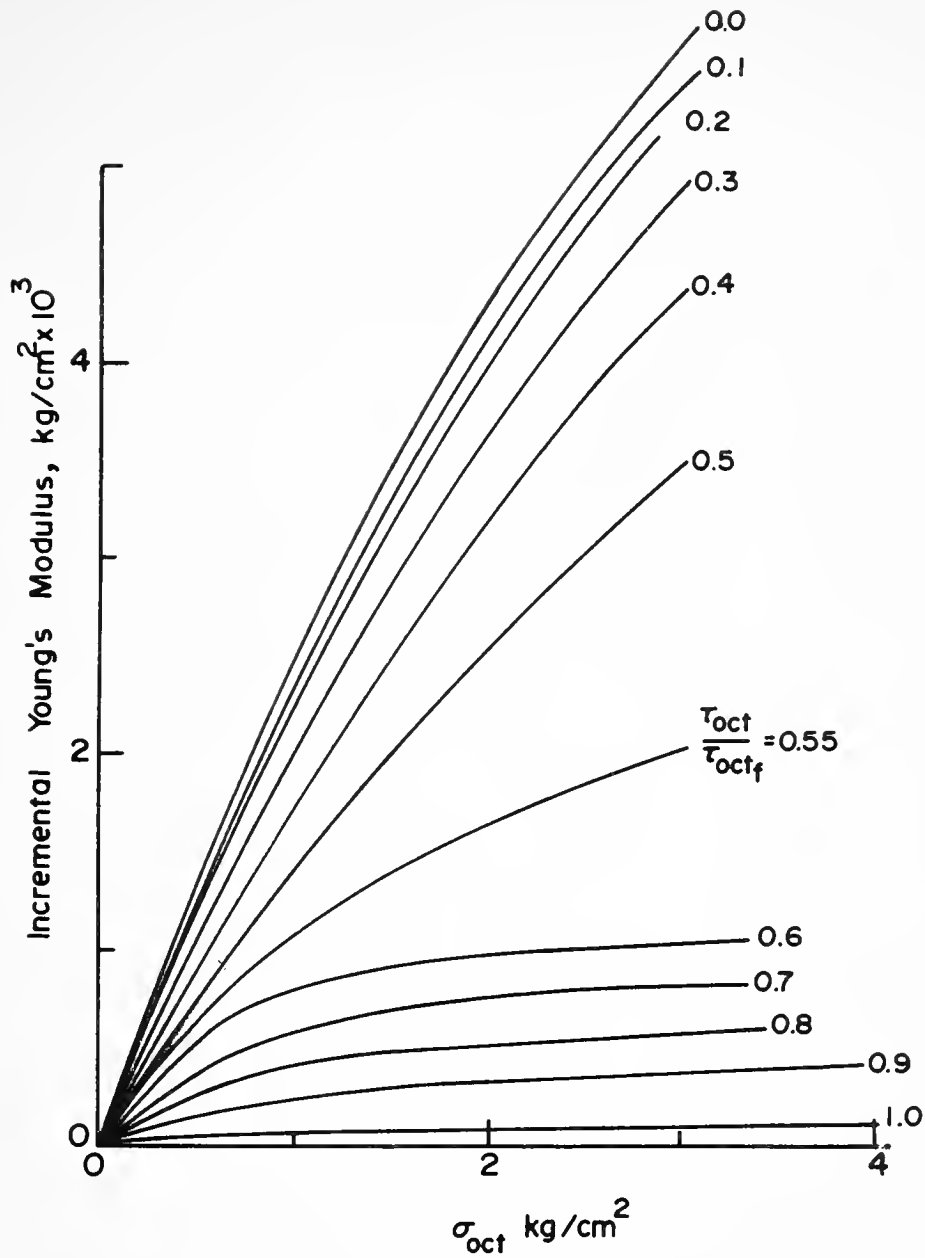


FIGURE 4.13 TANGENT MODULUS VS. OCTAHEADRAL NORMAL STRESS AND FAILURE RATIO FOR DENSE SAND.

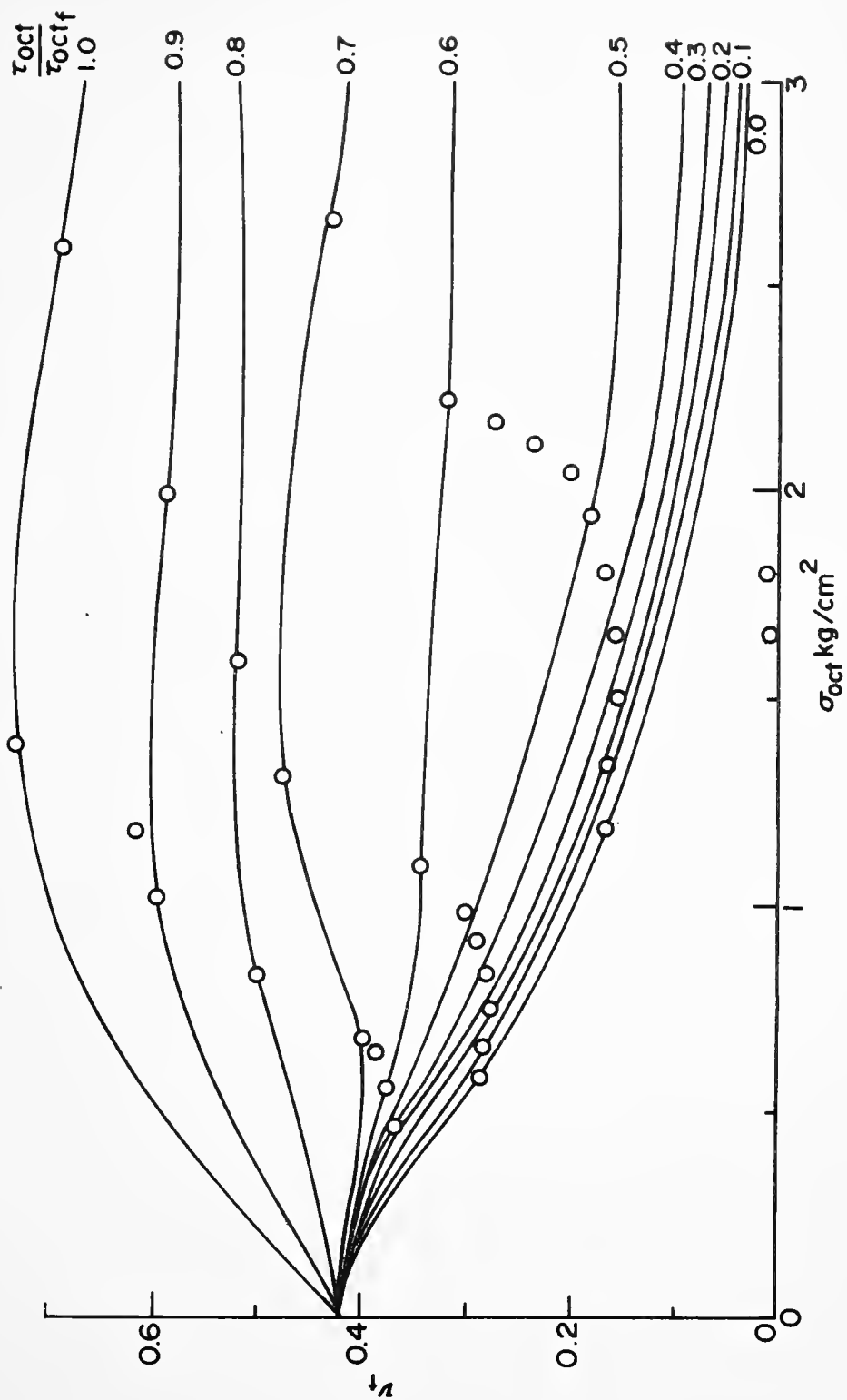


FIGURE 4.14 TANGENT POISSON'S RATIO VS. OCTAHEDRAL NORMAL STRESS AND FAILURE RATIO FOR DENSE SAND.

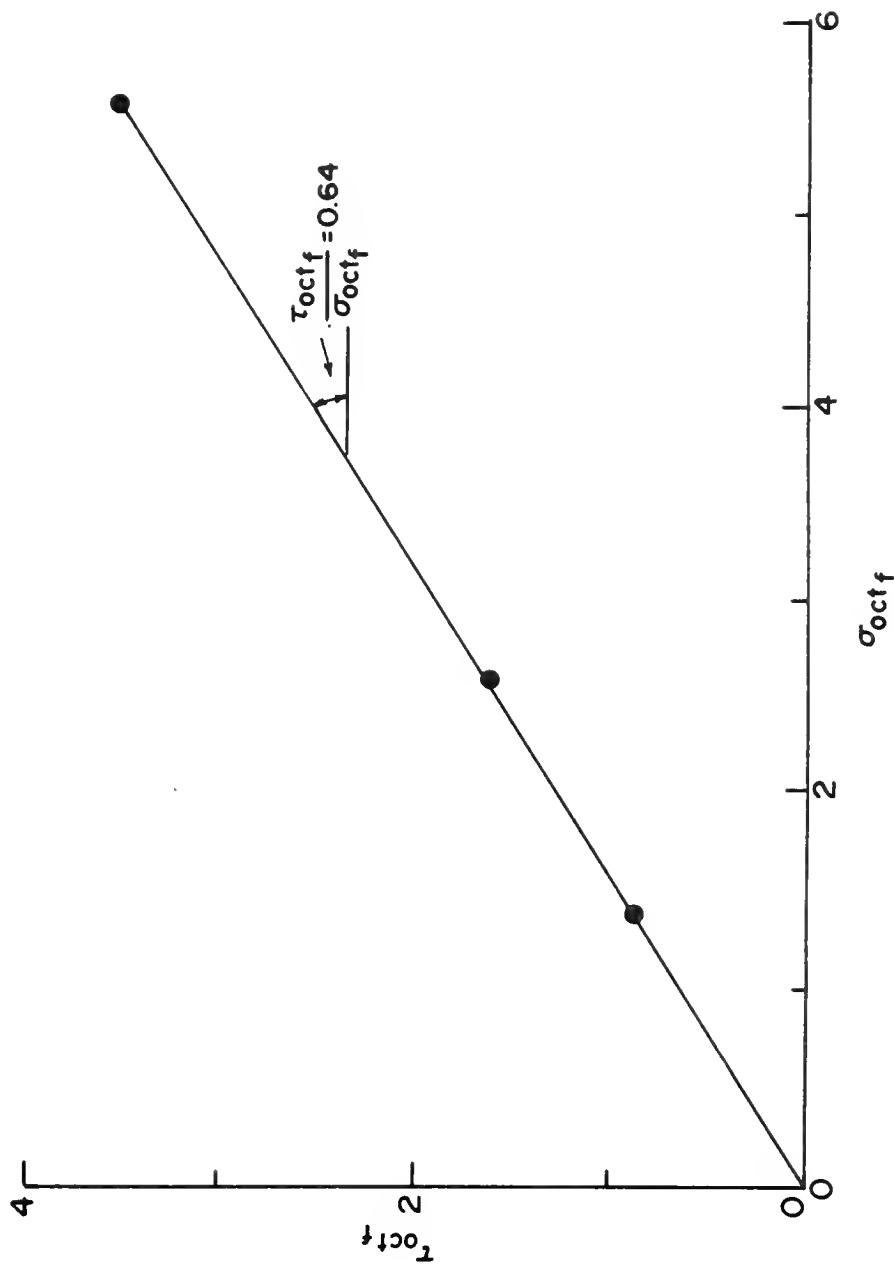


FIGURE 4.15 OCTAHEADRAL SHEAR STRESS VS. OCTAHEADRAL NORMAL STRESS AT FAILURE, DENSE SAND.

CHAPTER V

COMPUTER PROGRAM

5.1 Introduction

In Chapter II the need for a realistic analytical tool for the solution of culvert problems was described in some detail. The vehicle for solution, that is, the finite element method was discussed in Chapter III and methods for considering representative material properties were treated in Chapter IV. It is apparent that the number of variables encountered in culvert problems can be handled only with the help of a large digital computer, and that an efficient technique for numerical analysis as required. In this chapter, computer program, data structure, and solution technique developed for this study will be presented with the aid of simplified flow charts.

The Computing Center at Purdue University has a CDC 6500/6400 system computer. Therefore, the program has been written using features of CDC system. The language is FORTRAN IV, and the program is called FINLIN, (Finite element, Isoparametric, Non-Linear with Interaction and No-tension).

The following attractive features were utilized in developing the computer program:

(1) Isoparametric triangular finite elements with one curved boundary, and independent of the local coordinate system, was used to represent soil materials. The displacement function is quadratic resulting in linear strain distribution within the element.

(2) Nonlinear, stress dependent anisotropic soil properties can be used. Tangent Young's modulus and tangent Poisson's ratio for any state of stress is determined by fitting spline functions to actual test data which are represented in terms of octahedral stresses.

(3) A soil-pipe interaction element was introduced consisting of a curvilinear rectangle of zero thickness, i.e., two adjacent corners of the rectangle have the same coordinates.

(4) Bilinear stress-strain behavior, which includes slip at a critical ratio of shear stress to normal stress, was used to represent soil-pipe interface behavior.

(5) A "no-tension" analysis was used both for soil and interaction elements.

(6) Realistic representation of pipe, including rotational stiffness at nodes has been introduced using a segment of a curved bar with six degrees of freedom.

(7) Self-weight of soil is distributed throughout the soil mass, and different types of materials in different zones can be handled.

(8) By selecting appropriate options analysis using linear or nonlinear soil properties can be performed.

(9) The program is capable of incremental analysis in layers, which realistically models the construction sequence.

Limitations of the computer program are as follows:

(1) Only plane-strain conditions have been considered, so that three-dimensional effects are ignored. However, the program can be used for two-dimensional problems in plane stress conditions.

(2) Time-dependent soil properties and prestressing due to compaction has not been accounted for.

(3) Yielding or cracking of the pipe has not been considered.

(4) Only static loads can be analyzed.

(5) There is no provision for automatic mesh generation.

5.2 Program Outline

Any finite element scheme requires the following sequence of operations.

(1) Reading information about nodes, elements and boundary conditions.

(2) Input of material properties.

(3) Generation of element stiffness matrix and assembly to form the structure stiffness matrix with modifications for given boundary conditions.

(4) Solution of stiffness equations for given internal and external loads.

(5) Determination of element strains and stresses.

(6) Recycling according to given options for analysis.

The computer program FINLIN follows a similar sequence of operations. Descriptions of each of these steps are presented in later section. First, some special features of the computer system will be discussed, which are helpful in writing programs which require large memory locations and involve very large numbers of numerical operations.

Overlay

Overlay is a high speed loader system which transfers relocatable program sources to central memory for execution. Each overlay consists of a main program and associated subroutines. Each overlay is identified with a pair of integer numbers, the first number is for primary and the second for secondary levels. Transfer of all information from one overlay to another can be achieved by using blank common, labelled common or by disc tape units. All overlays excepting the main overlay (0,0) are stored outside the central memory. Any primary or secondary overlay can be loaded to the memory when called by an appropriate control card. The main advantage of using an overlaid system is that portions of a program which are not needed at one time can remain outside the central memory and does not occupy these

valuable spaces. As a result, more storage space is available for usage. For example, when the program is evaluating the stiffness matrix and solving for displacements, routines for stress or strain are not needed. Hence, routines for stress and strain can be stored elsewhere.

(Disc) Tape Unit

These units are used for temporary READ/WRITE operations for unformatted and/or formatted operations. Large amounts of information (e.g., nodal and element data), which are used several times in the program can be written on tape units and the memory locations thus released can be used for some other purpose. Necessary sets of data can be read from the tape unit when required; a desired set of data can be found by following the sequence in which the data has been written on the unit. So a bookkeeping of the sequence has to be maintained throughout. Also READ and WRITE operations can not be mixed. Though rewinding a tape unit is permitted at any stage, the READ or WRITE operations have to be sequential. This limitation causes some difficulty for general use.

Random Mass Storage

This technique is similar to the disc tape unit but the need for bookkeeping has been eliminated. This is done by assigning an index number for each record and defining the length of each record. The READ/WRITE operations can be

arbitrary rather than in sequential form. This facility can be used very efficiently for nonlinear analysis where the state of stress and strain are required very often. The element numbers can be used as index number.

The above mentioned features have been fully utilized in writing the computer program. The scheme of operations has been subdivided into several OVERLAY's whose functions are described here.

Figure 5.1 shows the organization of a complete program which consists of several OVERLAYS. Figure 5.2 shows the flow chart for OVERLAY (0.0) which happens to be the main OVERLAY. Calling and execution of all other OVERLAYS are controlled by this section depending upon the type of analysis desired.

The flow diagram for OVERLAY (1,0) is shown in Figure 5.3. Description of problem geometry, materials, number of nodes and elements are read here. Semi-band width of the stiffness matrix, number of degrees of freedom are calculated. Nonlinear material properties are read for each type of material. Data reduction and spline fitting is performed and pertinent parameters, such as tangent modulus and tangent Poisson's ratio, are evaluated and stored for future use. Geometry, properties and location of pipe is also read here. Evaluation of area for triangular elements, and other values are computed here.

OVERLAY (2.0) plots the finite element mesh from the data read earlier, Figure 5.4.

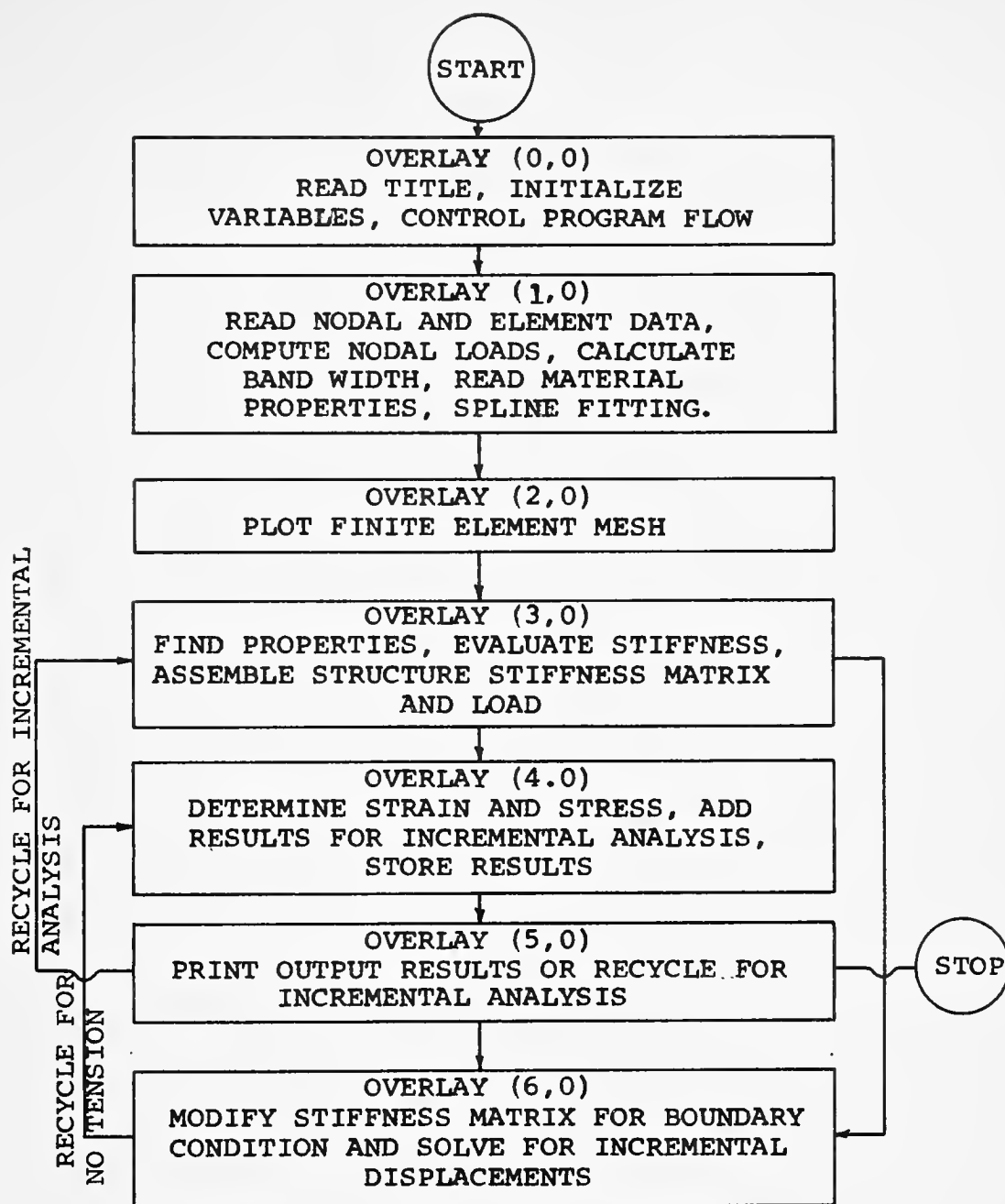


Figure 5.1 General Flow Chart of Program FINLIN

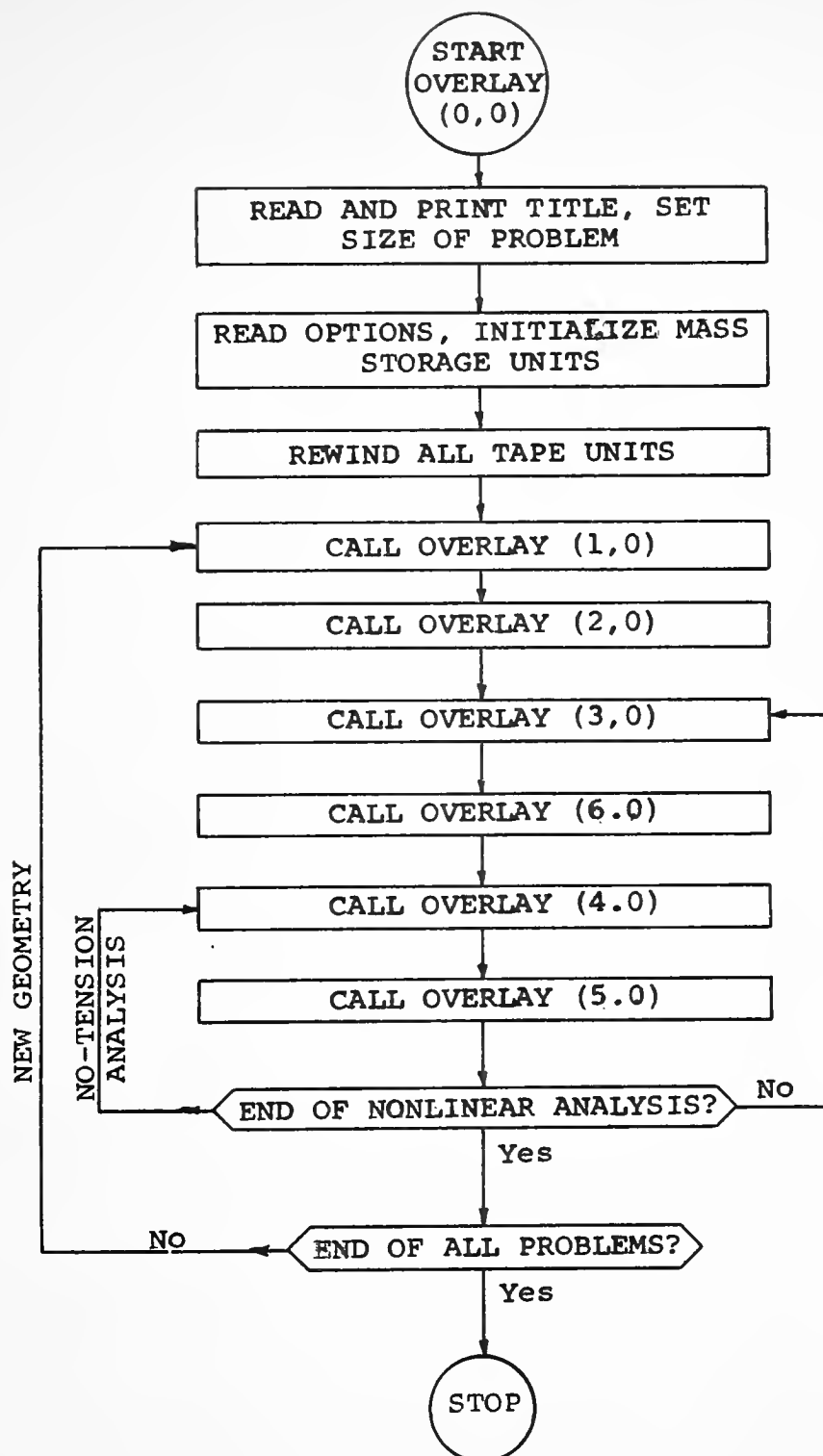


Figure 5.2. Flow Chart for OVERLAY (0,0)

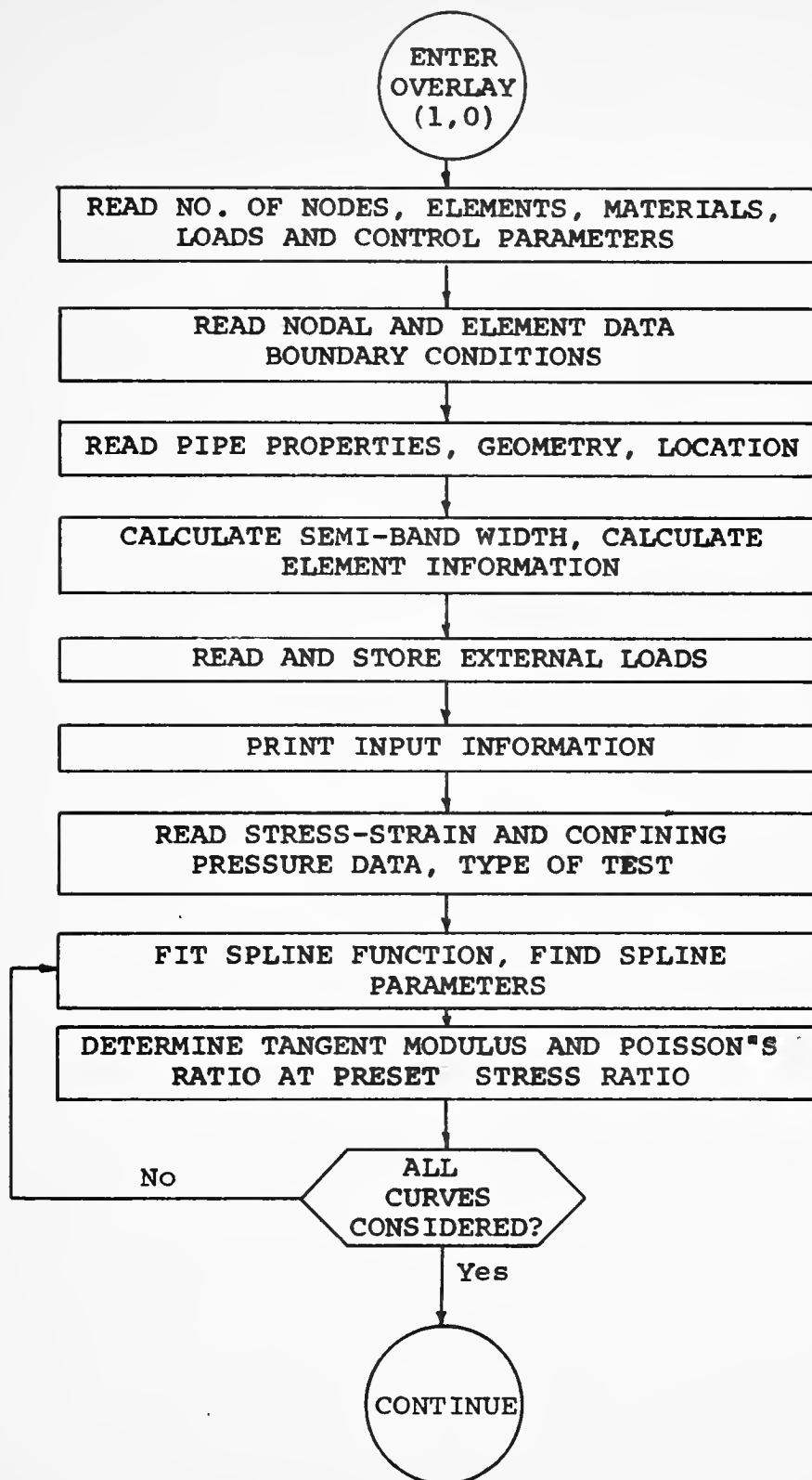


Figure 5.3 Flow Chart for OVERLAY(1,0) , (Continued)

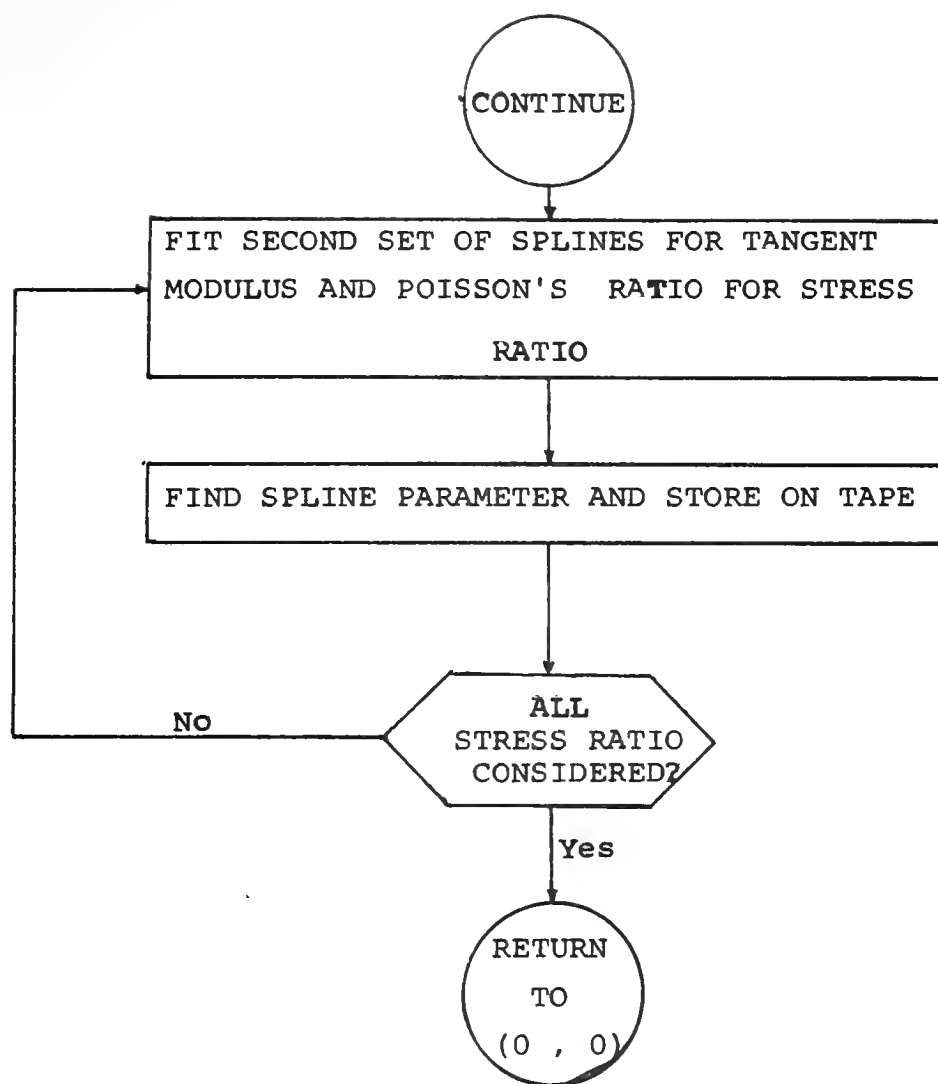


Figure 5.3 Flow Chart for OVERLAY (1,0)

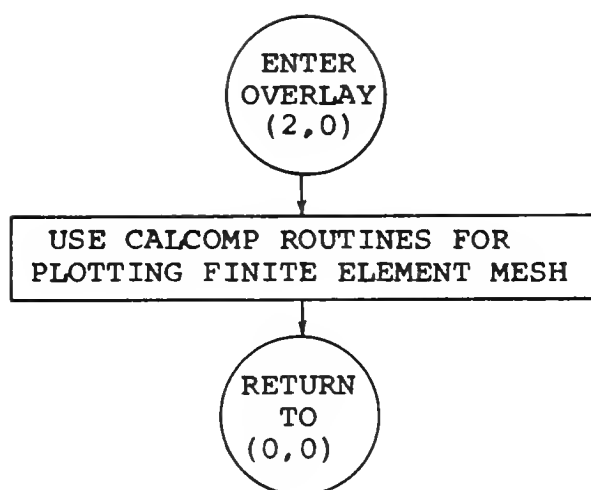


Figure 5.4 Flow Chart for OVERLAY (2,0)

The most important portion of the program is OVERLAY (3.0), which is shown in Figure 5.5. In this section evaluation of the stiffness matrix, structural assembly, and estimation of nodal loads is carried out. Because of limited capacity of the computer's core memory, all elements in the structure can not be assembled at one time. This is done in blocks the size of which should be at least a square array of the size of semi-band-width of the assembly [semi-band-width is evaluated and stored in OVERLAY (1,0)]. Then a searching scheme locates which of the nodes and corresponding elements should fit in the first block. Evaluation of stiffness matrix is performed element-by-element. The three types of elements, curved bar, interaction, and triangular elements, are each treated separately because of their different characteristics, and are described here.

Type 1, Curved Bar Element

The pipe radius, EI value, angle β , (Figure B.1), position of center of pipe and angles ϕ_1 and ϕ_2 (Figure B.2) need to be calculated from the information supplied by OVERLAY (1,0). As properties of the pipe remain constant, no particular attention is required for non-linear behavior. Stiffness coefficients for element 1-2 (Figure B.1) are evaluated and transformed to the global axes using equation (B.16).

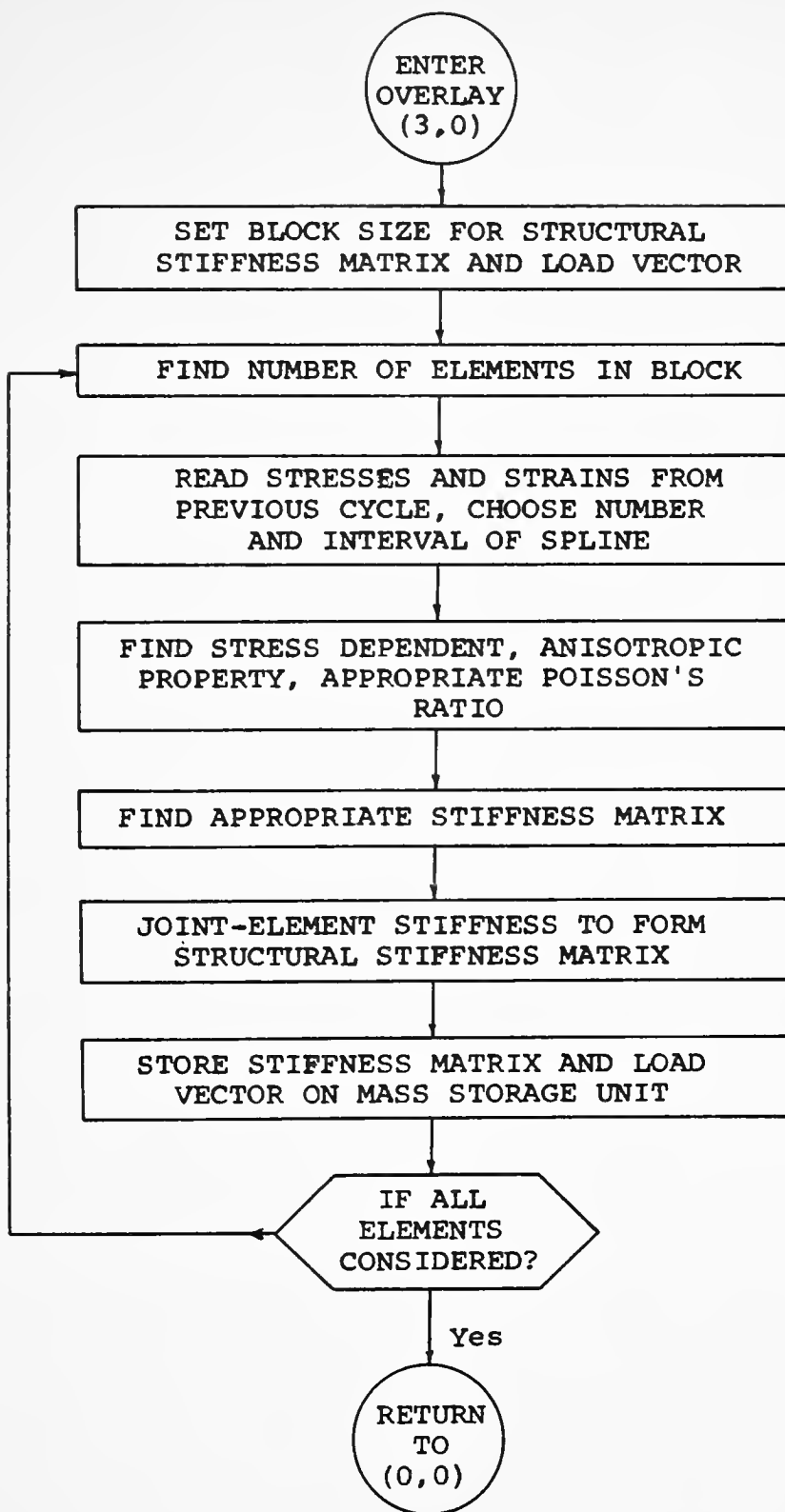


Figure 5.5. Flow Chart for OVERLAY (3,0)

Type 2, Interaction Element

There are two alternatives depending whether interaction behavior is desired or not. If interaction is not required, properties of interaction are maintained constant throughout and evaluation of stiffness matrix proceeds as described in Appendix C.

If interaction behavior is required then for the first step the scheme follows the procedure for a no-interaction situation. In subsequent steps, the normal stress on the element due to all previous increments are read from mass storage data. If the normal stress is compressive, and the ratio of shear stress to normal stress is less than the limiting value, the modulus in tangential direction, E_t is maintained at the same high value as that for normal direction, E_n

$$E_n = E_t \rightarrow \infty \quad (5.1)$$

If the normal stress on the interaction element is zero in nature, both E_t and E_n are set to small values (because zero values for E_n and E_t will create ill-conditions).

If the normal stress on the interaction element is compressive but the ratio of shear stress to normal stress is larger than the limiting value, the E_n value is kept unchanged while E_t is set to a small value, which simulates slip.

In case of failure of the interaction element either due to excessive shear stress or to tension, a message will be printed to that effect. In case of tension, excess tension is eliminated by "no-tension" analysis, as described later.

Triangular Element

This type of element is used for the soil mass. It can have linear elastic or nonlinear properties depending upon the option. Anisotropy parallel to the general coordinate system is also permitted and can be handled as described in section 4.8. For linear elastic properties, the modulus value in vertical direction, Poisson's ratio, and the anisotropy ratios need to be defined. Elasticity matrix [D] is evaluated using equation (4.41) and the stiffness matrix is developed following the procedure described in Appendix A.

For nonlinear properties an incremental procedure is required. In the first step initial values for Young's modulus and Poisson's ratio are used. In subsequent steps the state of stress due to all previous steps are read from mass storage data. To determine the appropriate values of tangent modulus and Poisson's ratio, the interval of octahedral normal stress and the interval of the ratio of octahedral shear stress to octahedral shear stress at failure must be available.

For octahedral normal stress, the program conducts a search in a table generated in OVERLAY (1,0) and stores the limits of that particular interval. Then the octahedral shear stress at failure for a given octahedral normal stress is determined directly from the test data, in the case of plane strain tests or from the following expression in the case of plane stress tests:

$$\left. \frac{\tau_{\text{oct}}}{\sigma_{\text{oct}}} \right|_{\text{failure}} = \frac{1}{1+\psi} \sqrt{2(\psi^2 - \psi + 1) - \frac{6N_{\phi}}{(N_{\phi} + 1)^2}} \quad (5.2)$$

$$\psi = \frac{\sigma_1 + \sigma_3}{\sigma_2}, \quad N_{\phi} = \frac{1+\sin\phi}{1-\sin\phi}$$

where

τ_{oct} = octahedral shear stress at failure

σ_{oct} = octahedral normal stress at failure

ϕ = friction angle of soil

σ_1 = major principal stress

σ_2 = intermediate principal stress

σ_3 = minor principal stress.

Derivation of expression (5.2) can be found in Appendix D.

In equation (5.2), for given values of ψ and ϕ , values of $\left. \frac{\tau_{\text{oct}}}{\sigma_{\text{oct}}} \right|_f$ can be determined. Multiplying this ratio by σ_{oct} , the value of τ_{oct} at failure is known.

Dividing τ_{oct} of the element by $\tau_{\text{oct}}|_f$ the failure stress ratio can be determined. This ratio is the second parameter required to find appropriate value of tangent modulus and Poisson's ratio; the program automatically interpolates the stored data to obtain values corresponding to the actual state of stress.

The elasticity matrix [D] for the soil element is calculated using equation (4.41). The rest of the procedure is same as described in Appendix A.

Structural Assembly

Knowing the stiffness matrix of an element, the structure can be assembled by a routine operation of adding appropriate coefficients in the total stiffness matrix using element information supplied by OVERLAY (1,0). In such a way the first block of equations are formed. As the stiffness matrix is symmetric in nature, only the above diagonal portion of the matrix is generated and stored in a random mass storage unit. The same memory space can now be used to assemble the second and subsequent blocks of equations until all nodes are considered.

To calculate the nodal load vector due to gravity load, total weight of each soil element is determined by multiplying unit weight by the area. Total load of an element is distributed in all six nodes. One-twelfth of total load is carried by each of corner node and one-quarter of total load is carried by each mid-side node. Total load at

a node is the summation of nodal loads from each element connected at the node. This nodal load vector is also stored in a random mass storage unit.

Solution of Stiffness Equation:

Several approaches for solution of simultaneous linear equations have been tried, including Cholesky's method, and modified Cholesky's scheme. These schemes take advantages of banded nature and symmetry of equations. The Cholesky's scheme is difficult to use in large problems because the method requires the complete matrix to remain in central memory during the solution process, and requires taking square root. The square root of a negative argument is imaginary, so the scheme requires a very well conditioned matrix (which may not be true for conditions like slip in the interface element or very low tangent modulus value at stress ratio 1). This difficulty can be overcome by using modified Cholesky's method which avoids taking square root, but for large problems the computer time needed for solution is prohibitive.

Christian (1973) reviewed the existing schemes for solution of simultaneous equations. He pointed out advantages and disadvantages of different methods. But none of the methods reviewed can be considered efficient (and economic) under all conditions. Klyuyev and Kokovkin-Scherbak (1965) pointed out that for solution of a system of equations the Gauss elimination process requires the least number of

arithmetic operations. Based on this finding a scheme for solution has been developed using Gauss elimination. In this process, the equations are stored on disc unit sequentially. During the reduction process only a block of equations of the size of a semi-band width by semi-band width remains in central memory. After reduction, one block of reduced equations is written on a tape unit and one block of equation is read. Solution is obtained by backsubstitution in the reduced equation. This is done in a similar fashion as in the reduction process itself. Solution of the stiffness equations for given nodal load and boundary condition is performed in OVERLAY (6,0) whose flow-chart is shown in Figure 5.8.

From the node point deflections, the stresses and strains are determined. This is done in OVERLAY (4.0) and is shown in Figure 5.6. Different components of strain can be determined from geometric properties, shape functions and nodal displacements by using equation (3.12). Once strains are known, the stresses can be determined by multiplying the strain matrix with $[D]$ matrix for the same element. Stress and strain increments for each increment cycle are evaluated and added to the values of the previous cycle.

The last and final step in the scheme is to print the results. This is done in OVERLAY (5.0) and shown in Figure 5.7. In this OVERLAY the node point deflections are added to those from previous cycles and all components of element

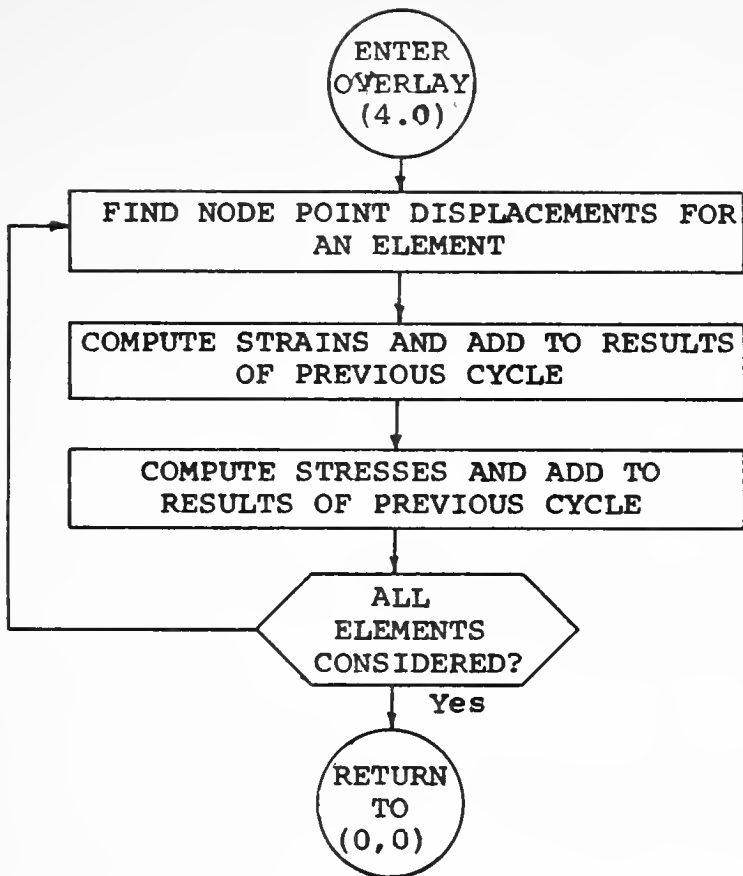


Figure 5.6. Flow Chart for OVERLAY (4,0)

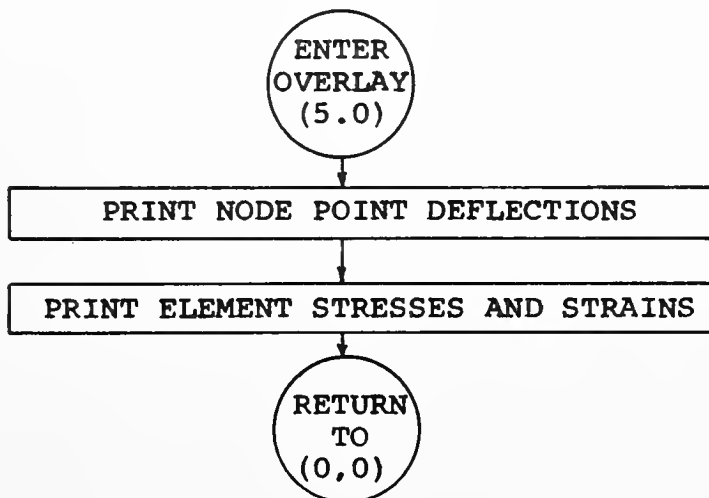


Figure 5.7 Flow Chart for OVERLAY (5,0)

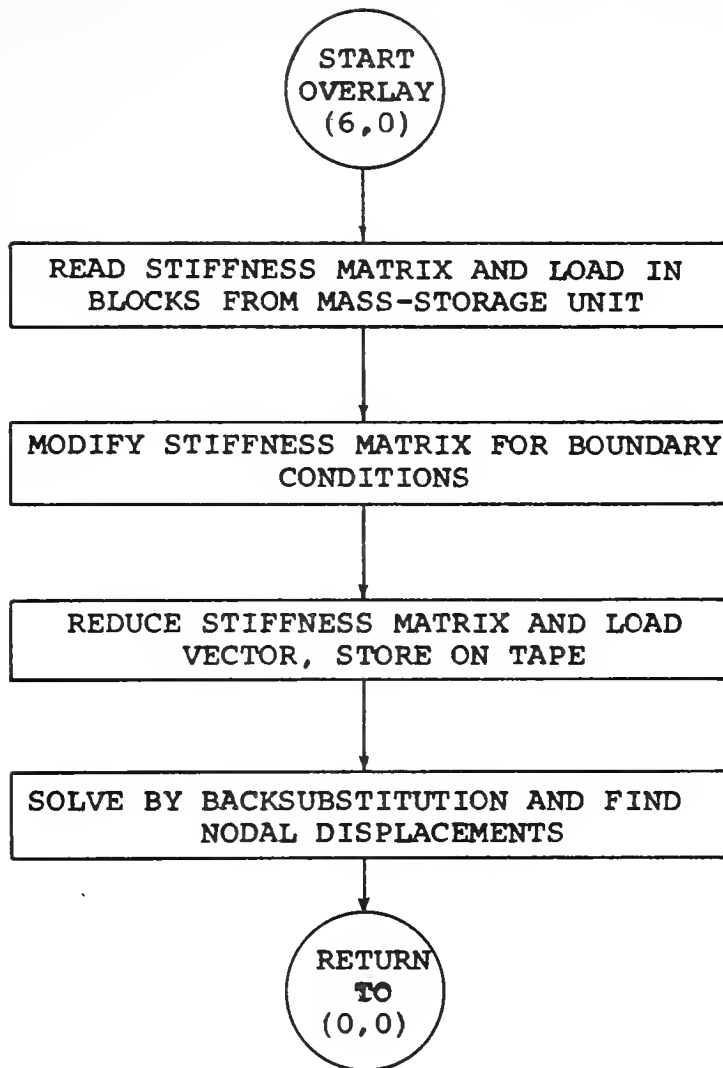


Figure 5.8. Flow Chart for OVERLAY (6,0)



stress and strains and displacements are printed.

In incremental analysis OVERLAYS (4.0), (6,0) and (5,0) are repeated for the desired number of load increments. For analysis of sequence of construction, in steps, the height of each layer has to be defined. According to the given height, the program will select which elements will appear in a particular layer. Accordingly, nodal loads due to self-weight for those elements only will be considered for analysis. This follows the routine procedure of assembly and solutions described above.

No-tension Analysis

It is well-known that most soils have very poor resistance to tensile force, and in most cases can be assumed to have no resistance in tension. For this purpose the analysis has to be modified so that tension is reduced to zero (or to a specified small value). In other words, the tensile forces have to be eliminated from those elements which experience tension and the effect of this stress release in the adjoining elements has to be evaluated. Unfortunately, very limited research has been done in this particular area. Zienkiewicz, et. al. (1968) developed a concept for 'no-tension' analysis. The major steps in the analysis are summarized below:

- (1) Determine those elements in which tension exists.

(2) Calculate the nodal loads that produced the tensile stresses.

(3) Apply equal and opposite nodal forces in each element where tension exists and recalculate the stresses in all the elements.

(4) If, at the end of step (3), tensile stresses are still present steps (2) and (3) are repeated until convergence is reached.

Chang and Nair (1973) reported that use of this technique requires a large number of iterations and in some cases the solution may never converge. The reason for this uncertainty lies in the fact that there is no rational basis for evaluating equivalent nodal loads in step (3) for a two-dimensional state of stress. Chang and Nair (1973) proposed a modification by altering the value of Poisson's ratio, which may increase the rate of convergence but does not alter the uncertainty of convergence.

Development of tensile stresses in interaction element causes a similar problem. Also when the ratio of shear stress to normal stress in the interaction element exceeds the limiting value, excess shear stress also has to be eliminated. A method for estimating nodal loads to eliminate excess tension or shear is proposed, considering the following aspects:

(1) The state of stress before application of the load.

(2) Increments of stresses due to the current load increment.

(3) In this manner the stiffness matrix is kept unchanged, which eliminates the need for reevaluation of element stiffnesses and then assembly to form the complete structure.

The procedure for no-tension analysis adopted in this study is described below. Figure 5.9 shows a state of stress σ_i in an element, which represents the summation of stresses up to i th increment of load. $\Delta\sigma_{i+1}$ represents change in stress due to $(i+1)$ th load increment and σ_{i+1} is the total stress at the end of this increment which is a net tension in the element. The tensile stress, σ_{i+1} has to be eliminated by applying equivalent nodal loads on each node of the element. Equivalent nodal load for an element is given by the following expression

$$\{P\} = [k] \cdot \{du\} \quad (5.3)$$

where

$\{P\}$ = Equivalent nodal load vector

$[k]$ = Element stiffness matrix

$\{du\}$ = Nodal displacement vector.

Equivalent nodal load for this element is evaluated using equation (5.3) where $\{du\}$ is the nodal displacement vector for $(i+1)$ th increment of load. The load increment is modified by multiplying by a load factor F , which is given by the following equation:

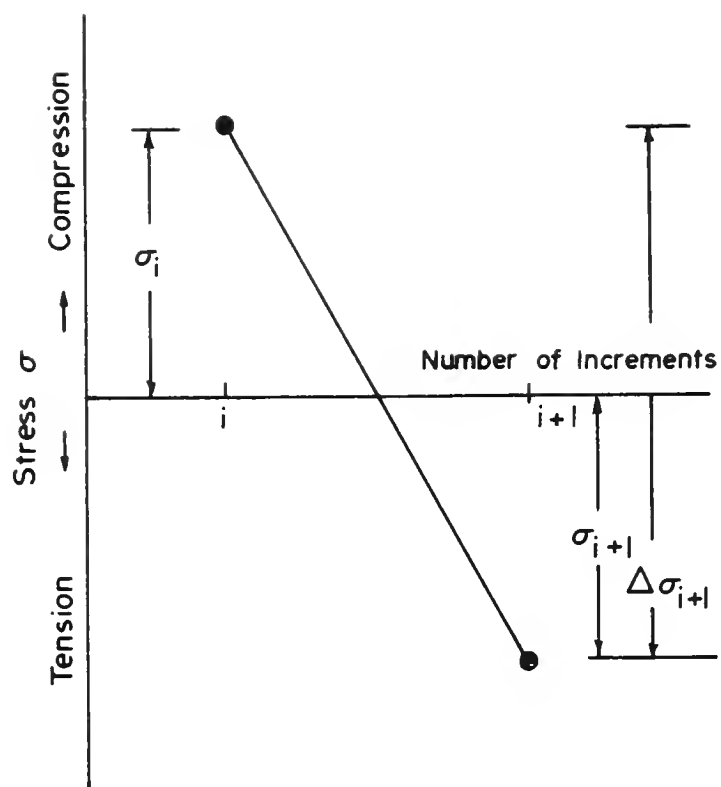


FIGURE 5.9 SCHEME FOR 'NO-TENSION' ANALYSIS.



$$F = 1 - \frac{|\sigma_i|}{|\Delta\sigma_{i+1}|}, \text{ where } | | \text{ denotes absolute value} \quad (5.4)$$

Then the correcting nodal load is given by

$$\{P\}_C = - F \cdot \{P\} \quad (5.5)$$

where

$\{P\}_C$ = Correcting load vector.

The correcting nodal loads $\{P\}_C$ are applied to all nodes of an element which developed tension. A similar procedure is applied to all elements in tension. The complete structure is solved again with only the correcting loads with the structure stiffness matrix kept unchanged. Increments in stress are added to those from previous increment and checked for tension. If the tension is within a small acceptable limit, the next load increment is applied. On the other hand, if tension exists, the procedure of stress release is repeated for a specified number of times. If the procedure fails to converge after the specified number of iterations, further execution is stopped.

Development of tension, or of stress ratio in excess of the specified limit, in the interaction element causes similar problems, and a similar procedure is applied in such cases. The load factor, F in equation (5.5) is determined in the following manner.

Let τ and σ be the total shear and normal stresses in an interaction element at the end of i th load increment. $\Delta\tau$ and $\Delta\sigma$ are increments of τ and σ due to $(i+1)$ th increment.

$$R_i = \frac{\tau}{\sigma} = \text{stress ratio after } i\text{th load increment.}$$

$$R_{i+1} = \frac{\tau + \Delta\tau}{\sigma + \Delta\sigma} = \text{stress ratio after } (i+1)\text{ load increment.}$$

R_{i+1} is greater than limiting value of stress ratio, R_L .

Also let $Q = \frac{\Delta\tau}{\Delta\sigma}$ for $(i+1)$ th increment.

$$\Delta R = R_L - R_i = \frac{\sigma \cdot \Delta\tau - \tau \cdot \Delta\sigma_r}{\sigma \cdot (\sigma + \Delta\sigma_r)} \quad (5.6)$$

or

$$\Delta R = \frac{\Delta\sigma_r \cdot (\sigma \cdot Q - \tau)}{\sigma \cdot (\sigma + \Delta\sigma_r)} \quad (5.7)$$

Solving for $\Delta\sigma_r$ from (5.7)

$$\Delta\sigma_r = \frac{\Delta R \cdot \sigma}{(Q - R_L - \Delta R)} \quad (5.8)$$

where $\Delta\sigma_r$ is the increment of σ required to maintain the stress ratio of the limiting value.

For release of excess shear, i.e., to maintain stress ratio within allowable limit, equivalent nodal loads given by equation (5.5) has to be applied in which F is given as

$$F = 1. - \frac{\Delta\sigma_r}{\Delta\sigma} \quad (5.9)$$

and $\Delta\sigma_r$ is defined in equation (5.8).

This procedure also suffers from uncertainty of convergence, and further research is needed in this area.

CHAPTER VI

FINITE ELEMENT ANALYSIS

6.1 Selection of Boundaries and Boundary Conditions.

To analyze the culvert problem by the finite element method, a set of finite boundaries must be established and the conditions at these boundaries defined realistically. A decision must be taken to establish (a) the size of the region to be considered, (b) the size of elements in different parts of the region, and (c) what boundary conditions should be used at each boundary. Depending on the type of problem, type of analysis, major points of interest, time and resources available for the study, the answer to the above questions may vary over a wide range. However, insight into the problem, past experience, and some trial solutions help in the decision making process.

In the usual case, symmetry across a vertical axis through the center of culvert may be assumed except for special cases like nonsymmetric external loading, non-uniform backfilling sloping surfaces and similar situations. The assumption of symmetry across the axis reduces the problem to one-half size. Trial runs revealed that the lateral (vertical) boundary should be at a distance three

to four times the radius of pipe, and the bottom (horizontal) boundary at least one diameter below the pipe invert.

Selection of the same size of element throughout the medium is uneconomical both in terms of time required to digitize the problem and cost of run. The general practice is to use smaller sized elements in zones of primary interest and in areas of relatively high stress gradients. Large elements can be used elsewhere, but the transition between large and small elements should be gradual. In the culvert problem, the major area of interest is in the zone near the pipe, hence smaller-sized elements are used in a zone of half the radius of pipe and the size increased gradually towards the boundaries. For numerical stability, "flat" triangles are avoided.

Conditions at boundaries may be defined either by defining nodal forces or displacements. Both approaches are acceptable but it is generally easier to visualize boundary conditions in terms of displacements rather than nodal forces. The boundary conditions used in this study are as given below.

(1) Vertical Axis of symmetry - Zero horizontal displacement; free movement vertically.

(2) Horizontal Lower Boundary - Zero vertical and zero horizontal displacement.

(3) Vertical boundary laterally from center of pipe - Conditions at this boundary are the same as those for the axis of symmetry.

These assumptions of boundary conditions are reasonable and are commonly used (Corotis, Farzin, Krizek, 1974).

6.2 Selection of Example Problems

The main purpose of this study is to develop an analytical tool which can adequately predict the performance of culverts buried in soil under various situations. The scheme for analysis and the computer code developed has been checked for internal consistency using problems for which known solutions exist. To examine the capability of this program to analyze culvert problems in a realistic fashion a pipe culvert of varying stiffness was chosen and its behavior analyzed for different soil conditions, various construction procedures and different amounts of limiting slip at the soil-pipe interface. A corrugated aluminum pipe was selected as an example problem for study. The pipe has a nominal diameter of 10 feet and is embedded in soil with 20 feet (or 40 feet) height of cover (Figure 6.1). The problem has been idealized using 340 nodes and 174 elements (Figure 6.2). The lower boundary has been fixed at 10 feet below the bottom of the pipe and the lateral boundary has been chosen at a distance of 32 feet from the center line of pipe.

Properties of Soil

The backfill material selected is Monterey No. 0 sand which is mainly composed of quartz and feldspar grains.

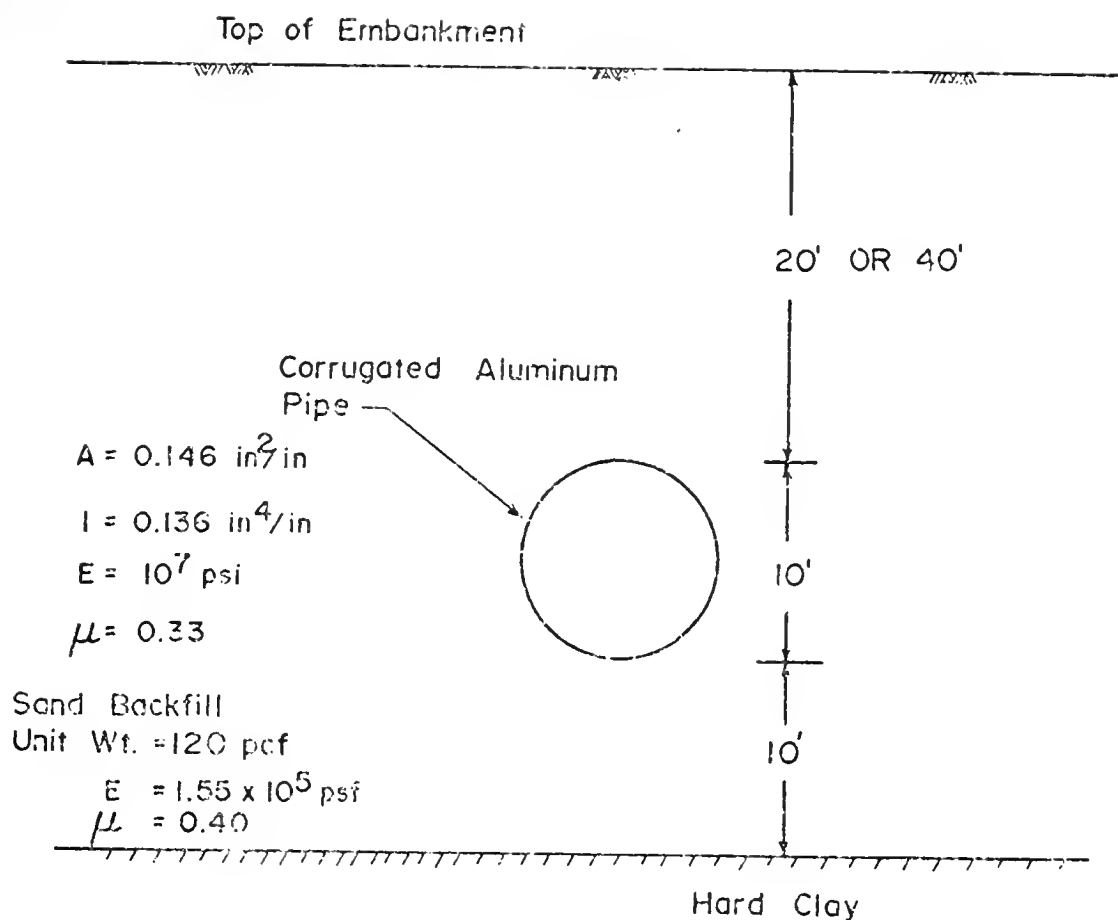


FIGURE 6.1 GEOMETRY OF SAMPLE CULVERT PROBLEM.

FINITE ELEMENT MESH

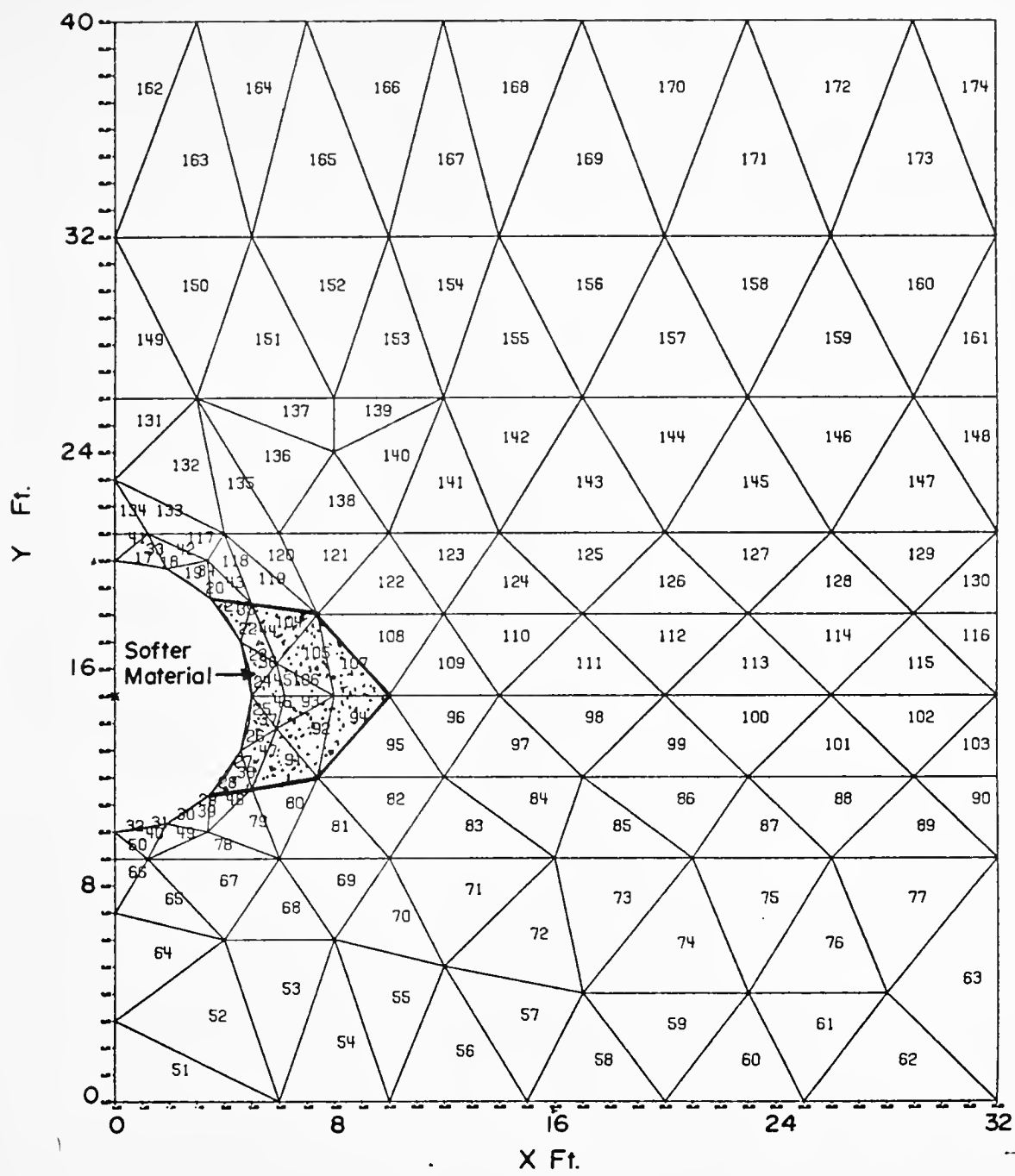


FIGURE 6.2 FINITE ELEMENT MESH FOR EXAMPLE PROBLEM.

It is a uniform medium sand with uniformity coefficient $C_u = d_{60}/d_{10} = 1.53$, and an average diameter of $d_{50} = 0.43$ mm. Specific gravity is 2.645. Minimum and maximum void ratios are $e_{\min} = 0.656$, $e_{\max} = 0.860$. From triaxial tests, the friction angle ϕ for the sand is 34.6 degrees when $e = 0.78$.

Lade (1972) conducted plane strain tests on rectangular prismatic specimens 10.6 cm high, 4.6 cm wide and 11.5 cm long confining pressures σ_3 of 0.3, 0.6 and 1.2 kg/cm² in drained conditions. Stress-strain and volume change characteristics obtained are shown in Figure 4.8. These results have been used to represent nonlinear stress dependent soil properties (Figures 4.9 and 4.10).

Finite Element Idealization

Sixteen curved bar elements were utilized to idealize the pipe, i.e., the angle made by each segment of pipe at the center is 11.25 degrees. The total number of interaction elements is 16. 340 nodes and 174 elements have been used to idealize the problem. The problem being symmetric, only a half-section passing through center-line of pipe was analyzed. The finite element mesh is shown in Figure 6.2.

Problems Selected

In order to study effects of different material parameters and of considering construction layers with and without allowing slip to occur at the soil-pipe interface, a variety of problems was analyzed.

Pipe Properties. Corrugated aluminum pipe

$$EI = 1.36 \times 10^6 \text{ lb. in}^2/\text{inch}$$

$$E = 10^7 \text{ lb/in}^2$$

$$\mu = 0.33$$

$$I = 0.136 \text{ in}^4/\text{in}$$

$$\text{Radius } R = 60 \text{ inch}$$

$$\text{Area } A = 0.146 \text{ in}^2/\text{inch}$$

Soil Properties. Moderately loose sand

$$\text{Unit weight } \gamma_m = 120 \text{ lbs/cu. ft.}$$

$$(\text{Elastic}) \text{ Tangent Modulus, } E = 1.55 \times 10^5 \text{ psf.}$$

$$(\text{Elastic}) \text{ Poisson's Ratio, } \mu = 0.40$$

The effect of varying E was examined

Nonlinear properties = direct input of plane strain test data. The effect of soft inclusions shown as a speckled zone in Figure 6.2 was analyzed.

The construction sequence was broadly classified into the following categories:

- I. Single Layer - Culvert and backfill are placed in a single operation with the weight applied either as a single load, or in increments.
- II. Multi-layer - In this case the pipe and backfill are constructed in layers. The layer heights and number of load increments per layer are shown in Table 6.1.

The height of backfill was also varied, with 20 feet and 40 feet heights of cover considered. Table 6.2 lists the range in parameters analysed for a single layer of backfill.

Table 6.1(a) Layer Heights for Incremental Analysis, 20 Ft. Fill.

Layer No.	Layer Height (Ft.)		No. of Increments	
	From	To	A	B
1	0	9.5	1	2
2	9.5	12.0	1	2
3	12.0	15.0	1	2
4	15.0	18.0	1	2
5	18.0	21.0	1	2
6	21.0	26.0	1	2
7	26.0	32.0	2	3
8	32.0	40.0	2	3
Total			10	18

Table 6.1(b) Layer Heights for Incremental Analysis, 40 Ft. Fill.

Layer No.	Layer Height (Ft.)		No. of Increments
	From	To	
1	0	9.5	2
2	9.5	12.0	2
3	12.0	15.0	2
4	15.0	18.0	2
5	18.0	22.0	2
6	22.0	32.0	2
7	32.0	44.0	6
8	44.0	60.0	6
Total			24

Table 6.2

Example Problem Description - I. Single Layer, 20 Feet of Cover

No.	E_{Soil}	EI_{Pipe}	No. of Increments	Interface Slip
L-1	$E_i = 1.55 \times 10^5 \text{ psf}$ $\nu_i = 0.4$	$EI = 1.13 \times 10^5 \text{ lb ft}^2/\text{ft}$ $\nu = 0.33$	1	No
L-2	E_i	$EI/2$	1	No
L-3	E_i	$EI/5$	1	No
L-4	E_i	$EI/10$	1	No
L-5	E_i	$2EI$	1	No
L-6	E_i	$5EI$	1	No
L-7	E_i	$10EI$	1	No
L-8	E_i	$20EI$	1	No
L-9	E_i	$50EI$	1	No
L-10	E_i	$100EI$	1	No
L-11	$E_i/10$	$EI/10$	1	No
L-12	$E_i/10$	$EI/5$	1	No
L-13	$E_i/10$	$EI/2$	1	No
L-14	$E_i/10$	EI	1	No
L-15	$E_i/10$	$2EI$	1	No
L-16	$E_i/10$	$5EI$	1	No
L-17	$E_i/10$	$10EI$	1	No
L-18	$E_i/10$	$20EI$	1	No
L-19	$E_i/10$	$50EI$	1	No
L-20	$E_i/10$	$100EI$	1	No
L-21	$10E_i$	$EI/10$	1	No

Table 6.2 (Continued)

No.	E_{Soil}	EI_{Pipe}	No. of Increments	Interface Slip
L-22	$10E_i$	$EI/5$	1	No
L-23	$10E_i$	$EI/2$	1	No
L-24	$10E_i$	EI	1	No
L-25	$10E_i$	$2EI$	1	No
L-26	$10E_i$	$5EI$	1	No
L-27	$10E_i$	$10EI$	1	No
L-28	$10E_i$	$20EI$	1	No
L-29	$10E_i$	$50EI$	1	No
L-30	$10E_i$	$100EI$	1	No
L-31	E_i	$EI/100$	1	No
L-32	E_i	$EI/50$	1	No
L-33	E_i	$EI/20$	1	No
L-34*	E_i	EI	1	No
L-35*	E_i	$EI/10$	1	No
L-36	E_j, ν_j	$144EI$	1	No
L-37**	E_j, ν_j	$144EI$	1	No
L-38*	E_i	$100EI$	1	No
L-39*	E_i	$30EI$	1	No

L = Linear elastic soil properties

$$E_j = 1.0 \times 10^6 \text{ psf}, \nu_j = 0.47$$

$$* E_{\text{soil}} = \frac{E_i}{100} \text{ near springline}$$

** 40 ft. height of cover

Table 6.2 (Continued)

No.	E_{Soil}	EI_{Pipe}	No. of Increments	Interface Slip
NL-1	NL	144EI	5	No
NL-2	NL	144EI	5	Yes
NL-3	NL	144EI	10	No
NL-4	NL	144EI	10	Yes
**NL-5	NL	144EI	5	No
**NL-6	NL	144EI	5	Yes
**NL-7	NL	14.4EI	5	No
**NL-8*	NL	144EI	5	No
**NL-9*	NL	144EI	5	Yes

Parameters analyzed using 8 layers to simulate actual construction are in Table 6.3. The number of increments per layer are as shown in Table 6.1(a) and 6.1(b) for 20 and 40 feet of cover, respectively.

Table 6.3

Example Problem Description - II. Multi-Layer, Nonlinear Soil, 20 Feet of Cover

No.	E_{Soil}	EI_{Pipe}	Total No. of Increments	Interface Slip
ML-1	NL	144EI	10	No
ML-2	NL	144EI	10	Yes
ML-3	NL	144EI	18	No
ML-4	NL	144EI	18	Yes
**ML-5	NL	144EI	24	No

NL = Nonlinear soil properties, direct input of test data

* $E_{\text{soil}} = \frac{E_i}{10}$ near spring line; **40 feet of cover

1.04

1.04

1.04

1.04

1.04

1.04

1.04

1.04

1.04

1.04

1.04

1.04

1.04

1.04

1.04

1.04

1.04

1.04

1.04

1.04

1.04

1.04

CHAPTER VII

PRESENTATION AND DISCUSSION OF RESULTS

The primary purpose of the example problems is to study changes in response of the pipe to different input parameters, and to recognize which of the variables have significant effects on the behavior of pipe. The factors chosen for comparison to reflect culvert response were:

- (1) Deformed shape of pipe and percent change in vertical diameter, $\Delta Y\%$.
- (2) Maximum thrust in pipe, P_{\max} .
- (3) Maximum moment in pipe, M_{\max} .
- (4) Maximum extreme fiber stress in pipe, $\sigma_{\theta_{\max}}$.
- (5) Marston-Spangler E' value back-calculated from equation (2.4).
- (6) Horizontal and vertical stress in the soil adjacent to the springline of the pipe, σ_x and σ_y , respectively.
- (7) Vertical stress in the soil at the crown of the pipe, σ_n .
- (8) Maximum value of ratio of shear stress to normal stress at the soil-pipe interface, $\left. \frac{\tau}{\sigma} \right|_{\max}$.

When the effects of slip at the pipe-soil interface was being examined, the limiting value of $\frac{\tau}{\sigma}$ was set at 0.33. To increase the rate of convergence a 10% tolerance in this ratio was allowed; also, a small amount of tensile stress [not exceeding 120 psf] was allowed in the no-tension analysis.

Solutions to example problems were organized into three groups:

- (1) Problems using linear elastic soil properties, varying the relative stiffness of pipe and soil.
- (2) Problems using non-linear soil properties in which the effects of construction sequence are analyzed.
- (3) Problems similar to (2) but using a larger fill height.

Group One:

A listing of problems solved in the first group is given in Table 6.2. Problems L-1 to L-10 show the effect of changing pipe stiffness keeping the surrounding soil unchanged. Problems L-11 to L-12 and L-21 to L-31 cover the same range in pipe stiffness but the soil modulus is reduced by a factor of 10, and increased by a factor of 10, respectively. In all cases the problems were solved with the full gravitational load due to self-weight of soil applied in one operation. A summary of the results obtained is presented in Table 7.1. Percent change in vertical diameter, $\Delta Y\%$, for various values of EI are plotted on a semilog scale and shown in Figure 7.1a for each soil stiffness. It is seen that compression of the pipe in the vertical direction is dependent on the stiffness of pipe and on the modulus value of the surrounding soil. The soil modulus has an enormous influence on the deflection of flexible pipes but the effect becomes less and less pronounced as the pipe stiffness increases. If the soil and pipe properties are homogeneous and linear, the change in pipe diameter is significant only if the soil is weak and the pipe is flexible.

Table 7.1 Comparison of Results for Linear Soil Properties, Single Layer, No Interface Slip, 20 Feet Cover

Identification No. (Table 6.2)	Change in Vertical Diameter $\Delta\%$	Max. Thrust in Pipe P_{max} lb/ft. $\times 10^4$	Max. Moment in Pipe M_{max} ft.lb/ft. $\times 10^3$	Max. Extreme Fiber Stress $\sigma_{\theta max}$ lb/in $^2 \times 10^3$	Marston-Spangler E' lb/ft $^2 \times 10^5$	Horizontal Soil Stress at Springline lb/ft $^2 \times 10^3$	Vertical Soil Stress at Springline lb/ft $^2 \times 10^3$	Vertical Soil Stress at Crown lb/ft $^2 \times 10^3$	Interface Stress Ratio τ/σ max
L-1	0.823	1.70	0.96	15.3	3.49	2.84	2.40	2.25	.38
L-2	0.846	1.69	0.67	25.4	3.42	2.86	2.42	2.23	.38
L-3	0.861	1.68	0.47	58.3	3.38	2.90	2.43	2.21	.39
L-4	0.866	1.68	0.42	118.0	3.36	2.93	2.44	2.21	.39
L-5	0.780	1.70	1.48	10.1	3.61	2.79	2.38	2.29	.38
L-6	0.676	1.72	2.32	6.3	3.97	2.67	2.32	2.40	.38
L-7	0.654	1.75	4.22	4.5	4.57	2.52	2.25	2.53	.38
L-8	0.407	1.78	5.99	3.1	5.77	2.34	2.17	2.70	.38
L-9	0.227	1.81	8.28	1.6	9.34	2.11	2.07	2.90	.37
L-10	0.130	1.83	9.59	0.9	15.3	1.99	2.01	3.01	.38
L-11	8.23	1.70	0.96	153.0	0.35	2.84	2.40	2.25	.38
L-12	7.80	1.70	1.48	100.0	0.36	2.79	2.38	2.29	.38
L-13	6.76	1.72	2.74	63.3	0.40	2.67	2.32	2.40	.38
L-14	5.54	1.75	4.22	45.1	0.46	2.52	2.25	2.53	.38
L-15	4.07	1.78	5.99	30.6	0.58	2.34	2.17	2.70	.37
L-16	2.27	1.81	8.28	16.2	0.93	2.11	2.07	2.90	.37
L-17	1.30	1.83	9.59	9.4	1.53	1.99	2.01	3.01	.38
L-18	0.700	1.84	10.6	5.1	2.73	1.92	1.98	3.07	.39
L-19	0.296	1.85	11.8	2.3	6.33	1.87	1.96	3.12	.39
L-20	0.150	1.85	13.2	1.3	12.3	1.85	1.95	3.14	.40
L-21	0.090	1.63	0.33	107.0	34.5	3.04	2.53	2.23	.39
L-22	0.088	1.65	0.34	55.7	33.7	3.03	2.49	2.24	.39

Table 7.1 (Continued)

Identifi- cation No. (Table 6.2)	Change in Vertical Diameter $\Delta Y, \%$	Max. Thrust in Pipe P_{\max} $\text{lb/ft.} \times 10^4$	Max. Moment in Pipe M_{\max} $\text{ft. lb/ft} \times 10^3$	Max. Extreme Fiber Stress $\sigma_e \max$ $\text{lb/in}^2 \times 10^3$	Marston- Spangler E, $\text{lb/ft}^2 \times 10^5$	Horizontal Soil Stress at Springline $\text{lb/ft}^2 \times 10^3$	Vertical Soil Stress at Springline $\text{lb/ft}^2 \times 10^3$	Vertical Soil Stress at Crown $\text{lb/ft}^2 \times 10^3$	Interface Stress Ratio τ/σ max
L-23	0.087	1.67	0.34	23.2	33.5	2.98	2.46	2.22	.39
L-24	0.087	1.68	0.39	11.8	33.6	2.93	2.44	2.21	.39
L-25	0.086	1.68	0.47	5.8	33.8	2.90	2.43	2.21	.39
L-26	0.085	1.69	0.66	2.5	34.2	2.86	2.42	2.23	.38
L-27	0.082	1.70	0.96	1.5	34.9	2.84	2.40	2.25	.38
L-28	0.078	1.70	1.48	1.0	36.1	2.79	2.38	2.29	.38
L-29	0.068	1.72	2.74	0.63	39.7	2.67	2.32	2.40	.38
L-30	0.055	1.75	4.22	0.45	48.9	2.52	2.25	2.53	.38
L-31	0.903	1.63	0.33	1070.0	3.45	3.04	2.53	2.23	.39
L-32	0.877	1.65	0.36	557.0	3.37	3.03	2.49	2.24	.39
L-33	0.868	1.67	0.40	232.0	3.35	2.98	2.46	2.22	.39
L-34	4.03	0.97	6.03	59.8	0.062	0.36	0.29	0.60	.40
L-35	4.91	0.67	1.19	181.0	0.055	0.51	0.38	0.69	.34
L-36	0.015	1.57	1.93	0.17	42.3	2.71	2.63	2.58	.21
L-37**	0.031	2.76	3.79	0.32	20.3	4.87	4.77	5.04	.13
L-38	0.343	1.98	24.8	2.4	0.353	0.13	0.12	3.36	0.84
L-39	2.01	1.62	16.8	16.2	0.092	0.20	0.18	1.66	0.53

**40 feet of cover

Maximum moment and maximum thrust in the pipe are plotted vs. pipe stiffness in Figure 7.1b for each soil stiffness. It is seen that the maximum moment increases sharply with increasing pipe stiffness--especially in the case of a soft soil--but the maximum thrust in the pipe is virtually unaffected [it depends primarily on height of fill and diameter of pipe].

The maximum extreme fibre stress in the pipe is shown plotted vs. pipe stiffness in Figure 7.1(c). Although soil stiffness is a factor--with weaker soils inducing higher stresses--the predominant effect is due to pipe stiffness. The relative importance of thrust vs. moment on the maximum extreme fibre stress is shown in Figure 7.1(d). For a typical corrugated metal pipe (normalized $EI = 1$) 85 percent of the maximum stress is due to moment (vs. 15 percent due to thrust) in a weak soil; even in a moderately good soil ($E_1 = 1$) the ratio is still 57 percent. Thus, very small moments in flexible pipes can cause yielding of the pipe wall. If local buckling does not develop, the soil pressures on the pipe will redistribute to reduce the induced moments; if not, there is danger of collapse. Thus, local buckling may be viewed as a key performance criterion for flexible culverts. In stiff pipes, the induced moments dominate pipe performance.

In all the above cases the Marston-Spangler values of soil modulus E' were back-calculated; they are listed in Table 7.1 and shown plotted in Figure 7.1e. If E' were a soil property its value would be constant for a given E_{soil} and a given pipe diameter. It can be seen that for weak soils the E' values are strongly dependent on pipe stiffness for the same E_{soil} [E' is also greatly dependent on the height of cover]. Accordingly, E' is not a soil property, and there is no hope of empirically

- \square $E_{\text{soil}} = E_1 / 10$ (PROB. L-11 TO L-20)
 \circ $E_{\text{soil}} = E_1$ (PROB. L-1 TO L-10)
 \triangle $E_{\text{soil}} = 10E_1$ (PROB. L-21 TO L-30)

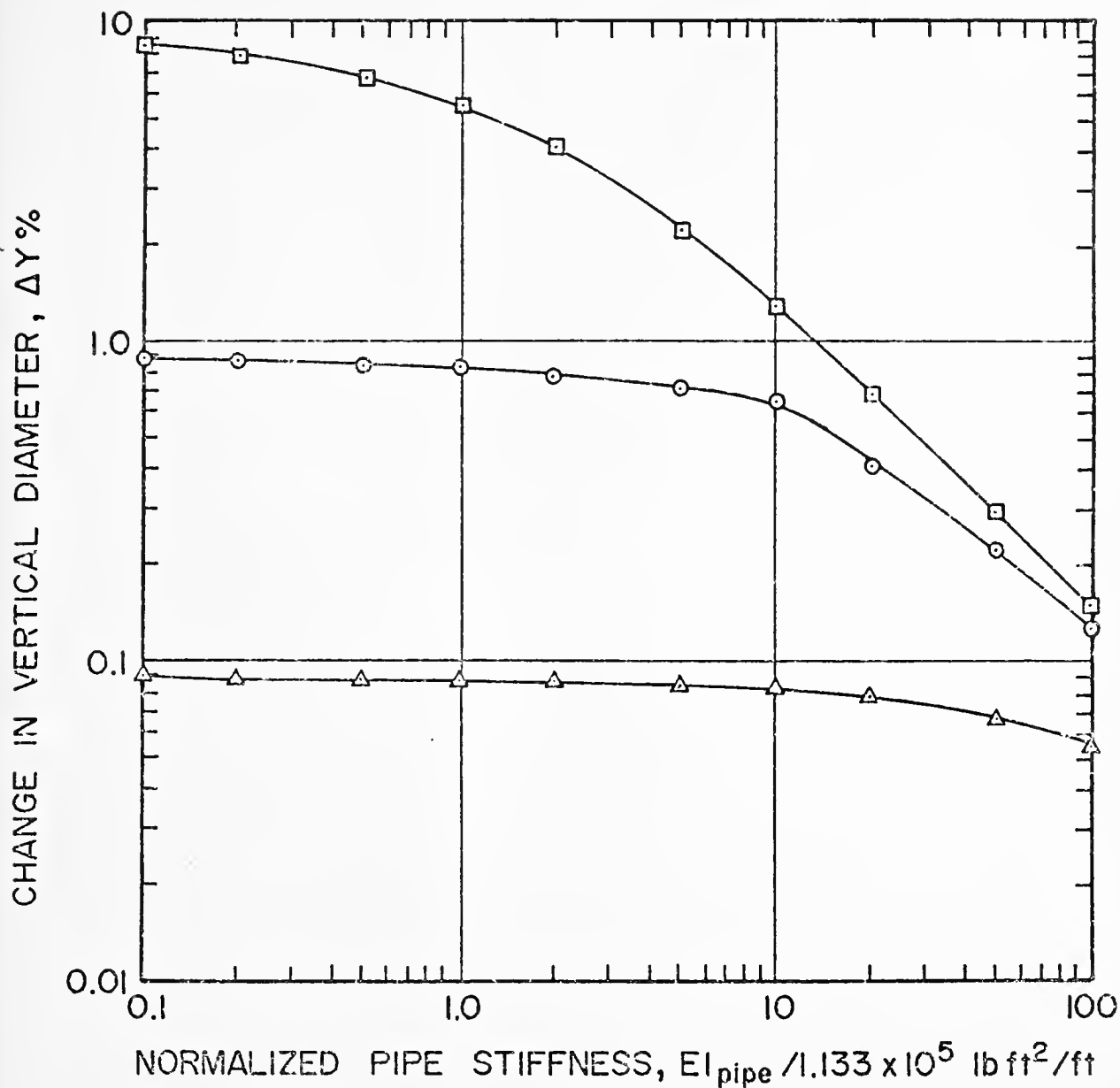


FIGURE 7-1(a) EFFECT OF RELATIVE STIFFNESS OF PIPE AND SOIL ON CHANGE IN VERTICAL DIAMETER OF PIPE.

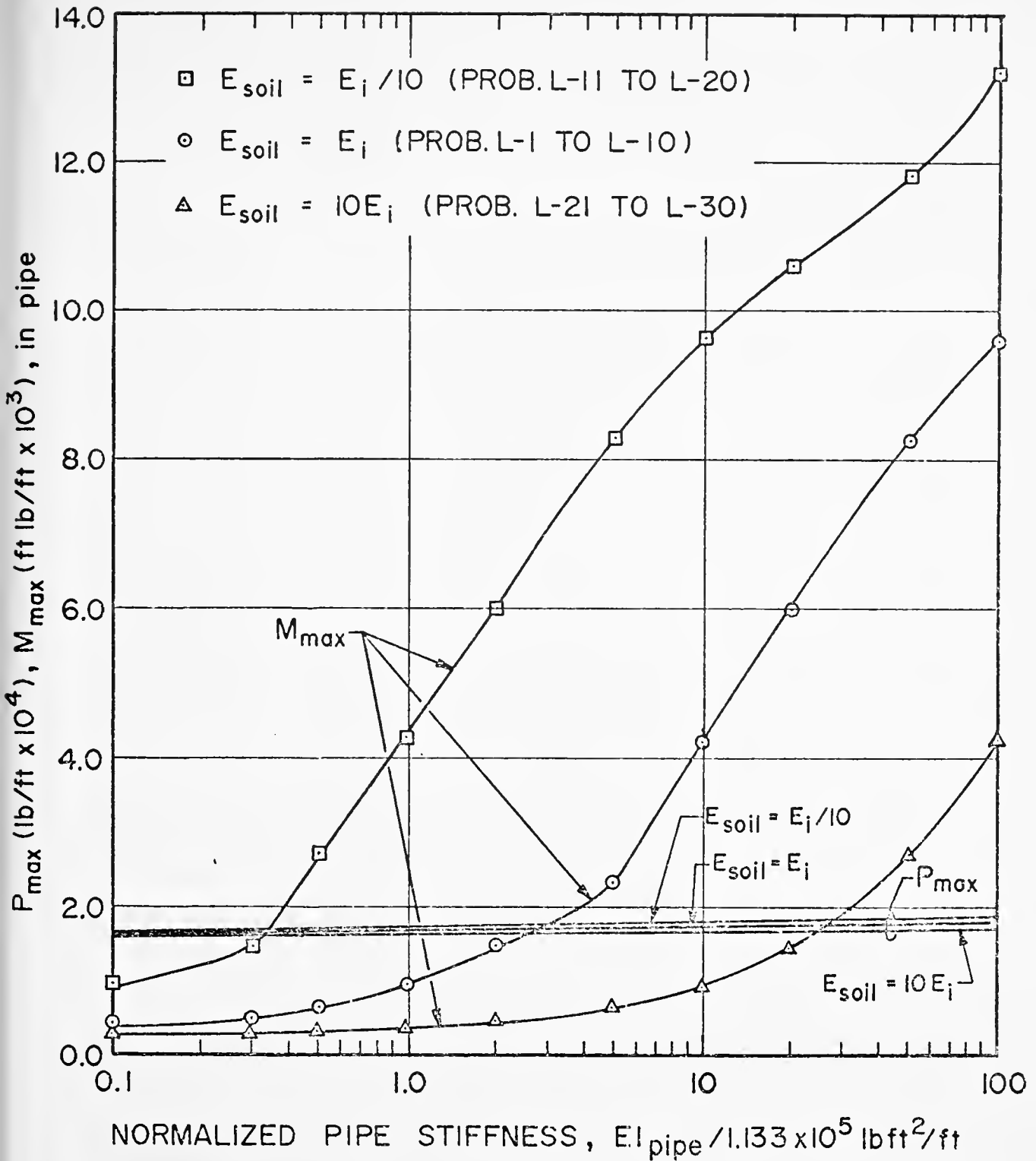


FIGURE 7-1(b) EFFECT OF RELATIVE STIFFNESS OF PIPE AND SOIL ON MAXIMUM MOMENT (M_{max}) AND MAXIMUM THRUST (P_{max}) IN THE PIPE.

- $\square E_{\text{soil}} = E_i / 10$ (PROB. L-11 TO L-20)
 $\circ E_{\text{soil}} = E_i$ (PROB. L-1 TO L-10)
 $\triangle E_{\text{soil}} = 10E_i$ (PROB. L-21 TO L-30)

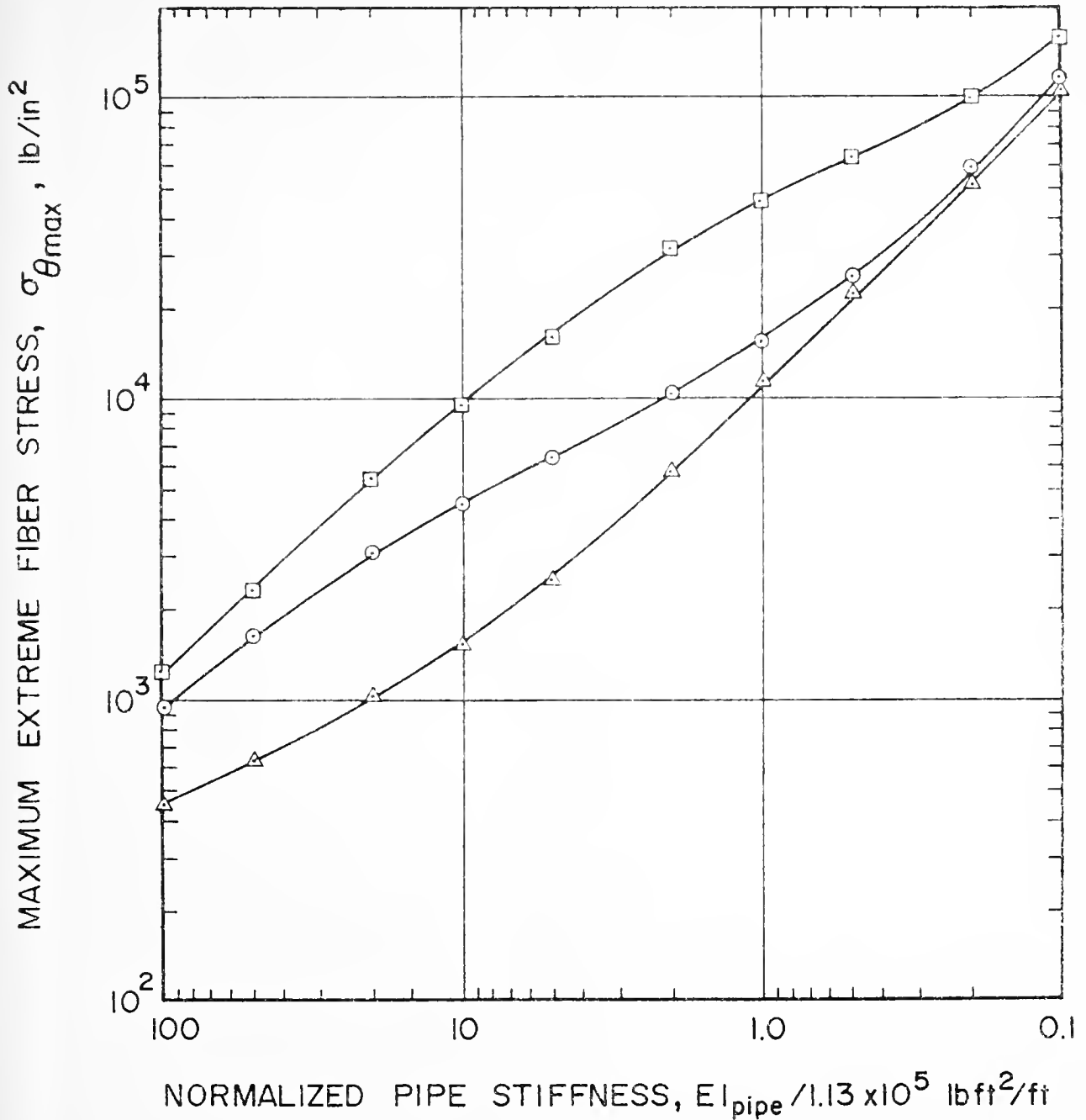


FIGURE 7-1(c) EFFECT OF RELATIVE STIFFNESS OF PIPE AND SOIL ON MAXIMUM EXTREME FIBER STRESS ($\sigma_{\theta_{\max}}$) IN THE PIPE.

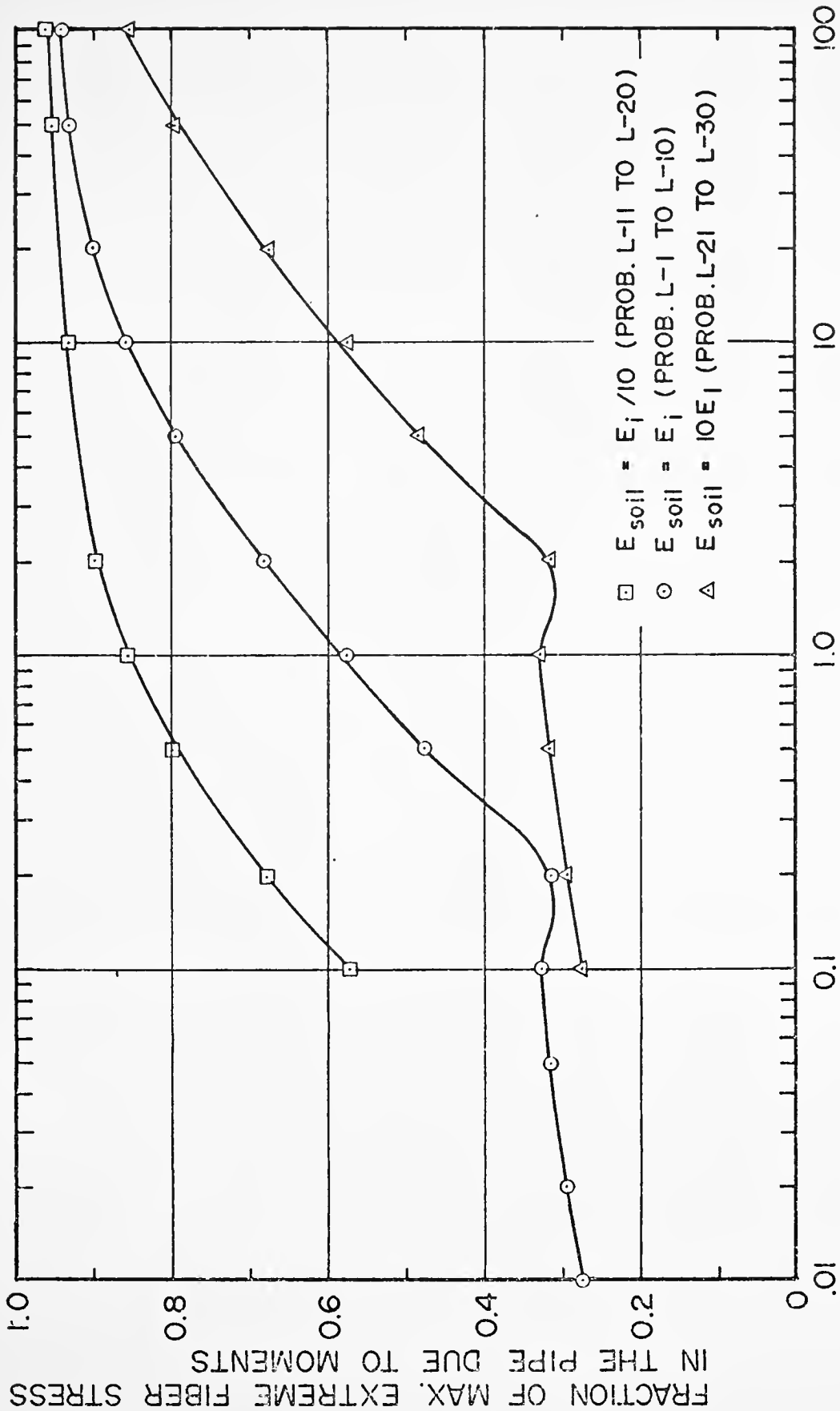


FIGURE 7-1(d) FRACTION OF MAXIMUM EXTREME FIBER STRESS IN PIPE INDUCED BY MOMENT vs. NORMALIZED PIPE STIFFNESS

- \square $E_{\text{soil}} = E_i / 10$ (PROB. L-11 TO L-20)
 \circ $E_{\text{soil}} = E_i$ (PROB. L-1 TO L-10)
 \triangle $E_{\text{soil}} = 10E_i$ (PROB. L-21 TO L-30)

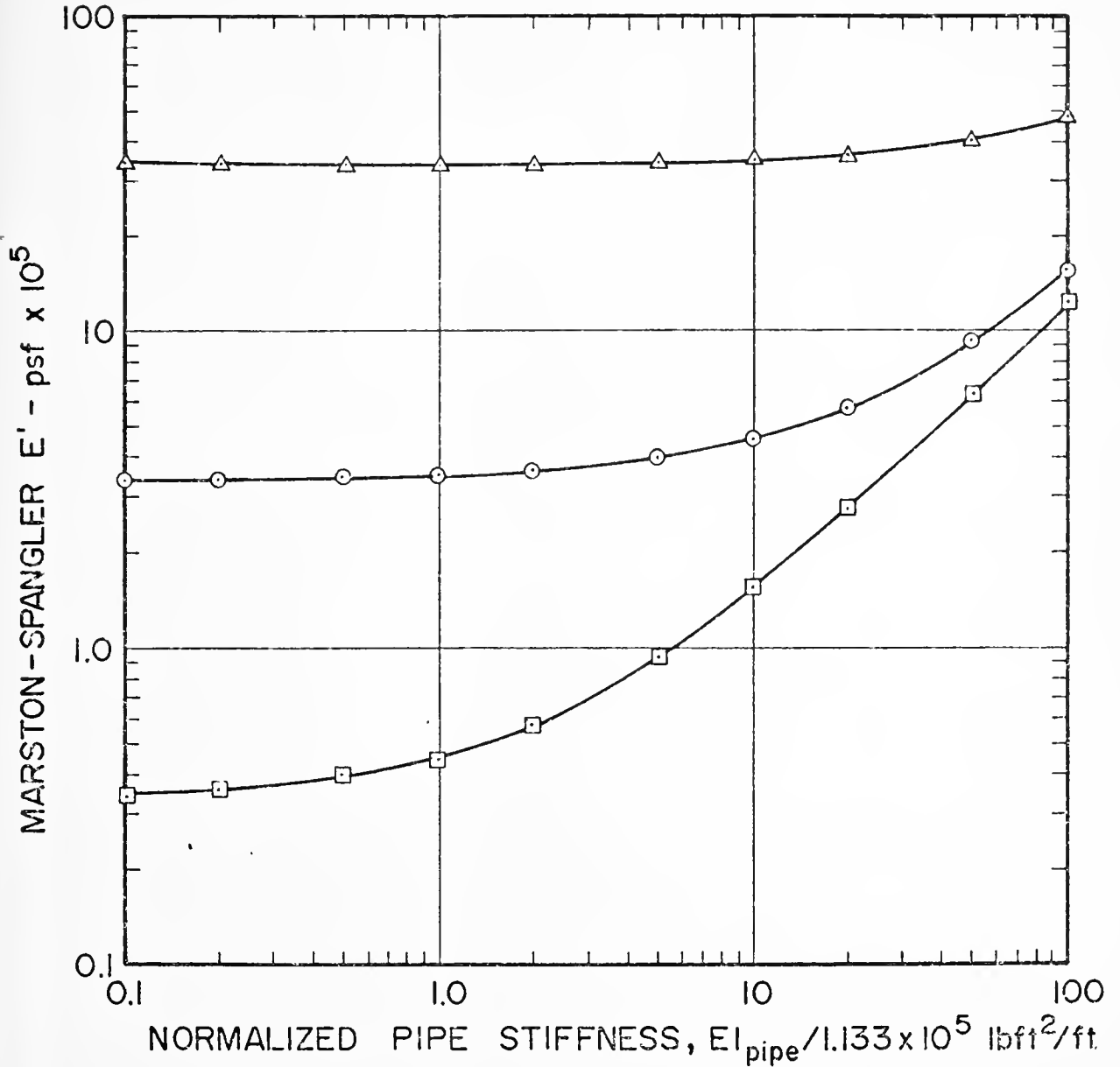


FIGURE 7-1(e) INFLUENCE OF PIPE STIFFNESS ON MARSTON-SPANGLER SOIL MODULUS, E' .

correlating values of E' that would be valid for a wide range of culvert problems.

To investigate the effect of poor backpacking near the springline two problems (L-34, L-35) were solved where very loose material is placed in this location (see Figure 6.2). Results are given in Table 7.1 and compared below.

	<u>EI</u>	<u>$\frac{\Delta Y}{\%}$</u>	<u>σ_{θ} (max) psi x 10^3</u>	<u>σ_x at spring psf x 10^3</u>
$E_{\text{soil}} = 1$; uniform	1	0.82	15.3	2.25
$E_{\text{soil}} = 1$; 1/100 at springline	1	4.03	59.8	0.36

In this case the same pipes are subjected to much higher extreme fibre stresses and the deflections at the crown are increased by a factor of 5. Lack of confinement of the pipe near the springline adversely affects culvert performance, a fact which is well known from experience.

In problem L-35, the pipe is ten times more flexible than in problem L-34, but the reductions in vertical diameter are approximately the same. This is explained by the formation of a soil arch over the pipe which transfers load away from the crown. Formation of the "arch" is also reflected in an increase in vertical stress in the soil away from the springline. The formation of a soil arch is the principal reason why it is possible to construct 'super-span' corrugated metal culverts (Fisher, 1969). It is seen that considerable insight into culvert behavior [but not the prediction of culvert performance] can be gained from simple elastic analysis.

Figures 7.2 through 7.4 show the distribution of parameters reflecting pipe response around the circumference

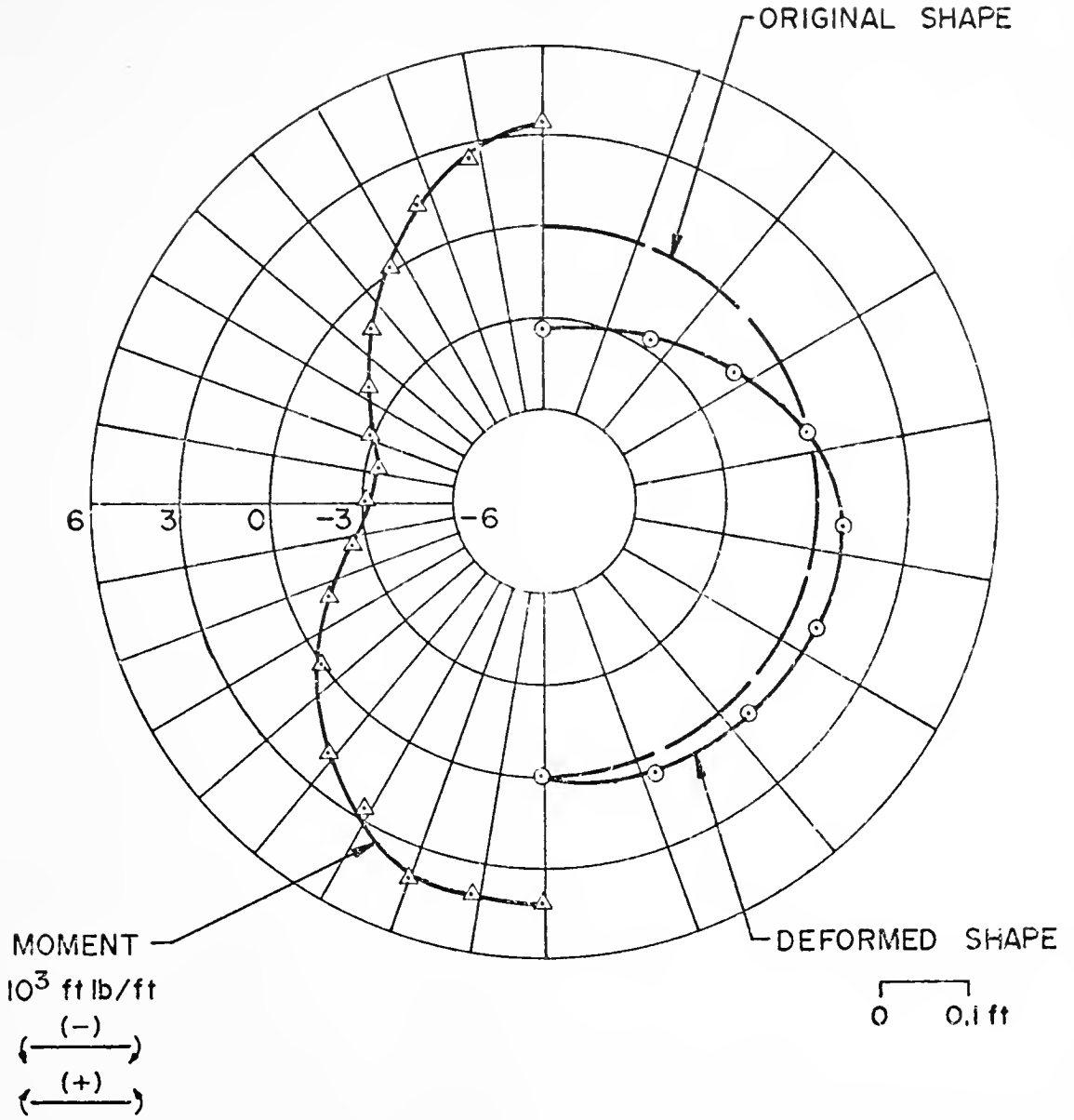


FIGURE 7.2 DISTRIBUTION OF MOMENT AND DEFORMED SHAPE OF PIPE, PROBLEM L-14.

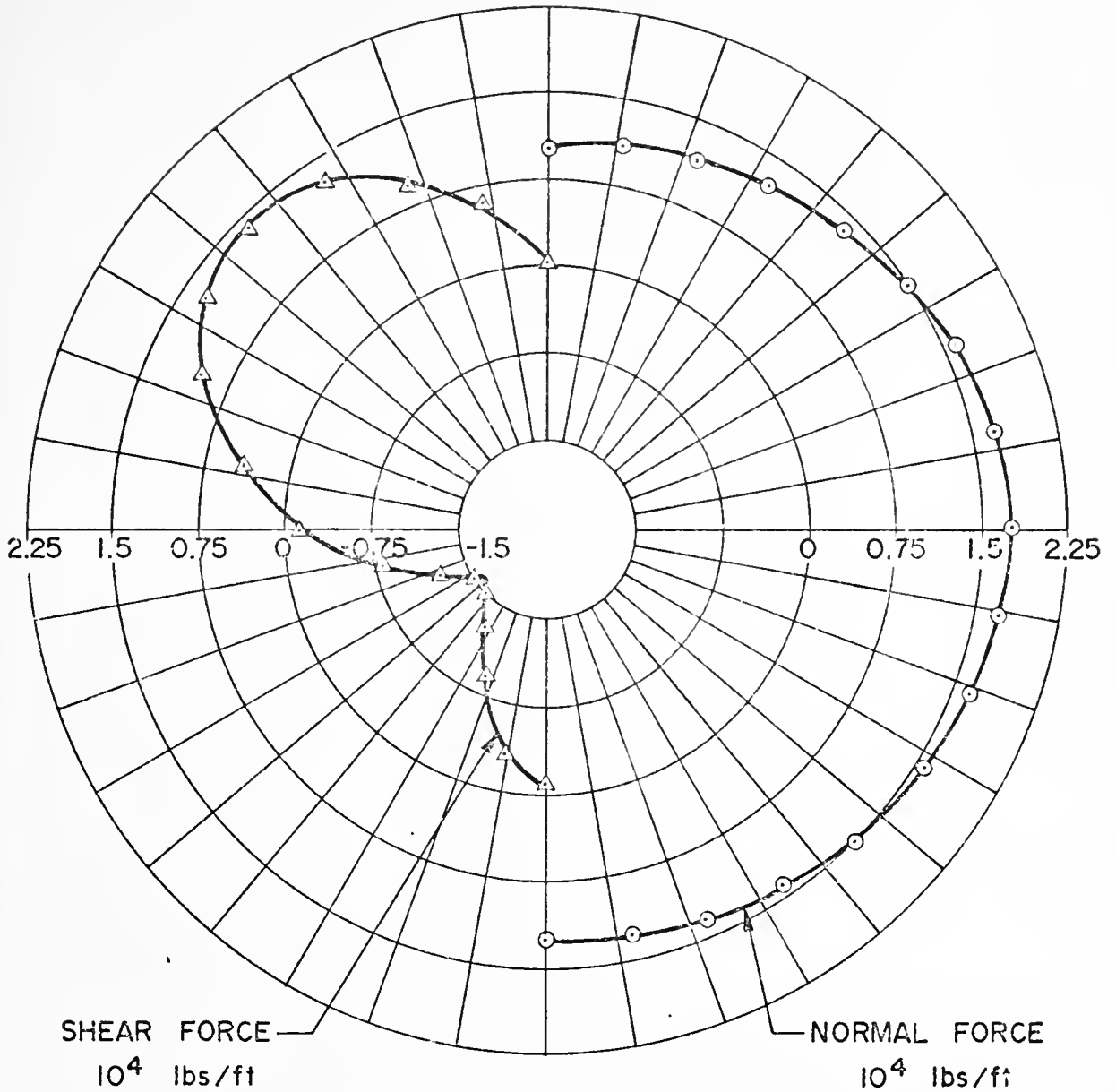


FIGURE 7.3 DISTRIBUTION OF NORMAL AND SHEAR FORCES IN PIPE, PROBLEM L-14.

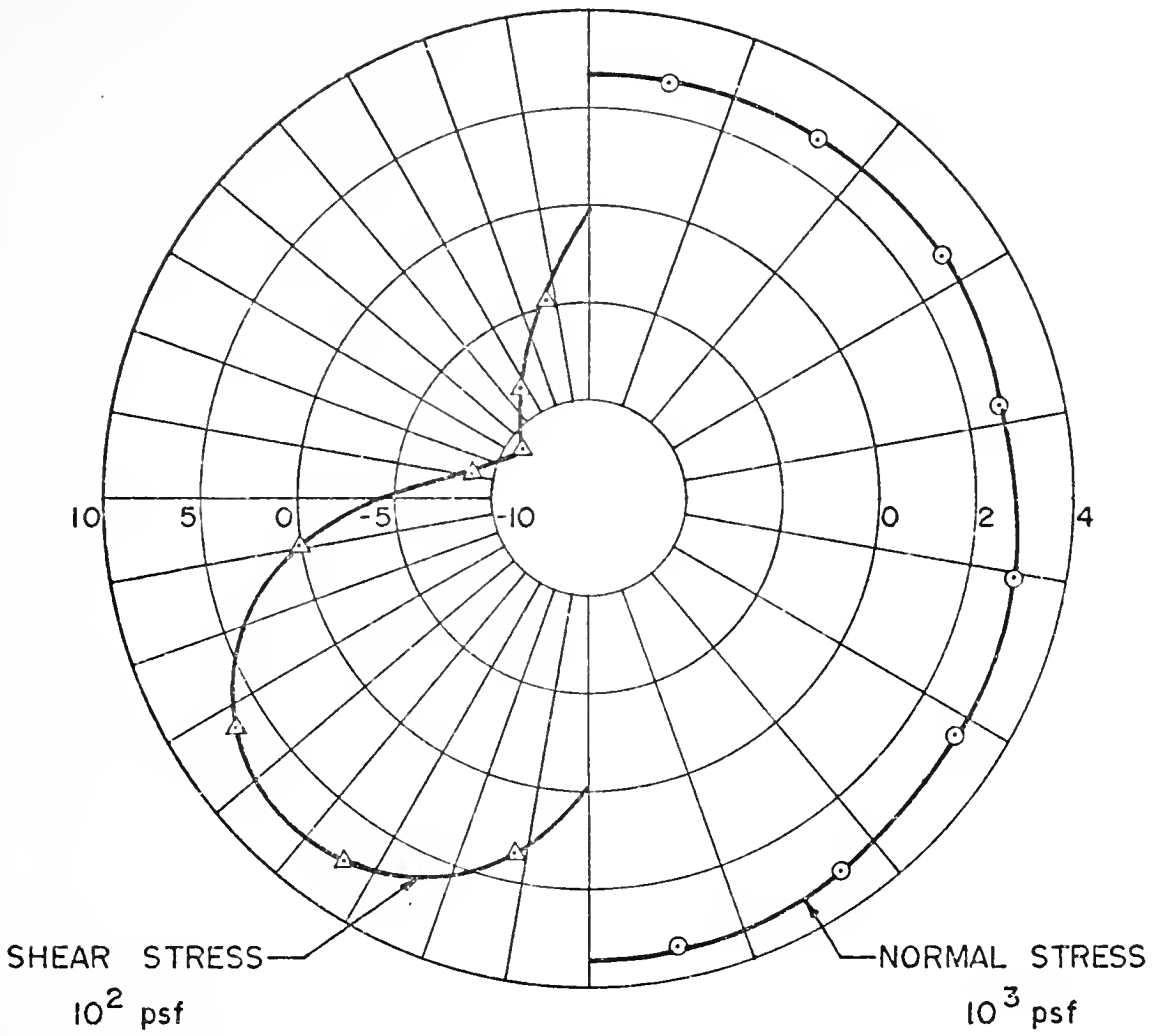


FIGURE 7.4 NORMAL AND SHEAR STRESS IN INTERACTION LAYER, PROBLEM L-14.

of the pipe for problem L-14. In Figure 7.2, deformed shape of pipe and distribution of nodal moments in the pipe are shown. Distribution of thrust and shear force in the pipe are shown in Figure 7.3. Distribution of normal and shear stresses in interaction layer (soil-pipe interface) is plotted in Figure 7.4. The results are typical for problems in Group 1, except for L-34 through L-39.

Group Two

The main purpose of the problems in Group 2 is to study the effects of nonlinear soil properties and simulation of construction sequence. Results of problems NL-1 to NL-4 and ML-1 to ML-4 are listed in Table 7.2. Also for comparison, results from problem L-36 (which is ^{the} one layer, linear elastic solution) have been included in the same table, because Young's modulus and Poisson's ratio for the soil is the same as the initial values in the non-linear analysis.

In problems NL-1 to NL-4 construction is completed in a single layer but the total load is applied in 5 (for NL-1 and NL-2) and 10 (for NL-3 and NL-4) increments. (See Table 6.2). Results obtained for 10 increments of load are very similar to that obtained with 5 increments, which shows that convergence was reached after 5 increments of load were applied to a single soil layer. For other geometries and degrees of non-linearity convergence may not be so rapid.

Comparison of results with and without interface slip shows very little or no variation. This is because

7.2 Comparison of Results, Single and Multilayer Construction, Nonlinear, Soil Properties, With and Without Interface Slip, 20 Feet Soil Cover

Identification No. (Table 6.2 and 6.3)	Change in Vertical Diameter, $\Delta Y\%$	Max. Thrust in Pipe, P_{max} $lb/ft \times 10^4$	Max. Moment in Pipe, M_{max} $ft \cdot lb/ft \times 10^3$	Max. Extreme Fiber Stress, $\sigma_{\theta max}$ $lb/in \times 10^3$	Marston-Spangler E' $lb/in^2 \times 10^5$	Horizontal Stress in Soil at Springline $lb/ft^2 \times 10^3$	Vertical Stress in Soil at Springline $lb/ft^2 \times 10^3$	Vertical Stress in Soil at Crown $lb/ft^2 \times 10^3$	Stress Ratio Inter-action $\frac{I}{\sigma} max$
L-36*	0.015	1.57	1.93	0.17	42.28	2.71	2.63	2.58	0.214
NL-1	0.057	1.74	6.06	0.43	11.18	2.29	2.14	2.64	0.395
NL-2	0.056	1.74	6.06	0.43	11.18	2.28	2.14	2.64	0.367
NL-3	0.059	1.73	6.29	0.44	10.72	2.24	2.12	2.65	0.398
NL-4	0.061	1.73	6.42	0.45	10.40	2.27	2.13	2.64	0.351
ML-1	0.061	1.60	6.51	0.46	10.35	2.06	1.87	2.39	0.379
ML-2	0.061	1.59	6.47	0.45	10.36	2.07	1.87	2.39	0.296
ML-3	0.051	1.56	5.73	0.40	12.57	2.09	2.03	2.32	0.359
ML-4	0.053	1.56	5.93	0.42	11.94	2.03	2.27	2.32	0.309

*E and v for soil is same as the initial values in the non-linear analysis

very few interaction elements have reached failure conditions corresponding to slip, and these by only a small margin.

Comparison of results between linear (L-36) and non-linear soil properties (NL-1) shows relatively large differences in deflected shape and in the extreme fibre stresses. Also, the results from single layer (5 to 10 increment) nonlinear analysis are comparable to the results from multi-layer (8 layer) nonlinear analysis which shows that for a corrugated metal culvert, 10 feet in diameter, with 20 foot of cover consisting of a granular soil the effects of considering nonlinear soil properties are very significant but consideration of the construction sequence is unimportant as long as it is symmetrical.

Problems ML-1 to ML-4 have 8 construction layers (see Table 6.3) and were solved using nonlinear soil properties and incremental analysis. In this case also interaction has very little effect on the behavior of pipe. The total number of load increments (Table 6.3) has an influence on the results but the differences between 10 and 18 increments are not large.

In the construction process, the pipe is placed on a prepared bedding and the placement of backfill material and compaction proceeds in layers. It is observed during this backpacking operation that the pipe elongates in the vertical direction, and that any untied vertical struts will topple. In the finite element simulation of construction in layers the same phenomenon is observed; in all solutions

(ML-1 to ML-4) the pipe actually elongated during the placement of 4th and 5th layer of backfill material.

Figures 7.5 to 7.7 show the distribution of parameters reflecting pipe response around the circumference of the pipe for problem NL-1. The deformed pipe shape and distribution of moments are shown in Figure 7.5. Distribution of thrust and shear force in the pipe are plotted in Figure 7.6. Distribution of normal and shear stress in interaction layer (at pipe interface) is shown in Figure 7.7. Similar plots for multi-layer solutions are given in Figures 7.8 to 7.10.

Group Three

Problems in group three were selected to show the influence of increased height of fill. In this case the height of cover has been increased from 20 feet to 40 feet. Results for linear (L-37), nonlinear (NL-5 to NL-9) and multi-layer (ML-5) analyses are tabulated in Table 7.3. The differences between elastic and nonlinear solutions are very prominent in this case, but the influence of slip at the soil-pipe interface is of no importance. Decreasing pipe stiffness [NL-6 vs. NL-7] causes increased shortening in vertical diameter, lower moment, and higher extreme fibre stresses. Making the pipe more flexible creates an arching effect which is evidenced by reduced vertical stress in the soil near crown of pipe and increased vertical stress at the springline.

Table 7.3 Comparison of Results, Single and Multilayer Construction, Nonlinear Soil Properties, With and Without Interface Slip, 40 Feet of Soil Cover

Identifi- cation No. (Table No. 6.2 and 6.3)	Change in Vertical Diameter $\Delta Y\%$	Max. Thrust in Pipe P_{max} $lb/ft \cdot 10^4$	Max. Moment in Pipe M_{max} $ft \cdot lb/ft \cdot 10^3$	Max. Extreme Fiber Stress, $\sigma_{\theta max}$ $lb/in^2 \cdot 10^3$	Marston- Spangler E' $lb/in^2 \cdot 10^3$	Horizontal Stress in Soil at Springline $lb/ft^2 \cdot 10^3$	Vertical Stress in Soil at Springline $lb/ft^2 \cdot 10^3$	Vertical Stress in Soil at Crown $lb/ft^2 \cdot 10^3$	Stress Ratio Inter- action $\frac{I}{\sigma}$ max
L-37	0.031	2.76	3.79	0.32	20.3	4.87	4.77	5.04	0.131
NL-5	0.119	3.17	12.30	0.85	43.2	4.00	3.84	5.26	0.367
NL-6	0.119	3.17	12.30	0.85	43.2	4.00	3.84	5.26	0.367
NL-7	0.275	3.04	3.48	2.95	19.8	5.34	4.31	4.35	0.358
NL-8	0.247	3.25	26.00	1.76	19.7	2.04	1.92	5.62	0.277
NL-9	0.247	3.25	26.00	1.76	19.7	2.04	1.92	5.62	0.277
NL-5	0.119	2.97	12.7	0.57	42.7	3.74	3.73	4.82	0.369

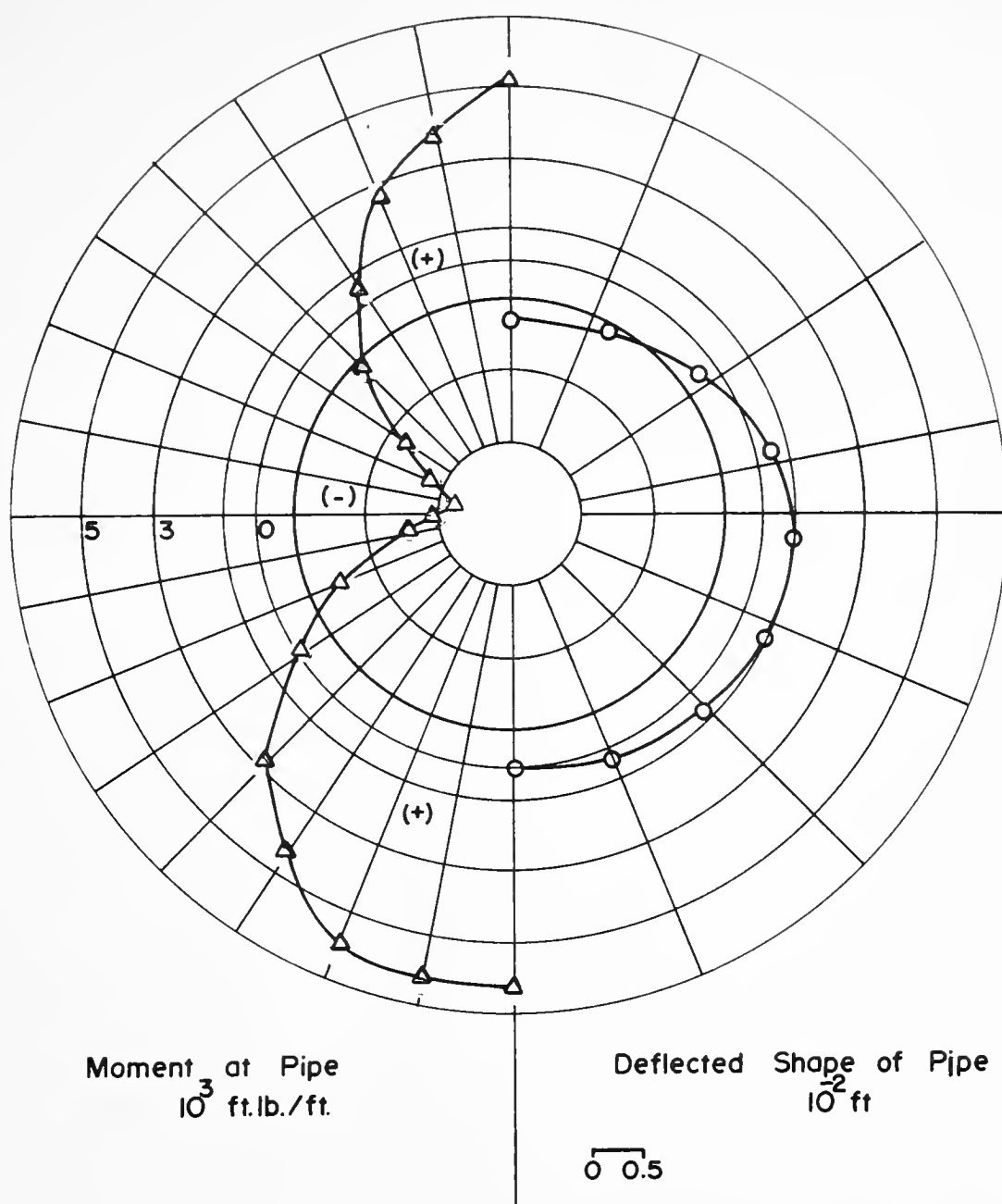


FIGURE 7.5 DEFLECTED SHAPE AND DISTRIBUTION OF MOMENT IN PIPE, NONLINEAR ANALYSIS, PROBLEM NL-1.

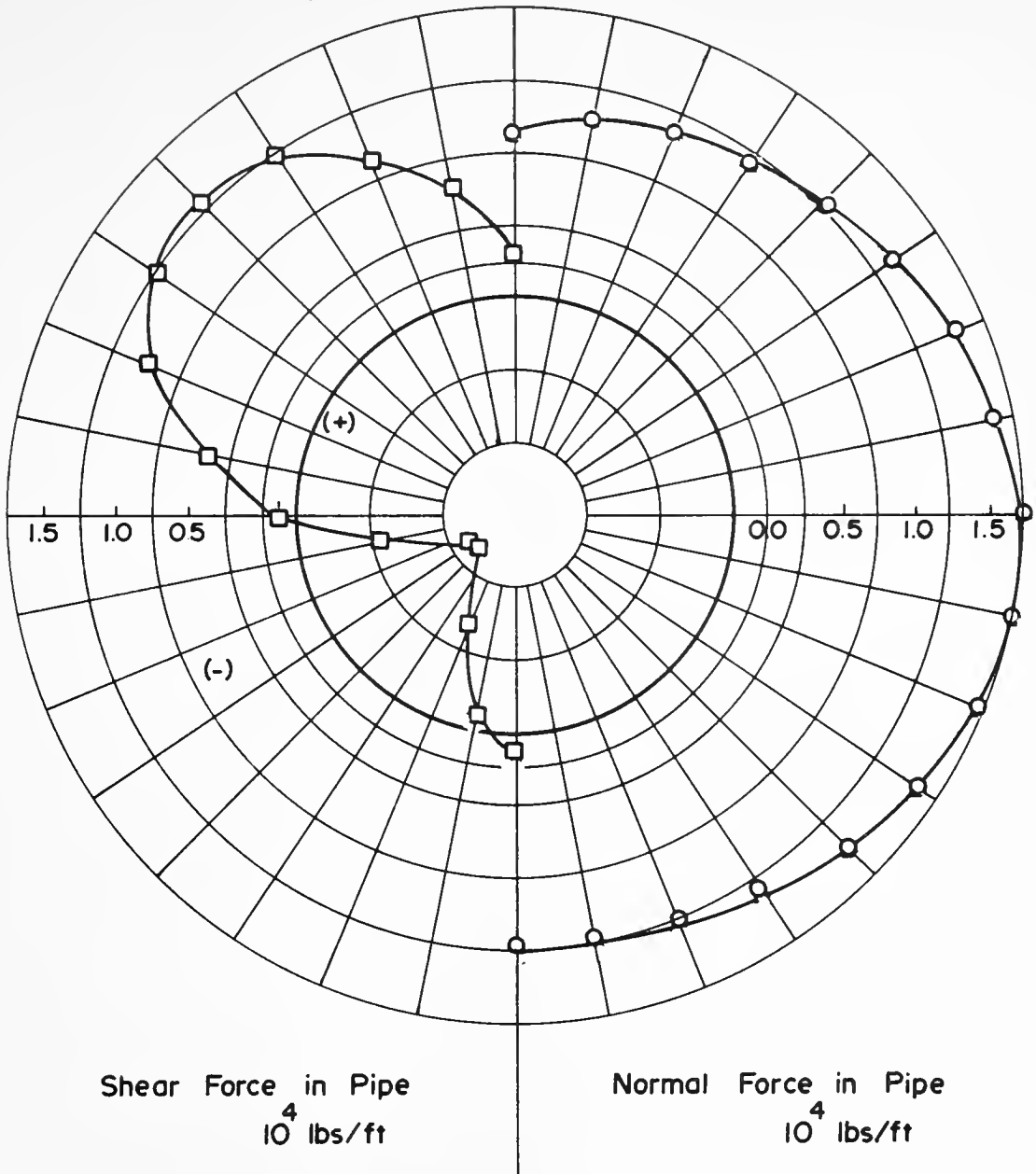


FIGURE 7.6 DISTRIBUTION OF NORMAL AND SHEAR FORCE IN PIPE, NONLINEAR ANALYSIS, PROBLEM NL-1.



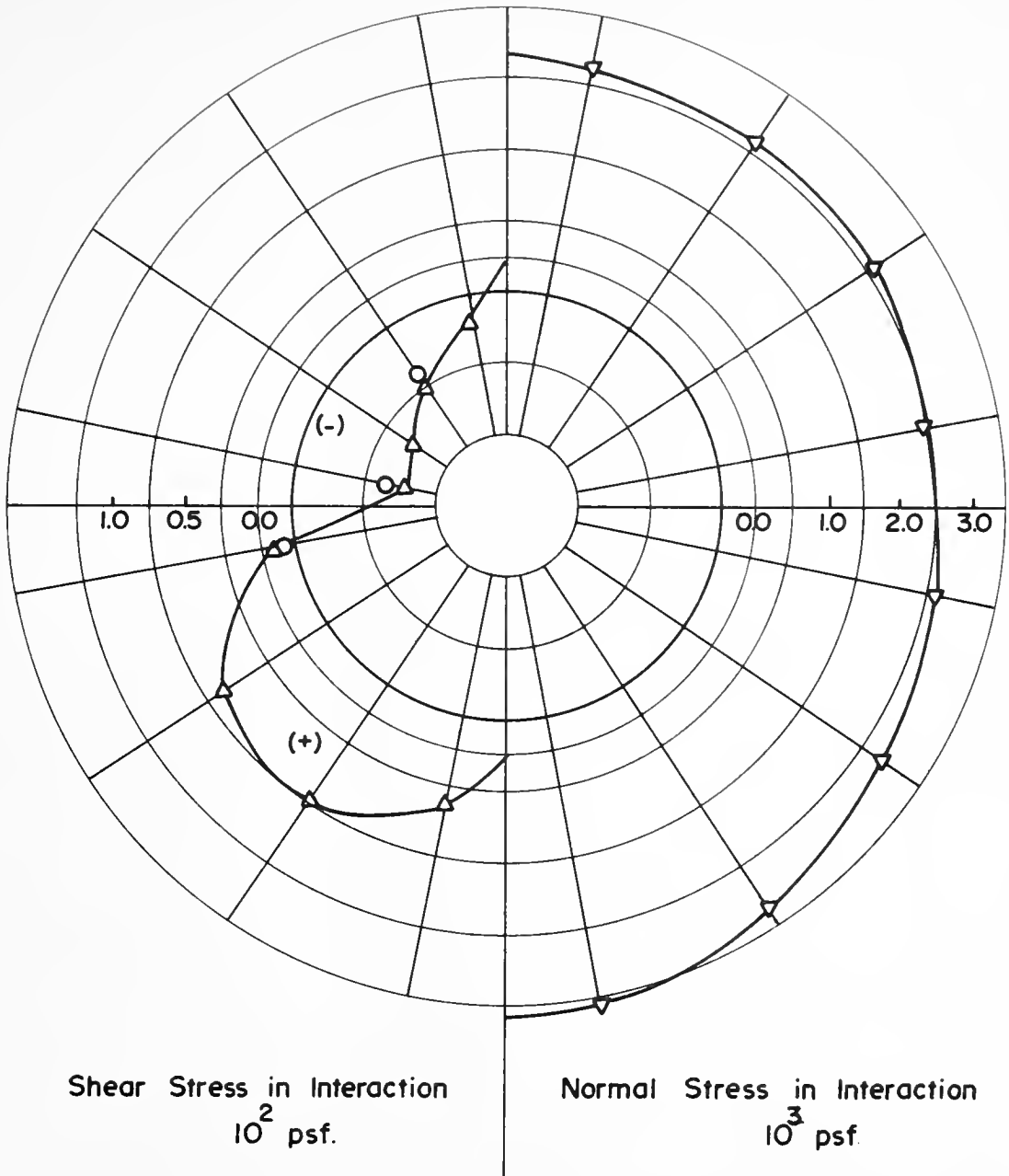


FIGURE 7.7 DISTRIBUTION OF NORMAL AND SHEAR STRESS IN INTERACTION LAYER, NON-LINER ANALYSIS, PROBLEM NL-1.



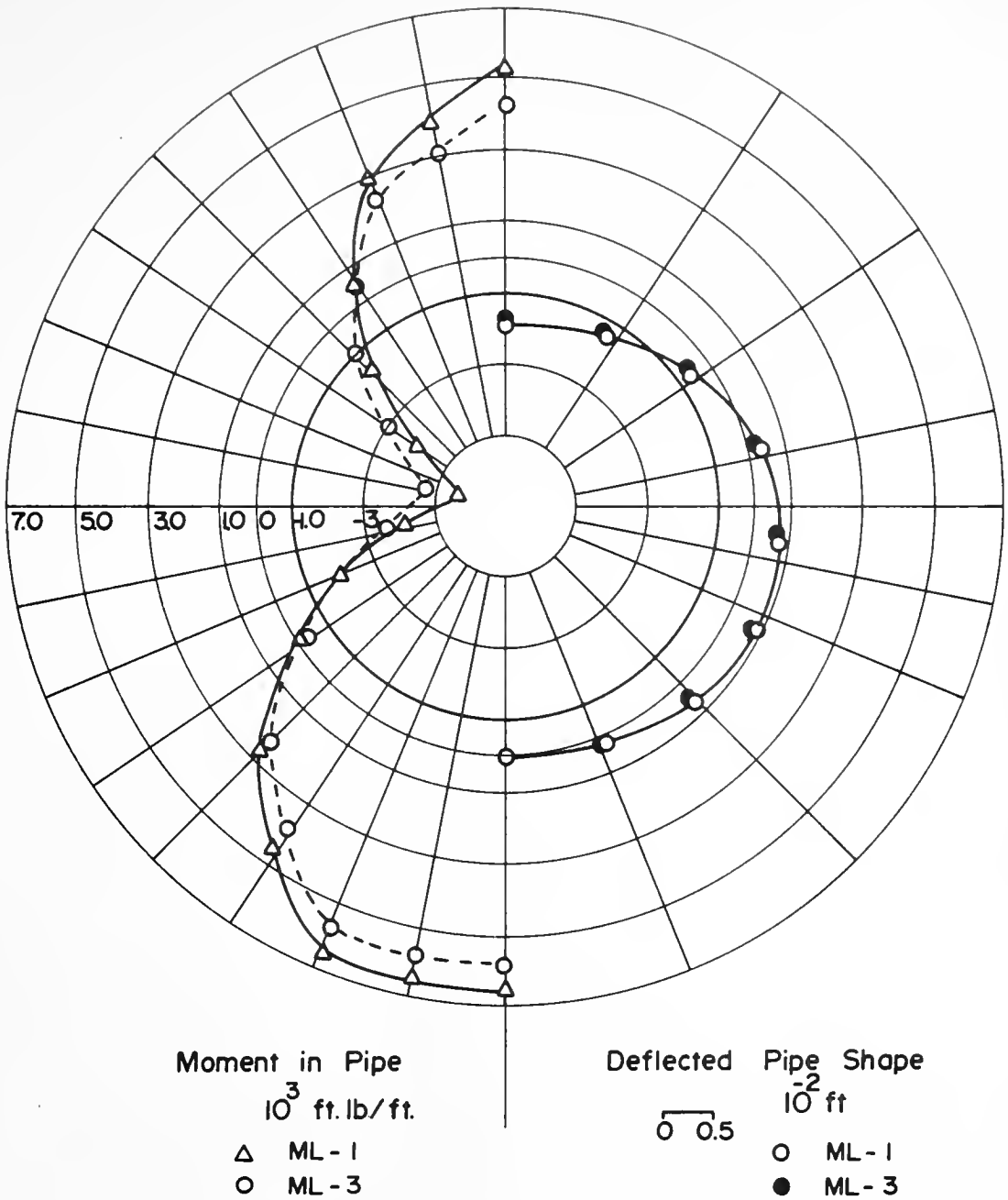


FIGURE 7.8 DEFLECTED SHAPE AND DISTRIBUTION OF MOMENT IN PIPE, MULTI LAYER ANALYSIS, PROBLEM ML-1, ML-3.

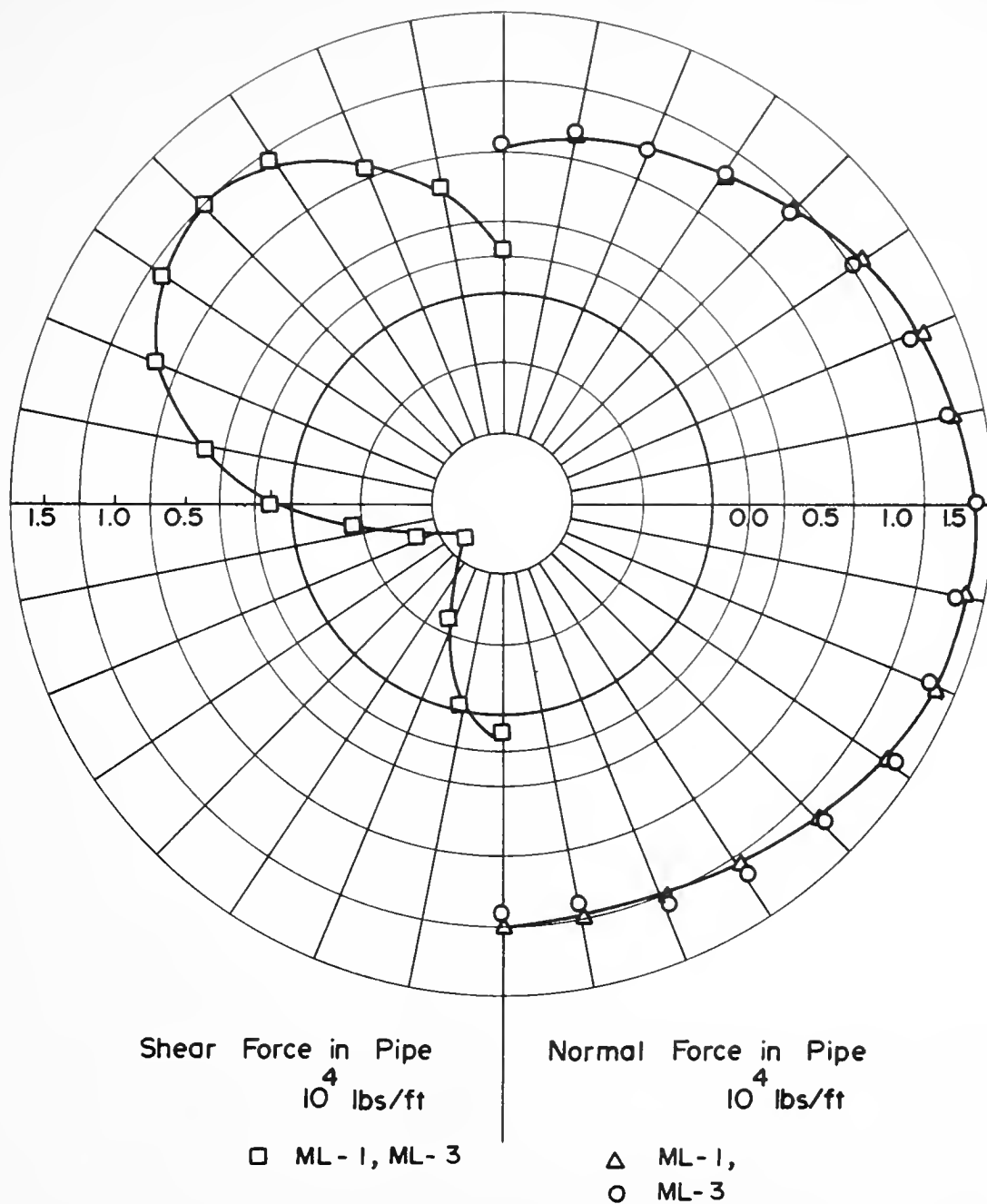


FIGURE 7.9 DISTRIBUTION OF NORMAL AND SHEAR FORCE IN PIPE ,MULTI LAYER ANALYSIS, PROBLEM ML-1, ML-3.

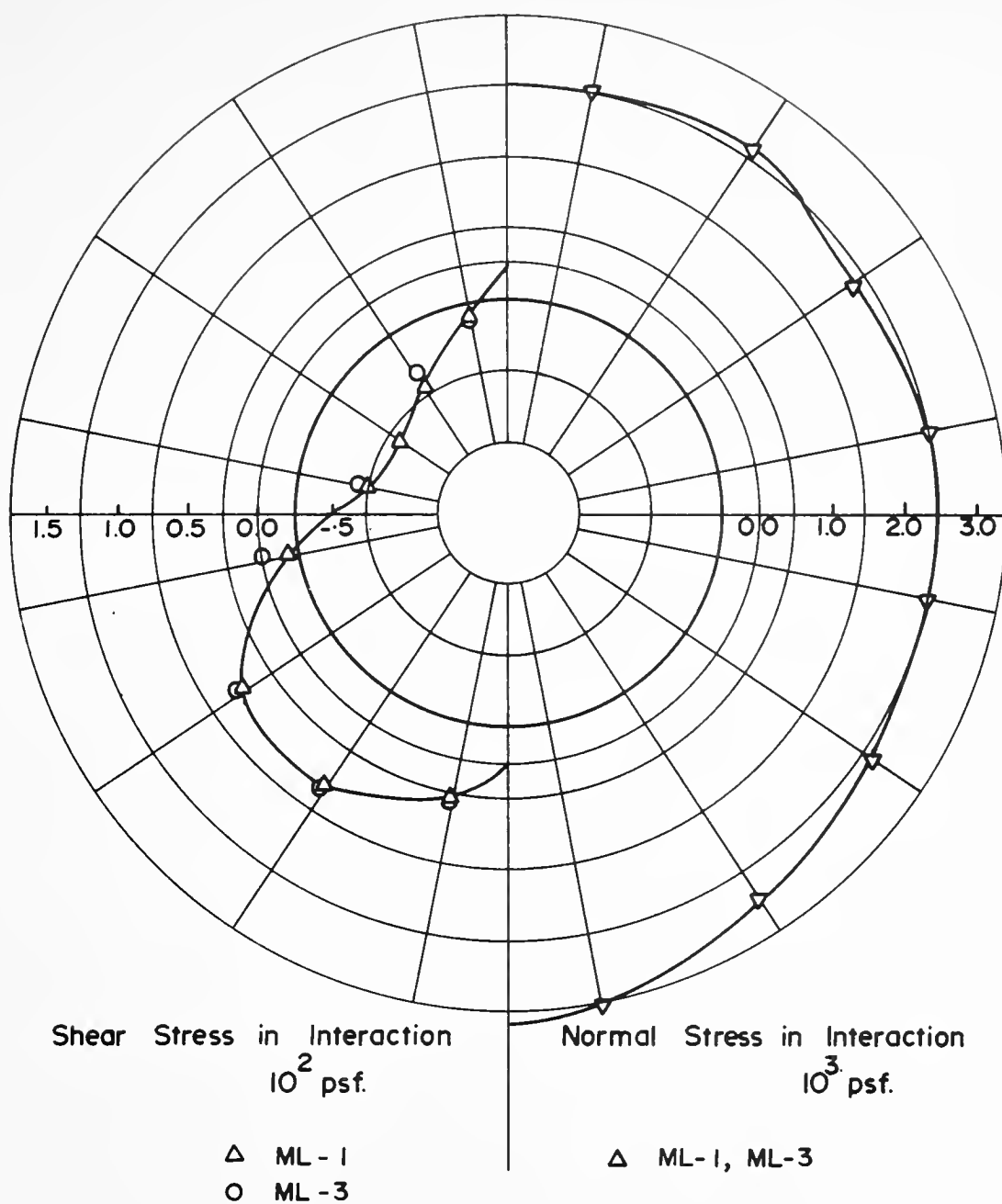


FIGURE 7.10 DISTRIBUTION OF NORMAL AND SHEAR STRESS IN INTERACTION LAYER, MULTI-LAYER ANALYSIS, PROBLEM ML-1, ML-3.



The problem with 40 feet fill has been solved using less stiff material near springline of pipe (problems NL-8, NL-9). This caused increased distortion of pipe, and a 35% increase in the extreme fiber stresses. Again, slip at the soil-pipe interface with a limiting $\tau/\sigma = 0.33$ had no influence on the results--which means little slip occurred between soil and pipe. But in all cases the maximum thrust on pipe remains virtually unaffected by different modes of analysis.

The problem with increased height of fill has been analyzed using 8 construction layers and 24 load increments (ML-5). Results are shown in Table 7.3. Similarity of results between nonlinear analysis using single layer (NL-5) and multi-layer construction (ML-5) is striking. For a culvert beneath high fills, the mode of construction may not be of importance, as the total height of fill has a dominant effect. This may not be true with nonhomogeneous or anisotropic backfill material.

CHAPTER VIII

SUMMARY

8.1 Results

Three significant improvements were made in the models used to represent components of a culvert problem:

1. An element consisting of a curved bar with bending resistance at the nodes was introduced to represent segments of the pipe. It was shown that for flexible pipes (flexibility number < 10) large errors are introduced if conventional (triangular or rectangular) elements are used--unless the pipe is divided into a very large number of elements. For the purpose of this study, the properties of the pipe material were restricted to linear elastic behavior.

2. An isoparametric triangular element with one curved side (to fit the pipe), linear strain distribution, and three intermediate nodes was used to represent the soil. After many trials, considering a variety of ways to represent soil properties, it was decided to use the results of actual test data expressed in terms of octahedral stress and strain. The results are stored to memory and the computer automatically interpolates the appropriate soil properties for any element at a particular stress level and stress increment.

3. A new element was introduced--called the 'interaction' element--to represent behavior at the soil pipe interface. The element has zero thickness (essentially zero displacement normal to the pipe) but can induce slip when the ratio of shear stress to normal stress exceeds a prescribed limit (angle of wall friction).

A computer program was written incorporating the features described above which can handle situations in which the soil and/or interaction elements are incapable of resisting tension and in which the loads due to self-weight of the soil can be applied in convenient layers (to simulate the construction sequence). Anisotropic stress-strain properties in the pipe material and in the soil, and inclusions or zones of material with different properties, was accounted for.

8.2 Conclusions

Some example problems were solved to demonstrate the versatility of the program and to investigate the influence of such factors as non-linear soil properties, relative stiffness of pipe and soil, inclusion of weak materials near the spring line, and construction procedures. From these results the following preliminary conclusions are drawn:

- A. In the case of conventional circular, corrugated metal pipes buried in granular soil, if the fill is placed symmetrically



- a) considerable insight into culvert behavior can be gained even if the soil is represented by a linear elastic material
- b) the maximum circumferential thrust in the pipe depends mainly on pipe diameter and height of fill; the stiffness of the soil or the relative stiffness of the pipe is of little influence
- c) although the maximum moment in the pipe decreases as the pipe stiffness decreases the extreme fibre stresses increase sharply. This suggests that a key factor in the performance of corrugated metal pipes is adequate resistance to local buckling; in the absence of buckling, yielding of the pipe walls will redistribute the soil pressures to insure stability. Slip in bolted seams (which reduces the thrust in the pipe without impairing the bending resistance), is also beneficial.

- B. The use of non-linear soil properties is essential to the prediction of culvert performance, while simulating construction sequence (if symmetrical) is of lesser importance--especially as the height of fill increases (to 40 feet or more).
- C. Allowance for reduced friction at the pipe-soil interface is of little importance for 10 foot diameter corrugated metal pipes buried in granular fill



with 20 to 40 feet of soil cover. It is believed, however, that interface slip can play an important role in the behavior of large-span corrugated metal arches.

- D. The Marston-Spangler soil modulus E' is not a soil property--its value was back-calculated in the example problems solved and was shown to vary strongly with pipe stiffness, and amount of soil cover. Accordingly, empirical correlations of E' with pipe performance are tenuous and cannot be used as a rational basis for future predictions.

8.3 Recommendations for Future Research

Based on the present study, it is recommended that further research should be directed in the following areas.

(1) More study is required in the area of 'no-tension' analysis and in the allowances made for interface slip. A methodology is needed to reduce the number of iterations required to reach convergence.

(2) The displacement function for interaction is linear, for soil it is quadratic while that for pipe is cubic. Accordingly, there is incompatibility of displacements along the element interfaces between the nodes. The consequences of this incompatibility may be important and should be investigated further.

(3) The solution scheme needs additional study to see if further economies can be effected in the solution of large and complex problems, possibly including automatic generation of the finite element mesh.

(4) The development of plastic hinges and of local yielding of the pipe should be accounted for. This is necessary in realistic predictions of culvert performance, because if yielding is allowed (cracking in the case of concrete pipes), it plays an important role in the economy of the structure.

(5) Sensitivity studies should be made for other pipe geometries, especially for the pipe-arch.

(6) To investigate cases in which the differential settlements in the longitudinal direction are significant, a three-dimensional finite element analysis should be developed.

LIST OF REFERENCES



LIST OF REFERENCES

- Abel, J. F.; Mark, R.; and Richards, R., Jr. (1973), "Stresses Around Flexible Elliptic Pipes", Journal of the Soil Mechanics and Foundations Division of American Society of Civil Engineers, Vol. 99 No. SM7, July, pp. 509-526.
- Ahlberg, J. H.; Nilson, E. N.; and Walsh, J. L. (1967), "The Theory of Splines and Their Applications", Mathematics in Science and Engineering. Vol. 38, Academic Press, New York.
- Allgood, J. R. (1972), "Summary of Soil-Structure Interaction", Technical Report No. R-771 Y-F008-08-02-108, DNA 13.018, Defense Nuclear Agency, Naval Civil Engineering Laboratory, Port Hueneme, California.
- Allgood, J. R. and Takahashi, S. K. (1972), "Balanced Design and Finite Element Analysis of Culverts", Highway Research Record, No. 413, pp. 45-56.
- Barnard, R. E. (1957), "Design and Deflection Control of Buried Steel Pipe Supporting Earth Loads and Live Loads", Proceedings American Society for Testing and Materials, Vol. 57, pp. 1233-1258.
- Bishop, A. W. (1966), "The Strength of Soils as Engineering Material", 6th Rankine Lecture, Geotechnique, Vol. 16, No. 2, pp. 89-130.
- Brinch Hansen, J. (1963), Discussion of "hyperbolic Stress-Strain Response to Cohesive Soils", by Kondner, R. L., Journal of the Soil Mechanics and Foundations Division of American Society of Civil Engineers, Vol. 89, No. SM4, July, pp. 241-242.
- Brown, C. B. (1966), "Rigid Culverts under High Fills, Traction on the Barrel and in the Soil", Report No. 3-66a, State of California Highway Transportation Agency, U.S. Department of Commerce, Bureau of Public Roads, October.



- Brown, C. B.; Green, D. R; and Pawsey, S. (1968), "Flexible Culverts Under High Fills", Journal of the Soil Mechanics and Foundations Division of American Society of Civil Engineers, Vol. 94, No. ST4, April, p. 905-917.
- Brummund, W. F. and Leonards, G. A. (1973), "Experimental Study of Static and Dynamic Friction Between Sand and Typical Construction Materials", Journal of Testing and Evaluation, American Society for Testing and Materials, Vol. 1, No. 2, pp. 162-165.
- Burns, J. Q. and Richard, R. M. (1964), "Attenuation of Stresses for Buried Cylinders", Proceedings of the Symposium on Soil-Structure Interaction, University of Arizona, Tucson, Arizona, September, pp. 378-392.
- "California Culvert Practice", (1944), Reprint of a Series of Technical Abstracts from California Highways and Public Roads, 2nd Edition, Chapter VII, State of California, Dept. of Public Works, Division of Highways, August.
- Chang, C-Y and Nair, K. (1973), "Development and Applications of Theoretical Methods for Evaluating Stability of Openings in Rock", Final Report, U.S. Bureau of Mines, Contract No. H0220038, December.
- Chen, L. S. (1948), "An Investigation of Stress-Strain and Strength Characteristics of Cohesionless Soils by Triaxial Compression Tests", Proceedings, Second International Conference on Soil Mechanics and Foundation Engineering, Rotterdam, Vol. V, pp. 35-43.
- Christian, M. (1973), "Solution of Linear Equations - State of the Art", Journal of the Soil Mechanics and Foundations Division of American Society of Civil Engineers, Vol. 99, No. ST7, July, pp. 1507-1526.
- Clough, R. W. (1960), "The Finite Element Method in Plane Strain Analysis", Proceedings Second Conference on Electronic Computation, Journal of the Soil Mechanics and Foundations Division of American Society of Civil Engineers, Pittsburg.
- Clough, G. W. and Duncan, J. M. "Finite Element Analysis of Port Allen and Old River Locks", U.S. Army Engineers Waterways Experimentation Station, Vicksburg, Mississippi.

- Clough, R. and Tocher, J. (1965), "Finite Element Stiffness Matrices for Analysis of Plate Bending", Proceedings of (1st) Conference on Matrix Methods in Structural Mechanics, Wright-Patterson AFB, Ohio, AFFDL TR 66-80.
- Conforth, D. H. (1964), "Some Experiments on the Influence of Strain Conditions on the Strength of Sand", Geotechnique, Vol. 14, No. 2, pp. 143-167.
- Corotis, B.; Farzin, M. H.; and Krizek, R. J. (1974) "Non-Linear Stress-Strain Formulation for Soils", Journal of the Geotechnical Engineering Division of American Society of Civil Engineers, Vol. 100, No. GT9, September, pp. 993-1008.
- Costantino, C. J., Robinson, R. R., and Salmon, M. A. (1964), "A Simplified Soil Structure Interaction Model to Investigate the Response of Buried Silos and Cylinders", Proceedings of the Symposium on Soil-Structure Interaction, University of Arizona, Tucson, Arizona, September, pp. 303-314.
- Dar, S. M. and Bates, R. C. (1974), "Stress Analysis of Hollow Cylindrical Inclusions", Journal of the Geotechnical Engineering Division of American Society of Civil Engineers, Vol. 100, No. GT2, February, pp. 123-138.
- Davis, R. E. (1966), "Structural Behavior of a Reinforced Arch Culvert", Vol. 1, Vol. 2, Report No. SSR 3-66, State of California, Highway Transportation Agency, In cooperation with U.S. Department of Commerce Bureau of Public Roads, September.
- _____. (1969) "Structural Behavior of A Flexible Metal Culvert Under A Deep Embankment Using Method B Backfill", Vol. 1, R & D Report No. 4-69, State of California, Dept. of Public Roads, Division of Highways Bridge Dept.
- Davis, R. E.; Bacher, A. E. and Obermuller, J. C. (1974), "Concrete Pipe Culvert Behavior - Part 1", Journal of the Structural Engineering Division, of American Society of Civil Engineers, Vol. 100, No. ST3, March, pp. 599-614.
- _____. (1974), "Concrete Pipe Culvert Behavior - Part 2", Journal of the Structural Engineering Division, of American Society of Civil Engineers, Vol. 100, No. ST3, March, pp. 615-630.

- Desai, C. S. (1971), "Nonlinear Analysis Using Spline Functions", Journal of the Soil Mechanics and Foundations Division of American Society of Civil Engineers, Vol. 97, No. SM10, October, pp. 1461-1480.
- _____. (1972), Closure, "Nonlinear Analysis Using Spline Functions", Journal of the Soil Mechanics and Foundations Division of American Society of Civil Engineering, Vol. 98, No. SM9, September, pp. 967-971.
- Desai, C. S. and Abel, J. F. (1972), "Introduction to the Finite Element Method, A Numerical Method for Engineering Analysis", Von Nostrand Reinhold Co.
- Domaschuk, L. and Wade, N. H. (1969), "A Study of Bulk and Shear Moduli of a Sand", Journal of the Soil Mechanics and Foundations Division of American Society of Civil Engineers, Vol. 95, No. SM2, March, pp. 561-581.
- Duncan, J. M. and Chang, C. Y. (1970), "Nonlinear Analysis of Stress and Strain in Soils", Journal of the Soil Mechanics and Foundations Division of American Society of Civil Engineers, Vol. 96, No. SM5, September, pp. 271-290.
- Duncan, J. M. and Goodman, R. E. (1968), "Finite Element Analysis of Slopes in Jointed Rock", U.S. Army Engineers, Waterways Experiment Station, Corps of Engr., Vicksburg, Mississippi, February.
- Felippa, C. A. (1966), "Refined Finite Element Analysis of Linear and Non-linear Two-Dimensional Structures", Ph.D. Thesis, Dept. of Civil Eng., University of California, Berkeley.
- FHWA (1970), "Corrugated Metal Pipe, Structural Design Criteria and Recommended Installation Practice", U.S. Dept. of Transportation, Federal Highway Administration, Bureau of Public Roads, Prepared by E. W. Wolf and M. Townsend.
- Fisher, C. L. (1969), "World's Largest Culverts", Proceedings of Highway Engineering Conference, New Mexico State University, Las Cruces.
- Frydman, S. (1974), "Yielding of Sand in Plane Strain", Journal of the Geotechnical Engineering Division of Civil Engineers, Vol. 100, No. GT5, May, pp. 491-501.

- Frydman, S. and Zeitlen, J. G. (1969), "Some Psuedo-Elastic Properties of Granular Media", Proceedings of 7th International Conference on Soil Mechanics and Foundation Engineering, Vol. 1, Mexico, pp. 135-141.
- Goodman, R. E. and Brown, C. B. (1963), "Dead Load Stresses and the Instability of Slopes, Journal of Soil Mechanics and Foundations Division of American ociety of Civil Engineers, Vol. 89, No. SM3, May, pp. 103-134
- Goodman, R. E.; Taylor, R. L.; and Brekke, T. L. (1968), "A Model for the Mechanics of Jointed Rock", Journal of the Soil Mechanics and Foundations Division of American Society of Civil Engineers, Vol. 94, No. SM3, May, pp. 637-659.
- Griffith, J. S. and Keeney, C. A. (1972) "Load Development On A Buried Rigid Conduit", Journal of Water Pollution Control Federation, Vol. 44, No. 9, September, pp. 1713-1717.
- Harr, M. E. (1966), Foundations of Theoretical Soil Mechanics, McGraw-Hill Book Co., New York.
- Holubec, I. (1968), "Elastic Behavior of Cohesionless Soil", Journal of the Soil Mechanics and Foundations Division of American Society of Civil Engineers, Vol. 94, NO. SM6, November, pp 1215-1230.
- Howard, A. K. (1973), "Laboratory Load Tests on Buried Flexible Pipe - Progress Report No. 6", Engineering and Research Center, Report No. REC-ER-73-9, Bureau of Reclamation, June.
- Howard, A. K. and Metzger, H. G. (1973), "RPM Pipe Deflections on Yuma Project Field Tests", Report No. REC-ERC-73-7, U.S. Dept. of the Interior, Bureau of Reclamation, April.
- Irons, B. M. (1970), "A Frontal Solution Program for Finite Element Analysis", International Journal for Numerical Methods in Engineering, Vol. 2, No. 1, January - March, pp. 5-32.
- Kirkland, J. L. and Walker, R. E. (1972), "Fundamental Studies of Medium-Structure Interaction", Report No. 1, Finite Element Analysis of Buried Cylinders, U. S. Army Engineer Waterways Experiment Station, Vicksburg, Mississippi, June.



- Klyuyev, V. V. and Kokovkin-Scherbak, N. I. (1965), "On the Minimization of Number of Arithemetic Operations for the Solution of Linear Algebraic Systems of Equations". Technical Report CS-24, Computer Science Dept., Stanford University, California.
- Kondner, R. L. (1963), "Hyperbolic Stress-strain Response: Cohesive Soils", Journal of the Soil Mechanics and Foundations Division of American Society of Civil Engineers, Vol. 89, No. SM1, February, pp. 115-143.
- Krizek, R. J.; Corotis, B.; and Farzin, M. H. (1975), "Field Performance of Reinforced Concrete Pipe". Transportation Research Record, No. 517, pp. 30-42.
- Krizek, R. J.; Parmelee, R. A.; Kay, J. N. and Elnaggar H. A. (1971), "Rational Structural Analysis and Design of Pipe Culverts", National Cooperative Highway Research Program, Research Report No. 116.
- Krizek, R. J. and Kay J. N. (1972), "Material Properties Affecting Soil Structure Interaction of Underground Conduits", Highway Research Record No. 413, Highway Research Board, pp. 13-29.
- Krizek, R. J. and Parmelee, R. A. (1968), "Bibliography on Analysis, Design and Installation of Highway Culverts", Dept. of Civil Eng., The Technological Institute, Northwestern University, Evanston, Illinois.
- Kulhawy, F. H. and Duncan, J. M. (1969), "Finite Element Analysis of Stresses & Movements in Embankments During Construction", Contract Report S-69-8, U.S. Army Engineer Waterways Experiment Station, Vicksburg, Mississippi, November.
- Lade, P. V. (1972), "e Stress-Strain and Strength Characteristics of Cohesionless Soils", Ph.D. Thesis, University of California, Berkeley.
- Lade, P. V. and Duncan, J. M. (1976). "Stress-Path Dependent Behavior of Cohesionless Soils", Journal of the Geotechnical Engineering Division, ASCE, Val. 102, No. GT1, pp. 51-68.
- Lee, K. L. and Seed, H. B. (1967), "Drained Strength Characteristics of Sands", Journal of the Soil Mechanics and Foundations Division of American Society of Civil Engineers, Vol. 93, NO. SM6, November, pp. 117-141.
- Lekhnitskii, S. G. (1963), (Translated from Russian by P. Fern), "Theory of Elasticity of an Anisotropic Elastic Body", Edited by J. J. Brandstatter, Chapter 1, Holden-Day Series in Mathematical Physics, Holden Day, Inc., San Francisco.



- Linger, D. A. (1972), "Historical Development of the Soil-Structure Interaction Problems", Highway Research Record, No. 413, pp. 5-12.
- Madhav, M. R. and Roy, M. B. (1970), "Anisotropy of a Bentonite Clay by Vane Shear Tests", Journal Indian National Society of Soil Mechanics and Foundation Engineering, Vol. 9, No. 3, July, pp. 333-340.
- Mallett, R. H. and Marcal, P. V. (1968), "Finite Element Analysis of Nonlinear Structures", Journal of the Soil Mechanics and Foundations Division of American Society of Civil Engineering Vol. 94, No. ST9, September, pp. 2081-2105.
- Marston, A. (1930), "The Theory of External Loads on Closed Conduits in the Light of the Latest Experiments", Iowa Engineering Experiment Station, Bulletin 96, Ames, Iowa.
- Marston, A. and Anderson A. O. (1913), "The Theory of Loads on Pipes in Ditches and Tests of Cement and Clay Drain Tile and Sewer Pipe", Iowa Engineering Experiment Station, Bulletin 31, Ames, Iowa.
- Martin, H. C. (1966), Introduction to Matrix Methods of Structural Analysis. McGraw Hill Book Co., New York, pp. 144-150.
- Melosh, R. J. (1961), "A Stiffness Matrix for the Analysis of Thin Plates in Bending", Journal of Aeronautical Science, Vol. 28, No. 4.
- _____. (1963), "Basis for Derivation of Matrices for the Direct Stiffness Method", Journal American Institute of Aeronautics and Astronautics, Vol. 1, No. 7.
- Neilson, F. D. (1972), "Experimental Studies in Soil-Structure Interaction", Highway Research Record, No. 413, pp. 30-44.
- Oden, J. T. (1967), "Finite Element Applications in Non-linear Structural Analysis", Proceedings of Symposium on Application of Finite Element Methods in Civil Engineering, American Society of Civil Engineers, Vanderbilt University, Nashville, Tennessee, November, pp. 419-456.
- Parmelee, R. A. (1973), "An Investigation of Soil-Structure Interaction of Buried Concrete Pipe", Paper presented at the Highway Research Board Meeting at Washington, DC., January.

- Parmelee, R. A. and Corotis, R. D. (1972), "The Iowa Deflection Formula: An Appraisal", Highway Research Record, No. 413, pp. 89-101.
- Perloff, W. H. (1972), "Strain Distribution Around Underground Openings", Technical Report No. 7, School of Civil Engineering, Purdue University, Sponsored by Advanced Research Projects Agency, Dept. of Defense.
- Poulos, H. G. (1972), "Difficulties In Prediction of Horizontal Deformation of Foundation", Research Report, No. R-160, School of Civil Engineering, University of Sydney, Australia.
- Przemieniecki, J. S. (1968), Theory of Matrix Structural Analysis, McGraw Hill Book Co., New York.
- Ramani, D. T. (1972), "The Finite Element Analysis of Sandwich 'Buckle-Shell' Structures", Ph.D. Thesis, Purdue University, Dept. of Civil Eng., W. Lafayette, Indiana, June.
- Ritz, W. (1909). "Über eine Methode zur Lösung gewissen Variations - Problems der mathematischen Physik", Journal Reine und Angewandte Math. 135, pp. 1-61.
- Roark, R. J. (1943), "Formulas for Stress and Strain", Second Edition, McGraw-Hill Book Co., New York, 1943.
- Rutledge, P. C. and Gould, J. P. (1973), "Movements of Articulated Conduits under Earth Dams on Compressible Foundations", Embankment-Dam Engineering, Casagrande Volume, John Wiley & Sons, pp. 209-237.
- Spangler, M. G. (1960), "Marston Theory for Soil Pressure on Conduits", Chapter 24, Soil Engineering, International Text Book Co., Pittsburgh, Pennsylvania.
- Spangler, M. G. (1962), "Culverts and Conduits", Chapter 11, in Foundation Engineering, edited by G. A. Leonards, McGraw Hill, New York.
- _____. (1971), Discussion of paper "Response of Corrugated Steel Pipe To External Soil Pressure" by Watkins and Moser, Highway Research Record No. 373, pp. 96-108.
- "State of the Art" (1964), Session 4, Proceedings of the Symposium on Soil-Structure Interaction, Univ. of Arizona, Tucson, Arizona, September, pp. 189-282.

- Stavsky, Y. and Hoff, H. J. (1969), "Mechanics of Composite Structures", Chapter 1, Composite Engineering Laminates, Edited by A. G. H. Dietz, M.I.T. Press.
- Strutt, J. W. (Lord Rayleigh), (1870), "On the Theory of Resonance", Transaction, Royal Society (London), A-161, pp. 77-118.
- Townsend, M. (1963), "Reinforced Concrete Pipe Culverts, Criteria for Structural Design and Installation", U. S. Dept. of Commerce, Bureau of Public Roads, August.
- Turner, M. J. (1959), "The Direct Stiffness Method of Structural Analysis", Structures and Materials Panel Paper, AGARD Meeting, Aachen, Germany.
- Turner, M. J.; Clough, R. W. and Topp, L. T. (1956), "Stiffness and Deflection Analysis of Complex Structures", Journal of the Aeronautical Sciences, Vol. 23, No. 9, September.
- Washizu, K. (1968), "Variational Methods in Elasticity and Plasticity", Pergamon Press, Oxford.
- Watkins, R. K. and Moser A. P. (1971), "Response of Corrugated Steel Pipe to External Soil Pressures", Highway Research Record, No. 373, pp. 86-92.
- White, H. L. and Layer, J. P. (1960), "The Corrugated Metal Conduit as a Compression Ring", Proceedings of the Highway Research Board, Vol. 39, pp. 389.
- Wolf, E. W. and Townsend, M. (1970), "Corrugated Metal Pipe, Structural Design Criteria and Recommended Installation Practice", U.S. Dept. of Transportation, Federal Highway Administration, Bureau of Public Roads.
- Wolford, D. S. (1954), "Sectional Properties of Corrugated Sheets Determined by Formula", Civil Engineering, February, pp. 59-60.
- Wright, S. G. and Duncan, J. M. (1972), "Analysis of Waco Dam Slide", Journal of the Soil Mechanics and Foundations Division of American Society of Civil Engineers, Vol. 98, No. SM9, September, pp. 869-677.
- Wu, T. H. (1971), "A Study of Soil-Structure Interaction: Reinforced Concrete Culvert Pipes", Report (Final): EES 314, Engr. Expt. Stn. Ohio State Univ., Columbus, Ohio, July.

- Zienkiewicz, O. C.; Irons, B. M.; Ahmed, S.; and Scott F. (1969), "Isoparametric and Associated Element Families for Two and Three Dimensional Analysis", Finite Element Methods in Stress Analysis, Edited by Holland, I., and Bell K. Published by TAPIR, The Technical University of Norway, Trondheim.
- Zienkiewicz, O. C. (1971), "The Finite Element Method in Engineering Science." McGraw Hill Book Co. London.
- Zienkiewicz, O. C.; Villiappan, S. and King, I. P. (1968), "Analysis of Rock as a 'No Tension' Material", *Geotechnique*, Vol. 18, March, 1968.

APPENDICES



APPENDIX - A

ISOPARAMETRIC LINEAR-STRAIN TRIANGULAR
ELEMENT WITH ONE CURVED BOUNDARY

Derivation of isoparametric linear strain triangular finite elements has been presented in section 3.5 in brief.

A more detailed treatment is described here. Figure A.1 shows an element with corner nodes marked 1, 2, 3 and intermediate midpoint nodes are 4, 5, 6. $P(x,y)$ is any floating point inside the triangular area. Side 1-4-2 may be curved. The triangle may be subdivided into four areas

$$P23 = \text{area } A_1$$

$$P31 = \text{area } A_2$$

$$1P2 \text{ and the curved side} = \text{area } A_3$$

$$\text{Side } 12 \text{ and curved side} = \text{area } A_4$$

$$\text{Total area of triangle } 123 = A^*$$

$$A^* = A_1 + A_2 + A_3 + A_4 \quad (\text{A.1})$$

The area ratios are

$$\xi_1 = \frac{A_1}{A^*}, \quad \xi_2 = \frac{A_2}{A^*}, \quad \xi_3 = \frac{A_3}{A^*}$$

$$\text{and} \quad \xi_1 + \xi_2 + \xi_3 = 1 - 2\eta \quad (\text{A.2})$$

where

$$2\eta = \frac{A_4}{A^*}$$

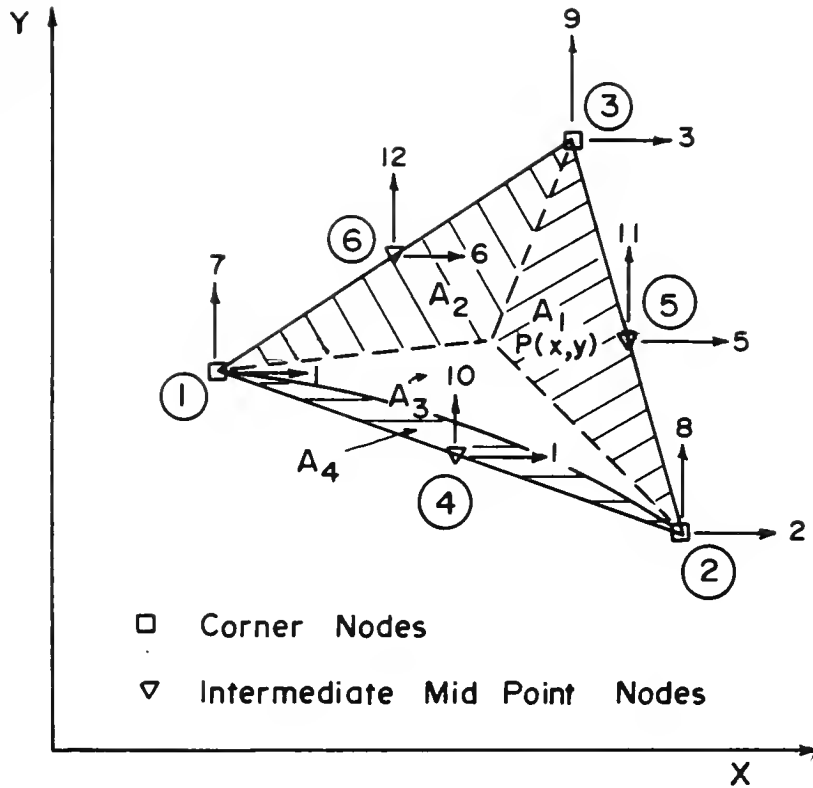


FIGURE A-1 ISOPARAMETRIC LINEAR STRAIN TRIANGULAR ELEMENT.

Relations between ξ_i and x, y system are given in equation (3.2). Displacement functions F_1 and F_4 have been derived in equation (3.5) and (3.6) respectively. Expressions for F_2 , F_3 , F_5 and F_6 follows the same procedure and are summarized in equation (3.7) and shown here.

$$\begin{aligned}
 F_1 &= \xi_1 \left[\frac{2}{1-2\eta} \xi_1 - 1 \right] \\
 F_2 &= \xi_2 \left[\frac{2}{1-4\eta} \xi_2 - \frac{1}{1-4\eta} \right] \\
 F_3 &= \xi_3 \left[2\xi_3 - 1 + 4\eta \right] \\
 F_4 &= \frac{4}{(1-2\eta)^2} \xi_1 \xi_2 \\
 F_5 &= \frac{4}{(1-4\eta)} \xi_2 \xi_3 \\
 F_6 &= \frac{4}{(1-4\eta)} \xi_3 \xi_1
 \end{aligned} \tag{A.3}$$

In vector notation

$$\underline{F}^T = \{F_1 \ F_2 \ F_3 \ F_4 \ F_5 \ F_6\}$$

where T refers to transpose of matrix.

Displacement at P (Figure A.1) can be written in terms of nodal displacement in the following manner

$$\underline{f} = \begin{Bmatrix} u \\ v \end{Bmatrix} = \begin{bmatrix} \underline{F} & \underline{0} \\ \underline{0} & \underline{F} \end{bmatrix} \cdot \begin{Bmatrix} \underline{u} \\ \underline{v} \end{Bmatrix} \tag{A.4}$$

where \underline{u} and \underline{v} are nodal displacement vectors in x and y directions, respectively.

Strain in the element can be determined by taking the partial derivative of equation (A.3) with respect to x , and y . Chain rule for partial derivatives will be used, which is

$$\frac{\delta \underline{f}}{\delta x} = \sum_{i=1}^3 \frac{\delta \underline{F}_i}{\delta \xi_i} \cdot \frac{\delta \xi_i}{\delta x}$$

or

$$\frac{\delta \underline{f}}{\delta x} = \sum_{i=1}^6 \frac{\delta \underline{F}_i}{\delta \xi_i} \cdot \frac{\delta \xi_i}{\delta x} = \frac{\delta \underline{F}_1}{\delta \xi_1} \cdot \frac{\delta \xi_1}{\delta x} + \frac{\delta \underline{F}_2}{\delta \xi_2} \cdot \frac{\delta \xi_2}{\delta x} + \frac{\delta \underline{F}_3}{\delta \xi_3} \cdot \frac{\delta \xi_3}{\delta x}$$

(A.5)

From (A.3)

$$\frac{\delta F_1}{\delta \xi_1} = \frac{1}{1-2\eta} \{4\xi_1 - 1 + 2\eta\}$$

$$\frac{\delta F_2}{\delta \xi_2} = \frac{1}{1-4\eta} \{4\xi_2 - 1\}$$

$$\frac{\delta F_3}{\delta \xi_3} = \{4\xi_3 - 1 + 4\eta\}$$

$$\frac{\delta F_4}{\delta \xi_1} = \frac{4\xi_2}{(1-2\eta)^2}$$

$$\frac{\delta F_4}{\delta \xi_2} = \frac{4\xi_1}{(1-2\eta)^2}$$

$$\frac{\delta F_5}{\delta \xi_3} = \frac{4}{(1-4\eta)} \xi_2$$

$$\frac{\delta F_5}{\delta \xi_2} = \frac{4}{(1-4\eta)} \xi_3$$

$$\frac{\delta F_6}{\delta \xi_1} = \frac{4}{(1-4\eta)} \xi_3$$

$$\frac{\delta F_6}{\delta \xi_3} = \frac{4}{(1-4\eta)} \xi_1$$

To determine derivatives like $\frac{\delta \xi_i}{\delta x}$ and $\frac{\delta \xi_i}{\delta y}$, equation (3.2a) will be used and the derivatives can be written as

$$\frac{\delta \xi_1}{\delta x} = \frac{1}{2(\text{Area})} \cdot y_{23}$$

$$\frac{\delta \xi_2}{\delta x} = \frac{1}{2(\text{Area})} \cdot y_{31}$$

$$\frac{\delta \xi_3}{\delta x} = \frac{1}{2(\text{Area})} \cdot y_{12}$$

where $y_{ij} = y_i - y_j$

In vector notation

$$\frac{\delta \xi}{\delta x} = \frac{1}{2(\text{Area})} \{y_{23} \quad y_{31} \quad y_{12}\} = \frac{1}{2A^*} B_1 \quad (\text{A.6})$$

where $A^* = \text{Area of triangle 1-2-3}$ and $B_1 = \{y_{23} \quad y_{31} \quad y_{12}\}$

In a similar fashion

$$\frac{\delta \xi}{\delta y} = \frac{1}{2A^*} B_2 \quad (A.7)$$

$$\text{where } B_2 = \{ x_{32} \quad x_{13} \quad x_{21} \}$$

$$\text{and } x_{ij} = x_i - x_j$$

Now equation (A.5) can be written as

$$\frac{\delta F}{\delta x} = \frac{1}{2A^*} B_1 \underline{\psi} \quad (A.8)$$

where

$$\underline{\psi} = \begin{bmatrix} \frac{1}{1-2\eta}(4\xi_1-1+2\eta) & 0 & 0 \\ 0 & -\frac{1}{(1-4\eta)}(4\xi_1-1) & 0 \\ 0 & 0 & (4\xi_3-1+4\eta) \\ \frac{4\xi_2}{(1-2\eta)^2} & 0 & \frac{4}{(1-4\eta)}\xi_3 \\ \frac{4\xi_1}{(1-2\eta)^2} & \frac{4}{(1-4\eta)}\xi_3 & 0 \\ 0 & \frac{4}{(1-4\eta)}\xi_2 & \frac{4}{(1-4\eta)}\xi_1 \end{bmatrix}$$

In a similar way

$$\frac{\delta F}{\delta y} = \frac{1}{2A^*} B_2 \underline{\psi} \quad (A.9)$$

Now the element strain vector can be written from equation (A.4) as

$$\underline{e} = \begin{Bmatrix} e_x \\ e_y \\ e_{xy} \end{Bmatrix} = \begin{Bmatrix} \frac{\delta u}{\delta x} \\ \frac{\delta v}{\delta y} \\ \frac{\delta u}{\delta y} + \frac{\delta v}{\delta x} \end{Bmatrix} = \begin{Bmatrix} f_x \cdot \underline{u} \\ f_y \cdot \underline{v} \\ f_y \cdot \underline{u} + f_x \cdot \underline{v} \end{Bmatrix} \quad (A.10)$$

where $f_x = \frac{\delta F}{\delta x}$ and $f_y = \frac{\delta F}{\delta y}$

$$\underline{e} = \frac{1}{2A^*} \cdot \begin{Bmatrix} B_1 & 0 \\ 0 & B_2 \\ B_2 & B_1 \end{Bmatrix} \cdot \begin{bmatrix} \underline{\psi} & 0 \\ 0 & \underline{\psi} \end{bmatrix} \cdot \begin{Bmatrix} \underline{u} \\ \underline{v} \end{Bmatrix} \quad (A.11)$$

or

$$\underline{e} = \underline{b} \cdot \begin{Bmatrix} \underline{u} \\ \underline{v} \end{Bmatrix}$$

By definition, stiffness matrix of the element is

$$\underline{k} = \iiint_{\text{volume}} [\underline{b}]^T \cdot [\underline{D}] \cdot [\underline{b}] \, d(\text{vol}) \quad (A.12)$$

where $[\underline{D}]$ is the elasticity matrix and \underline{k} is the element stiffness matrix.

Equation (A.12) can be expanded as

$$\underline{k} = \frac{1}{4A^*} \iiint_{\text{volume}} \begin{bmatrix} \underline{\psi}^T & 0 \\ 0 & \underline{\psi}^T \end{bmatrix} \cdot \begin{bmatrix} B_1^T & 0 & B_2^T \\ 0 & B_2^T & B_1^T \end{bmatrix} \cdot \begin{bmatrix} D_{11} & D_{12} & D_{13} \\ D_{21} & D_{22} & D_{23} \\ D_{31} & D_{32} & D_{33} \end{bmatrix} \cdot \begin{bmatrix} B_1 & 0 \\ 0 & B_2 \\ B_2 & B_1 \end{bmatrix} \cdot \begin{bmatrix} \underline{\psi} & 0 \\ 0 & \underline{\psi} \end{bmatrix} \cdot d(\text{vol}) \quad (\text{A.13})$$

(1) (2) (3)

(4) (5)

where D_{ij} are coefficients of elasticity matrix, as shown in (4.41).

Multiplying (2), (3), and (4) for uniform thickness of the element, t

$$\underline{k} = \frac{t}{4A^*} \iint_{\text{area}} \begin{bmatrix} \underline{\psi}^T & 0 \\ 0 & \underline{\psi}^T \end{bmatrix} \cdot \begin{bmatrix} C_{11} & \dots & C_{16} \\ C_{61} & \dots & C_{66} \end{bmatrix} \cdot \begin{bmatrix} \underline{\psi} & 0 \\ 0 & \underline{\psi} \end{bmatrix} \cdot d(\text{area})$$

(1) (2) (3) (A.14)

where C_{ij} are the coefficients of the product of (2), (3) and (4) forms a symmetric matrix by nature.

Only above diagonal coefficients are shown here:



$$C_{1,1} = y_{23} \cdot (D_{11}y_{23} + D_{13}x_{32}) + x_{32} \cdot (D_{31}y_{23} + D_{33}x_{32})$$

$$C_{1,2} = y_{23} \cdot (D_{11}y_{31} + D_{13}x_{13}) + x_{32} \cdot (D_{31}y_{31} + D_{33}x_{13})$$

$$C_{1,3} = y_{23} \cdot (D_{11}y_{12} + D_{13}x_{21}) + x_{32} \cdot (D_{31}y_{12} + D_{33}x_{21})$$

$$C_{1,4} = y_{23} \cdot (D_{12}x_{32} + D_{13}y_{23}) + x_{32} \cdot (D_{32}x_{32} + D_{33}y_{23})$$

$$C_{1,5} = y_{23} \cdot (D_{12}x_{13} + D_{13}y_{31}) + x_{32} \cdot (D_{32}x_{13} + D_{33}y_{31})$$

$$C_{1,6} = y_{23} \cdot (D_{12}x_{21} + D_{13}y_{12}) + x_{32} \cdot (D_{32}x_{21} + D_{33}y_{12})$$

$$C_{2,2} = y_{31} \cdot (D_{11}y_{31} + D_{13}x_{13}) + x_{13} \cdot (D_{31}y_{31} + D_{33}x_{13})$$

$$C_{2,3} = y_{31} \cdot (D_{11}y_{12} + D_{13}x_{21}) + x_{13} \cdot (D_{31}y_{12} + D_{33}x_{21})$$

$$C_{2,4} = y_{31} \cdot (D_{12}x_{32} + D_{13}y_{23}) + x_{13} \cdot (D_{32}x_{32} + D_{33}y_{23})$$

$$C_{2,5} = y_{31} \cdot (D_{12}x_{13} + D_{13}y_{31}) + x_{13} \cdot (D_{32}x_{13} + D_{33}y_{31})$$

$$C_{2,6} = y_{31} \cdot (D_{12}x_{21} + D_{13}y_{12}) + x_{13} \cdot (D_{32}x_{21} + D_{33}y_{12})$$

$$C_{3,3} = y_{12} \cdot (D_{11}y_{12} + D_{13}x_{21}) + x_{21} \cdot (D_{31}y_{12} + D_{33}x_{21})$$

$$C_{3,4} = y_{12} \cdot (D_{12}x_{32} + D_{13}y_{23}) + x_{21} \cdot (D_{32}x_{32} + D_{33}y_{23})$$

$$C_{3,5} = y_{12} \cdot (D_{12}x_{13} + D_{13}y_{31}) + x_{21} \cdot (D_{32}x_{13} + D_{33}y_{31})$$

$$C_{3,6} = y_{12} \cdot (D_{12}x_{21} + D_{13}y_{12}) + x_{21} \cdot (D_{32}x_{21} + D_{33}y_{12})$$

$$C_{4,4} = x_{32} \cdot (D_{22}x_{32} + D_{23}y_{23}) + y_{23} \cdot (D_{32}x_{32} + D_{33}y_{23})$$

$$C_{4,5} = x_{32} \cdot (D_{22}x_{13} + D_{23}y_{31}) + y_{23} \cdot (D_{32}x_{13} + D_{33}y_{31})$$

$$C_{4,6} = x_{32} \cdot (D_{22}x_{21} + D_{23}y_{12}) + y_{23} \cdot (D_{32}x_{21} + D_{33}y_{12})$$

$$C_{5,5} = x_{13} \cdot (D_{22}x_{13} + D_{23}y_{31}) + y_{31} \cdot (D_{32}x_{13} + D_{33}y_{31})$$

$$C_{5,6} = x_{13} \cdot (D_{22}x_{21} + D_{23}y_{12}) + y_{31} \cdot (D_{32}x_{21} + D_{33}y_{12})$$

$$C_{6,6} = x_{21} \cdot (D_{22}x_{21} + D_{23}y_{12}) + y_{12} \cdot (D_{32}x_{21} + D_{33}y_{12})$$

Carrying out matrix multiplication in (A.14), the 12x12 coefficients of the stiffness matrix can be determined. The last step in the derivation is to integrate the coefficients over the area of the triangle, multiply by thickness and divide by four times the area squared. The formula given in equation (3.16) is helpful for integration of stiffness coefficients. As the coefficients are symmetric in nature, only diagonal and below-diagonal terms of the final stiffness coefficients are given here and designated as Sk_{ij} where i and j refer to degrees of freedom.

Note $A = A^*$

$$Sk_{1,1} = \frac{C_{11}t}{4A} \left(\frac{1}{1-2\eta} \right)^2 \left[1 + \frac{4}{3}\eta + 4\eta^2 \right]$$

$$Sk_{2,1} = - \frac{C_{12}t}{12A(1-4\eta)}$$

$$Sk_{2,2} = \frac{C_{22}t}{4A(1-4\eta)^2}$$

$$Sk_{3,1} = \frac{C_{13}t}{4A(1-2\eta)} \left[-\frac{1}{3} + 2\eta + 8\eta^2 \right]$$

$$sk_{3,2} = - \frac{C_{23}t}{12A}$$

$$sk_{3,3} = \frac{C_{33}t}{4A} \left[1 + \frac{8}{3}\eta + 16\eta^2 \right]$$

$$sk_{4,1} = \frac{t}{4A(1-2\eta)^3} \left[2 \cdot C_{11}\eta + C_{12} \left(\frac{4}{3} + \frac{8}{3}\eta \right) \right]$$

$$sk_{4,2} = \frac{C_{21}t}{(1-2\eta)^2 \cdot 3A(1-4\eta)}$$

$$sk_{4,3} = \frac{4t\eta}{(1-2\eta)^2 \cdot 3A} (C_{31} + C_{32})$$

$$sk_{4,4} = \frac{t}{(1-2\eta)^4 \cdot 3A} (2C_{11} + C_{12} + C_{21} + 2C_{22})$$

$$sk_{5,1} = \frac{t \cdot 2\eta}{3A(1-2\eta)(1-4\eta)} (C_{11} + C_{13})$$

$$sk_{5,2} = \frac{C_{23}t}{3A(1-4\eta)^2}$$

$$sk_{5,3} = \frac{t}{3A(1-4\eta)} \left[(C_{32} \cdot (1+4\eta) + C_{33} \cdot 4\eta) \right]$$

$$sk_{5,4} = \frac{t}{(1-2\eta)^2} \cdot \frac{1}{3A(1-4\eta)} (C_{12} + 2C_{13} + C_{22} + C_{23})$$

$$sk_{5,5} = \frac{t}{3A(1-4\eta)^2} (2C_{22} + C_{23} + C_{32} + 2C_{33})$$

$$sk_{6,1} = \frac{t}{3A(1-4\eta) \cdot (1-2\eta)} \left[C_{13} + 2\eta(C_{11} + C_{13}) \right]$$

$$sk_{6,2} = 0$$

$$sk_{6,3} = \frac{t}{3A(1-4\eta)} \left[C_{31} + 4\eta(C_{31} + C_{33}) \right]$$

$$sk_{6,4} = \frac{t}{(1-2\eta)^2 3A(1-4\eta)} (C_{11} + C_{13} + C_{21} + 2C_{23})$$

$$sk_{6,5} = \frac{t}{3A(1-4\eta)^2} (2C_{21} + C_{23} + C_{31} + C_{33})$$

$$sk_{6,6} = \frac{t}{3A(1-4\eta)^2} (2C_{11} + C_{13} + C_{31} + 2C_{33})$$

$$sk_{7,1} = \frac{C_{14}t}{4A(1-2\eta)^2} \left(1 + \frac{4}{3}\eta + 4\eta^2 \right)$$

$$sk_{7,2} = - \frac{C_{24}t}{12A(1-4\eta)}$$

$$sk_{7,3} = \frac{C_{34}t}{12A(1-4\eta)} (1 - 6\eta - 24\eta^2)$$

$$sk_{7,4} = \frac{t}{(1-2\eta)^2 3A(1-2\eta)} \left[C_{14} 2\eta + C_{24} (1 + 2\eta) \right]$$

$$sk_{7,5} = \frac{t 2\eta}{3A(1-2\eta)(1+2\eta)} (C_{24} + C_{34})$$

$$sk_{7,6} = \frac{t}{3A(1-4\eta)(1-2\eta)} \left[2 \cdot C_{14}\eta + C_{34} (1 + 2\eta) \right]$$

$$sk_{7,7} = \frac{C_{44}t}{4A(1-2\eta)^2} \left(1 + \frac{4}{3}\eta + 4\eta^2 \right)$$

$$sk_{8,1} = \frac{C_{15}t}{12A(1-4\eta)(1-2\eta)} (-1 + 2\eta)$$

$$sk_{8,2} = \frac{C_{25}t}{4A(1-4\eta)^2}$$

$$Sk_{8,3} = - \frac{C_{35} t}{12A}$$

$$Sk_{8,4} = \frac{C_{15} t}{(1-2\eta)^2 3A (1-4\eta)}$$

$$Sk_{8,5} = \frac{C_{35} t}{3A (1-4\eta)^2}$$

$$Sk_{8,6} = 0$$

$$Sk_{8,7} = - \frac{C_{45} t}{12A (1-4\eta)}$$

$$Sk_{8,8} = \frac{C_{55} t}{4A (1-4\eta)^2}$$

$$Sk_{9,1} = - \frac{C_{16} t}{12A (1-2\eta)} (1 - 2\eta - 8\eta^2)$$

$$Sk_{9,2} = - \frac{C_{26} t}{12A}$$

$$Sk_{9,3} = \frac{C_{36} t}{4A} (1 + \frac{8}{3}\eta + 16\eta^2)$$

$$Sk_{9,4} = \frac{4 t \cdot \eta}{3A (1-2\eta)^2} (C_{16} + C_{26})$$

$$Sk_{9,5} = \frac{t}{3A (1-4\eta)} \left[C_{26} \cdot (1 + 4\eta) + 4 \cdot C_{36}\eta \right]$$

$$Sk_{9,6} = \frac{t}{3A (1-4\eta)} \left[C_{16} (1 + 4\eta) + C_{36} (4\eta) \right]$$

$$Sk_{9,7} = - \frac{C_{46} t}{12A (1-2\eta)} (1 - 6\eta - 24\eta^2)$$

$$Sk_{9,8} = - \frac{C_{56} t}{12A}$$

$$Sk_{9,9} = \frac{C_{66} t}{4A} (1 + \frac{8}{3}\eta + 16\eta^2)$$

$$Sk_{10,1} = \frac{t}{3A (1-2\eta)^3} \left[2\eta C_{14} + C_{15} (1 + 2\eta) \right]$$

$$Sk_{10,2} = \frac{C_{24} t}{3A (1-4\eta)} \cdot \frac{1}{(1-2\eta)^2}$$

$$Sk_{10,3} = \frac{4\eta t}{3A (1-2\eta)^2} \cdot (C_{34} + C_{35})$$

$$Sk_{10,4} = \frac{t}{3A (1-2\eta)^4} (2 C_{14} + C_{15} + C_{24} + 2 C_{25})$$

$$Sk_{10,5} = \frac{1}{(1-2\eta)^2} \frac{t}{3A (1-4\eta)} (C_{24} + C_{25} + 2C_{34} + C_{35})$$

$$Sk_{10,6} = \frac{1}{(1-2\eta)^2} \frac{t}{3A (1-4\eta)} (C_{14} + C_{15} + C_{34} + C_{35})$$

$$Sk_{10,7} = \frac{t}{3A (1-2\eta)^3} \left[2\eta C_{44} + (1 + 2\eta) C_{45} \right]$$

$$Sk_{10,8} = \frac{t}{3A (1-4\eta)} \cdot \frac{C_{54}}{(1-2\eta)^2}$$

$$Sk_{10,9} = \frac{4\eta t}{3A (1-2\eta)^2} (C_{64} + C_{65})$$

$$Sk_{10,10} = \frac{t}{3A (1-2\eta)^4} (2 C_{44} + C_{45} + C_{54} + 2 C_{55})$$

$$Sk_{11,1} = \frac{2\eta t}{3A (1-2\eta) (1-4\eta)} (C_{15} + C_{16})$$

$$Sk_{11,2} = \frac{t}{3A (1-4\eta)^2} C_{26}$$

$$Sk_{11,3} = \frac{t}{3A (1-4\eta)} \left[C_{35} (1 + 4\eta) + 4\eta \cdot C_{36} \right]$$

$$Sk_{11,4} = \frac{t}{3A (1-2\eta)^2 (1-4\eta)} \cdot \left[C_{15} + 2 C_{16} + C_{25} + C_{26} \right]$$

$$Sk_{11,5} = \frac{t}{3A (1-4\eta)^2} (2 C_{25} + C_{26} + C_{35} + 2 C_{36})$$

$$Sk_{11,6} = \frac{t}{3A (1-4\eta)^2} (2 C_{15} + C_{16} + C_{35} + C_{36})$$

$$Sk_{11,7} = \frac{2\eta t}{3A (1-2\eta) (1-4\eta)} (C_{45} + C_{46})$$

$$Sk_{11,8} = \frac{t}{3A (1-4\eta)^2} C_{56}$$

$$Sk_{11,9} = \frac{t}{3A (1-4\eta)} \left[C_{65} (1 + 4\eta) + 4\eta C_{66} \right]$$

$$Sk_{11,10} = \frac{t}{3A (1-4\eta) (1-2\eta)^2} (C_{45} + 2 C_{46} + C_{55} + C_{56})$$

$$Sk_{11,11} = \frac{t}{3A (1-4\eta)^2} (2 C_{55} + C_{56} + C_{65} + 2 C_{66})$$

$$Sk_{12,1} = \frac{t}{3A (1-2\eta)} \left[2\eta C_{14} + (1 + 2\eta) C_{16} \right]$$

$$Sk_{12,2} = 0$$

$$Sk_{12,3} = \frac{t}{3A (1-4\eta)} \left[C_{34} (1 + 4\eta) + 4\eta C_{36} \right]$$

$$Sk_{12,4} = \frac{t}{3A (1-4\eta) (1-2\eta)^2} (C_{14} + C_{16} + C_{24} + 2 C_{26})$$

$$Sk_{12,5} = \frac{t}{3A (1-4\eta)^2} (2 C_{24} + C_{26} + C_{34} + C_{36})$$

$$Sk_{12,6} = \frac{t}{3A (1-4\eta)^2} (2 C_{14} + C_{16} + C_{34} + 2 C_{36})$$

$$Sk_{12,7} = \frac{t}{3A (1-4\eta) (1-2\eta)} \left[2\eta C_{44} + (1 + 2\eta) C_{46} \right]$$

$$Sk_{12,8} = 0$$

$$Sk_{12,9} = \frac{t}{3A (1-4\eta)} \left[C_{64} (1 + 4\eta) + 4\eta C_{66} \right]$$

$$Sk_{12,10} = \frac{t}{3A (1-4\eta) (1-2\eta)^2} (C_{44} + C_{46} + C_{54} + 2 C_{56})$$

$$Sk_{12,11} = \frac{t}{3A (1-4\eta)^2} (2 C_{54} + C_{56} + C_{64} + C_{66})$$

$$Sk_{12,11} = \frac{t}{3A (1-4\eta)^2} (2 C_{44} + C_{46} + C_{64} + C_{66})$$

This completes evaluation of the stiffness matrix for isoparametric triangular elements.

Determination of Element Strain and Stress

In general finite element scheme, stiffness of each element is joined according to their nodal and element configuration to form the structural stiffness matrix which is the distribution of stiffness coefficients at all nodes. This matrix is modified for given boundary conditions and

the system of equations is solved for given nodal loads. The solution is the distribution of x and y displacements at all nodes. To determine strain in an element, nodal displacements of the element are grouped in vector \underline{u} and \underline{v} for x and y directions. Then equation (A.11) can be used to find element strain.

To evaluate element stresses, only the elasticity matrix $[D]$ and strain vector \underline{e} are required. The coefficients of $[D]$ matrix are the same as used in equation (A.13). Element stress can be found by the following expression:

$$\{ \underline{\sigma} \} = [D] \cdot \{ \underline{e} \} \quad (A.15)$$

If incremental analysis is used, the displacement vectors \underline{u} and \underline{v} , strain vector \underline{e} and stress vector $\underline{\sigma}$ are increments in one increment of load. Total displacements, strain and stress can be obtained by algebraic summation of these quantities for all increments in the analysis.

APPENDIX - B

CURVED BAR ELEMENT

Figure B.1 shows a segment of a curved bar element 1-2 of uniform thickness, which has a radius R , and subtends an angle β at the center. E is Young's modulus of the bar material and I is the moment of inertia of cross section per unit length. S is a variable point along the arc which makes an angle ϕ at the center and dS is the small increment in S corresponding to $d\phi$, the increment in ϕ . The segment is acted upon by a radial force Q , tangential force P and moment M at each end, corresponding deflections are v , u and θ .

The following sign conventions have been used. v is always radial and positive when directed towards the center. u is always tangential and positive in the counter clockwise direction. θ is positive in counter clockwise direction.

Total moment at S due to all forces and moments at 1 is given by

$$M = M_1 + P_1 R (1 - \cos\phi) - Q_1 R \sin\phi \quad (B.1)$$

$$\text{Strain energy: } U = \frac{1}{2EI} \int M^2 dS$$

$$\text{But } dS = R d\phi$$

$$\text{So } U = \frac{R}{2EI} \int_0^\beta M^2 d\phi \quad (B.2)$$

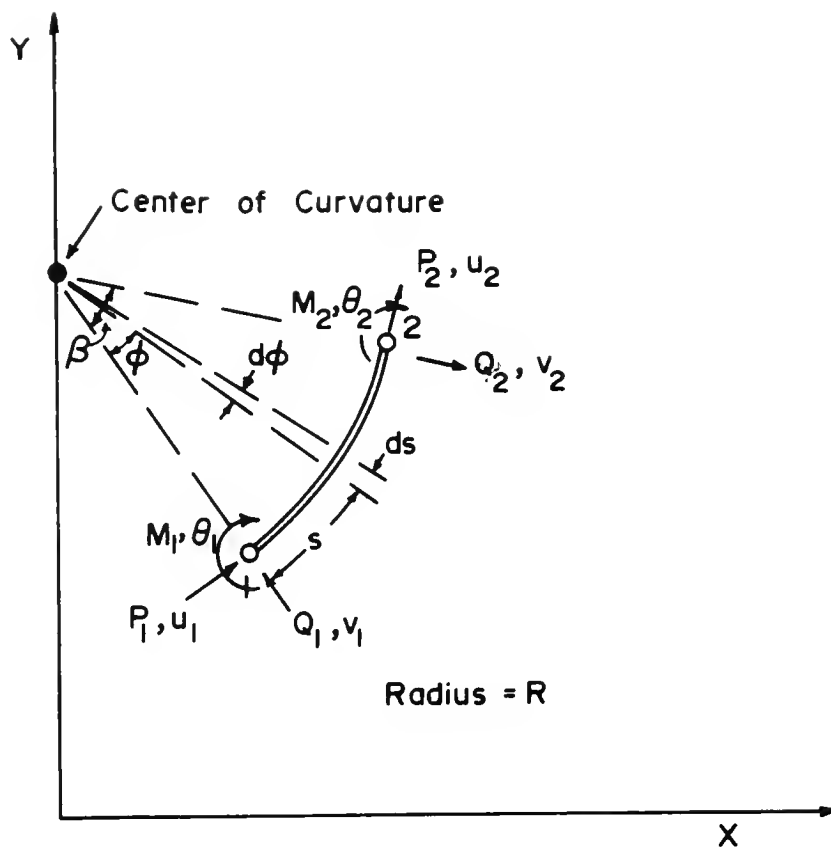


FIGURE B.1 CURVED BAR ELEMENT.

Displacement in any direction can be found by Castigliano's theorem, namely $\frac{\delta U}{\delta P_i} = \delta_i$

Displacements at node 1 are

$$u_1 = \frac{\delta U}{\delta P_1} = \frac{R}{EI} \int_0^\beta M \frac{\delta M}{\delta P_1} d\phi \quad (B.3a)$$

$$v_1 = \frac{\delta U}{\delta Q_1} = \frac{R}{EI} \int_0^\beta M \frac{\delta M}{\delta Q_1} d\phi \quad (B.3b)$$

$$\theta_1 = \frac{\delta U}{\delta M_1} = \frac{R}{EI} \int_0^\beta M \frac{\delta M}{\delta M_1} d\phi \quad (B.3c)$$

Substituting for M from equation (B.1) in above equations, taking the derivative, multiplying and integrating, one obtains the following:

$$\begin{Bmatrix} u_1 \\ v_1 \\ \theta_1 \end{Bmatrix} = \frac{R^2}{EI} \begin{bmatrix} c & b & a \\ b & d & e \\ \frac{a}{R} & \frac{e}{R} & \frac{\beta}{R} \end{bmatrix} \cdot \begin{Bmatrix} P_1 R \\ Q_1 R \\ M_1 \end{Bmatrix} \quad (B.4)$$

where

$$a = \beta - \sin\phi$$

$$b = \cos\beta + \frac{\sin^2\beta}{2} - 1$$

$$c = \frac{3\beta}{2} - 2 \sin\beta + \frac{\sin 2\beta}{4}$$

$$d = \frac{\beta}{2} - \frac{\sin 2\beta}{4}$$

$$e = \cos \beta - 1$$

Solving (B.4) for P_1 , Q , and M_1

$$\begin{Bmatrix} P_1 \\ Q_1 \\ M_1 \end{Bmatrix} = \frac{EI}{R^3 G} \begin{bmatrix} A & B & \frac{C}{\beta} R \\ B & D & \frac{E}{\beta} R \\ \frac{C}{\beta} R & \frac{E}{\beta} R & \frac{F}{\beta} R^2 \end{bmatrix} \begin{Bmatrix} u_1 \\ v_1 \\ \theta_1 \end{Bmatrix} \quad (B.5)$$

(k_{11})

where

$$\begin{aligned} A &= \frac{e^2}{\beta} - d, & B &= -\frac{ae}{\beta} \\ C &= ad - be & D &= \frac{a^2}{\beta} - c \\ E &= ce - ab & F &= b^2 - ad \\ G &= b(b - 2\frac{ae}{\beta}) + c(\frac{e^2}{\beta} - d) + \frac{a^2 d}{\beta} \end{aligned}$$

Considering equilibrium of the segment 1-2 under the system of forces, the following set of equations can be written

$$\begin{aligned} P_1 + P_2 \cos\beta - Q_2 \sin\beta &= 0 \\ Q_1 + P_2 \sin\beta + Q_2 \cos\beta &= 0 \\ M_1 + P_1 R (1 - \cos\beta) - Q_1 R \sin\beta + M_2 &= 0 \end{aligned} \quad (B.6)$$

Solving for P_2 , Q_2 and M_2 in terms of P_1 , Q_1 and M_1

$$\begin{Bmatrix} P_2 \\ Q_2 \\ M_2 \end{Bmatrix} = \begin{bmatrix} -\cos\beta & -\sin\beta & 0 \\ \sin\beta & \cos\beta & 0 \\ -R(1 - \cos\beta) & R \sin\beta & -1 \end{bmatrix} \cdot \begin{Bmatrix} P_1 \\ Q_1 \\ M_1 \end{Bmatrix} \quad (B.7)$$

Substituting in (B.7) for P_1 , Q_1 and M_1 from equation (B.5) and carrying the matrix multiplication, the following is obtained:

$$\begin{Bmatrix} P_2 \\ Q_2 \\ M_2 \end{Bmatrix} = \frac{EI}{R^3 G} [k_{21}] \begin{Bmatrix} u_1 \\ v_1 \\ \theta_1 \end{Bmatrix} \quad (\text{B.8})$$

where

$$[k_{21}] = \begin{bmatrix} a_{11} & a_{12} & a_{13} \\ a_{21} & a_{22} & a_{23} \\ a_{31} & a_{32} & a_{33} \end{bmatrix}$$

and a_{ij} are defined as below:

$$a_{11} = - (A \cos\beta + B \sin\beta)$$

$$a_{12} = - (B \cos\beta + D \sin\beta)$$

$$a_{13} = - (C \cos\beta + E \sin\beta) \cdot \frac{R}{\beta}$$

$$a_{21} = (A \sin\beta - B \cos\beta)$$

$$a_{22} = (B \sin\beta - D \cos\beta)$$

$$a_{23} = (C \sin\beta - E \cos\beta) \cdot \frac{R}{\beta}$$

$$a_{31} = [A (\cos\beta - 1) + B \sin\beta - \frac{C}{\beta}] \cdot R$$

$$a_{32} = [B (\cos\beta - 1) + D \sin\beta - \frac{E}{\beta}] \cdot R$$

$$a_{33} = [C (\cos\beta - 1) + E \sin\beta - F] \cdot \frac{R^2}{\beta}$$



Following a similar procedure for node 2 one can write

$$\begin{Bmatrix} P_2 \\ Q_2 \\ \theta_2 \end{Bmatrix} = \frac{EI}{R^3 G} [k_{22}] \cdot \begin{Bmatrix} u_2 \\ v_2 \\ \theta_2 \end{Bmatrix} \quad (B.9)$$

where $[k_{22}]$ is given by

$$[k_{22}] = \begin{bmatrix} A & -B & \frac{C}{\beta} R \\ -B & D & -\frac{E}{\beta} R \\ \frac{C}{\beta} R & -\frac{E}{\beta} R & \frac{F}{\beta} R^2 \end{bmatrix} \quad (B.10)$$

and

$$\begin{Bmatrix} P_1 \\ Q_1 \\ \theta_1 \end{Bmatrix} = \frac{EI}{R^3 G} [k_{21}] \cdot \begin{Bmatrix} u_2 \\ v_2 \\ \theta_2 \end{Bmatrix} \quad (B.11)$$

where k_{21} is the transpose of matrix k_{12} .

Combining equations (B.5), (B.8), (B.9) and (B.11) the stiffness matrix for the curved bar 1-2 can be written as:

$$\begin{Bmatrix} P_1 \\ Q_1 \\ M_1 \\ P_2 \\ Q_2 \\ M_2 \end{Bmatrix} = [k] \cdot \begin{Bmatrix} u_1 \\ v_1 \\ \theta_1 \\ u_2 \\ v_2 \\ \theta_2 \end{Bmatrix} \quad (\text{B.12})$$

where

$$[k] = \frac{EI}{R^3 G} \cdot \begin{bmatrix} k_{11} & k_{12} \\ k_{21} & k_{22} \end{bmatrix}_{6 \times 6}$$

or

$$[k] = \begin{bmatrix} SR(1,1) & SR(1,2) & \dots & SR(1,6) \\ \vdots & \vdots & & \vdots \\ \vdots & \vdots & & \vdots \\ SR(6,1) & SR(6,2) & \dots & SR(6,6) \end{bmatrix}$$

$SR(i,j)$ are the stiffness coefficients in the local co-ordinate system.

The final step is to transform the stiffness matrix $[k]$ to the global co-ordinate system $x-y$. Figure B.2 shows the local co-ordinate system u,v, θ and global co-ordinates $x-y$. Angle ϕ is always measured from the horizontal line passing through the center. ϕ is positive counter clockwise and negative clockwise.

Expressions for transformation u, v, θ and $x-y$ system can be written as:

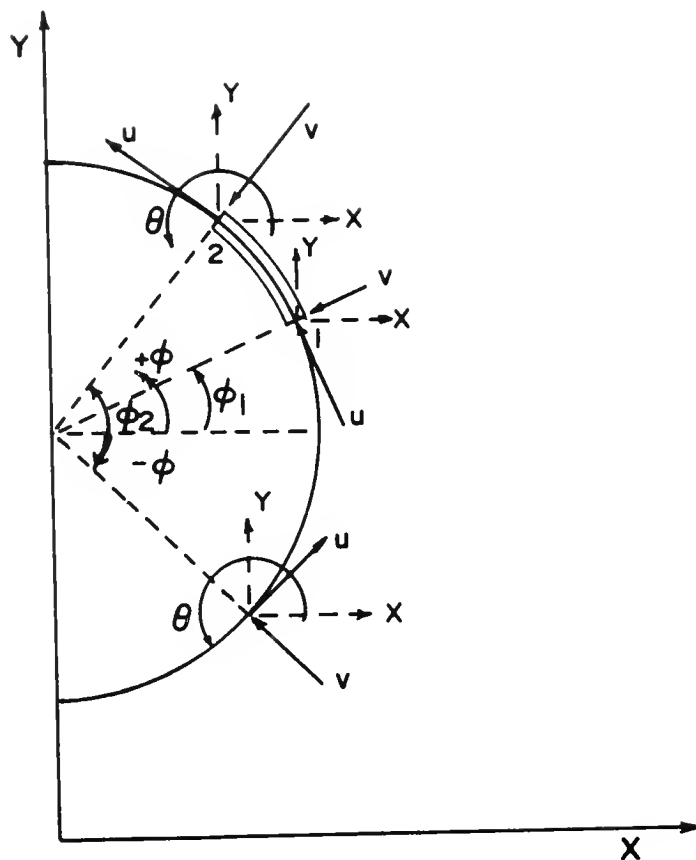


FIGURE B.2 TRANSFORMATION OF COORDINATE SYSTEM FOR CURVED BAR ELEMENT.

$$u = -x \sin\phi + y \cos\phi \quad (\text{B.13a})$$

$$v = -x \cos\phi - y \sin\phi \quad (\text{B.13b})$$

$$\theta = \theta \quad (\text{B.13c})$$

In Matrix form

$$\begin{Bmatrix} u \\ v \\ \theta \end{Bmatrix} = [\bar{L}] \cdot \begin{Bmatrix} x \\ y \\ \theta \end{Bmatrix} \quad (\text{B.14})$$

$$\text{where } [\bar{L}] = \begin{bmatrix} -\sin\phi & \cos\phi & 0 \\ -\cos\phi & -\sin\phi & 0 \\ 0 & 0 & 1 \end{bmatrix}$$

Complete transformation matrix for element 1-2 can be written as

$$\begin{Bmatrix} u_1 \\ v_1 \\ \theta_1 \\ u_2 \\ v_2 \\ \theta_2 \end{Bmatrix} = [L] \begin{Bmatrix} x_1 \\ y_1 \\ \theta_1 \\ x_2 \\ y_2 \\ \theta_2 \end{Bmatrix} \quad (\text{B.15})$$

where

$$[L] = \begin{bmatrix} -\sin\phi_1 & \cos\phi_1 & 0 & 0 & 0 \\ -\cos\phi_1 & -\sin\phi_1 & 0 & 0 & 0 \\ 0 & 0 & 1 & 0 & 0 \\ 0 & 0 & 0 & -\sin\phi_2 & \cos\phi_2 \\ 0 & 0 & 0 & -\cos\phi_2 & -\sin\phi_2 \\ 0 & 0 & 0 & 0 & 1 \end{bmatrix}$$

Inverting matrix L and denoting by T ,

$$[T] = [L]^{-1}$$

pre-multiplying $[k]$ matrix by transpose of $[T]$ and post-multiplying by $[T]$, the stiffness matrix for curved element 1-2 in global co-ordinate system can be written as

$$\begin{matrix} [SRG] \\ 6 \times 6 \end{matrix} = \begin{matrix} [T]^T \\ 6 \times 6 \end{matrix} \cdot \begin{matrix} [k] \\ 6 \times 6 \end{matrix} \cdot \begin{matrix} [T] \\ 6 \times 6 \end{matrix} \quad (B.16)$$

where $[SRG]$ is the stiffness matrix for curved bar element in global co-ordinate system.

APPENDIX - C INTERACTION ELEMENT

Figure C-1 shows an interaction element with four nodes 1 to 4 with eight degrees of freedom. Initially co-ordinates of node 4 are same as for node 1 and those of node 3 are the same as of node 2, which ensures zero thickness. The local co-ordinate system is chosen so that the origin is at the midpoint of the element, the x direction is parallel to and the y direction is perpendicular to the length of the element. The stiffness matrix will be developed using the local co-ordinate system.

If the interaction element is acted upon by a vector of force per unit length $\{P\}$, which produces a relative displacement vector $[w]$, then the expression for total potential energy Φ , of the element can be written as

$$\Phi = \frac{1}{2} \int_{-L/2}^{L/2} [w]^T \cdot \{P\} \cdot dx \quad (C.1)$$

where

$$[w] = \begin{bmatrix} w_s^{\text{top}} & - & w_s^{\text{bottom}} \\ w_n^{\text{top}} & & w_n^{\text{bottom}} \end{bmatrix}$$

$$P = \begin{Bmatrix} P_s \\ P_n \end{Bmatrix}$$

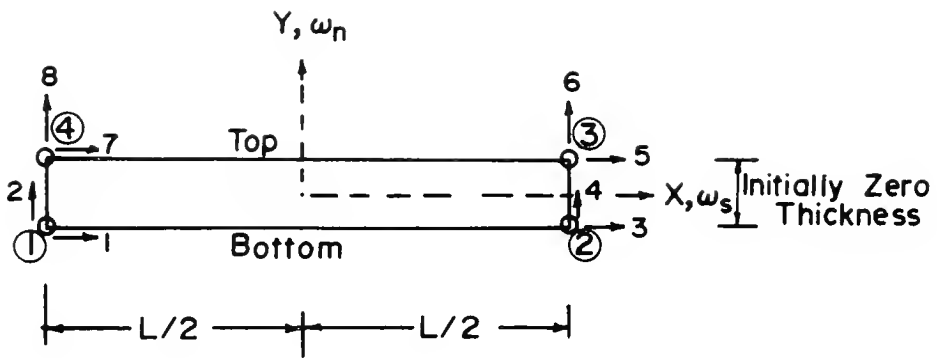


FIGURE C.1 REPRESENTATION OF INTERACTION ELEMENT.

in which subscripts n and s refer to normal and tangential directions respectively.

The vector {P} may be expressed as a product of unit stiffness and displacements, or

$$\{P\} = [E] \cdot [w] \quad (C.2)$$

where [E] = diagonal interaction stiffness property matrix

$$= \begin{bmatrix} E_s & 0 \\ 0 & E_n \end{bmatrix}$$

in which E_n and E_s are the stiffnesses in directions, normal to and parallel to the element.

Substituting equation (C.2) into (C.1)

$$\Phi = \frac{1}{2} \int_{-L/2}^{L/2} [w]^T [E] [w] dx \quad (C.3)$$

The next step is to write the relative displacement vector [w] in terms of nodal displacements. Along the bottom line of interaction element

$$\begin{Bmatrix} w_s^{\text{bottom}} \\ w_n^{\text{bottom}} \end{Bmatrix} = \frac{1}{2} \begin{bmatrix} 1 - \frac{2x}{L} & 0 & 1 + \frac{2x}{L} & 0 \\ 0 & 1 - \frac{2x}{L} & 0 & 1 + \frac{2x}{L} \end{bmatrix} \cdot \begin{Bmatrix} u_1 \\ u_2 \\ u_3 \\ u_4 \end{Bmatrix} \quad (C.4)$$

where x is a floating point along x - direction (Figure C.1).
Similarly for top line of interaction element

$$\begin{Bmatrix} w_s^{\text{top}} \\ w_n^{\text{top}} \end{Bmatrix} = \frac{1}{2} \begin{bmatrix} 1 + \frac{2x}{L} & 0 & 1 - \frac{2x}{L} & 0 \\ 0 & 1 + \frac{2x}{L} & 0 & 1 - \frac{2x}{L} \end{bmatrix} \cdot \begin{Bmatrix} u_5 \\ u_6 \\ u_7 \\ u_8 \end{Bmatrix} \quad (\text{C.5})$$

where u_i is the total displacement in the i^{th} degree of freedom.

Now the relative displacement vector $[w]$ can be written in terms of equation (C.4) and (C.5)

$$[w] = \frac{1}{2} \begin{bmatrix} -A & 0 & -B & 0 & B & 0 & A & 0 \\ 0 & -A & 0 & -B & 0 & B & 0 & A \end{bmatrix} \cdot \begin{Bmatrix} u_1 \\ u_2 \\ u_3 \\ u_4 \\ u_5 \\ u_6 \\ u_7 \\ u_8 \end{Bmatrix} \quad (\text{C.6})$$

or $[w] = \frac{1}{2} [D] \cdot \{u\}$

$$\text{where } A = 1 - \frac{2x}{L}$$

$$\text{and } B = 1 + \frac{2x}{L} .$$

Substitution of $[w]$ into equation (C.3) yields

$$\phi = \frac{1}{2} \int_{-L/2}^{L/2} \frac{1}{4} \{u\}^T \cdot [D]^T \cdot [E] \cdot [D] \cdot \{u\} \cdot dx \quad (C.7)$$

Performing matrix multiplication of $[D]^T$ $[E]$ $[D]$ and integrating over $-L/2$ to $L/2$ yields $[k]$, which on substitution into equation (C.7) gives the expression for total potential energy.

$$\phi = \frac{1}{2} \cdot L \cdot \{u\}^T \cdot [k] \cdot \{u\} \quad (C.8)$$

where $[k]$ per unit length ($L = 1$) is given by

$$[E] = \frac{1}{6} \begin{bmatrix} 2E_s & 0 & E_s & 0 & -E_s & 0 & -2E_s & 0 \\ 0 & 2E_n & 0 & E_n & 0 & -E_n & 0 & -2E_n \\ E_s & 0 & 2E_s & 0 & -2E_s & 0 & -E_s & 0 \\ 0 & E_n & 0 & 2E_n & 0 & -2E_n & 0 & -E_n \\ -E_s & 0 & -2E_s & 0 & 2E_s & 0 & E_s & 0 \\ 0 & -E_n & 0 & -2E_n & 0 & 2E_n & 0 & E_n \\ -2E_s & 0 & -E_s & 0 & E_s & 0 & 2E_s & 0 \\ 0 & -2E_n & 0 & -E_n & 0 & E_n & 0 & 2E_n \end{bmatrix}_{8 \times 8} \quad (C.9)$$

By definition of minimum potential energy, equation (C.9) is the $[8 \times 8]$ stiffness matrix per unit length of interaction element.

In the culvert problem, the value of E_n is maintained very high as long as the element is in compression which ensures essentially zero displacement normal to the pipe. Values of E_s are also very high before a limiting value of

shear stress to normal stress (stress ratio) is reached. For values of the stress ratio above the limiting quantity, E_s is also reduced to zero permitting slip between the top and bottom faces of the interaction element.

So far the development is based on the local coordinate system only, depending upon the element's position, the normal and tangential directions change. The next step is to transform the stiffness matrix to the global coordinate system, which follows a standard procedure of coordinate transformation as described in Appendix - B, equations similar (B.13 to B.16).

APPENDIX - D

DERIVATION OF $\frac{\tau_{\text{oct}}}{\sigma_{\text{oct}}} \Big|_{\text{failure}}$

In equation (5.2) ratio of octahedral shear stress to octahedral normal stress at failure is presented. The derivation of equation (5.2) follows.

σ_1 , σ_2 and σ_3 are the principal stresses at failure for a soil whose angle of friction is ϕ .

$$\sigma_{\text{oct}} = \frac{\sigma_1 + \sigma_2 + \sigma_3}{3} \quad (\text{D.1})$$

$$\tau_{\text{oct}} = \frac{1}{3} \sqrt{(\sigma_1 - \sigma_2)^2 + (\sigma_2 - \sigma_3)^2 + (\sigma_3 - \sigma_1)^2} \quad (\text{D.2})$$

For plane strain conditions from the generalized Hook's law, σ_2 may be represented as

$$\sigma_2 = \psi(\sigma_1 + \sigma_3) \quad (\text{D.3})$$

where

$$\psi = \nu$$

Substituting for σ_2 from equation (D.3) into (D.1) and (D.2)

$$\sigma_{\text{oct}} = \frac{(\sigma_1 + \sigma_3)(1 + \psi)}{3} \quad (\text{D.4})$$

and

$$\tau_{\text{oct}} = \frac{1}{3} \sqrt{2(\sigma_1 + \sigma_3)^2 (\psi^2 - \psi + 1) - 6\sigma_1\sigma_3} \quad (\text{D.5})$$

Dividing (D.5) by (D.4)

$$\frac{\tau_{\text{oct}}}{\sigma_{\text{oct}}} = \frac{\sqrt{2(\sigma_1 + \sigma_3)^2 (\psi^2 - \psi + 1) - 6\sigma_1\sigma_3}}{(\sigma_1 + \sigma_3)(1 + \psi)} \quad (\text{D.6})$$

$$\text{At failure } \frac{\sigma_1}{\sigma_3} = \frac{1 + \sin\phi}{1 - \sin\phi} = N_\phi \quad (\text{D.7})$$

From equation (D.7) one can write the following

$$(\sigma_1 + \sigma_3) = (N_\phi + 1) \cdot \sigma_3$$

$$\sigma_1 = N_\phi \sigma_3$$

$$\sigma_1 \sigma_3 = N_\phi \sigma_3^2$$

Substituting for σ_1 , σ_3 etc. from above identities into (D.6) and simplifying, one can write

$$\left. \frac{\tau_{\text{oct}}}{\sigma_{\text{oct}}} \right|_{\text{failure}} = \frac{1}{1 + \psi} \sqrt{\left[2(\psi^2 - \psi + 1) - \frac{6N_\phi}{(N_\phi + 1)^2} \right]} \quad (\text{D.8})$$

APPENDIX - E

DERIVATION OF TANGENT MODULUS (E_t) AND TANGENT
POISSON'S RATIO (ν_t)

For a three dimensional state of stress

σ_1 = major principal stress

σ_2 = intermediate principal stress

σ_3 = minor principal stress

ϵ_1 = major principal strain

ϵ_2 = intermediate principal strain

ϵ_3 = minor principal strain

E = Young's modulus of the material

ν = Poisson's ratio

Generalized Hook's law:

$$E \cdot \epsilon_1 = \sigma_1 - \nu \sigma_2 - \nu \sigma_3 \quad (E.1)$$

$$E \cdot \epsilon_2 = \sigma_2 - \nu \sigma_1 - \nu \sigma_3 \quad (E.2)$$

$$E \cdot \epsilon_3 = \sigma_3 - \nu \sigma_1 - \nu \sigma_2 \quad (E.3)$$

For plane strain condition $\epsilon_2 = 0$ and from equation

(E.2)

$$\sigma_2 = \nu (\sigma_1 + \sigma_3) \quad (E.4)$$



Substituting σ_2 from equation (E.4) into (E.1) and (E.3) and simplifying

$$\varepsilon_1 = \frac{1 - \nu^2}{E} \left[\sigma_1 - \frac{\nu}{1 - \nu} \sigma_3 \right] \quad (\text{E.5})$$

$$\varepsilon_3 = \frac{1 - \nu^2}{E} \left[\sigma_3 - \frac{\nu}{1 - \nu} \sigma_1 \right] \quad (\text{E.6})$$

$$\frac{\varepsilon_1}{\varepsilon_3} = K = \frac{\sigma_1 - \left(\frac{\nu}{1 - \nu}\right) \sigma_3}{\sigma_3 - \left(\frac{\nu}{1 - \nu}\right) \sigma_1} \quad (\text{E.7})$$

or

$$\frac{\nu}{1 - \nu} = \frac{\sigma_1 - K\sigma_3}{\sigma_3 - K\sigma_1}$$

or

$$\nu = \frac{\sigma_1 - K\sigma_3}{(1 - K)(\sigma_1 + \sigma_3)} \quad (\text{E.8})$$

Substituting for K from (E.7) in (E.8) and simplifying

$$\nu = \frac{\sigma_1 \varepsilon_3 - \varepsilon_1 \sigma_3}{(\varepsilon_3 - \varepsilon_1)(\sigma_1 + \sigma_3)} \quad (\text{E.9})$$

To get tangent Poisson's ratio, ν_t incremental values of stresses and strains have to be used. If Δ denotes incremental values, the expression for tangent Poisson's ratio is given

$$\nu_t = \frac{\Delta\sigma_1 \Delta\varepsilon_3 - \Delta\varepsilon_1 \Delta\sigma_3}{(\Delta\varepsilon_3 - \Delta\varepsilon_1)(\Delta\sigma_1 + \Delta\sigma_3)} \quad (\text{E.10})$$

Subtracting (E.6) from (E.5) and simplifying

$$E = \frac{1 - \nu^2}{\epsilon_1 - \epsilon_3} \left[\frac{\sigma_1 - \sigma_3}{1 - \nu} \right]. \quad (E.11)$$

or

$$E = (1 + \nu) \left[\frac{\sigma_1 - \sigma_3}{\epsilon_1 - \epsilon_3} \right] \quad (E.12)$$

Substituting for ν from equation (E.8)

$$E = \left\{ 1 + \frac{\sigma_1 - K \sigma_3}{(1 - K)(\sigma_1 + \sigma_3)} \right\} \cdot \left\{ \frac{\sigma_1 - \sigma_3}{\epsilon_1 - \epsilon_3} \right\} \quad (E.13)$$

$$= \frac{\sigma_1 (2 - K) + \sigma_3 (1 - 2K)}{(1 - K)(\sigma_1 + \sigma_3)} \cdot \left\{ \frac{\sigma_1 - \sigma_3}{\epsilon_1 - \epsilon_3} \right\} \quad (E.14)$$

or

$$E = \left\{ \frac{\sigma_1 - \sigma_3}{\epsilon_1 - \epsilon_3} \right\} \cdot \left[1 - \frac{\sigma_1 \epsilon_3 - \epsilon_1 \sigma_3}{(\sigma_1 + \sigma_3)(\epsilon_1 - \epsilon_3)} \right] \quad (E.15)$$

To obtain tangent modulus E_t , incremental values of stress and strains are used in equation (E.15)

$$E_t = \frac{(\Delta \sigma_1 - \Delta \sigma_3)}{(\Delta \epsilon_1 - \Delta \epsilon_3)} \cdot \left[1 - \frac{\Delta \sigma_1 \Delta \epsilon_3 - \Delta \epsilon_1 \Delta \sigma_3}{(\Delta \sigma_1 + \Delta \sigma_3)(\Delta \epsilon_1 - \Delta \epsilon_3)} \right] \quad (E.16)$$

$$E = \frac{1}{1 - \frac{v^2}{c^2}}$$

10

11

12

13

14

$$E_f = \frac{1}{1 - \frac{v^2}{c^2}}$$

